Final Rapid Science Synthesis Report: Findings from the Second Texas Air Quality Study (TexAQS II)

A Report to the
Texas Commission on Environmental Quality

by the
TexAQS II Rapid Science Synthesis Team

Prepared by the
Southern Oxidants Study Office of the Director at
North Carolina State University

by
Ellis B. Cowling, Director of SOS
Cari Furiness, Research Associate
Basil Dimitriades, Adjunct Professor
and
David Parrish
Earth System Research Laboratory,
National Oceanic and Atmospheric Administration

In cooperation with Mark Estes of TCEQ and
47 other members of the Rapid Science Synthesis Team

Acknowledgments

Department of Energy (DOE)
    Pacific Northwest Laboratory (PNL)
    Argonne National Laboratory (ANL)
    Los Alamos National Laboratory (LNL)

Department of Interior (DOI)
    Minerals Management Service (MMS)

Environment Canada (EC)
    Meteorological Service of Canada (MSC)

National Aeronautics and Space Administration
    Headquarters Science Mission Directorate and science teams for the
        Atmospheric Infrared Sounder (AIRS),
        Cloud-Aerosol Lidar Infrared Pathfinder Satellite Observations (CALIPSO),
        Moderate Resolution Imaging Spectroradiometer (MODIS),
        Multi-angle Imaging SpectroRadiometer (MISR)
        Ozone Monitoring Instrument (OMI), and
        Tropospheric Emission Spectrometer (TES)
    Jet Propulsion Laboratory (JPL)
    Langley Research Center (LRC)

National Oceanic and Atmospheric Administration (NOAA)
    Office of Oceans and Atmospheric Research (OAR)
        Earth System Research Laboratory (ESRL)
        Pacific Marine Environmental Laboratory (PMEL)
        Atlantic Oceanographic and Meteorological Laboratory (AOML)
        Air Resources Laboratory (ARL)
        National Weather Service (NWS)
        National Environmental Satellite Data and Information Service (NESDIS)
        Office of Marine and Aviation Operations (OMAO)

National Science Foundation (NSF)
    National Center for Atmospheric Research (NCAR)

Tennessee Valley Authority (TVA)

United States Environmental Protection Agency (USEPA)

    Office of Air Quality Planning and Standards

    Air Quality Analysis Division

        Air Quality Modeling Group

Cooperating Research Universities

Baylor University

California Institute of Technology

Chalmers University of Technology, Göteborg, Sweden

Fort Hayes State University

Georgia Institute of Technology

Howard University

Lamar University

Texas Air Research Center (TARC)

North Carolina State University

Pennsylvania State University

Portland State University

Rice University

Scripps Institution of Oceanography

Texas A&M University

Texas Tech University

University of Alabama in Huntsville

University of California at Los Angeles

University of California at Santa Cruz

University of Colorado
Cooperative Institute for Research in Environmental Science (CIRES)

University of Houston

University of Manchester, Manchester, UK

University of Maryland Baltimore County

University of Massachusetts

University of Miami

University of New Hampshire

University of Rhode Island

University of Texas in Austin

University of Washington
Joint Institute for Study of Atmosphere Oceans (JISAO)

Valparaiso University

Washington State University

Cooperating Private Sector Organizations

Aerodyne Research Inc.

Baron Advanced Meteorological Systems

Exxon Mobil Corporation

Houston Regional Monitoring Network

Science Systems and Applications, Inc.

SensorSense, The Netherlands

Shell Oil Corporation

Sonoma Technology, Inc.

URS Corporation

Other Cooperating Organizations

Houston Advanced Research Center (HARC)

Texas Environmental Research Consortium (TERC)

Executive Summary

The Rapid Science Synthesis Team (RSST) for the Second Texas Air Quality Study (TexAQS II) has been charged to address a series of 12 High Priority SIP-Relevant Science Questions identified by the Texas Commission on Environmental Quality (TCEQ). Answers to these important questions were needed by TCEQ and other stakeholders in Texas to help fulfill the Commission's responsibility to develop scientifically sound State Implementation Plans (SIPs) by which to attain the recently implemented 8-hour National Ambient Air Quality Standard (NAAQS) for Ozone. SIPs for both the Houston-Galveston-Brazoria and the Dallas-Fort Worth Ozone Non-Attainment Areas were submitted to EPA in June 2007.

This Final Report of the Rapid Science Synthesis Team for TexAQS II is designed to provide statements of Findings in response to each of TCEQ's 12 High Priority SIP-Relevant Science Questions. This report addresses:

1) Significant sources of ozone and aerosol pollution in eastern Texas,

2) Photochemical and meteorological processes involved in the production, transport, and accumulation of these pollutants in various parts of Texas,

3) An assessment of the adequacy of emissions inventories for both biogenic and anthropogenic sources of ozone and aerosol precursor chemicals, and

4) An assessment of the skill of current air quality modeling and forecasting systems and recommendations for improvement of these systems.

This Executive Summary provides a short introduction to the scientific Findings from TexAQS II research for use by TCEQ managers and other air-quality decision makers and stakeholders in Texas. It contains a complete list of the 12 High Priority SIP-Relevant Science Questions that TCEQ asked our Rapid Science Synthesis Team to address a series of carefully crafted statements of Findings that have been developed in response to each of these questions.

We emphasize that the statements of scientific Findings developed as part of the Rapid Science Synthesis effort are based on analysis and interpretation of results from TexAQS II research within the limited time that was available between completion of the last TexAQS II field measurements on 15 October 2006 and our Rapid Science Synthesis contract ending date – 31 August 2007. More thorough and comprehensive analyses are already underway and will yield a great deal of additional important information in the future.

The institutional affiliations of the scientists responsible for the analyses leading to these Findings are given in the Acknowledgments section, immediately preceding this Executive Summary. Each section of this report is structured to contain one of the 12 SIP-Relevant Science Questions, then a numbered sequence of Findings in response to that question. Following each Finding, acknowledgment of the individuals whose analyses and data contributed to that Finding are listed. It also provides a brief discussion of the evidence that supports each Finding. The concerned reader should carefully consider the caveats contained in these discussions. For the convenience of all readers, a glossary of acronyms is provided in Appendix 1.

Please note that questions printed in **blue** were designated by TCEQ for special emphasis.

Findings

Question A
Which local emissions are responsible for the production of high ozone in Houston, Dallas, and eastern Texas?
Are different kinds of emissions responsible for transient high ozone and 8-hour-average high ozone (i.e., ≥84 ppbv)?

Finding A1: The highest (i.e. > 125 ppbv) ozone concentrations in the HGB area result from rapid and efficient ozone formation in relatively narrow, concentrated plumes, which originate from HRVOC and NO_x co-emitted from petrochemical facilities. The Houston Ship Channel (HSC) is the origin of the plumes with the highest ozone concentrations.

Finding A2a: Winds carry the emission plumes from the Ship Channel throughout the Houston area. The wind direction determines the location of the ozone maximum relative to the Ship Channel; shifts in wind direction lead to the transient high ozone events observed at monitoring sites within the Houston area.

Finding A2b: The general characteristics of the highest (i.e. > 125 ppbv) ozone formation in Houston did not change between 2000 and 2006, although the maximum observed ozone concentrations were lower in 2006 than in 2000.

Finding A3: Emissions from the Houston Ship Channel play a major role in the formation of the highest 8-hour average ozone concentrations (and ozone design values) observed in the Houston area.

Finding A4: Observations during TexAQS 2006 showed that nitryl chloride ($ClNO_2$) is formed within the nocturnal boundary layer when NO_x emissions and marine influences are both present. Following sunrise, $ClNO_2$ photolyzes to yield chlorine atoms, which may lead to earlier and more rapid O_3 production in the Houston region.

Question B
How do the structure and dynamics of the planetary boundary layer and lower troposphere affect the ozone and aerosol concentrations in Houston, Dallas, and eastern Texas?

Finding B1: Boundary layer structure and mixing height near and over Galveston Bay and the eastern Houston ship channel area are spatially complex and variable from day to day. Vertical mixing profiles often do not fit simple models or conceptual profiles. High concentrations of pollutants are sometimes found above the boundary layer.

Finding B2: Complex coastal winds, resulting from weak larger-scale winds over the area, occurred during many, but not all, ozone exceedance days in the Houston-Galveston-Brazoria nonattainment area. Almost no high-ozone days during TexAQS 2000 resembled any high ozone days from TexAQS 2006, but collectively the 2000 and 2006 field intensives sampled the full range of meteorological conditions associated with high ozone events.

Finding B3: After sea breeze days, the Houston plume was broadly dispersed at night through the formation of low-level jets.

Finding B4: The Dallas ozone plume can extend well beyond the monitoring network.

Question C
Are highly reactive VOC and NO$_x$ emissions and resulting ambient concentrations still at the same levels in Houston as they were in 2000?
How have they changed spatially and temporally? Are there specific locations where particularly large quantities of HRVOC are still being emitted?
Are those emissions continuous or episodic?
How well do the reported emissions inventories explain the observed concentrations of VOC and NO$_x$?

Finding C1: There are indications that ethene (the lightest HRVOC) emissions from industrial sources in the Houston area decreased by 40 (±20)%, i.e., by a factor of between 1.25 and 2.5, between 2000 and 2006.

Finding C2: Measurements of ethene emission fluxes from petrochemical facilities during TexAQS 2006 indicate that the 2004 TCEQ point source database underestimates these 2006 emissions by one to two orders of magnitude. Repeated sampling of the same petrochemical facility showed that the ethene emission flux remained constant to within a factor of two.

Finding C3: Close to petrochemical HRVOC sources, the OH reactivity of propene is generally greater than that of ethene.

Finding C4: The latest available emission inventories underestimate ethene emissions by approximately an order of magnitude.

Finding C5: Inventories for NO$_x$ point sources at petrochemical facilities equipped with CEMS appear to be relatively accurate. Substantial decreases in NO$_x$ emissions in the Houston Ship Channel are suggested by the inventories, and measurements from aircraft are qualitatively consistent with the NO$_x$ decreases.

Question D
What distribution of anthropogenic and biogenic emissions of ozone and aerosol precursors can be inferred from observations?

Finding D1a: Several rural electric generation units (EGU) in the Houston area and in eastern Texas have substantially decreased their NO$_x$ emissions per unit power generated since the TexAQS 2000 study. With one exception, SO$_2$ emissions have not changed appreciably since 2000 for the plants sampled in 2006.

Finding D1b: Comparisons of emissions derived from ambient observations with those measured by continuous emission monitoring systems (CEMS) indicate that the emissions from point sources equipped with CEMS are very accurately known.

Finding D1c: Underreporting of CO emissions at several EGU noted in 2000 (Nicks et al., 2003) has been reconciled by large increases (by factors of 5 to 50) in the inventory values between 2000 and 2006, as a result of newly implemented CEMS monitoring of CO at these plants.

Finding D2: On-road mobile emission inventories developed from MOBILE6 have significant shortcomings. MOBILE6 consistently overestimates CO emissions by about a factor of 2. It accurately estimated NO_x emissions in the years near 2000, but it indicates decreases in NO_x emissions since then, while ambient data suggest NOx emissions have actually increased. Consequently in 2006, NO_x to VOC emission ratios in urban areas are likely underestimated by current inventories.

Finding D3: Emissions from ships constitute a significant NO_x source in the HGB region. Literature results provide accurate emission factors for inventory development.

Finding D4: Mixing ratios of isoprene over Texas measured from the WP-3D were used for evaluation of the BEIS-3 emission inventory. On average, the isoprene emissions from the inventory and emissions derived from the measurements agree within a factor of ~2. There may be areas south of Dallas-Fort Worth and southwest of Houston, where isoprene emissions are lower than indicated by the BEIS3 inventory based upon the biogenics emission land cover data (BELD-3.0).

Finding D5: The speciation of VOC from mobile sources in the Houston and Dallas-Forth Worth areas agrees with detailed measurements in the northeastern U.S. However, initial results suggest that the agreement with the NEI-99 emission inventory is poor.

Question E
Are there sources of ozone and aerosol precursors that are not represented in the reported emissions inventories?

Finding E1: The observed mixing ratios and regional distribution of ambient formaldehyde are broadly consistent with daytime photochemical production from reactive VOC. An upper limit for primary formaldehyde emissions from mobile sources is obtained from nighttime measurements, and is small in comparison with the secondary, daytime formation.

Finding E2: Concentrated plumes of ammonia were observed occasionally in the Houston Ship Channel area. These plumes often led to the formation of ammonium nitrate aerosol.

Finding E3: Concentrated plumes of gaseous elemental mercury from at least one point source were observed repeatedly in the Houston Ship Channel area and once in the Beaumont-Port Arthur area. The sources of the plumes could not be identified with current inventory sources of mercury.

Question F

How do the mesoscale chemical environments (NOx-sensitive ozone formation vs radical-sensitive ozone formation) vary spatially and temporally in Houston, Dallas, and eastern Texas?
Which mesoscale chemical environments are most closely associated with high ozone and aerosol?

Finding F1: Both Eulerian and Lagrangian plume modeling approaches indicate that in 2000 high ozone concentrations in the HGB area were sensitive to both VOC and NO_x emission reductions.

Finding F2: An observation-based approach to determine the sensitivities of high ozone in the HGB non-attainment area to the precursor VOC and NO_x emissions has been investigated; it has yielded ambiguous results.

Finding F3: At the highest ozone concentrations, the observed relationship between ozone and the products of NO_x oxidation indicates less efficient ozone production in the Dallas area than in the Houston area. In the observation-based indicator species approach, this behavior corresponds to less NO_x-sensitive and more VOC- or radical-sensitive ozone formation in Dallas compared to Houston.

Finding F4: Tests of the ability of models to reproduce observed relationships between ozone and other photochemical products have the potential to provide very fruitful approaches to improving models.

Question G

How do emissions from local and distant sources interact to determine the air quality in Texas?
What meteorological and chemical conditions exist when elevated background ozone and aerosol from distant regions affect Texas?
How high are background concentrations of ozone and aerosol, and how do they vary spatially and temporally?

Finding G1: The maximum background ozone concentrations encountered in 2006 exceeded the 8-hour NAAQS. On average, air of continental origin had higher background concentrations than marine air. The average background ozone concentrations measured in 2006 in eastern Texas complement a previously developed climatology.

Finding G2: The net ozone flux transported out of Houston averages about a factor of two to three larger than the corresponding flux from Dallas. The fluxes from these urban areas are significant contributors to the background ozone in the eastern Texas region.

Finding G3: Elevated background ozone concentrations for urban areas can include contributions from the recirculation of locally produced ozone or local precursor emissions.

Finding G4: **Plumes from Texas urban areas make substantial contributions to the ozone, aerosol, and precursor concentrations in the rural regions of eastern Texas.**

Finding G5: **Dust of African origin and sulfate aerosol advected into the Houston area, under southerly flow conditions from the Gulf of Mexico, can make significant contributions to the background aerosol in the eastern Texas region.**

Finding G6: Nighttime chemistry influences the availability of oxides of nitrogen (NO_x), highly reactive VOC (HRVOC), and O_3.

Finding G7: **Low rural nighttime ozone concentrations have been observed at some, but not all, rural locations in northeast Texas; these low nighttime ozone concentrations are not replicated in the regulatory modeling.**

Question H
Which areas within Texas adversely affect the air quality of non-attainment areas in Texas?
Which areas outside of Texas adversely affect the air quality of non-attainment areas in Texas?

Finding H1: **Ozone can be transported into the Dallas area from the Houston area.**

Finding H2: **High ozone concentrations in eastern Texas result from both in-state sources and transport of continental air from the east and northeast.**

Finding H3: **A synthesis of satellite and in situ measurements with photochemical modeling and Lagrangian trajectory analyses provides a quantification of regional influences and distant sources on Houston and Dallas air quality during TexAQS 2006.**

Finding H4: **In the Dallas area, local emissions and transport each contributed about equally to the average 8-hr ozone exceedance in 2002. Transported ozone alone can bring the Dallas area close to exceeding the 8-hour ozone standard.**

Finding H5: **In the Houston area, local emissions and transport each contributed about equally to the average 8-hr ozone exceedances investigated by aircraft flights in 2000 and 2006. As in Dallas, transported ozone alone can bring the Houston area close to exceeding the 8-hour ozone standard.**

Question I
Why does the SAPRC chemical mechanism give different results than the carbon bond (CB-IV) mechanism?
Which replicates the actual chemistry better?

Finding I1: **Air quality modeling for both 2000 and 2006 shows substantial differences in ozone concentrations predicted by the SAPRC99 and CB-IV chemical mechanisms.**

Finding I2: **In regions with very high VOC reactivity and high NO$_x$ emission density, differences in ozone formation and accumulation predicted by regional photochemical models using the SAPRC99 and CB-IV mechanisms are due to differences in: (1) the chemistry of aromatics, especially mono-substituted aromatics (e.g., toluene), (2) nitric acid formation rates, and (3) the rates of free radical source terms in the SAPRC and CB-IV mechanisms.**

Finding I3: **The differences in the predictions of the SAPRC99 and CB-IV mechanisms can be probed using simulations of model compounds and comparisons of the simulations to environmental chamber data. For simulations involving CO and NO$_x$ (inorganic chemistry), the predictions of the CB-IV and SAPRC99 mechanisms that are used in regional photochemical models (with no chamber wall corrections) converge if the rate constants for the OH + NO$_2$ reaction are made consistent between the two mechanisms. The predictions of the Carbon Bond mechanism, version 5 (CB05) also converge to the same predicted values if the OH + NO$_2$ rate constant is made consistent with the other mechanisms.**

Finding I4: **The performance of the mechanisms in simulating olefins chemistry can be improved through more explicit representation of internal olefin chemistry, which has been added in CB05. In addition, performance of the SAPRC99 mechanism in simulating chamber data was improved for some experiments when propene was modeled explicitly, as opposed to being represented by a lumped chemical species.**

Finding I5: **For high reactivity chamber experiments involving olefins, sensitivity analyses indicated that mechanism adjustments that would lead to increased radical concentrations (increasing the radical yield in olefin-ozone reactions and changing the OH+NO$_2$ termination rate constant) had little impact on predicted ozone concentrations.**

Finding I6: **The SAPRC99 mechanism performed better than the CB mechanisms in simulating some chamber experiments with toluene; the mechanism performances were more comparable for xylenes and other multiply substituted aromatics.**

Finding I7: **The differences between the SAPRC and CB-IV mechanism predictions for toluene chemistry decrease substantially if the yield for the lumped species CRES, and rate constant for the OH + NO$_2$, are made consistent between the two mechanisms. The predictions of the CB05 mechanism also converge to the same predicted values if the CRES yield and the OH + NO$_2$ rate constant are made consistent with the other mechanisms.**

Finding I8: **For simulations of ambient surrogate mixture experiments in the UCR EPA chamber, all mechanisms underpredict O$_3$ at low ROG/NO$_x$ ratios, with the bias decreasing as the ROG/NO$_x$ ratio increases. In simulations of mixture experiments in chambers without aromatics, CB05 performs the best, and with no dependence of bias on the ROG/NO$_x$ ratio.**

31 August 2007

Finding I9: SAPRC99, CB-IV, and CB05 all successfully predicted concentrations of ozone and other species during simulation of a stagnation event, if the chemical mechanisms were initialized after initial high concentrations of olefins had reacted. None of the mechanisms successfully predicted a rapid rise in radical concentrations and ozone concentration concurrent with initially high C2, C3, and CMBO concentrations during the event.

Question J

How well do air quality forecast models predict the observed ozone and aerosol formation? What are the implications for improvement of ozone forecasts?

Finding J1a: Most forecast models exhibit skill in predicting maximum 8-hr-average O_3 but none of the models is better than persistence in predicting 24-hr-average $PM_{2.5}$ levels.

Finding J1b: Seven air quality forecast models and their ensemble were generally unable to forecast 85 ppbv 8-hr-average O_3 exceedances with any reliability.

Finding J2: Sophisticated data assimilation of meteorological and even chemical observations is essential for improving photochemical model forecasts.

Finding J3: Model performance evaluations and intercomparisons require a comprehensive, best-guess emissions inventory for the TexAQS 2006 Field Intensive.

Question K

How can observation and modeling approaches be used for determining (i) the sensitivities of high ozone in the HGB non-attainment area to the precursor VOC and NO_x emissions, and (ii) the spatial/temporal variation of these sensitivities?

Finding K1: A simple, heuristic model based upon the Empirical Kinetic Modeling Approach (EKMA) method suggests that the HGB region may ultimately require drastic NO_x emissions controls to reach compliance with the NAAQS for ozone.

Finding K2: The same model suggests that in a projected future scenario with very strict VOC emission controls, but without drastic NO_x emission controls, biogenic VOC emissions plus background concentrations of CO and methane may be sufficient to cause ozone exceedances.

Question L

What existing observational databases are suitable for evaluating and further developing meteorological models for application in the HGB area?

The Final Report for Question L can be found in Appendix 2 of this Report, as submitted 31 October 2006.

Introduction

The Rapid Science Synthesis Team (RSST) for the Second Texas Air Quality Study (TexAQS II) was charged to address the series of 12 High Priority SIP-Relevant Science Questions listed in the text box below. The Texas Commission on Environmental Quality (TCEQ) posed these questions to elicit responses needed to help TCEQ fulfill its responsibility to develop State Implementation Plans (SIPs) by which to attain the recently implemented 8-hour National Ambient Air Quality Standards (NAAQS) for ozone in the 8-county Houston-Galveston-Brazoria and 8-county Dallas-Fort Worth ozone non-attainment areas. TCEQ's interests and questions also deal, to a lesser extent, with fine particulate matter. This report presents the final Responses of the RSST to these 12 TCEQ Science Questions.

As part of the Rapid Science Synthesis effort, TCEQ and the Office of the Director for the Southern Oxidants Study (SOS-OD) established Working Groups to address each Science Question. Each Working Group consisted of 8-15 experts drawn from various university-, state-, federal-, and private-sector organizations. The members of the Working Groups are listed in the text box below; contact information is given in Appendix 3.

The Working Groups developed research approaches for responding to each of the 12 TCEQ Science Questions; the approaches are described in a Progress Report from the RSST dated 31 July 2006. On 12 and 13 October 2006, shortly before completion of the TexAQS II Field Study, the Rapid Science Synthesis Team participated in a day-and-a half-long meeting in Austin, Texas. Presentations from this initial Rapid Science Synthesis Workshop were posted on the TCEQ website, http://www.tceq.state.tx.us/implementation/air/airmod/texaqs-files/TexAQSII.html. These presentations formed the basis for an RSST report, *Preliminary Findings from the Second Texas Quality Study (TexAQS II)*, dated 31 October 2006 [8 November revision].

The RSST participated in the Principal Findings and Data Analysis Workshop for TexAQS II/ GoMACCS 2006, held 29 May – 1 June 2007, in Austin, Texas. Presentations from this Workshop were also posted on the TCEQ website, http://www.tceq.state.tx.us/implementation/air/airmod/committee/scc.html#workshops. These presentations and subsequent analyses of research results by various TexAQS II researchers provided the foundation for this final report of the Rapid Science Synthesis Team, *Final Rapid Science Synthesis Report: Findings from TexAQS II*. The sections of this Final Report present carefully crafted statements of scientific findings in response to each of TCEQ's High Priority SIP-Relevant Science Questions. In this connection, we found very helpful the "Guidelines for Formulation of Scientific Findings to be Used for Policy Purposes" shown in Appendix 4.

Electronic copies of the three RSS reports to TCEQ are available on websites maintained by TCEQ (listed above) and by the National Oceanic and Atmospheric Administration (NOAA) (http://esrl.noaa.gov/csd/2006/).

The following introductory information provides some background and perspective for the Science Questions and the Responses developed by the RSST.

TCEQ's High Priority SIP-Relevant Science Questions and Leaders (L), Participants (P) and Observers (O) in Working Groups within the Rapid Science Synthesis Team

A Which local emissions are responsible for the production of high ozone in Houston, Dallas, and eastern Texas? Are different kinds of emissions responsible for transient high ozone and 8-hour-average high ozone (i.e., $\geq$84 ppbv)?
L – David Parrish, P – Tom Ryerson, Joost deGouw, Basil Dimitriades, David Allen, Mark Estes, Bernhard Rappenglück, O – Noor Gillani

B How do the structure and dynamics of the planetary boundary layer and lower troposphere affect ozone and aerosol concentrations in Houston, Dallas, and eastern Texas?
Co-L – Robert Banta & John Nielsen-Gammon, P – Allen White, Christoph Senff, Wayne Angevine, Bryan Lambeth, Lisa Darby, Bright Dornblaser, Daewon Byun, Bernhard Rappenglück, O – Carl Berkowitz, Noor Gillani

C Are highly-reactive VOC and NO_x emissions and resulting ambient concentrations still at the same levels in Houston as they were in 2000? How have they changed spatially and temporally? Are there specific locations where particularly large quantities of HRVOC are still being emitted? Are those emissions continuous or episodic? How well do the reported emissions inventories explain the observed concentrations of VOC and NO_x?
L – David Parrish, P – David Allen, Joost deGouw, Tom Ryerson, Mark Estes, David Sullivan, John Jolly, Eric Williams, Barry Lefer, O – Yulong Xie, Carl Berkowitz, Noor Gillani. **Note:** To answer the last part of question C, TCEQ must define the inventory to which the observations must be compared.

D What distribution of anthropogenic and biogenic emissions of ozone and aerosol precursors can be inferred from observations?
Co-L – David Allen & David Parrish, P – Tom Ryerson, Charles Brock, Joost deGouw, David Sullivan, Mark Estes, John Jolly, Eric Williams, Barry Lefer, Bernhard Rappenglück, O – Yulong Xie, Carl Berkowitz, Noor Gillani

E Are there sources of ozone and aerosol precursors that are not represented in the reported emissions inventories?
L – David Parrish, P – Tom Ryerson, Charles Brock, Joost deGouw, David Sullivan, John Jolly, David Allen, Eric Williams, Barry Lefer, Bernhard Rappenglück

F How do the mesoscale chemical environments (NO_x-sensitive ozone formation vs radical-sensitive ozone formation) vary spatially and temporally in Houston, Dallas and eastern Texas? Which mesoscale chemical environments are most closely associated with high ozone and aerosol?
Co-L – Basil Dimitriades & David Parrish, P – David Allen, Harvey Jeffries, William Vizuete, Daewon Byun, Mark Estes, Kenneth Schere, Barry Lefer, Bernhard Rappenglück, O – Yulong Xie, Carl Berkowitz

Note: Letter designations are for convenience only and do not denote priority. Questions in blue have been designated by TCEQ to receive special emphasis.

TCEQ's High Priority SIP-Relevant Science Questions and Leaders (L), Participants (P) and Observers (O) in Working Groups within the Rapid Science Synthesis Team (continued)

G How do emissions from local and distant sources interact to determine the air quality in Texas? What meteorological and chemical conditions exist when elevated background ozone and aerosol from distant regions affect Texas? How high are background concentrations of ozone and aerosol, and how do they vary spatially and temporally?
Co-L – David Allen & David Parrish, P –Bryan Lambeth, David Sullivan, Basil Dimitriades, Charles Brock, Michael Hardesty, Steve Brown, Joost deGouw, Bernhard Rappenglück, Brad Pierce, Wallace McMillan, Kevin Bowman, David Winker, Tim Bates

H Which areas within Texas adversely affect the air quality of non-attainment areas within Texas? Which areas outside of Texas adversely affect the air quality of non-attainment areas within Texas?
Co-L – David Allen & David Parrish, P – Mark Estes, Greg Yarwood, Basil Dimitriades, David Sullivan, Charles Brock, Michael Hardesty, John Jolly, Bryan Lambeth, Brad Pierce, Wallace McMillan, Kevin Bowman, David Winker

I Why does the SAPRC chemical mechanism give different results than CB-IV? Which replicates the actual chemistry better?
Co-L – David Allen & Greg Yarwood, P – Harvey Jeffries, William Vizuete, Bill Carter, David Parrish, Stuart McKeen, Daewon Byun, Joost deGouw, Barry Lefer, Bernhard Rappenglück, O – Mark Estes, Noor Gillani

J How well do forecast air quality models predict the observed ozone and aerosol formation? What are the implications for improvement of ozone forecasts?
L – Stuart McKeen, P – Gregory Carmichael, Bryan Lambeth, Kenneth Schere, James Wilczak, Greg Yarwood, Daewon Byun, John Nielsen-Gammon, Michael Hardesty

K How can observation and modeling approaches be used for determining (i) the sensitivities of high ozone in the HGB non-attainment area to the precursor VOC and NOx emissions, and (ii) the spatial/temporal variation of these sensitivities?
Co-L – Basil Dimitriades & David Parrish, P – Ted Russell, Harvey Jeffries, William Vizuete, Mark Estes, David Sullivan, Tom Ryerson, Greg Yarwood, Barry Lefer, Bernhard Rappenglück, O – Noor Gillani

L What existing observational databases are suitable for evaluating and further developing meteorological models for application in the HGB area?
L – Lisa Darby, P – Robert Banta, John Nielsen-Gammon, Daewon Byun, Wayne Angevine, Mark Estes, Bryan Lambeth, Stuart McKeen

Note: Letter designations are for convenience only and do not denote priority. Questions in blue have been designated by TCEQ to receive special emphasis.

Non-attainment Areas Requiring SIP Development

TCEQ initiated TexAQS II to obtain additional SIP-relevant understanding of the processes that lead to formation and accumulation of ozone and particulate matter in two very different ozone non-attainment areas within Texas:

1) The Houston-Galveston-Brazoria (HGB) ozone non-attainment area is a *coastal* urban region of about 5 million people. It consists of eight counties in southeastern Texas and is subject to distinctive coastal (sea-breeze) meteorological conditions and large petrochemical sources of industrial emissions, especially the Houston Ship Channel (HSC) and other nearby industrial sites. In 2005 HGB was classified as a non-attainment area of "moderate" status, with an attainment deadline of June 2010. The most recent SIP revision (June 2007) does not demonstrate attainment by that date, and the state of Texas has requested a reclassification of the HGB non-attainment area to "severe," which requires an attainment date of June 2019 and a SIP revision deadline of March 2010. HGB is in attainment of the $PM_{2.5}$ NAAQS.

2) The Dallas-Fort Worth (DFW) ozone non-attainment area is an *inland* urban region, also of about 5 million people. The DFW non-attainment area includes 8 counties in north-central Texas, with relatively typical inland metropolitan meteorological conditions and only limited industrial sources within the non-attainment counties, but with several power plants in nearby locations within northeastern Texas. DFW also was classified as in "moderate" non-attainment of the ozone standard, with a June 2010 attainment date. The June 2007 SIP revision submitted to EPA demonstrates attainment of the 8-hour standard by that deadline. DFW is in attainment of the $PM_{2.5}$ NAAQS.

Recent Air Quality Studies in Texas

During recent years, the State of Texas provided substantial funding for scientific studies to improve understanding of ozone formation and accumulation in eastern Texas. These scientific studies have been focused around two major air-quality field research programs.

First Texas Air-Quality Study (TexAQS 2000)

TexAQS 2000 was a relatively short-term (six-week-long) intensive field measurement program conducted during the summer of 2000 that included aircraft-based, tall tower-based, and ground-based field measurements; the study period was imbedded in a 16-month long study on particulate matter in the Houston area. The research results demonstrated that the *extraordinarily stringent decrease in NO_x emissions* proposed in the 2000 SIP for the HGB non-attainment area of Texas was not an optimal approach; a more realistic plan for attainment of the NAAQS for ozone should involve decreases in emissions of *both VOC and NO_x* – with a particular focus on the highly reactive VOC (HRVOC) emissions in the industrial areas surrounding the Houston Ship Channel and Galveston Bay.

Second Texas Air Quality Study (TexAQS II and TexAQS 2006)

TexAQS II was a much longer-term (18-month-long) program focused on the photochemical and meteorological processes leading to the formation and accumulation of ozone and particulate matter air pollution in eastern Texas. The study began in June 2005 and extended through 15 October 2006. This period includes not only the 2005 and 2006 summer ozone seasons, but also the intervening fall, winter, and spring months when occasional exceedances of the 8-hour ozone standard did occur, both together with and separately from, occasional episodes of high

concentrations of airborne particulate matter. The field measurements of TexAQS II constitute one of the most comprehensive air quality field research studies ever undertaken in the United States; the analysis and interpretation phases of TexAQS II will extend for years after completion of the field measurements.

TexAQS II culminated during the months of August, September, and October 2006 with an intensive series of coordinated chemical and meteorological measurements and modeling studies. In order to distinguish this relatively short-term but very intensive study from the earlier parts of TexAQS II, the 2006 summer intensive study has been dubbed TexAQS 2006.

The air-quality measurement platforms during TexAQS 2006 included:
1) Multiple instrumented aircraft operating in both the HGB and DFW areas of Texas,
2) A series of ground-based sites with continuing measurements of air chemistry, a network of ground-based wind profiler and rawinsonde locations, a mobile solar occultation flux research van, and both aircraft-based and ship-based ozone and aerosol lidar measurements throughout eastern Texas,
3) NOAA's *Ronald H. Brown* Research Vessel operating within the Houston Ship Channel and Galveston Bay,
4) The 200-foot-tall Moody Tower at the University of Houston, and
5) The National Aeronautics and Space Administration (NASA) Aura, Aqua, Terra, and GOES satellites.

The multimillion-dollar 18-month-long TexAQS II field research study and its embedded short-term intensive study, TexAQS 2006, were conducted jointly by staff of TCEQ and by scientists and engineers working under contracts issued by TCEQ, the Texas Environmental Research Consortium (TERC), and through formal and/or informal agreements for cooperation with the many other research organizations listed in the *Acknowledgments* of this Report.

All the research studies and plans for analysis and interpretation of results obtained during TexAQS II and TexAQS 2006 were undertaken with specific scientific research objectives in mind. But many of these investigations also were designed, undertaken, and funded by various federal, state, and private-sector organizations with specific policy purposes in mind – and most particularly in order to be used by TCEQ in developing State Implementation Plans that were required by the US EPA in 2007 for the Houston-Galveston-Brazoria and Dallas-Fort Worth ozone non-attainment areas. The very limited time available between completion of many of the TexAQS II field measurements and the deadline for preparation and final submission of the SIPs required for Houston and Dallas-Forth Worth was extraordinarily short – thus the need for a rapid synthesis of SIP-relevant science.

History of Ozone Exceedances in Houston and Dallas
Figure 1 shows that maximum ozone concentrations throughout HGB and DFW decreased from 1978 to 2005. It is notable that:
1) Most of the decreases in HGB occurred before 1990;
2) The decreases were greater in HGB (from over 150 ppbv to near 100 ppbv) than in DFW (from about 120 ppbv to near 95 ppbv); and
3) The ozone design values in HGB are now approximately the same as in DFW. The large variability in ozone maxima since 1990 – both among monitoring sites and between years – make it difficult to determine whether these apparent decreases in ozone maxima since 1999 are due to changes in emissions or to meteorological variations.
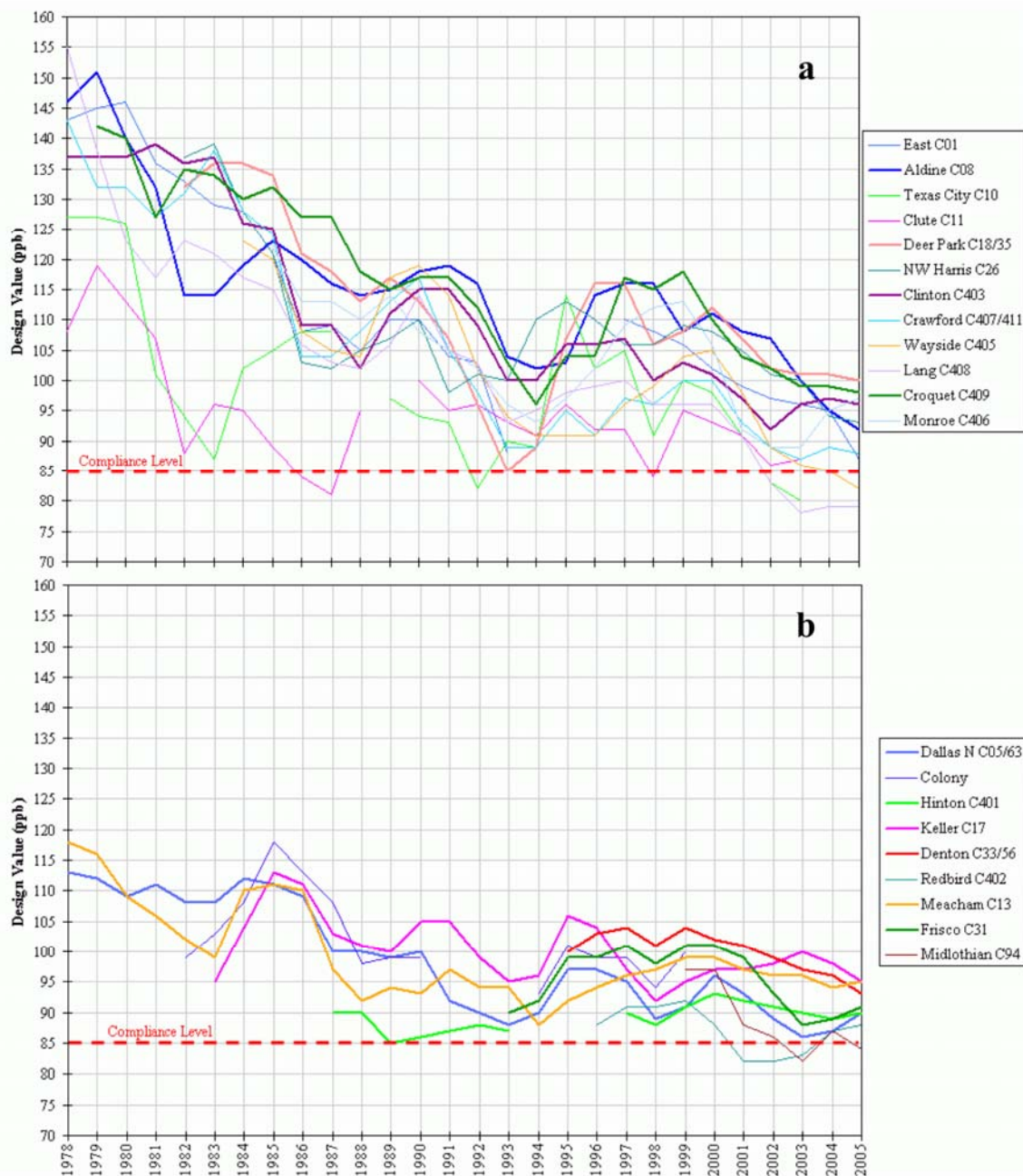
Figure 1. Temporal trends of 8-hour O_3 design values at a) HGB and b) DFW monitoring sites. The 8-hour O_3 design value for each monitor is the 3-year average of the fourth-highest daily maximum 8-hour-average ozone concentration measured at that monitor; these values are representative of the maximum ozone observed and the air concentrations of specific concern in developing control strategies. (Figure from Bryan Lambeth, TCEQ)

Although the ozone design values for the HGB and DFW areas are now very similar, acute ozone episodes are much more frequent in Houston than Dallas. During 2000-2005, the HGB area had 219 8-hour ozone exceedance days while the DFW area had 203. In contrast, however, during this same period, the HGB area had 147 one-hour exceedance days (ozone concentrations

> 120 ppbv) but the DFW area had only 24 such days. Over 60 percent of the HGB 8-hour exceedances were accompanied by 1-hour exceedances. In the HGB area the local design value maxima have not changed locations during that period, and have persisted in the vicinity of Deer Park, Bayland Park, and Aldine. There is a local minimum in ozone design value at sites located in the urban core of Houston, presumably because of the abundant fresh NO emissions there, which can suppress ozone formation, or titrate ozone transported into the area.

Regional Character of Ozone Exceedances in Eastern Texas
Maximum daily ozone concentrations generally occur in multi-day episodes, and episodes often are region-wide, with similar patterns throughout eastern Texas (Figure 2). These region-wide episodes of high ozone concentrations are seen in all years. Two hypotheses can be suggested to explain this behavior:

    1) The episodes occur during meteorological conditions under which elevated ozone concentrations, produced in upwind regions, are transported into the whole region of eastern Texas.

    2) The high ozone episodes represent periods when the regional meteorology is particularly conducive (sunny, hot, stagnant) to local or regional formation of ozone from locally or regionally emitted precursors, and the intervening periods represent meteorological conditions that are particularly poor (cloudy, cool, windy) for ozone formation within the region.

Figure 2. Daily maximum 8-hour ozone averages for August-September 2004 for all monitoring sites in eastern Texas. Each column represents one day, and each row represents one monitor within each community (TLM-Tyler, Longview, Marshall; BPA-Beaumont, Port Arthur; Aus-Austin; SAo-San Antonio, CCV-Corpus Christi, Victoria). The increasing color intensity indicates increasing ozone concentrations (yellow ≥65 ppbv, orange ≥85 ppbv, red ≥105 ppbv, purple ≥125 ppbv. (Data from TCEQ; Figure adapted from David Sullivan-U. Texas)

A decreasing temporal trend in regional ozone concentrations and exceedances has occurred over the past 13 years. A trend analysis covering 1994 to 2004 shows that the average of the maximum 8-hour-average ozone concentrations observed at upwind surface monitoring stations in the Houston area have declined since about 2000 (Figure 3). Values were approximately 80 ppbv in the 1990s and have dropped to between 60 and 70 ppbv in 2002 – 2004. This suggests that background ozone concentrations during high ozone episodes in the Houston area have been declining in recent years. There has been a concomitant decrease in the total number of exceedance days recorded each year in August and September at twelve representative eastern Texas monitoring sites (Figure 4). These sites were selected for completeness of data coverage (>75% each year) and regional representation (one site per county, except for two in Harris County). It is important to note that the year of the TexAQS 2006 field study had the fewest number of regional exceedances during this 13-year period.
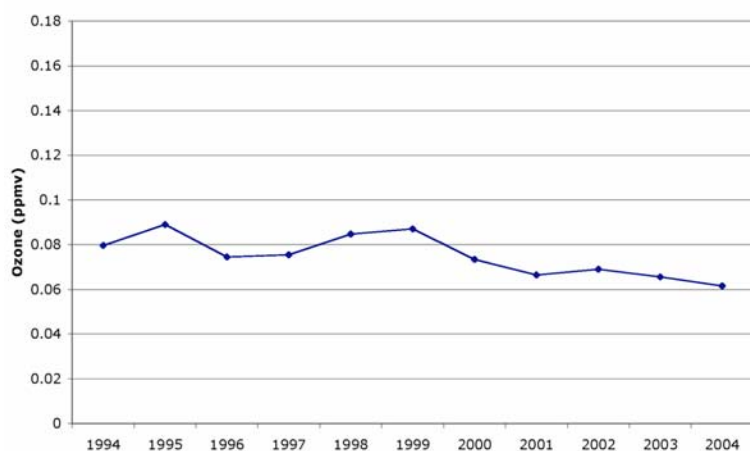

Figure 3. 1994 to 2004 trend of highest 3 - 6 values of 8-hour background ozone from upwind surface stations in Houston area (from Nielsen-Gammon et al., 2005).
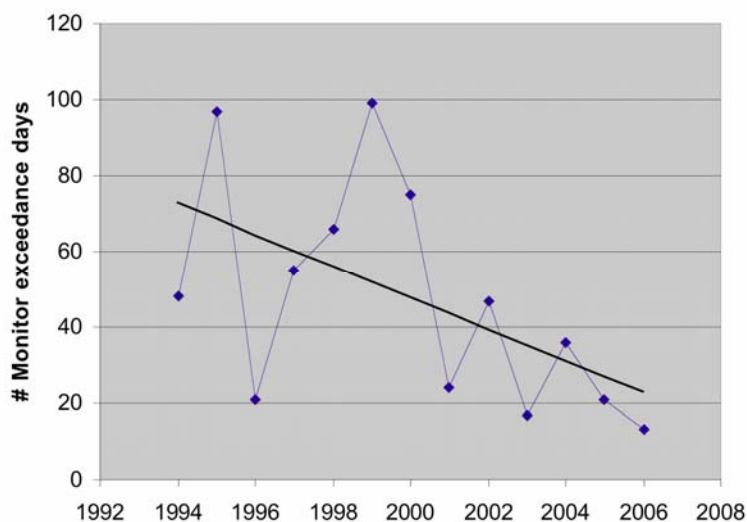

Figure 4. Total number of monitor-days with maximum 8-hour-average ozone above 85 ppbv in August and September during the years between 1994 and 2006. Twelve regional monitoring sites in eastern Texas were considered in this analysis. (Data from TCEQ; Figure from David Sullivan-U. Texas)

An Important Distinction: Ozone Production versus Accumulation
From the standpoints of understanding air quality science and the practical business of air quality management, it is important to recognize the distinction between ozone *formation* and/or ozone *production* (which are essentially synonymous)*,* on the one hand, and ozone *accumulation* on the other hand. The ambient concentration of ozone in a particular, near-surface volume of air at a fixed location is the net result of six processes that occur in the lower atmosphere:

- In situ ozone *formation (or production)* from chemical precursors in an air parcel,

- In situ ozone *destruction* by chemical reactions in that air parcel,

- *Deposition* of ozone from the air to vegetation or other surfaces,

- *Vertical transport* of ozone from an ozone reservoir aloft,

- *Horizontal transport* of ozone from up-wind locations, and

- *Dispersion and dilution* as a result of mixing with cleaner air during advection or vertical mixing when the height of the planetary boundary layer increases.

In effect, the rate of change in the concentration of ozone in a particular, near-surface volume of air is an "algebraic sum" of the rates of all six of these processes. The time-integral of this "algebraic sum" then represents the *accumulation* of ozone in that volume of air at that specific location (if the integral is positive, or a decrease in ambient ozone concentration if the integral is negative.)

Atmospheric scientists and engineers are well aware of these important processes and distinctions. They devote much effort to experimentally determining the rates of each of these processes, and to developing models that accurately calculate the resulting *accumulation* of ozone to compare with ambient observations of ozone concentrations.

Air quality managers are concerned with management of near-surface ozone concentrations; thus, they are not concerned with the *production* of ozone as such, so long as the ambient concentration of ozone does not exceed the NAAQS. Air quality managers are required to develop State Implementation Plans that are aimed at keeping ozone from *accumulating* in the atmosphere in concentrations that exceed these NAAQS.

In the mixed dialog that occurs between atmospheric scientists and air quality managers, this important distinction can be lost, and a degree of confusion may result. Some of this confusion arises because, among the six processes listed above, only the rate of ozone *formation* can be effectively addressed through local emission control efforts. Thus, ozone *formation* receives particular attention from both atmospheric scientists and air quality managers.

In this report, the term "*accumulation of ozone"* is used when the distinction is important. However, in many situations, the distinction between "*accumulation of ozone"* and "*ozone production*" is not so important. These situations arise when the rate of *production* dominates the "algebraic sum" above. In such situations, the discussion will focus on "*ozone production*" and the contribution of the other five processes will not be discussed.

Reactivity of VOC Ozone Precursors

Photochemical production of ozone requires two classes of precursors: oxides of nitrogen (NO_x, which include NO and NO_2) and volatile organic compounds (VOC). During ozone formation the VOC are photochemically oxidized while NO_x catalyzes the formation of ozone during that oxidation. Oxidation of carbon monoxide (CO) and methane also can contribute significantly to the formation of ozone.

Figure 5 shows the rate constants for the reactions of many different VOC with the hydroxyl radical (OH). This radical is the active agent

Figure 5. Rate constants and representative atmospheric lifetimes for some VOC. CO is included for comparison. Rate constant data are from the literature.

in the atmosphere that initiates the photochemical oxidation of VOC. The OH concentration in ambient air varies widely, but a representative, 24-hour average value is 1×10^6 OH radicals per cm^3 of air. The right hand axis in Figure 5 gives the lifetimes of various VOC at that representative OH concentration. The OH rate constants span such a wide range that the VOC lifetimes vary from many days to less than one hour. The effectiveness of any given VOC in ozone formation is approximately proportional to its OH reactivity, which is the product of the VOC concentration times its OH rate constant.

The TexAQS 2000 study highlighted the important role played by highly reactive VOC (HRVOC) in the HGB area. These species are the alkenes, five of which are included in Figure 5 (above the "Alkenes" label in the figure). Their importance is due to their high OH reactivities, which result from both their large OH rate constants and their high ambient concentrations. The high ambient concentrations result from large quantities of HRVOC emitted from petrochemical facilities in the HGB area.

The biogenic VOC, especially isoprene, are particularly important in forested regions of eastern Texas (Figure 6). Recently, new land cover and vegetation data have improved the spatial resolution and provided more quantifiable estimates of uncertainties for these emissions. Biogenic emissions derived from these new data are about 40% lower than previous calculations. It is important to recognize that some biogenic VOC, especially isoprene, are also emitted from anthropogenic sources in the industrial facilities in HGB.
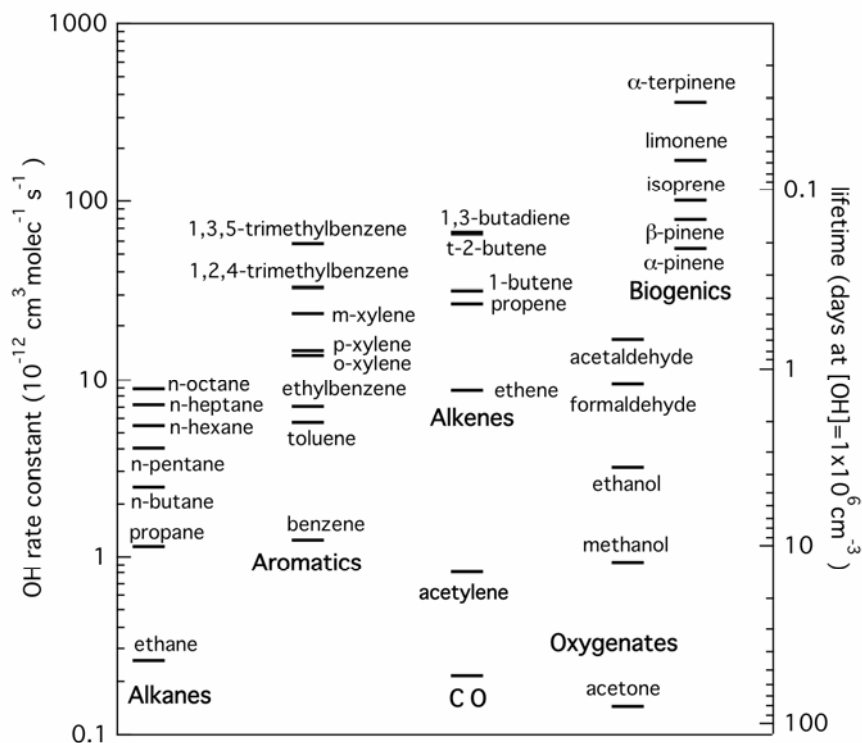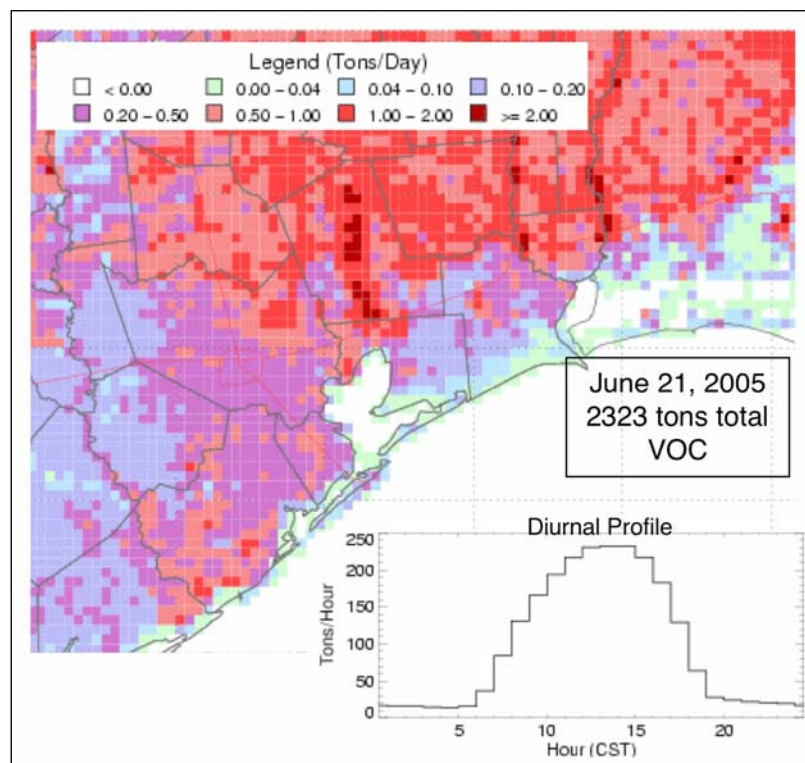
Figure 6. Biogenic VOC emissions in southeast Texas on a representative summer day. The emissions are calculated at 4 km x 4 km spatial resolution based on the latest University of Texas-Center for Space Research land cover data. (Figure adapted from Mark Estes, TCEQ)

A Reflective Note

Although this is the Final Report of the Rapid Science Synthesis Team, all of us on the RSST recognize that we have not yet derived maximum benefit from all the research data and information that was accumulated during TexAQS II. The accelerated pace of our analyses and interpretations did not allow full utilization of the results. Fortunately, however, the future will provide many additional opportunities for more detailed analyses, for more intercomparisons of results, and for more integrative interpretations. The findings developed in this Final Report will be subject to more rigorous examination when TexAQS II results are presented at scientific meetings and when papers deriving from TexAQS II research are submitted for publication in refereed scientific journals.

We are proud of what has been accomplished so far – the new scientific insights obtained, and the new policy insights provided. We hope this Final Report will be useful to TCEQ and the people of Texas, as they continue the practical business of air quality management in Houston and Dallas-Fort Worth.

We wish to express our thanks to the many staff in TCEQ who organized our several workshop meetings and helped us gain access to additional data and information from existing databases – especially those that go back in time to observations made long before both TexAQS 2000 and TexAQS II were conceived and implemented. We have also enjoyed the excellent cooperation among so many of the diverse groups of scientists, engineers, graduate students, and post-docs that joined in various parts of this very large study. It was fascinating to have the chance to understand more fully the very challenging chemical, biological, physical, meteorological, and mathematical factors that are involved, as well as some of the social, cultural, industrial, political, professional, and economic forces involved in managing air quality – especially in the Houston-Galveston, and Brazoria ozone non-attainment area.

Response to Question A

QUESTION A
Which local emissions are responsible for the production of high ozone in Houston, Dallas, and eastern Texas?
Are different kinds of emissions responsible for transient high ozone and 8-hour-average high ozone (i.e., ≥84 ppbv)?

BACKGROUND
Question A is related to Questions F and K, which focus on the sensitivities of high concentrations of ozone to VOC and NO_x emissions. Here the response to Question A gives an overview of the photochemical processes that produce the highest observed ozone concentrations, and the emissions that allow those processes to proceed rapidly. These highest ozone concentrations are limited to the HGB region, so the focus is on that area. Understanding 8-hour-average high ozone requires very different considerations and approaches than the understanding of transient high ozone; an initial investigation of the longer-term-average ozone in HGB is included.

FINDINGS

Finding A1: **The highest (i.e. > 125 ppbv) ozone concentrations in the HGB area result from rapid and efficient ozone formation in relatively narrow, concentrated plumes, which originate from HRVOC and NO_x co-emitted from petrochemical facilities. The Houston Ship Channel (HSC) is the origin of the plumes with the highest ozone concentrations.**

Analysis: Trainer-NOAA; Data: Ryerson, de Gouw et al.-NOAA, Fried et al.-NCAR, Atlas et al.-U. Miami.

The aircraft flights of TexAQS 2000 and 2006 reveal a persistent feature over Houston – on all days conducive to photochemical ozone production, narrow and concentrated plumes of ozone formed and were transported downwind from the HSC. Figure A1 shows measurements from one flight; on this day the wind was from the east-northeast. The top two graphs show the measurements of two primary ozone precursors. NO_y represents the NO_x emissions plus their oxidation products, primarily PAN and nitric acid. Ethene, a HRVOC, is an important ozone precursor. The concentrations of these two primary emissions were highest over the HSC, and defined a narrow downwind plume with decreasing concentrations. Figure A1 indicates that the NO_x and ethene emission sources are not precisely collocated, but the primary sources of both are in the HSC region. The downwind decrease in the concentration of NO_y was primarily due to dilution. Clearly, ethene concentrations decreased more rapidly than NO_y, due to its much faster removal through photochemical oxidation. The bottom two panels of Figure A1 show the concentrations of two secondary photochemical products, ozone and formaldehyde, formed within the plume of primary emissions. Formaldehyde, produced by the photochemical oxidation of ethene and other HRVOC, formed during the downwind transport as the HRVOC were oxidized; formaldehyde itself is an important ozone precursor. Ozone accumulated as a concentrated (up to 147 ppbv), narrow plume within the much less concentrated (≤ 100 ppbv), but wider ozone plume from the larger Houston urban area.
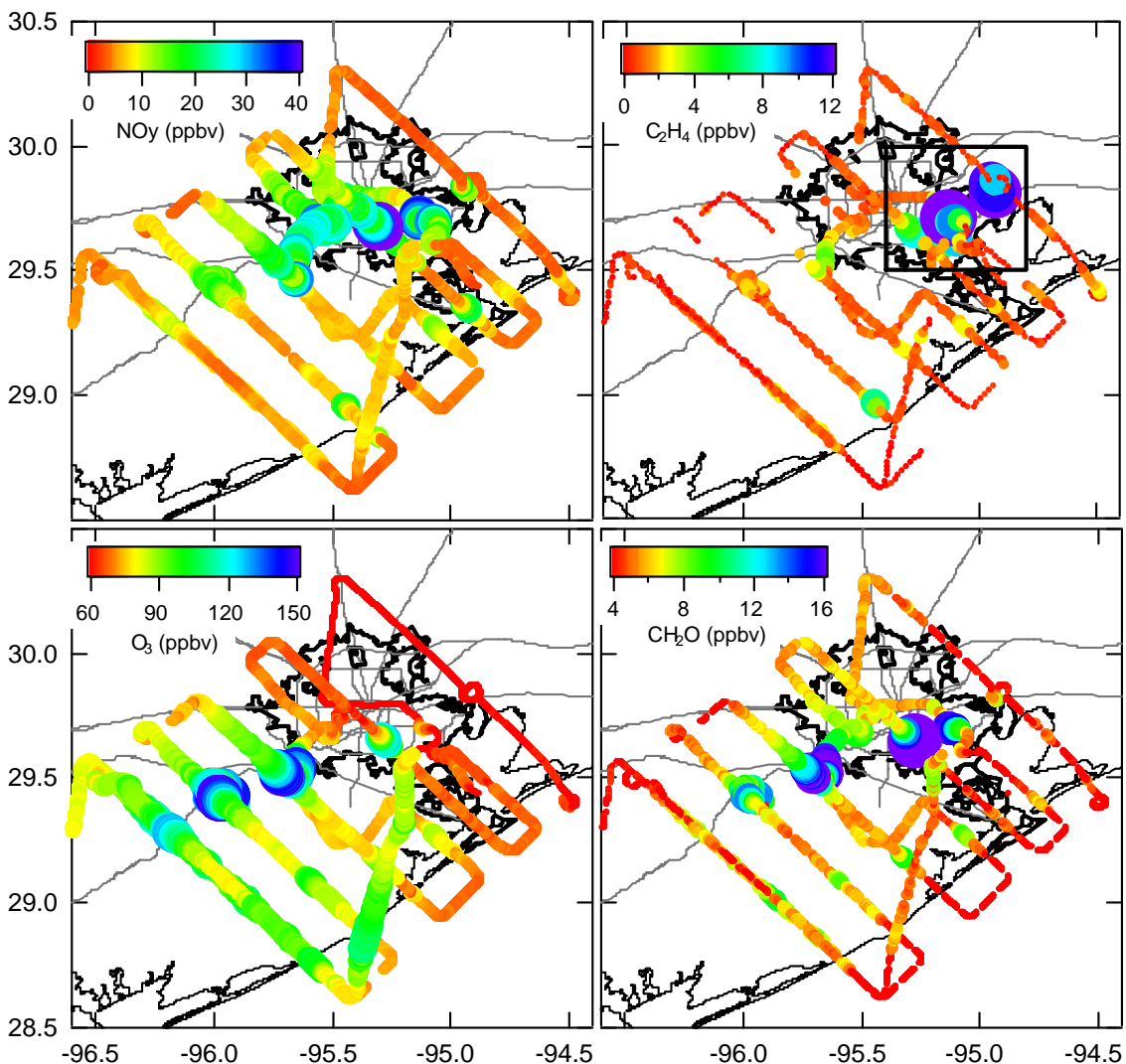
Figure A1. Measurements of NOy, ethene (C$_2$H$_2$), ozone, and formaldehyde (CH$_2$O), plotted along the flight track of the WP-3D on 6 October 2006. The symbols are sized and color-coded according to the indicated concentrations. Only measurements below 1.5 km altitude are shown. (A close approach to the Parish power plant has been removed from the NOy plot.)

The high temporal resolution measurements of ethene made by the laser photo-acoustic spectrometer (LPAS) and the wide species coverage of VOC measurements conducted on the canisters from the whole air sampler (WAS) provided detailed characterization of the HRVOC sources in HSC. The map in Figure A2 shows the concentration of ethene measured by these two systems downwind from six petrochemical complexes; the plumes of ethene emissions from the complexes are clearly delineated. The four pie charts in Figure A2 indicate the total OH reactivity of the VOC in four of the WAS samples, and show how that reactivity was divided among four of the lightest HRVOC species, and the total of all of the other alkanes, aromatics, and biogenic VOC measured in the canister samples. These four canister samples illustrate the general finding that the HRVOC dominate the VOC reactivity immediately downwind of the petrochemical facilities, and thus are responsible for a large fraction of the high ozone

production in the HGB area. The total reactivity and the fraction of the reactivity contributed by the HRVOC decrease downwind in the plumes, as expected from their very short lifetimes.

The pie charts in Figure A2 do not include aldehydes. These oxygenated VOC, which also account for a significant fraction of the OH reactivity, are primarily secondary products of the oxidation of the HRVOC. Thus, the contribution of the aldehydes to ozone production increases the fraction of the total VOC reactivity in the HSC area that is attributable to the emissions of the HRVOC.
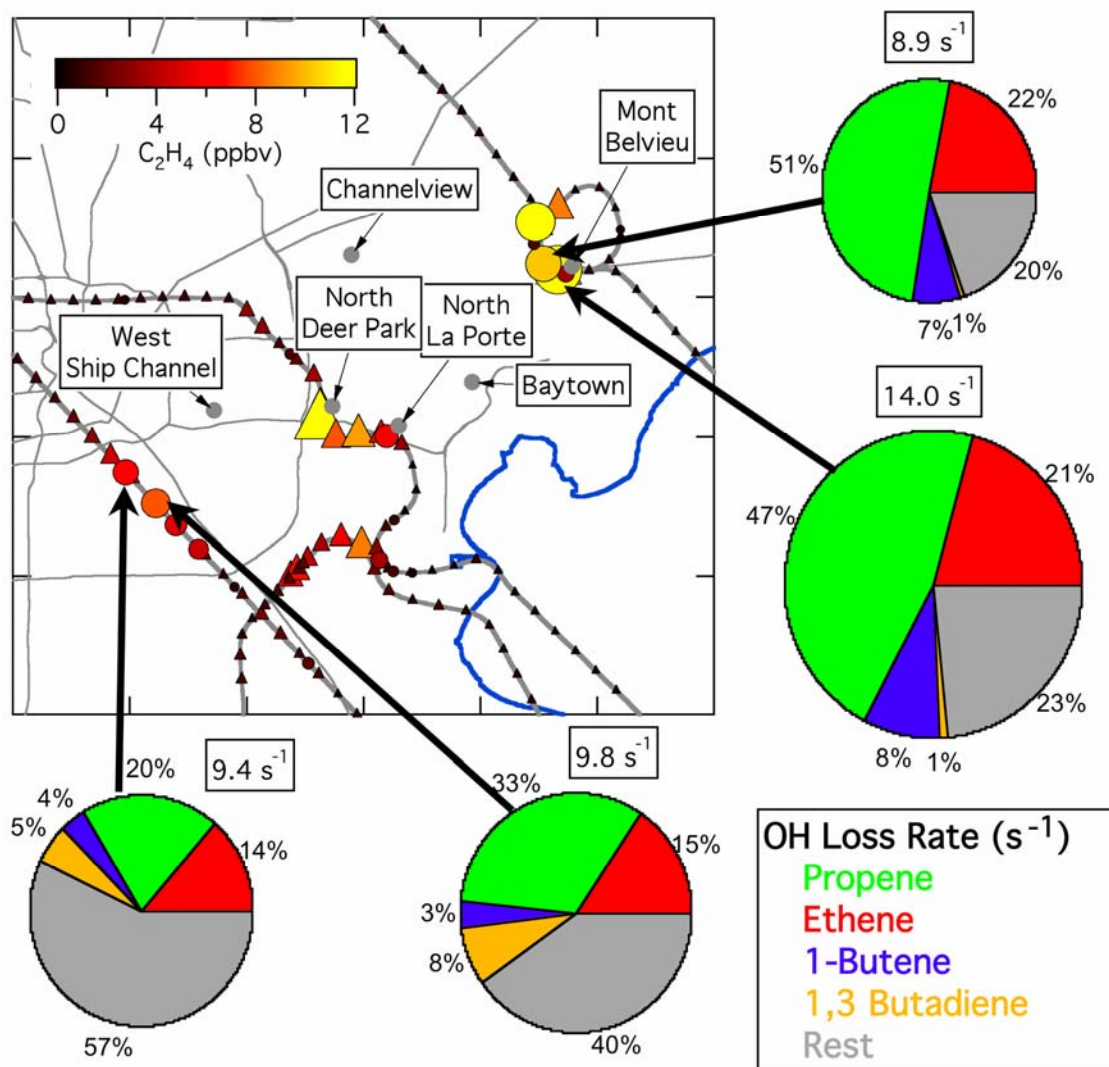

Figure A2. Measurements of ethene along the section of the WP-3D flight track included in the rectangle in the upper right panel of Figure A1. The symbols are sized and colored according to the indicated concentrations. The triangles indicate the 20-second-average measurements by LPAS, and the circles indicate the measurements from WAS. The pie charts are sized according to the total OH reactivity for four of the WAS samples, and the colors indicate the OH reactivity contributed by the four indicated HRVOC.

Finding A2a: **Winds carry the emission plumes from the Ship Channel throughout the Houston area. The wind direction determines the location of the ozone maximum relative to the Ship Channel; shifts in wind direction lead to the transient high ozone events observed at monitoring sites within the Houston area.**

Finding A2b: **The general characteristics of the highest (i.e. > 125 ppbv) ozone formation in Houston did not change between 2000 and 2006, although the maximum observed ozone concentrations were lower in 2006 than in 2000.**

Analysis: Ryerson et al.-NOAA; Data: Ryerson, Williams et al.-NOAA.

Ryerson et al. (2006) examined the four Electra flights during TexAQS 2000 that encountered ozone concentrations above 150 ppbv. Figure A3 shows the flight track segments where the highest ozone concentrations were observed. In each case, back-trajectory analysis attributed these high ozone concentrations to plumes from industrial emission sources in the HSC area. Measured chemical characteristics of the plumes (simultaneous high NO_x, SO_2, CO_2, and oxidation products of HVROC) confirmed this source attribution. The relationship between the transport times derived from the trajectory analysis and the observed enhancements in ozone concentration provided a measure of the net average ozone production rates in the plumes. Figure A3 also shows the observed relationship between ozone and the products of NO_x oxidation for those four flights; the slopes of these relationships provide an estimate of the net ozone production efficiencies in these plumes.
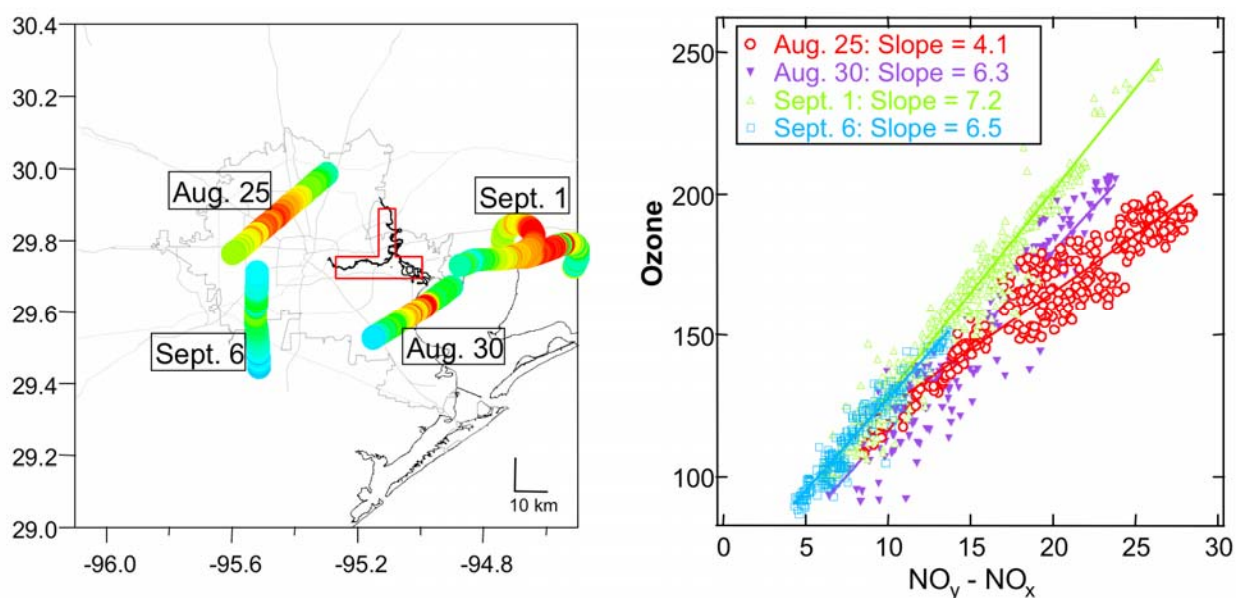

Figure A3. Highest ozone (red points) observed by the Electra aircraft during four flights in TexAQS 2000. In the left panel flight track segments are color-coded by observed ozone, and in the right panel the dependence of ozone on the products of NO_x oxidation are shown with approximate ozone production efficiencies estimated from fitted slopes (Ryerson et al., 2006).

Figure A4 presents a similar analysis for the three WP-3D daytime flights and the *RHB* ship cruise segment during TexAQS 2006 that encountered ozone concentrations near or above 120 ppbv. A simple wind direction analysis, coupled with the chemical plume signatures, indicate that in each case these plumes also originated from industrial emission sources in the Houston Ship Channel area. Figure A4 also shows the relationship between ozone and the products of NO_x oxidation in these plumes.
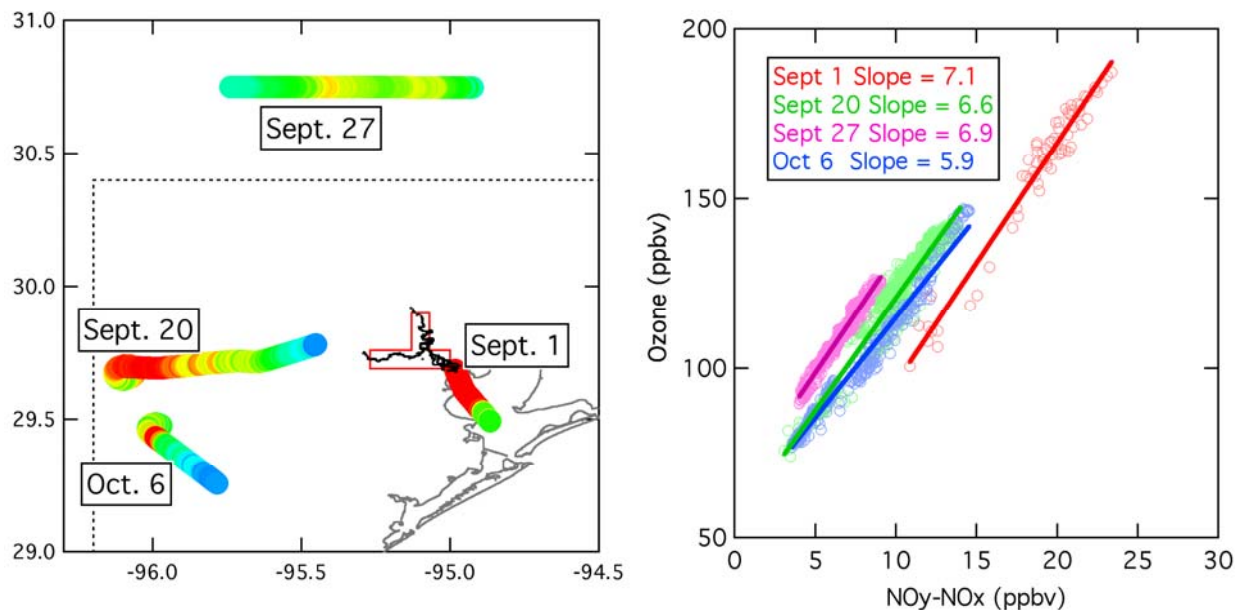

Figure A4. Highest ozone observed by the WP-3D aircraft and RHB research vessel during TexAQS 2006. The figure is in the same format as Figure A3. The dotted rectangle in the left panel indicates area covered in Figure A3.

Comparison of Figures A3 and A4 show that the ozone production environment in the Houston area was similar in 2000 and 2006. Similar ozone vs. $(NO_y$-$NO_x)$ slopes are seen in each year; the maximum concentrations of ozone observed in both years were associated with slopes near 7. Lower maximum ozone concentrations were observed in 2006, but this difference may be partially due to meteorological factors; the background ozone, as indicated by the y-intercepts in the two right panels in Figures A3 and A4, was lower in 2006 and lower background concentrations led to lower maximum concentrations. The lower 2006 background may indicate smaller effects of stagnation and recirculation that year. Finally, the maximum ozone concentrations were observed at greater distances from the HSC in 2006 than in 2000 (note difference in area covered in the two maps). This difference may be attributable to slower ozone production or to greater transport speeds in 2006 than in 2000.

Relationship between Ozone Production Efficiency and the Slope of the O_3 versus NO_y-NO_x Correlation – A Cautionary Note

Many investigations of atmospheric photochemistry have interpreted the slope of the correlation of the measured O_3 concentration versus the measured concentration of the oxidation products of NO_x (i.e. the difference between measured concentrations of NO_y and NO_x) as a direct measure of the ozone production efficiency (i.e. the number of O_3 molecules formed for each NO_x oxidized.) The first paper that examined this correlation noted that nitric acid deposition will affect the observed slope between O_3 and NO_y-NO_x correlations. If nitric acid is removed from the atmosphere, then a measurement of NO_y-NO_x will underestimate the concentration of NO_x oxidation products, and consequently, the slope of O_3 versus NO_y-NO_x will overestimate the ozone production efficiency. During TexAQS 2006, ozone production was studied under a variety of meteorological conditions. High wind speeds were found to enhance nitric acid loss, which caused the O_3 versus NO_x oxidation products correlation slope to increase, often dramatically. The observed slopes varied from 2 to 16 in the coalesced plume from Houston, which was followed up to 170 km downwind. In many cases, the particularly high O_3 versus NO_y-NO_x slopes were primarily caused by particularly rapid loss of nitric acid from the transported plume, rather than from particularly high ozone production efficiency within the plume. Thus, when interpreting the correlation slope of O_3 versus NO_y-NO_x as a measure of the ozone production efficiency, it is critical to consider the effect of nitric acid loss.

Finding A3: **Emissions from the Houston Ship Channel play a major role in the formation of the highest 8-hour average ozone concentrations (and ozone design values) observed in the Houston area.**

Analysis: Sullivan et al.-U. Texas; Data: TCEQ.

The general flow patterns that give rise to the highest 8-hour-average ozone concentrations in the HGB area have been investigated through back-trajectory analysis. Monitoring sites to the south and west of downtown Houston have the highest ozone design values in the HGB area (defined as the 3-year average of the fourth-highest daily maximum 8-hour-average ozone concentration). In Figure A5 the blue dots highlight the four highest design values: 104 ppbv at Tom Bass CAMS 558, 103 ppbv at Bayland Park CAMS 53, 102 ppbv at West Houston CAMS 554, and 98 ppbv at Monroe CAMS 406. The green dot indicates the Aldine site north of the city; as recently as 2002 Aldine had the maximum design value in the area, but it declined from 108 and 107 ppbv in 2001 and 2002, respectively, to 92 and 88 ppbv in 2005 and 2006, respectively.
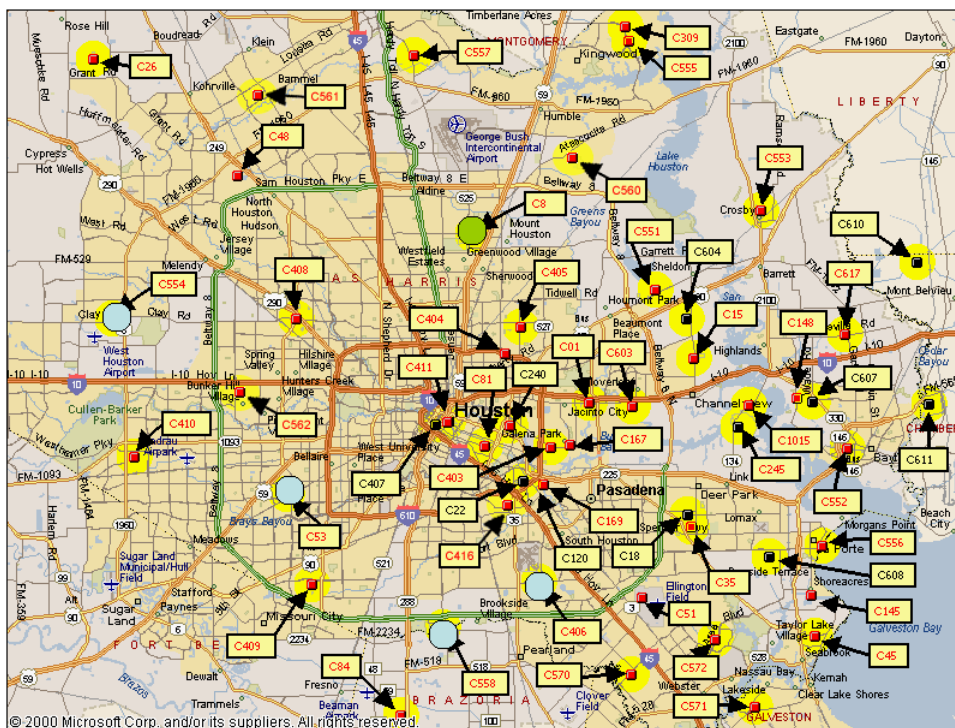
Figure A5. Harris County monitoring sites with the 4 highest 2006 design values marked in blue, and Aldine marked in green. In 2006, Bayland Park monitoring site (C53) had the area-wide highest regulatory design value of 104 ppbv.

A set of near-surface back-trajectory ensembles was generated for 8-hour ozone exceedance days at Bayland Park and Monroe, the two regulatory sites with the highest 2006 design values, and at Aldine to provide geographical contrast. The analysis covers the period from 2000 through 2006. On each day that a given monitor recorded an ozone exceedance, 7-hour back trajectories were calculated for all hours in which the measured ozone was above 85 ppbv. Hourly wind speed and direction data from 14 locations covering Harris County provided the data for the back-trajectory calculations. Wind speeds were adjusted to account for varying anemometer exposure among sites using factors provided by Bryan Lambeth of TCEQ, and further increased by 20 percent to account for generally higher speeds above each monitor's 10-meter anemometer tower. The data from all sites were pooled in an un-weighted average to provide one urban-scale wind speed and direction vector for each hour. Air parcel back trajectories were calculated in 10-minute time steps beginning from the start time of each appropriate hour. The resulting trajectory ensembles include 79 days at Aldine, 104 at Bayland Park, and 56 at Monroe. Since exceedance days generally had multiple hours with ozone concentrations over 85 ppbv, the number of trajectories totaled 252 at Aldine, 281 at Bayland Park, and 110 at Monroe. One composite trajectory was produced from each ensemble by averaging the x-y coordinates of all trajectories in the ensemble as a function of transport time. The resultant composites are expected to be biased short, but based on maps of the ensembles and their centerlines, this effect is judged to be minimal.

Figure A6 shows that each of these three composite back-trajectories reaches back to the HSC area earlier in the day, with approximately 7-hour transport times to the respective monitoring

sites. For Aldine the trajectories cluster to the south-southwest, for Bayland Park they wrap around the south side of central Houston, and for Monroe they cluster to the northeast. The consistency of the trajectories coming from the HSC provides strong support for the conclusion that emissions from the petrochemical industrial facilities in the HSC play a major role in the 8-hour ozone exceedances in the HGB area.
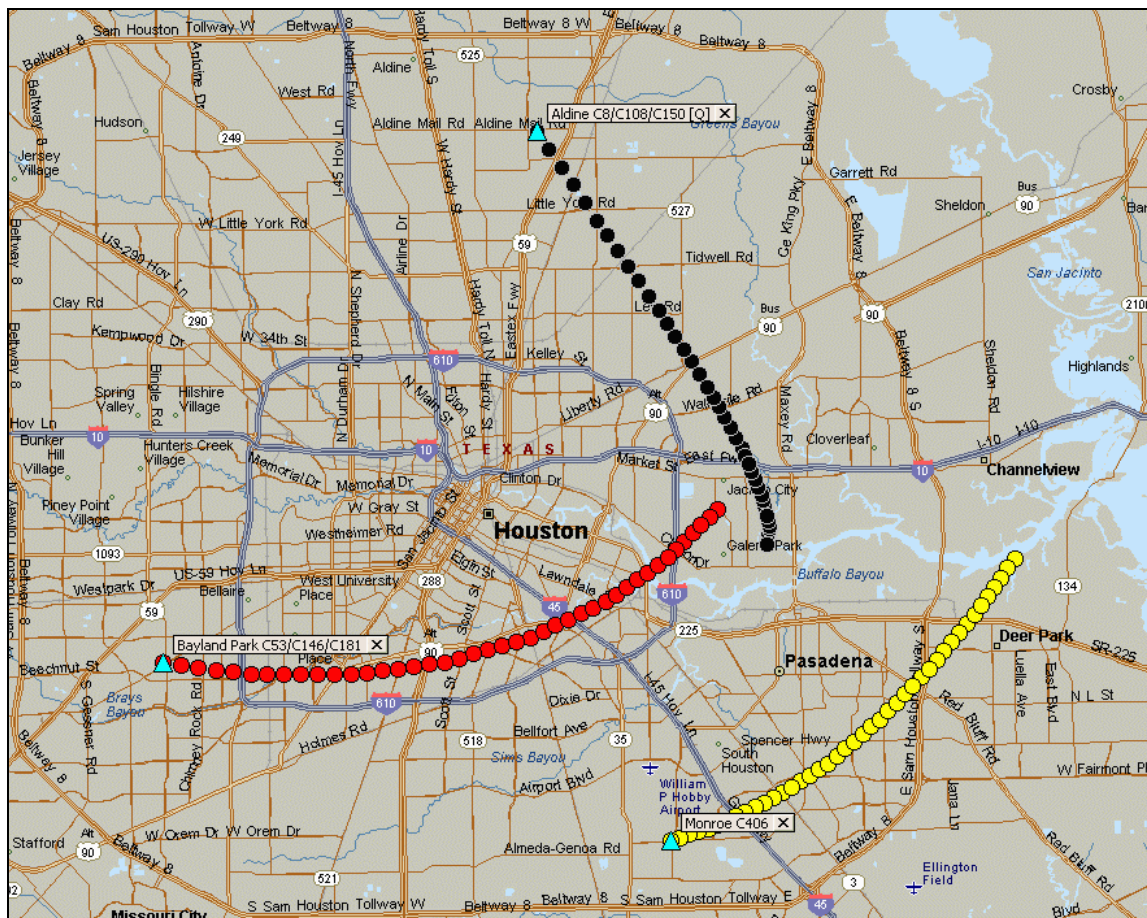

Figure A6. Composite 7-hour near-surface back trajectories for three Houston monitoring sites. All hours with $O_3 \geq 85$ ppbv on 8-hour exceedance days for the 2000-2006 period were included in the composite analysis.

Finding A4: **Observations during TexAQS 2006 showed that nitryl chloride ($ClNO_2$) is formed within the nocturnal boundary layer when NO_x emissions and marine influences are both present. Following sunrise, $ClNO_2$ photolyzes to yield chlorine atoms, which may lead to earlier and more rapid O_3 production in the Houston region.**

Analysis and Data: Roberts, Osthoff et al.-NOAA.

The first reported atmospheric observations of nitryl chloride, $ClNO_2$, were made aboard the *Ronald H Brown* during TexAQS 2006. Simultaneous measurements of $ClNO_2$, N_2O_5, and aerosol size and composition, show that $ClNO_2$ is a general product formed when N_2O_5 reacts on chloride-containing aerosol. N_2O_5 is produced from nighttime reactions of NO_2 with O_3. $ClNO_2$

is relatively stable at night, but photolyzes upon sunrise to yield Cl atoms and NO_2. These reactions link the nitrogen oxides to halogen activation.

An episode of high concentrations of $ClNO_2$ was observed on 2 September 2006 when the *RHB* was anchored in the Barbour's Cut inlet located off Galveston Bay near HSC. Figure A7 shows the measured N_2O_5 and $ClNO_2$ concentrations along with the Cl atom production rate calculated from the measured $ClNO_2$ and solar radiation flux. This Cl atom production reached almost 10^6 sec^{-1}, which is highly significant since Cl atoms react with VOC up to 100 times more rapidly than OH radicals. Figure A7 compares O_3 measured on 2 September with the average (± 1 standard deviation) of the O_3 levels observed during the other days that the RHB was in the Houston-Galveston area during TexAQS 2006. On 2 September the O_3 concentration increased more rapidly and reached a higher peak concentration compared to the average increase. This observation, while not definitive, is indicative of a potentially significant role for Cl atoms in O_3 production in polluted marine air.
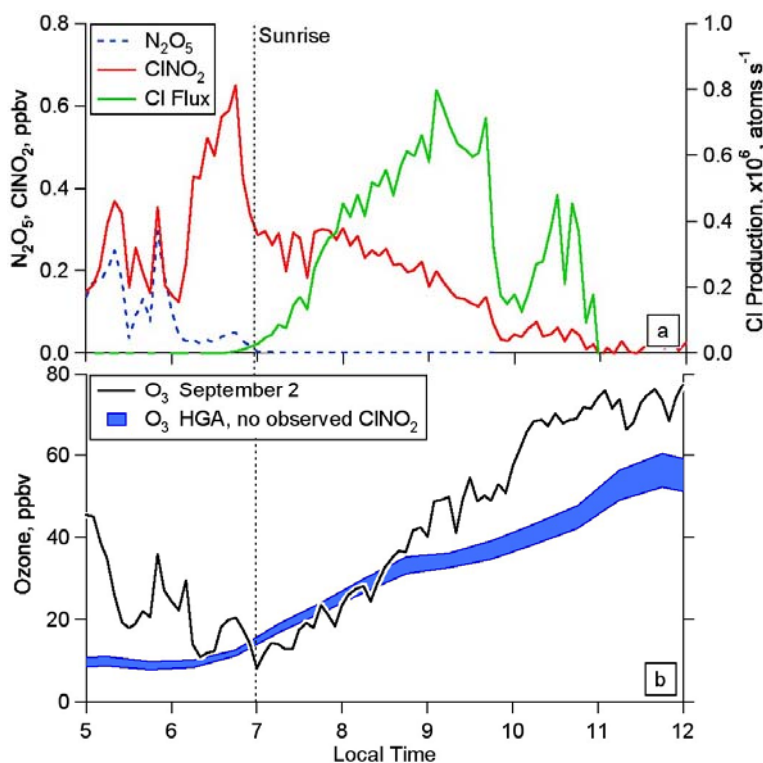

Figure A7. N_2O_5 and $ClNO_2$ measured on 2 September 2006, and calculated Cl atom production in the atmosphere (a); and the measured O_3 on 2 September, and the average from the other measurements in the Houston-Galveston area (b).

A preliminary box model study was conducted to investigate the $ClNO_2$ formation chemistry and to examine the effect of this Cl source on VOC-NO_x photochemistry. The model consisted of the Master Chemical Mechanism (Jenkin et al., 2003; Saunders et al., 2003), to which the N_2O_5 aerosol chemistry and $ClNO_2$ photochemistry were added. The model results show that a reaction efficiency of 25% for N_2O_5 on chloride-containing aerosol can account for the measurements in Figure A7. The Cl atoms produced upon sunrise led to a 2- to 3-fold increase in total peroxy radicals during the morning hours, which resulted in about a 15% higher O_3 concentration at the end of the afternoon production period. These results indicate the need to add this Cl atom source to current regional photochemical models.

KEY CITATIONS AND INFORMATION AND DATA SOURCES

Jenkin, M.E., S.M. Saunders, V. Wagner, and M.J. Pilling. 2003. Protocol for the development of the master chemical mechanism MCMv3 (Part B): Tropospheric degradation of aromatic volatile organic compounds. Atmospheric Chemistry and Physics, 3:181-193 (also Atmospheric Chemistry and Physics Discussions, 2:1905-1938 (2002)).

Ryerson, T.B., K.K. Perkins, M. Trainer, D.K. Nicks Jr., J.S. Holloway, J.A. Neuman, F. Flocke, A. Weinheimer, S.G. Donnelly, S. Schauffler, V. Stroud, E.L. Atlas, D.D. Parrish, R.W. Dissly, G.J. Frost, G. Hübler, R.O. Jakoubek, P.D. Goldan, W.C. Kuster, D.T. Sueper, A. Fried, B.P. Wert, R.J. Alvarez, R.M. Banta, L.S. Darby, C.J. Senff, and F.C. Fehsenfeld. 2006. Chemical and meteorological influences on extreme (>150 ppbv) ozone exceedances in the Houston metropolitan area. Draft Report to TCEQ, Contract No. 582-4-65613.

Saunders, S.M., M.E. Jenkin, R.G. Derwent, and M.J. Pilling. 2003. Protocol for the development of the master chemical mechanism MCMv3 (Part A): Tropospheric degradation of non-aromatic volatile organic compounds. Atmospheric Chemistry and Physics, 3:161-180 (also Atmospheric Chemistry and Physics Discussions, 2:1847-1903 (2002)).

Response to Question B

QUESTION B
How do the structure and dynamics of the planetary boundary layer and lower troposphere affect the ozone and aerosol concentrations in Houston, Dallas, and East Texas?

BACKGROUND
Meteorology in the boundary layer affects ozone levels through regulation of near-source concentrations (wind speed, mixing height), background levels (transport winds), photochemistry (solar radiation, temperature), and air parcel history (local winds).

FINDINGS

Finding B1: **Boundary layer structure and mixing height near and over Galveston Bay and the eastern Houston ship channel area are spatially complex and variable from day to day. Vertical mixing profiles often do not fit simple models or conceptual profiles. High concentrations of pollutants are sometimes found above the boundary layer.**

Analysis: Nielsen-Gammon-Texas A&M; Senff, Darby, Banta, Angevine, Tucker, White-NOAA; Breitenbach, Dornblaser, Lambeth-TCEQ; Morris-Valparaiso U.; Rappenglück, Perna-U. Houston. Data: Nielsen-Gammon-Texas A&M; Senff, Tucker, White, Darby, Angevine, Banta-NOAA; Morris-Valparaiso U.; Rappenglück, Perna-U. Houston.

Mixing depth (synonymous and used interchangeably here with the term "mixing height") exerts an important control on the concentrations of pollutants including ozone and its precursors. For example, when pollutants are released into a shallow mixed layer, high concentrations of emissions can accumulate; this was observed using airborne ozone lidar during TexAQS 2000 (Banta et al., 2005). On the other hand, deep mixing can significantly dilute pollutants.

Well away from the coastal region, the mixed layer was relatively uniform over broad spatial areas. Well inland, peak afternoon mixing heights were generally between 1½ and 2½ km, but could reach as high as 4 km. The mixed-layer heights generally grew into late afternoon, often leveling off above 2 km. Over the Gulf of Mexico, shipboard lidar and platform radar wind-profiler measurements indicated a relatively constant maritime mixed-layer depth of 600 m, with weak positive heat fluxes at the surface, both day and night.

The Houston urban area and major industrial sources are located in the coastal region, where the mixing depth is highly variable in space and time, as determined by shipboard lidar and land-based sensors. Reasons for this variability include land-sea contrast and the sea-breeze cycle, land-use differences, and along-shore coastal irregularities, the major one in this area being Galveston Bay. The meteorology of the previous day and night is another influence on mixed-layer variability, but that effect is much more difficult to generalize. The coastal zone of southeast Texas is a transition region between the maritime boundary layer, with the relatively constant 600-m mixed-layer depths over the Gulf of Mexico, and the deeper daytime mixed layers inland. The coastal influence on Houston mixed-layer heights can be seen in their diurnal behavior. In contrast to the inland sites, where the mixed-layer height generally increases until late afternoon, in the coastal zone the mixing height was observed to reach its maximum earlier

in the day (as early as late morning for sites near the shore) and then to decrease, as the sea-breeze front brought in cooler marine air through the afternoon.

Land-cover and land-use differences include the cross-region gradients in soil moisture and urban heat island processes. Climatologies and vegetation indicate moister conditions to the east of Houston and nearer to the coast, and drier conditions to the west and inland. Airborne lidar flights revealed a significantly deeper mixed layer over the arid regions to the west, consistent with mixing-depth data provided by the profiler array, which indicated increases in peak afternoon mixing depths with distance from the coast.

Urban heat island. The issue of the urban heat island (UHI) is also complicated in the coastal zone by the sea breeze. The effects of the sea breeze can be appreciated by contrasting Houston with an inland urban area, Dallas. Both Dallas and Houston have comprehensive networks of surface meteorology and chemistry sensors. The similarities of the networks and lack of terrain in Dallas and Houston allow for the comparison of their UHIs. The strength of the UHI is measured by taking the temperature difference from representative urban and rural sites. The Dallas UHI, unperturbed by thermal flows driven by land/sea temperature differences, was a well-defined phenomenon during the summers of 2000-2006 (Fig. B1a). Including all weather conditions, the average nighttime $T_{urban} - T_{rural}$ temperature difference was between 1.5º and 2.0º C and the average daytime difference was ~ 1.0º C. Analysis of Houston temperature data, however, revealed a different picture due to the Bay and Gulf breezes (Fig. B1b). Although the Houston UHI was a distinct phenomenon, even when including all weather conditions, the Bay or Gulf breezes modified the Houston UHI by cooling the city. Average nighttime $T_{urban} - T_{rural}$ temperature differences in Houston were between 1.75º and 2.75º C. However, during the day, the rural areas to the north and west of the city were often warmer than the downtown area during afternoon hours as a result of the sea breeze. Averaging the Houston $T_{urban} - T_{rural}$ temperature differences over the summers of 2000-2006 indicated a very small urban-rural temperature difference between 1400 and 1600 local standard time (LST), in contrast to Dallas, which had a $T_{urban} - T_{rural}$ temperature difference of ~1° C. In some individual years, such as 2000, 2003, 2005 and 2006, the Houston urban areas were actually cooler than the rural areas, on average, in the mid-afternoon. These years had more Bay-breeze/Gulf-breeze activity to cool the urban area.
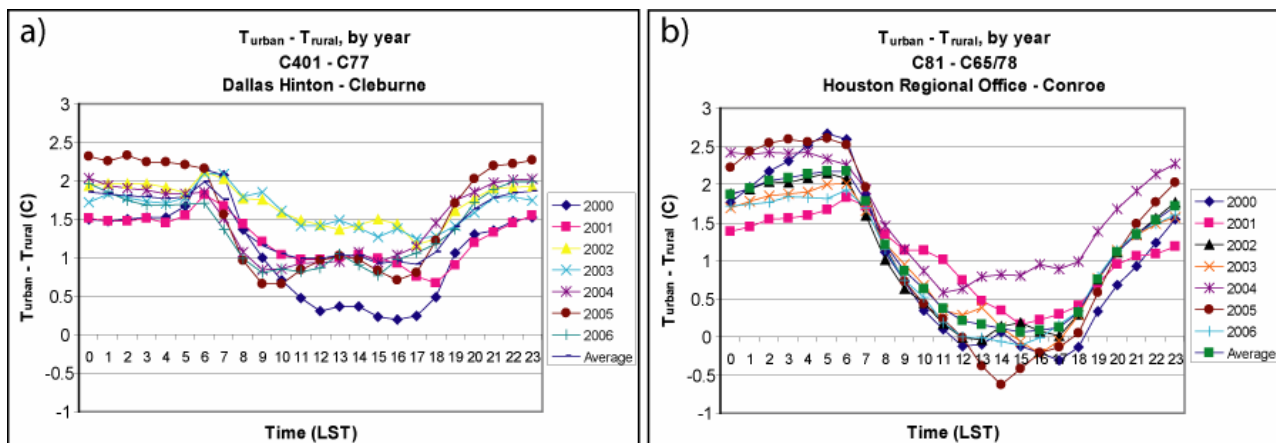

Figure B1. $T_{urban} - T_{rural}$ for each of the 7 summers analyzed, and the average for all summers. "Summer" includes all days from 1 June– 30 September. a) Dallas. b) Houston.

The effects of along-shore irregularity combined with the other coastal effects can be seen in the distributions of daytime mixed-layer heights. Midday mixed-layer heights measured at an inland site at Moody, Texas (near Waco) were relatively consistent from day to day, thus exhibiting a rather narrow distribution with a mean of ~1.5 km. Near the shore of Galveston Bay at LaPorte, a much broader distribution of mixed-layer heights, including high frequencies below 1 km, indicates the much more complex influences on mixing depth in the coastal zone. Spatial variability of mixing depth was evident in airborne lidar flights, with shallow mixing layers over Galveston Bay and deeper mixing layer depths over the Houston urban area as a result of heat-island effects. Variations in mixing depth at nearby locations often reflected advection of high or low mixing layer depths downwind of the urban area or Galveston Bay, for example.

Sounding observations from the University of Houston (UH) campus (e.g., Fig. B2) and from the *Ronald H. Brown* (when stationed in Galveston Bay) often showed a very complex vertical ozone structure, with no well-marked transition between the local boundary layer and the air above; this was consistent with shipboard Differential Absorption Lidar (DIAL) and Doppler lidar profiles. This complexity is likely to be underrepresented in numerical models.
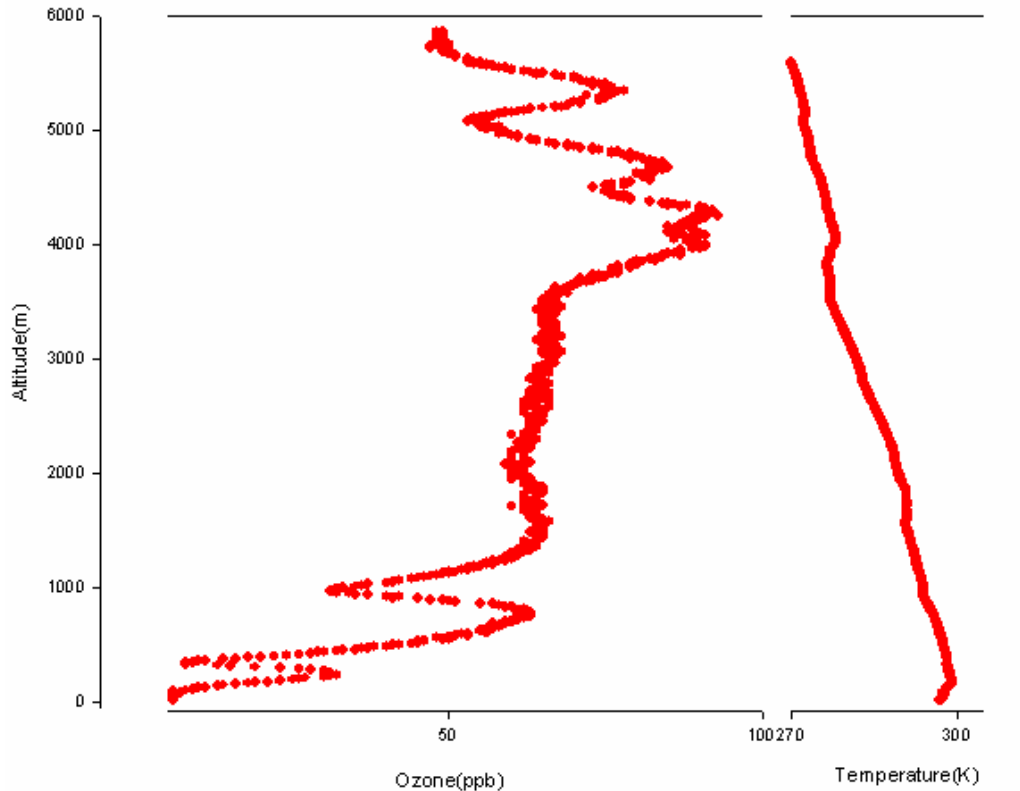

Figure B2. Ozonesonde profiles of ozone (left, 0-100 ppb) and temperature (right, 270-300 K) from the surface to 6,000 m above ground level (AGL), for a 1200 UTC ascent on 31 August 2006, released from the University of Houston campus. The minimum in the ozone profile near 1,000 m AGL was associated with a layer of high relative humidity and clouds.

Spatial variability of mixing height during TexAQS 2000 and TexAQS 2006. Multi-sensor spatial analyses of mixing heights, using data from the TexAQS field campaigns, illustrate the effects of these diverse influences, often showing mixing height varying by a factor of two or more across

Houston. An example of large spatial variability in mixing heights is shown in Figure B3. A combination of fixed-location ground-based sensors and mobile airborne sensors is essential for determining the spatial and temporal mixing height variability across the Houston metropolitan area.
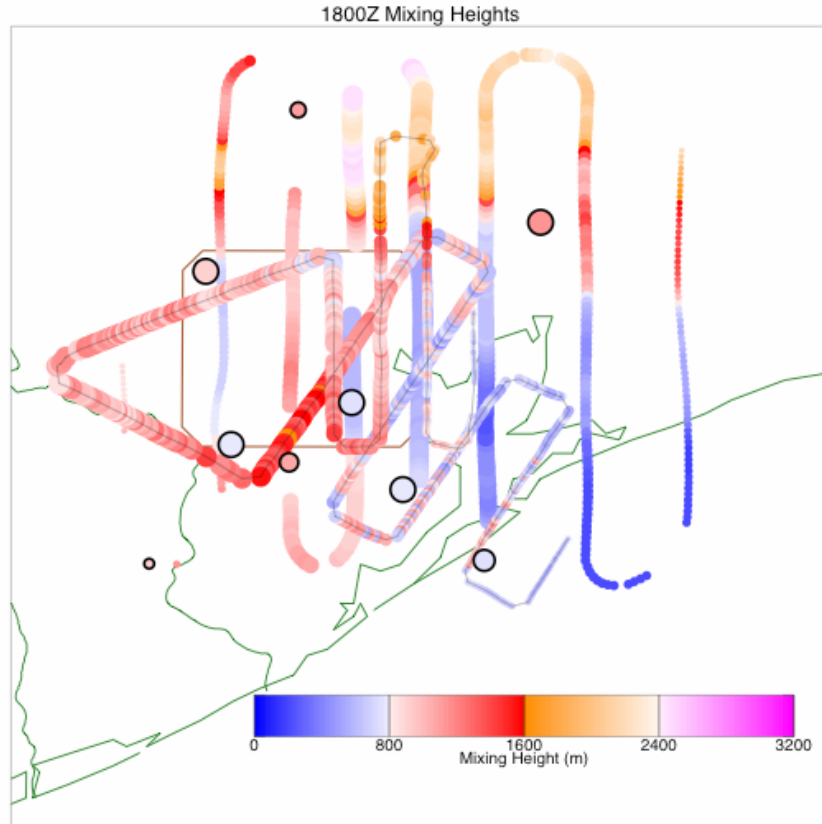

Figure B3. Mixing height measurements in early afternoon in Houston, 1 September 2000. Colors indicate observed or estimated mixing heights. Shown are mixing heights from airborne instruments (colored lines) and mixing heights from profilers, soundings, and aircraft ascents and descents (circles). Note the large spatial variability north and east of Houston (Nielsen-Gammon et al., 2007).

Mixing height and O_3 concentrations. Attempts to determine general relationships between daytime mixing heights and ozone concentrations have been mostly fruitless. The expected relationship is that higher concentrations would be associated with lower mixed-layer heights. Northerly or northeasterly large-scale flow, however, is often associated with higher concentrations from distant continental sources, and continental air masses often have higher mixing heights. Conversely, and also opposing the expected mixing-height/ozone relationship, out over Galveston Bay, large-scale southerly flow off the Gulf of Mexico was observed to be associated with more clean and moist air but shallower mixed layers. On the other hand, when pollutants are emitted into the shallow mixed layer of Galveston Bay and carried over the Bay, pollutant concentrations have been shown to remain very high – in agreement with expectation. In another scenario, aircraft sampling of urban or other plumes some distance downwind of the sources finds well mixed regions outside and inside of the plumes where the ozone is low and high, respectively, on the same day, but the mixing heights are essentially the same, yielding no

systematic relationship. All of these effects confound the search for general relationships, producing seemingly random or otherwise meaningless scatter plots of O_3 and mixing heights

Nighttime mixing. Nighttime boundary layer structure in the Houston-Galveston area is less easy to characterize. UH tethersonde and ozonesonde data indicate that nighttime depletion can occur at elevations as high as 200 m, implying that the top of the urban boundary layer tends to be ~200 m or less at night. Thus, nighttime mixing and transport effects in the Houston-Galveston area remain an area of longer-term research needs.

Layering of pollutants. O_3 and aerosol pollutants in the Houston-Galveston area were often confined to the mixed layer (Fig. B4a,b). But occasionally significant concentrations of pollutants were found above the mixed-layer height (Fig. B4c,d). Pollutants, especially aerosol, sometimes exhibited a complex layered structure, in which the origin of pollution in the individual layers was difficult to determine (Fig. B2). In the analysis performed to date, high concentrations of pollutants found in deep layers (more than a few hundred meters thick) above the mixed layer (Fig. B4d) were found to originate in distant regions outside of Texas to the northeast or east.
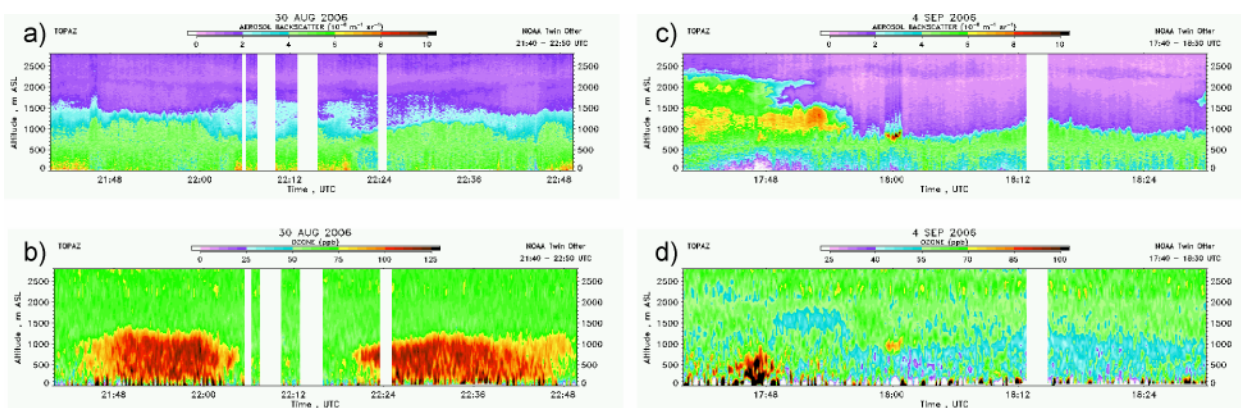

Figure B4. Airborne lidar time-height cross sections of aerosol backscatter (top, in units of 10^{-8} m^{-1} sr^{-1}) and ozone concentrations (bottom, in ppb) for a), b) 30 August 2006, when high ozone and aerosol concentrations were confined to the mixed layer, and c), d) 4 September 2006, when the mixed layer was indicated by higher aerosol concentrations, but the high ozone was above the boundary layer.

Finding B2: **Complex coastal winds, resulting from weak larger-scale winds over the area, occurred during many, but not all, ozone exceedance days in the Houston-Galveston-Brazoria nonattainment area. Almost no high-ozone days during TexAQS 2000 resembled any high ozone days from TexAQS 2006, but collectively the 2000 and 2006 field intensives sampled the full range of meteorological conditions associated with high ozone events.**

Analysis: Banta-NOAA; Nielsen-Gammon-Texas A&M; Bryan Lambeth-TCEQ; Gary Morris-Valparaiso U.; Perna, Rappenglück-U. Houston; Senff, Darby, Angevine-NOAA; Breitenbach, Dornblaser-TCEQ. Data: Nielsen-Gammon-Texas A&M; Senff, Tucker, White, Darby, Angevine, Banta-NOAA; Morris- Valparaiso U.; Rappenglück, Perna-U. Houston.

High ozone concentrations were most often associated with light winds and daytime sea-breeze reversals (often leading to stagnation occurrences; (Darby, 2005]), but some days with stronger

winds also had O_3 exceedances during both 2000 and 2006. The interplay between local wind patterns and large-scale transport produced a wide variety of meteorological scenarios for ozone events in the Houston area. Broadly speaking, when mean winds (here measured using 24-hr-mean resultant winds from nearshore buoy 42035) were light, recirculation was likely, whereas when mean winds were strong, the wind direction tended to be steady throughout the day. The direction of the mean wind determines when stagnation will occur if winds are light enough, and also determines the direction of transport of the Houston ozone plume.

By plotting the west-east and south-north components of the mean winds on a scatter diagram, the range of meteorological conditions during an ozone episode or an extended period may be determined. Such a diagram is shown in Fig. B5 for the late summer ozone season in Houston. During TexAQS 2000, most high-ozone events occurred when the mean wind was from the southeast (regime 1) or southwest (regime 2), but no light northeast wind events occurred at all. In contrast, during TexAQS 2006, wind conditions were much more representative of climatology, and several high-ozone events occurred under light northeast winds. Those days in which the wind was light from the southeast during 2006 tended to feature widespread clouds and precipitation. Thus, almost no high-ozone days during TexAQS 2000 resembled any high ozone days from TexAQS 2006, but collectively the 2000 and 2006 field intensives sampled the full range of meteorological conditions associated with high ozone events.
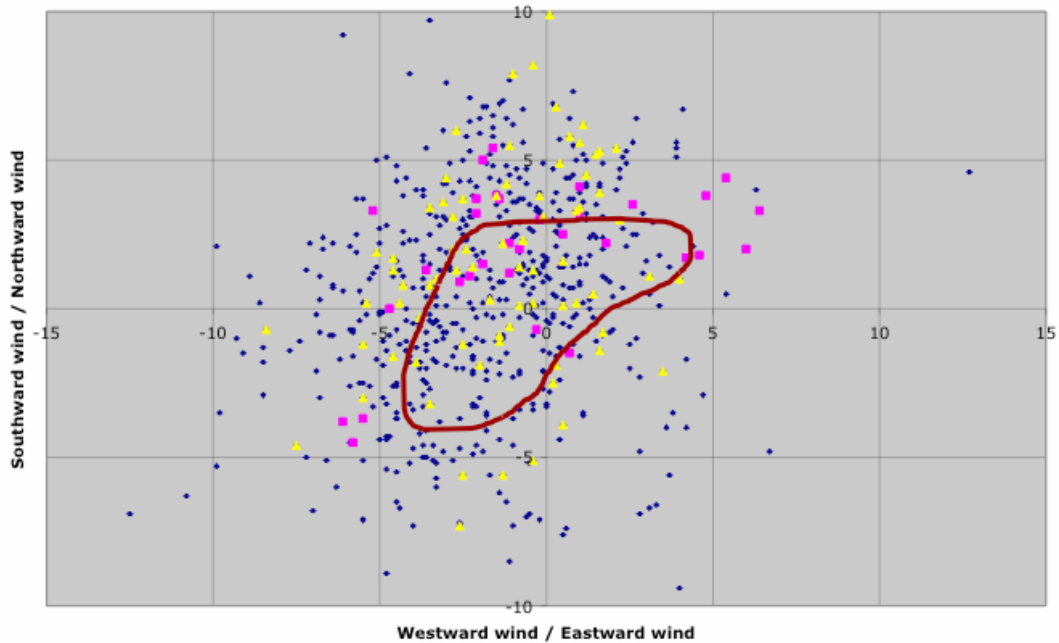

Figure B5. Scatter diagram of daily mean winds at buoy 42035, near Houston, during the period 1 August – 15 October, 1998-2006. Grid lines are every 5 m/s; a dot in the upper left quadrant implies winds from the southeast. The wind regimes most conducive to high 1-hr ozone in the Houston area are circled. Days during TexAQS 2000 are indicated with pink squares, and days during TexAQS 2006 are indicated with yellow triangles; blue dots represent data from all other years.

Peak ozone and wind speed. The overall relationship between peak O_3 concentrations and wind speed is shown in Fig. B6, which indicates the expected strong negative correlation between

maximum in-network ozone enhancements (or "add-on") above background and wind speed in the Houston area (see red data and line on Fig. B6). The 10-hr trajectory displacement is a surrogate for mean wind speed. Stronger winds (larger displacements) produce greater dilution of the pollution emissions, and thus lower concentrations of pollutants. Analysis of ground-based measurements over several years indicates a threshold effect in Houston (Nielsen-Gammon et al., 2005). Large local add-ons are typically present when large-scale winds are weaker than about 3 m s^{-1}, light enough to allow recirculation, and the add-on decreases rapidly for wind speeds larger than 3 m s^{-1}. This effect is evident especially in the airborne data in Fig. B6. A steady 3 m s^{-1} wind would produce a 10-hr displacement of 108 km, and below this value is where peak O_3 add-on concentrations become very large.
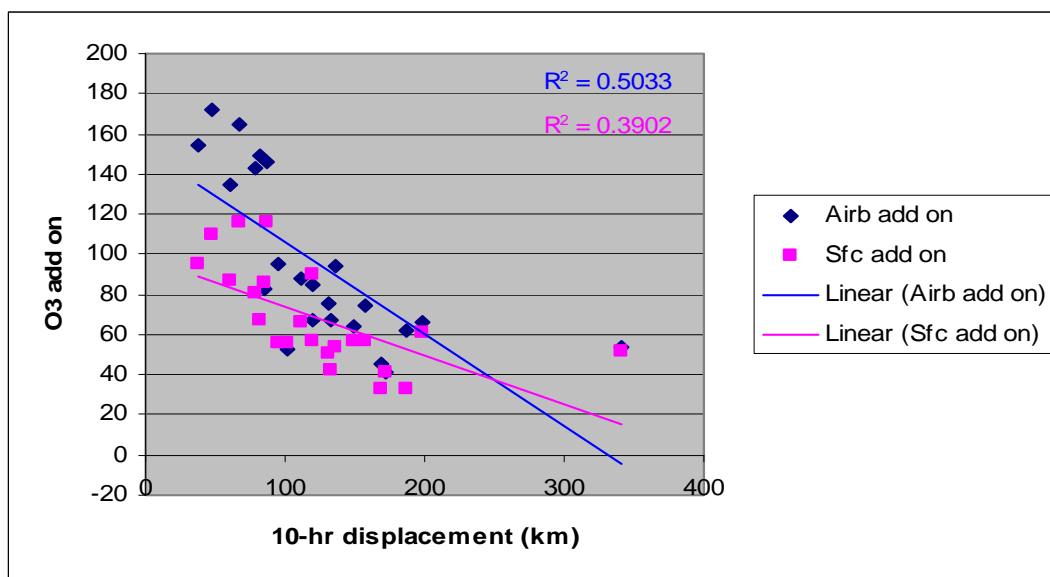

Figure B6. Houston ozone enhancement (peak ozone values in urban plume minus background values) plotted vs. displacement of 10-hr trajectories, representing the vector-mean wind for the period, starting at Houston at 8:00 a.m. CST. Red symbols indicate data from surface measurement network (1-hr average), and blue symbols indicate data from airborne ozone lidar and WP-3D. "Add on" represents peak ozone concentrations observed minus background concentrations. Lines are linear best-fit lines.

The blue points in Fig. B6 show the airborne-lidar-determined peak ozone concentrations vs. 10-hr trajectory displacements. The concentrations again decrease with increasing speed, but are everywhere larger than the surface measurements. Reasons for this discrepancy include that the airborne data represent conditions aloft not subject to surface processes such as removal, that the airborne lidar data represent averaging over shorter intervals, and that on days with stronger winds, plumes are narrower and harder to sample by fixed networks and also high concentrations may be blown out of the surface network before being sampled.

The last issue was expected to be a greater source of discrepancy between airborne and ground-network sampling, because the aircraft samples the pollution plume wherever it is, even though the maximum values may be occurring beyond the surface measurement network before the photochemical reactions are complete. Indeed, individual days have been identified with large discrepancies. However, Fig. B6 shows that, in general, light winds (small 10-hr displacements)

were associated with large O_3 enhancements by the Houston area, and stronger wind speeds, with smaller enhancements. Several cases of stronger-wind days have been identified when the total O_3 concentrations (background plus add-on) exceeded the 1-hr standard. Those days, most often associated with high background values, are being studied further to determine all processes responsible for the high concentrations.

On such stronger-wind days with high background levels, high pollutant concentrations were generally being advected into the Houston area under easterly or northerly continental flow. Airborne ozone lidar flights sampling air masses entering Texas from the east on three different days found concentrations of 50, 80, and 90 ppb in the inflow air. Another typical scenario is for post-cold-frontal northerly flow to be associated with high pollutant concentrations. When the offshore winds are weak enough, sea-breeze stagnation occurs, and when they are stronger, they are associated with high background. During 2006 all ozone episodes in the month of September occurred in a post-frontal environment. For example, a four-day sequence of ozonesonde profiles (Fig. B7) showed an increase in background ozone within the free troposphere up to 5000 m AGL, corresponding to transport from the continental United States after the passage of the front.
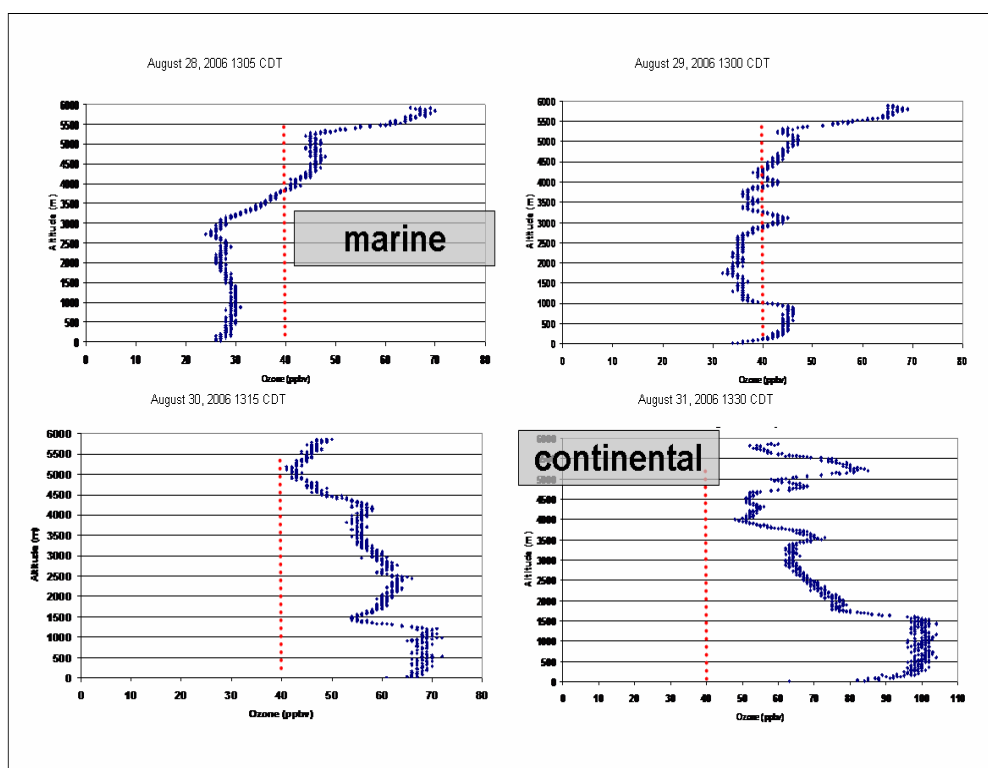

Figure B7. Ozonesonde profiles at ~1200 CST on 28, 29, 30, and 31 August 2006. Passage of cold front occurred on 29 August 2006. Before the passage of the front, marine air masses with O_3 concentrations of 30 ppb had concentrations even lower than the EPA boundary-condition benchmark values (40 ppb, red dotted vertical line). In subsequent days, background ozone increased throughout the troposphere up to 5000 m AGL due to the shift in wind direction after the frontal passage.

Many of these episodes were associated with strong elevated inversions. Higher afternoon ozone peaks occurred where there was an extremely dry air mass aloft, although it was not always associated with the strongest inversion observed. The air masses aloft with the strongest winds

(greater than 8 m s^{-1}) and driest air did not have extremely high ozone values associated with them, mainly because these episodes occurred right after a frontal passage where the northerly flow was strong enough to keep ozone peaks in check.

Thus, the Houston-Galveston-Brazoria area produces a tremendous amount of ozone. Even under relatively strong wind conditions, the result can be high pollutant concentrations, although the *very* highest concentrations are produced on days with weak-wind or sea-breeze-reversal conditions. Even with the 8-hr standard, most, but not all, 8-hr exceedances during the TexAQS II field intensive (and other 2005-6 episodes) occurred when winds were light enough to allow stagnation/recirculation.

Finding B3: After sea breeze days, the Houston plume was broadly dispersed at night through the formation of low-level jets.

Analysis: Nielsen-Gammon-Texas A&M; Banta, Senff, Ryerson, Darby, Tucker, White-NOAA; Lambeth-TCEQ. Data: Nielsen-Gammon-Texas A&M; Senff, Tucker, White, Darby, Angevine-NOAA.

Trajectory analysis of nighttime transport of the Houston plume, based on the wind profiler network, indicates that the Houston plume sometimes remains a coherent entity, subject to little wind shear (see Fig. B8a,b), but at other times is dispersed over a broad portion of Texas by strongly sheared winds (Fig. B8c,d). Broad dispersal is favored after sea breeze days when nighttime decoupling allows a strong low-level jet to form from the remains of the sea breeze circulation. The wind speed is strongest at 300-500 m, decreasing above and below.
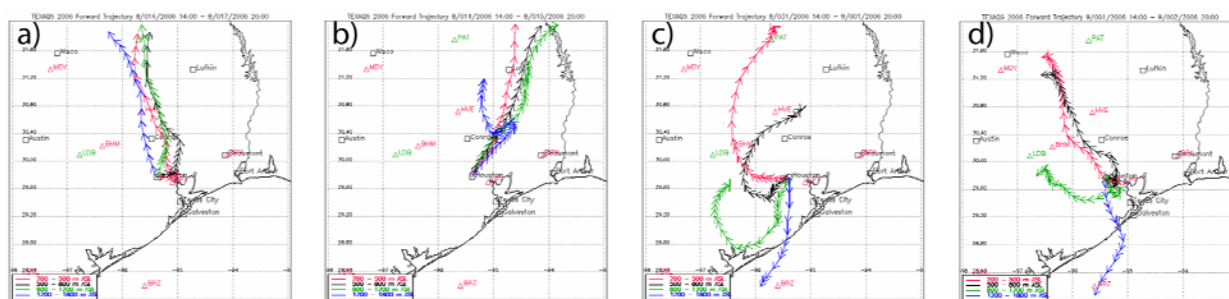

Figure B8. Overnight trajectories for four elevations above ground level, based on hourly radar wind profiler measurements, for the nights of a) 16-17 August, b) 14-15 August, c) 31 August-1 September, and d) 1-2 September. Red trajectories were averaged over the vertical interval from 200 to 500 m;, black, from 500-800 m; green, from 800-1200 m;, and blue, from 1200-1800 m. Lower trajectories or those ending up to the north of their origin are not likely to be contaminated by signal from migrating birds.

An inland surge of winds found in the 200-600 m layer at night has been called the sea-breeze low-level jet. The essential characteristics of this jet are shown in a sequence of images from an MM5 model forecast from 8 June 2006 (Fig. B9). In the first panel, at 1500 local standard time (LST), the winds are light and onshore. This wind pattern is particularly conducive to the formation of a sea-breeze low-level jet. Along the coast, a sea breeze has developed, and onshore wind speeds are locally 4-7 m s^{-1}. Around sunset, in the second panel, the sea breeze wind maximum has moved inland and has increased in speed to over 9 m s^{-1} in places. The LLJ occurs in a broad area along the coast, rather than a narrow along-wind band. In the lower left panel, at 2100 LST, the sea-breeze low-level jet is about 200 km inland and has continued to

increase in intensity, with peak wind speeds over 12 m s^{-1}. The leading edge of the jet is very sharp, implying a sudden increase in wind speed, whereas along the trailing edge the decline in wind speed is gradual. Note also that the wind direction, initially southeasterly, has veered to southerly under the influence of the Coriolis force. This veering continues through the night, and the wind direction is southwesterly by 0000 LST (final panel). By this time, with the winds no longer blowing toward lower pressure, the wind speed within the jet has begun to decrease. A similar wind evolution is simulated whenever winds are light and onshore during the day and precipitation is sparse or absent. Sea-breeze low-level jet passages are also evident in wind profiler observations from 2005-6.
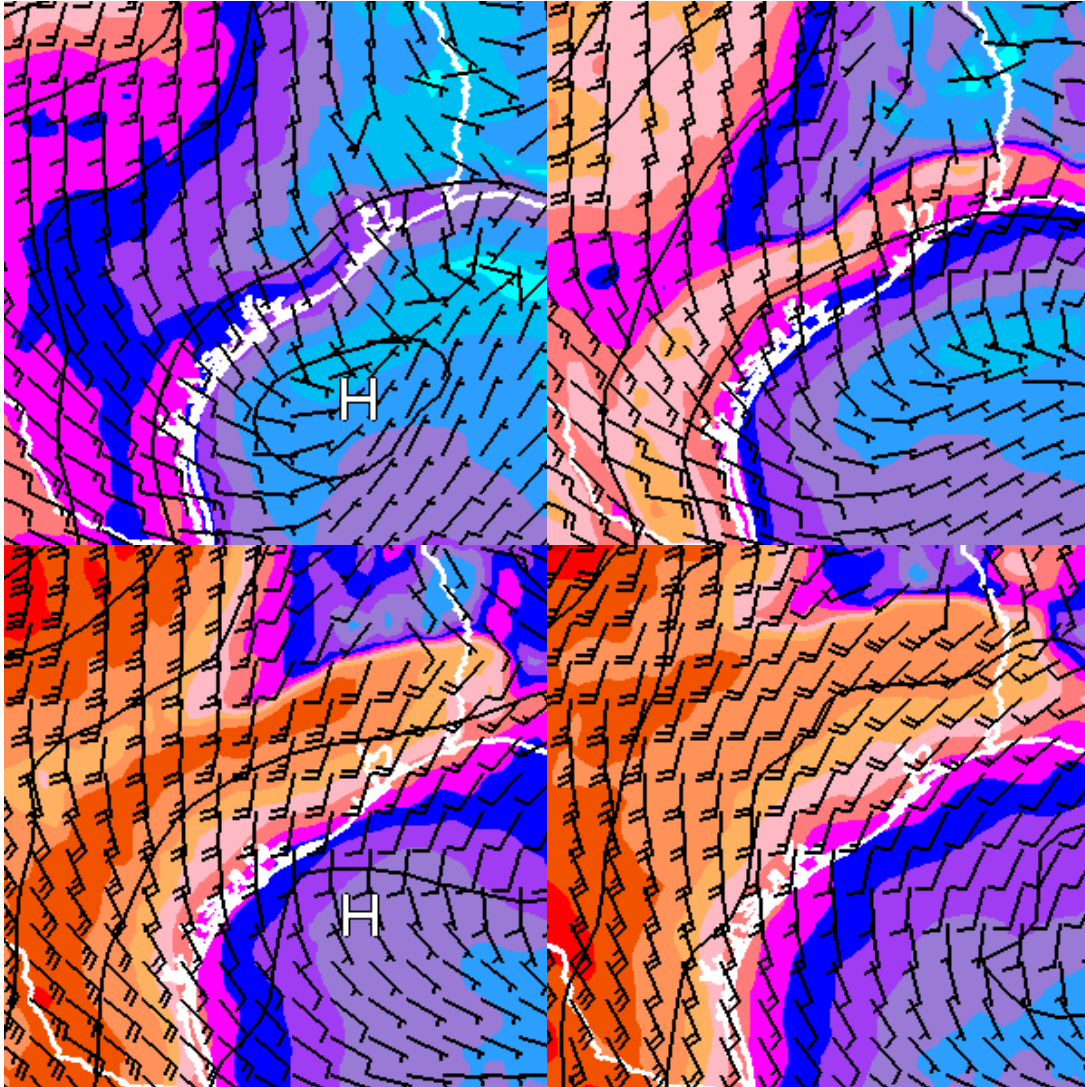

Figure B9. Forecasted 300 m winds (indicated with barbs and isotach shading) and pressure (black isobars), 1500 LST 8 June 2006 (upper left), 1800 LST (upper right), 2100 LST (lower left) and 0000 LST, 9 June (lower right). The sea-breeze low-level jet is the band of strong wind speeds originating along the coast at 1500 CST and accelerating inland through the evening.

A dramatic example of nocturnal transport has been documented for 8 September 2006, when high daytime concentrations of ozone that had accumulated over Houston during the previous day traveled to Dallas overnight, contributing to enhanced concentrations in Dallas the next day.

This episode is discussed in more detail in the Response to Question H. Other examples of overnight transport of the Houston plume were identified in data from the instrumented tower at Moody, Texas (near Waco) and in the Tyler-Longview areas of northeast Texas. In a further example from 1 September, the Houston plume moved to the south of the city overnight, and then was brought back in the sea breeze the next day to produce enhanced O_3 concentrations in the western suburbs. Calculations of the O_3 flux from Houston indicate that if these concentrations were spread over an area 100 by 100 miles by 2 km deep, it would raise the concentrations by 10 ppb over the entire volume. These calculations are further discussed in the Response to Question G.

Finding B4: **The Dallas ozone plume can extend well beyond the monitoring network.**

Analysis: Senff, Darby, Banta-NOAA; Breitenbach, Lambeth-TCEQ. Data: Senff, Darby, Banta-NOAA; Lambeth-TCEQ.

An airborne O_3 lidar flight, sampling the DFW plume on 13 September in northerly flow of ~ 5 m s^{-1}, found peak O_3 values of 90-95 ppb against a background of ~ 65 ppb (Fig. B10), representing an enhancement of 25-30 ppb, in agreement with previous estimates. These high O_3 values were observed in a distinct urban plume extending past the southernmost cross-wind flight leg at a distance of 85 km downwind of DFW, indicating that the plume extended much farther downwind than this. It seems likely that the highest ozone occurs beyond the margin of the monitoring network on such occasions, as was previously noted for the Houston network. Under southerly large-scale flow, recently installed ozone sensors in southern Oklahoma also indicated elevated ozone concentrations resulting from the DFW plume, at a distance of at least 240 km (near Lawton, Oklahoma).
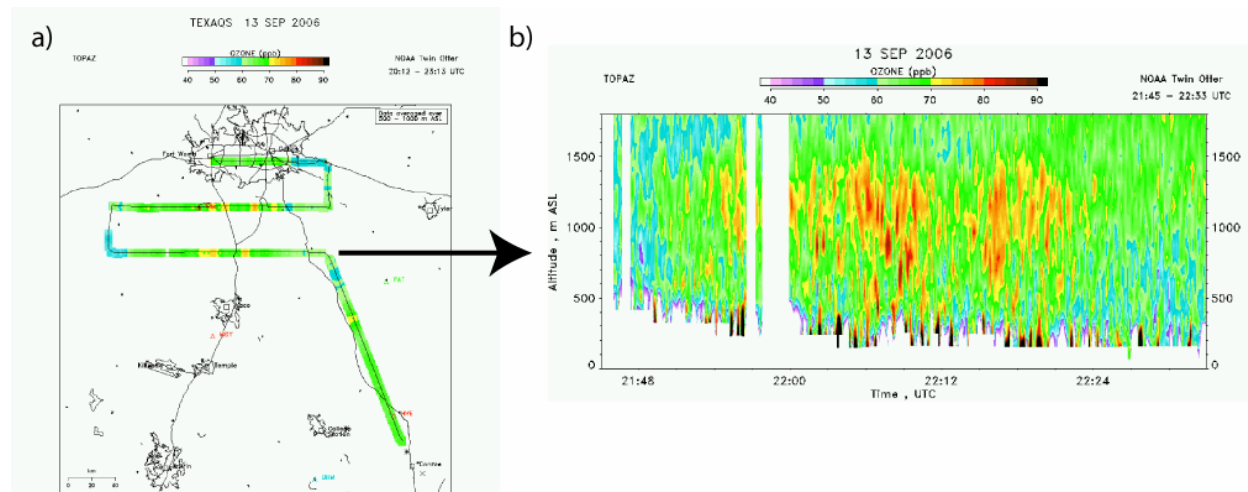
Figure B10. a) Flight track of the Twin Otter airborne ozone lidar, showing color-coded ozone concentrations averaged between 500 and 1000 m MSL (ozone scale from 50 to 100 ppb), for 13 September, a day with stiff north-northeasterly flow. b) Vertical time-height cross section of ozone [ppb, same scale as in a), vertical scale from 0 to 1800 m MSL, horizontal scale from 2145 to 2230 UTC] for southernmost cross-wind leg, showing plume of higher ozone from Dallas-Ft. Worth.

KEY CITATIONS AND INFORMATION AND DATA SOURCES

Banta, R.M., C.J. Senff, T.B. Ryerson, J. Nielsen-Gammon, L.S. Darby, R.J. Alvarez, S.P. Sandberg, E.J. Williams, and M. Trainer. 2005. A bad air day in Houston. Bull. Amer. Meteor. Soc., 86:657-669.

Darby, L.S. 2005. Cluster analysis of surface winds in Houston, Texas and the impact of wind patterns on ozone. J. Appl. Meteor. 44:1788-1806.

Nielsen-Gammon, J.W., J. Tobin, and A. McNeel. 2005. A Conceptual Model for Eight-Hour Ozone Exceedances in Houston, Texas. Part II: Eight-Hour Ozone Exceedances in the Houston-Galveston Metropolitan Area. HARC/TERC/TCEQ Report, 79 pp. http://www.harc.edu/Projects/AirQuality/Projects/Projects/H012.2004.8HRA

Nielsen-Gammon, J.W., C.L. Powell, M.J. Mahoney, W.M. Angevine, C. Senff, A. White, C. Berkowitz, C. Doran, and K. Knupp. 2007. Multisensor estimation of mixing heights over a coastal city. J. Appl. Meteor. Clim., in press.

Response to Question C

QUESTION C
Are highly reactive VOC and NO$_x$ emissions and resulting ambient concentrations still at the same levels in Houston as they were in 2000?
How have they changed spatially and temporally? Are there specific locations where particularly large quantities of HRVOC are still being emitted?
Are those emissions continuous or episodic?
How well do the reported emissions inventories explain the observed concentrations of VOC and NO$_x$?

BACKGROUND
Questions C, D, and E all deal with emissions. Here, Question C specifically addresses highly reactive VOC and co-located NO$_x$ emissions in the Houston area. Question D addresses all other ozone and aerosol precursor emissions, biogenic as well as anthropogenic, that are included in emission inventories. Question E addresses evidence for additional, unrecognized sources of precursor emissions.

FINDINGS

Finding C1: **There are indications that ethene (the lightest HRVOC) emissions from industrial sources in the Houston area decreased by 40 (±20)%, i.e., by a factor of between 1.25 and 2.5, between 2000 and 2006.**

Comparison of ethene/NO$_x$ emission ratios measured during TexAQS 2000, TexAQS 2006, and one 2002 aircraft flight

Analysis: de Gouw et al.-NOAA. Data: de Gouw, Ryerson et al.-NOAA; Atlas et al.–U. Miami

The emissions of ethene from numerous point sources were individually characterized using the Electra and WP-3D aircraft measurements made in TexAQS 2000, TexAQS 2006, and on one flight in the southeast Texas region in April 2002. Determination of ethene/NOx emission ratios was most straightforward for the isolated petrochemical plants to the south of Houston. These facilities were extensively investigated in 2000 and 2006, and an additional research flight was made in 2002 when the WP-3D transited to a study in California. Figure C1 shows the flight track in 2002 (Ryerson et al., 2003) and an example of a flight made in 2006, along with results of the NO$_x$ and ethene measurements. Apart from Texas City, there appear to be changes in the ethene/NO$_x$ emission ratios. The results are summarized in Table C1, and show decreases in the ratio by a factor of 3-7 for Sweeny, Freeport, and Chocolate Bayou. Further research is necessary to determine if the lower emission ratios were systematic, or only happened to be lower on the 29 September flight; preliminary analyses have shown that emission ratios are variable within factors of 2-3 between different flights. In addition, the high-time-resolution ethene data from the WP-3D have indicated that ethene and NO$_x$ enhancements are not always well correlated. Evidently the sources of these species are sometimes not co-located, making it difficult to define emission ratios in those cases.
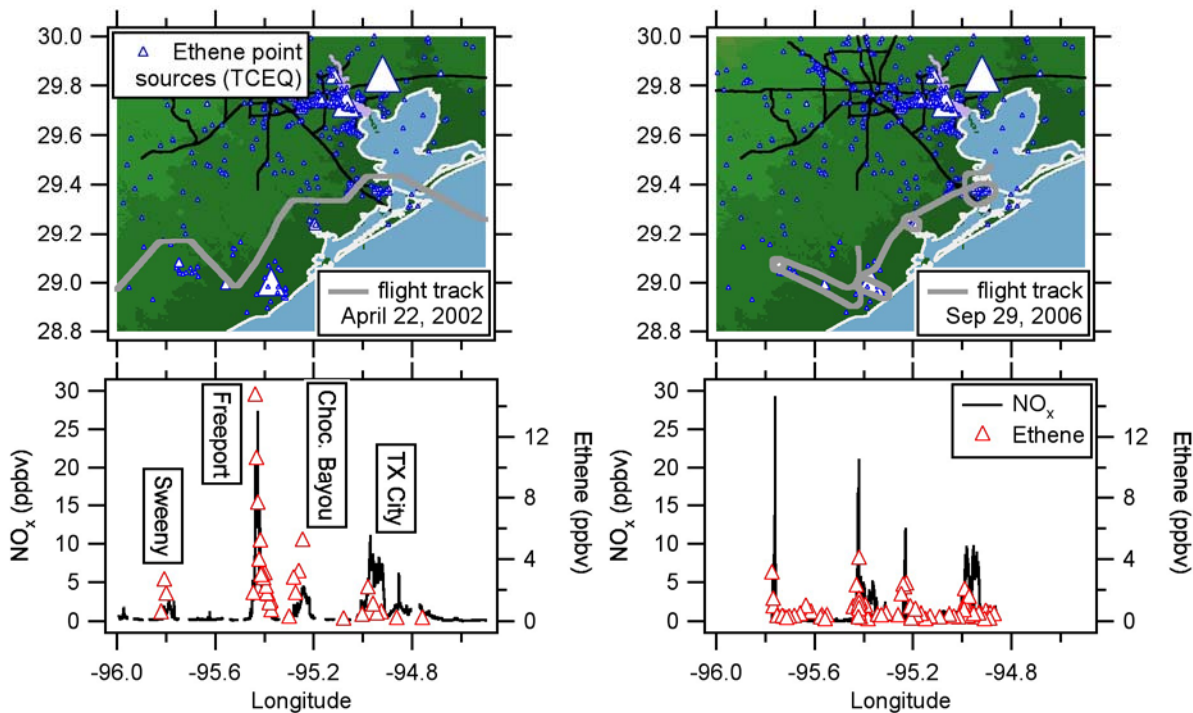
Figure C1. Measurements of NO_x and ethene downwind from 4 isolated petrochemical plants to the south of Houston. The top panels show the flight tracks of the WP-3D on 22 April 2002, (Ryerson et al., 2003) and on 29 September 2006. The lower panels show the measurement results plotted as a function of longitude.

Table C1. Ethene/NO_x emission ratios for petrochemical complexes determined from measurements in 2000, 2002, and 2006, compared with emission inventories.

	Ethene/NO_x Emission Ratios				
	Inventories		Measured		
	1999 [a]	2004 [b]	2000 [c]	2002 [c]	2006
Sweeny	0.05	0.019	3.6	1.7	0.5
Freeport	0.05	0.030	1.5	0.62	0.32
Choc. Bayou	0.08	0.048	2.0	1.2	0.62

[a] TNRCC emission inventory.

[b] TCEQ point source emission inventory with 1999 VOC speciation.

[c] Ryerson et al. (2003.)

Comparison of ethene and formaldehyde concentration distributions during TexAQS 2000 and 2006

Analysis: de Gouw et al.-NOAA. Data: de Gouw, Ryerson, Holloway, et al.-NOAA; Atlas et al.– U. Miami; Fried et al.-NCAR.

Figure C2 compares the 2000 and 2006 airborne ethene measurements made below 1000 m altitude inside a box around Houston (Figure C2, panel A). The median ethene from the whole air samples (WAS) was 40% lower in 2006 than in 2000 (Figure C2, panel B). The median ethene from the laser photo-acoustic spectroscopy (LPAS) measurements was even lower; one can show that the targeted filling of WAS inside pollution plumes leads to a bias in the WAS median. A similar comparison of the 2006 data from the *Ronald H. Brown* while in Barbour's Cut with the 2000 data from La Porte airport (these two locations are in close proximity) indicates a similar 40% decrease (not shown here).
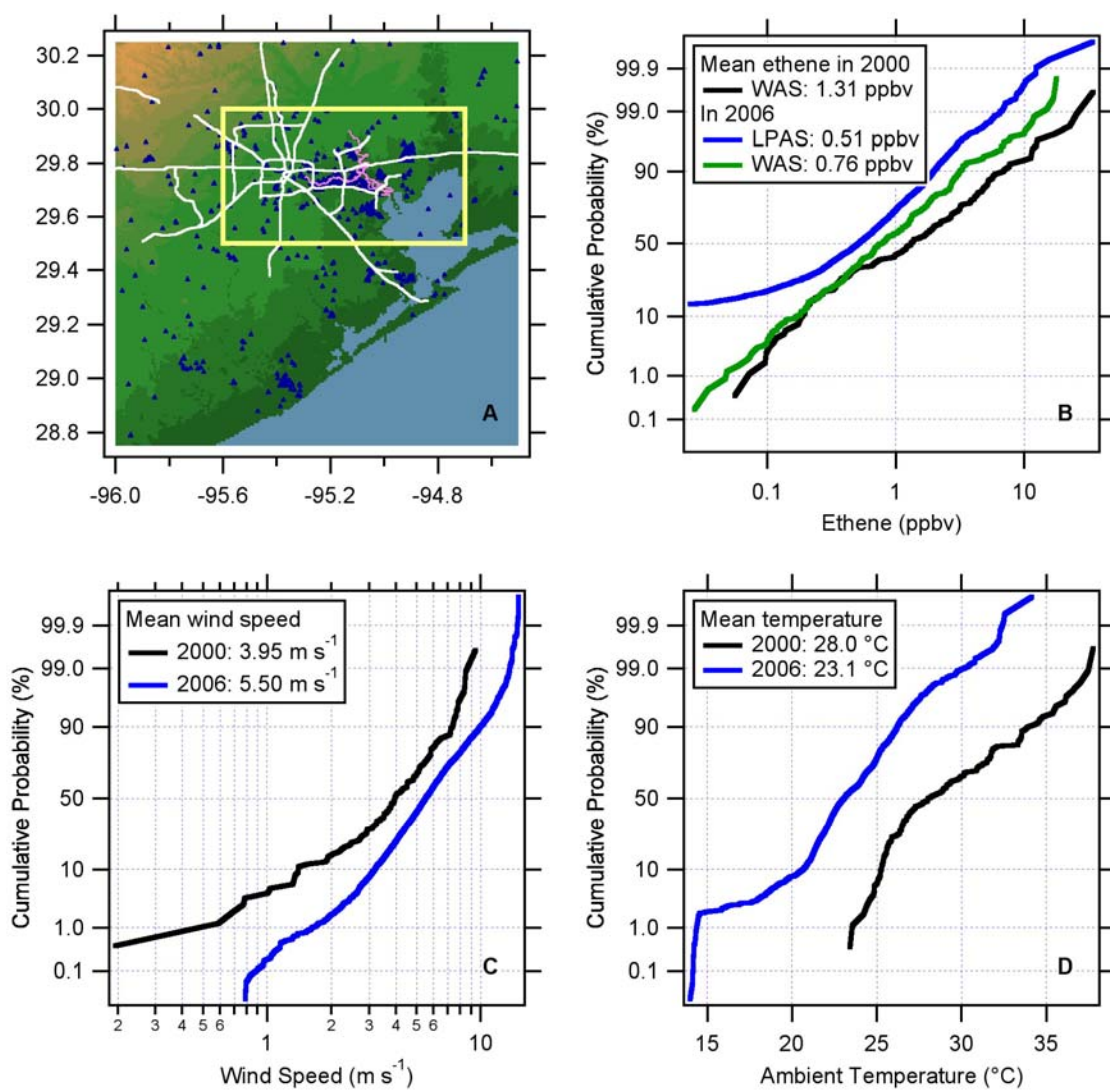

Figure C2. Cumulative probability diagrams for ethene, wind speed, and temperature measured from the NOAA WP-3D inside the box around Houston shown in panel A and below 1000 m altitude.

The question arises whether the differences between 2000 and 2006 are due to a decrease in HRVOC emissions or to a difference in meteorology. Average wind speeds in 2006 were higher than in 2000 (Figure C2, panel C), which would lead to a greater dilution of ethene emissions and lower mixing ratios in 2006. However, average temperatures in 2006 were lower than in 2000 (Figure C2, panel D). Higher temperatures can be associated with deeper boundary layers and thus a larger volume within which the emissions are mixed and diluted, which would imply higher mixing ratios in 2006.

All emissions are subject to the same meteorology. Comparison of other emitted species between 2000 and 2006 can provide additional insight into possible meteorological differences. If the decrease in ethene between 2000 and 2006 were due to meteorology, then other trace gases should exhibit similar trends. If, on the other hand, the decrease were due to a decrease in emissions, then other trace gases would show ambient concentration trends characteristic of their own emission trends. Figure C3 shows the difference in median mixing ratio between 2000 and 2006 for six species. On-road mobile emissions dominate the emissions of ethyne and CO; their mixing ratios showed only small changes between 2000 and 2006. (The CO mixing ratios were corrected for the observed background mixing ratios.) A decrease in CO is expected because of the modernization of the vehicle fleet between 2000 and 2006; the observed decrease of ~3% per year is slightly smaller than the reported historical trend of 4.6% per year (Parrish, 2006). NO_y showed a significant decrease between 2000 and 2006; this is attributed to the installation of emissions reduction technologies in power plants and other industrial NO_x point sources (see Finding C3 below). SO_2 increased slightly between 2000 and 2006; reductions were not expected as emissions controls have focused on NO_x. The largest decreases were observed in the mixing ratios of ethene and formaldehyde (HCHO), its main photoproduct. From this comparison we conclude that the meteorological differences had compensating effects on the two years, and that the decrease in ethene between 2000 and 2006 was due to a reduction in its industrial emissions.
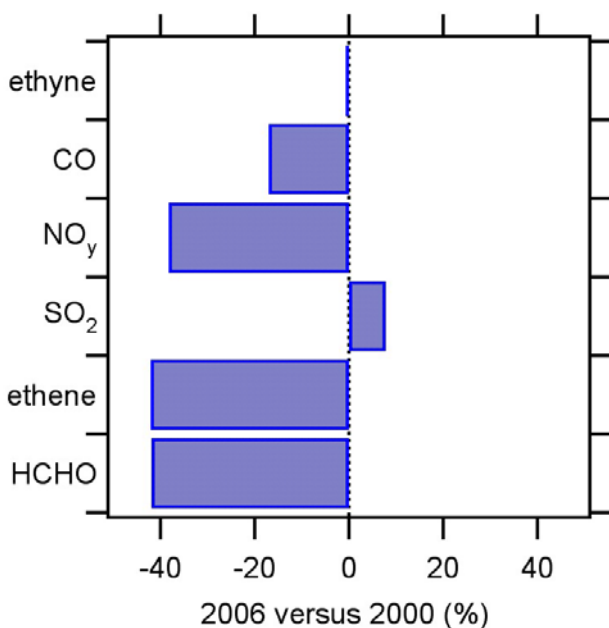

Figure C3. Difference in median mixing ratio for several trace gases measured from the WP-3D inside a box around Houston and below 1000 m altitude.

Long-term data sets

Analysis: Estes et al.-TCEQ; Data: TCEQ.

In the Houston area there have been extensive VOC measurements made by as many as eight auto-GC systems and by canister-based methods. Measurements were begun at some sites as early as 1997, giving temporal coverage over one decade by the end of 2006. Figure C4 presents results from two sites near the Ship Channel. The median ambient ethene levels at both sites decreased by about a factor of two between 1997 and 2005. Similar decreases were also seen for propene (not shown). Analysis by Sather and Cavender (2007) also shows significant decreases of ambient concentrations of ethene and propene, in qualitative agreement with Figure C4.
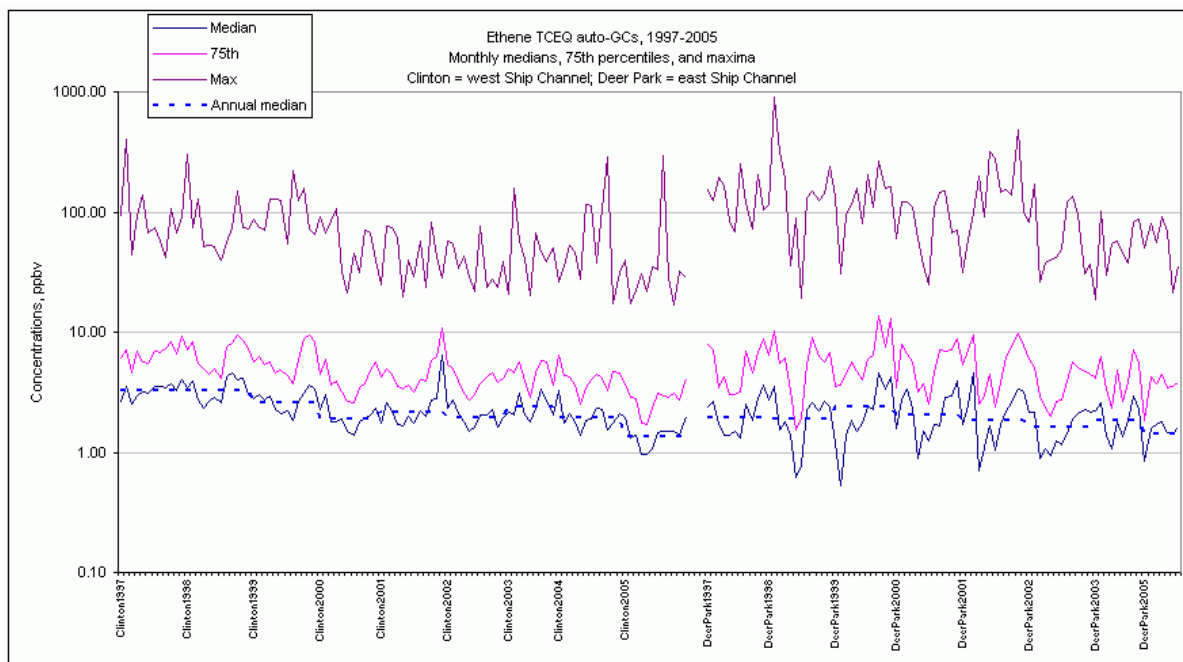

Figure C4. Results of ethene measurements by auto-GCs at two sites near the Houston Ship Channel: 9 years of data from Clinton (on the western end) and 8 years of data from Deer Park (on the eastern end).

Summary of evidence

Emission ratios of ethene relative to NO_x from several isolated petrochemical plants in 2006 were lower in comparison with results from 2000 and 2002. This decrease in ratios must be due to a decrease in ethene emissions, since the NO_x emissions have also decreased in many cases (see Finding G3). Further, lower mixing ratios of ethene and formaldehyde were observed in 2006 in comparison with 2000, and this change cannot be explained by differences in dilution rates between the two years.

Thus, analyses based on four different measured parameters (ethene/NO_x emission ratios in plumes of petrochemical facilities, the ambient distribution of ethene concentrations, the ambient distribution of formaldehyde, and long-term auto-GC ethene measurements) have all found evidence for a significant decrease in ethene emissions. The unanimity of these four analyses

increases our confidence that a significant decrease in HRVOC emissions from Houston area petrochemical facilities has actually occurred in the period between 2000 and 2006. Considering all of these analyses, the best estimate is that ethene emissions have decreased by about 40% (i.e., a factor of 1.7) between 2000 and 2006. The much more limited evidence available for propene suggests that emissions of this HRVOC may have decreased similarly.

It is important but difficult to assign confidence limits to the magnitude of the decrease. Our best estimate is that the decrease is $40 \pm 20\%$, which corresponds to a decrease by a factor of 1.25 to 2.5. We consider it unlikely, but cannot categorically exclude the possibility that there has in fact been no significant decrease.

Finding C2: **Measurements of ethene emission fluxes from petrochemical facilities during TexAQS 2006 indicate that the 2004 TCEQ point source database underestimates these 2006 emissions by one to two orders of magnitude. Repeated sampling of the same petrochemical facility showed that the ethene emission flux remained constant to within a factor of two.**

Analysis and data: de Gouw et al.-NOAA; Mellqvist et al.–Chalmers U.

Emissions of ethene were determined during TexAQS 2006 by two completely independent methods. First, column measurements of ethene by absorption of solar IR radiation were obtained from the solar occultation flux (SOF) mobile laboratory operated by Chalmers University (Gothenburg, Sweden). In this method, the ethene emission flux was estimated by combining the column data with measured vertical wind profiles and then integrating across the width of the plume in close proximity to the emission source. Second, ethene was measured onboard the WP-3D aircraft using a new laser photo-acoustic spectroscopy (LPAS) instrument. An example of the resulting data is shown from 25 September when the WP-3D and the SOF van both sampled the emissions from the Mont Belvieu complex (Figure C5).
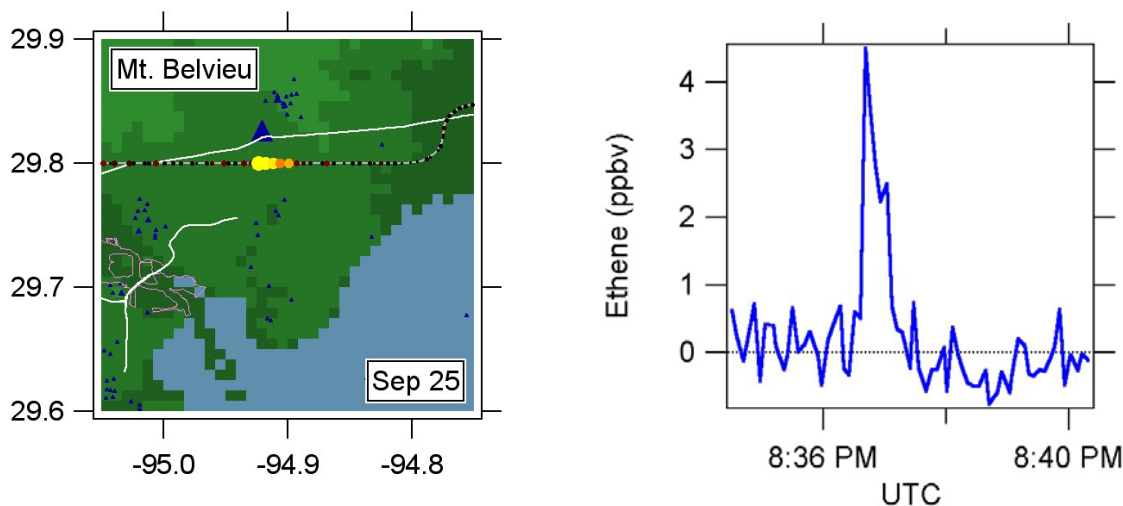

Figure C5. Transect of the WP-3D just downwind from the Mont Belvieu complex to the northeast of HSC, color-coded by ethene measured by LPAS. Ethene sources from the 2004 TCEQ point source database are indicated by the blue triangles, with the size proportional to the source strength. The measured time series of ethene for this transect is shown on the right.

The ethene flux was estimated from the aircraft measurements by integrating across the width of the plume and by assuming that the plume was homogeneously distributed over the height of the boundary layer. A flux of 280 kg h^{-1} is the result for this example. The result from the SOF van from the same complex on the same day was 500 kg h^{-1}, i.e., agreement within a factor of 2. Flux estimates from the SOF and WP-3D measurements were compared for different sources (Sweeny, Freeport, Texas City) and generally agreed within a factor of 2, with no systematic difference as to which technique was higher or lower.

The WP-3D determined the flux from Mont Belvieu on a total of 10 downwind transects. Figure C6 shows a histogram of the WP-3D results (grey bars); the average calculated flux is 470 kg h^{-1} with a standard deviation of 160 kg h^{-1}. Two considerations can serve to put these fluxes in perspective. First, the 2004 TCEQ point source database estimated the ethene emissions from Mont Belvieu to be 29 kg h^{-1}, a factor of 10-40 lower than the values measured during TexAQS 2006. Second, Murphy and Allen (2005) investigated the role of large, accidental releases of HRVOC in ozone formation in the HGB area. They identified 763 HRVOC emission events in a one-year period (31 January 2003 to 30 January 2004). More than half of these events released less than 1000 lbs (454 kg) total HRVOC. Thus, the Mont Belvieu complex, as an example of petrochemical facilities in the HGB area, routinely emits more ethene each hour than the total released in most of the individual accidental release events considered by Murphy and Allen. These facilities represent a significantly larger source of HRVOC and more substantial contribution to ozone formation than indicated by current emission inventories.
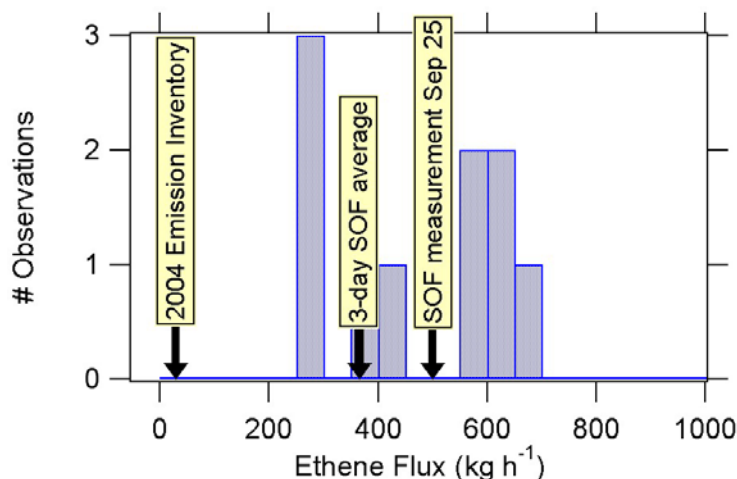
Figure C6. Histogram of ethene fluxes determined from aircraft measurements of 10 transects. Also indicated are the SOF result from September 25, the average SOF result from 3 days of measurements, and the 2004 TCEQ point source database.

Finding C3: **Close to petrochemical HRVOC sources, the OH reactivity of propene is generally greater than that of ethene.**

Analysis: de Gouw et al.-NOAA; Data: Atlas et al.-U. Miami.

Close to emission sources, the reactivity of propene generally outweighs that of ethene. To illustrate, Figure C7 shows the OH reactivity of propene (the product of the propene concentration and the rate coefficient for its reaction with OH) versus that of ethene from all the

whole air sample measurements onboard the WP-3D. At high reactivity (>0.5 s^{-1}) the data points are well above the blue line that indicates equal reactivity of ethene and propene. At lower reactivity (<0.1 s^{-1}), the reactivity of ethene is higher than that of propene; the lifetime of ethene is longer by about a factor of 3, and therefore it persists further downwind from sources. Thus, VOC measurements made at routine monitoring sites, generally located relatively distant from the facilities, will not accurately reflect the propene OH reactivity contributions unless the relative lifetimes of the HRVOC are carefully considered.
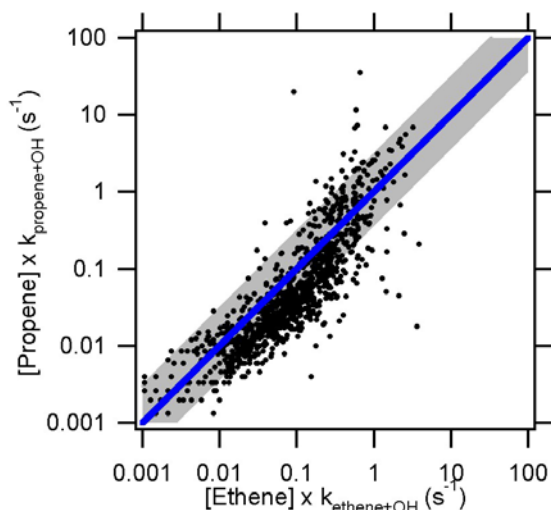

Figure C7. OH reactivity of propene versus that of ethene from all the data from the WP-3D. The blue line indicates equal reactivity of ethene and propene; the gray area shows the range where the reactivities of ethene and propene differ by no more than a factor of 3, higher or lower.

***Finding C4*: The latest available emission inventories underestimate ethene emissions by approximately an order of magnitude.**

Analysis: Jolly et al.-TCEQ; Data: TCEQ.

The TexAQS 2000 study established that inventories underestimated emission fluxes of HRVOC from petrochemical facilities by one to two orders of magnitude (Ryerson et al., 2003.) A remarkable feature of Table C1 and Figure C6 is that appreciation of this finding has not been reflected in the inventory evolution. For example, total HRVOC emissions included in the Harris County Point Source EI for 2000-2004 were fairly steady across those years, with the lowest year (2002, at 3300 tons) being about 83 percent of the highest year (2004, 4000 tons). Total VOCs in the county in the 2000-2005 period differed approximately 13 percent between the lowest year (2003, ~29,000 tons) and the highest year (2000, ~33,500 tons). Consequently, the latest available emission inventories still underestimate HRVOC emissions (as judged by the ethene comparisons summarized in Table C1 and Figure C6) by at least an order of magnitude.

In an effort to improve this situation, TCEQ collected the special 2006 Hourly Emission Inventory during the TexAQS 2006 intensive from 15 August through 15 September. During this period, 141 sites in eastern Texas reported their hourly emissions of VOC, NO$_x$, CO, and SO$_2$ from predetermined industrial sources, which were selected based upon the following criteria: sources subject to HRVOC rules, NO$_x$ and sulfur dioxide sources equipped with CEMS,

and emissions sources located near ambient air monitoring sites. For HRVOC the reported emissions were based upon process flow monitoring (flares, cooling towers) that was required beginning in January 2006. This inventory was the first in HGB conducted since compliance deadlines passed for key HRVOC regulations promulgated by the TCEQ. These hourly estimates were made only for a subset of process units and emission points within the reporting plants, and only a subset of plants that normally report in the HGB EI did so in the Hourly EI. Both of these factors add uncertainty to how well this inventory represents the total HGB VOC inventory. In HGB, about 10-11% of the process units and emission points that emit ethene and propene in the annual (periodic) emission inventory were included in the Hourly EI. However, these units accounted for 23-24% of all ethene/propene emissions reported in the annual EI.
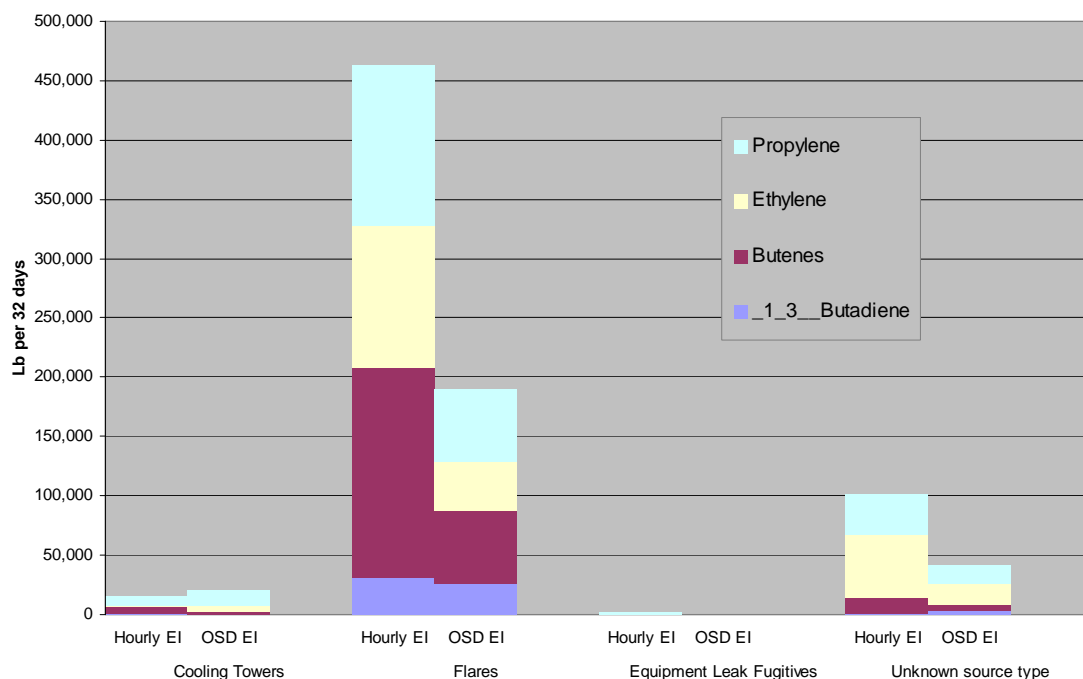

Figure C8. HRVOC emissions, by process unit type and compound/group. The special 2006 Hourly Emission Inventory is compared to the Ozone Season Daily Emission Inventory (OSD EI) summed over the 32 days (15 August – 15 September) included in the special inventory.

The results from the hourly EI suggests that reported emissions of total VOC and HRVOC species may increase in the coming years. Figure C8 shows emissions changes in inventoried emissions from cooling towers and flares, as well as for equipment leak fugitives (which were poorly represented in the hourly EI). The total HRVOC emissions from inventoried flares, increased about 2.4 fold (95 tons to 231 tons), although the much smaller emissions from cooling towers decreased by 28% (9.9 to 7.7 tons in the 32 day period). Overall, the total reported ethene and propene emissions in HGB approximately doubled.

In summary, the discrepancy between the HRVOC emission measured in the field and those included in inventories has improved to some degree between the 2000 and 2006 TexAQS studies. The measured emissions have decreased by about 40%, while the inventoried emissions (at least as indicated by the limited Special 2006 Hourly Emission Inventory) have increased by

about a factor of 2. However, in spite of this progress, the latest available emission inventories still underestimate ethene emissions by approximately an order of magnitude.

***Finding C5*: Inventories for NO_x point sources at petrochemical facilities equipped with CEMS appear to be relatively accurate. Substantial decreases in NO_x emissions in the Houston Ship Channel are suggested by the inventories, and measurements from aircraft are qualitatively consistent with the NO_x decreases.**

Analysis: Trainer et al.-NOAA; Data: Ryerson, et al.-NOAA.

Data from the WP-3D flights in 2006 compared to similar data from the Electra aircraft in 2000 indicate that substantial reductions in NO_x emissions from certain petrochemical facilities have occurred in the intervening period. Figure C9 presents an example of a transect downwind of HSC that was flown under similar conditions during both field studies. Plumes with well-defined correlations between NO_y and CO_2 concentrations were seen in both years from the east end of the HSC and from the Cedar Bayou complex (at the northern end of Galveston Bay). The slopes of these correlations give the NO_x/CO_2 emission ratio from the respective sources. These observed slopes compared well to the ratios calculated from the CEMS systems for the times of emissions of these plumes. It is clear that the NO_x/CO_2 emission ratio decreased dramatically for the Cedar Bayou complex (by a factor of 6) as a result of NO_x emission controls implemented at this plant. NO_x emissions also decreased detectably (by about 30%) from the facilities at the eastern end of the HSC.
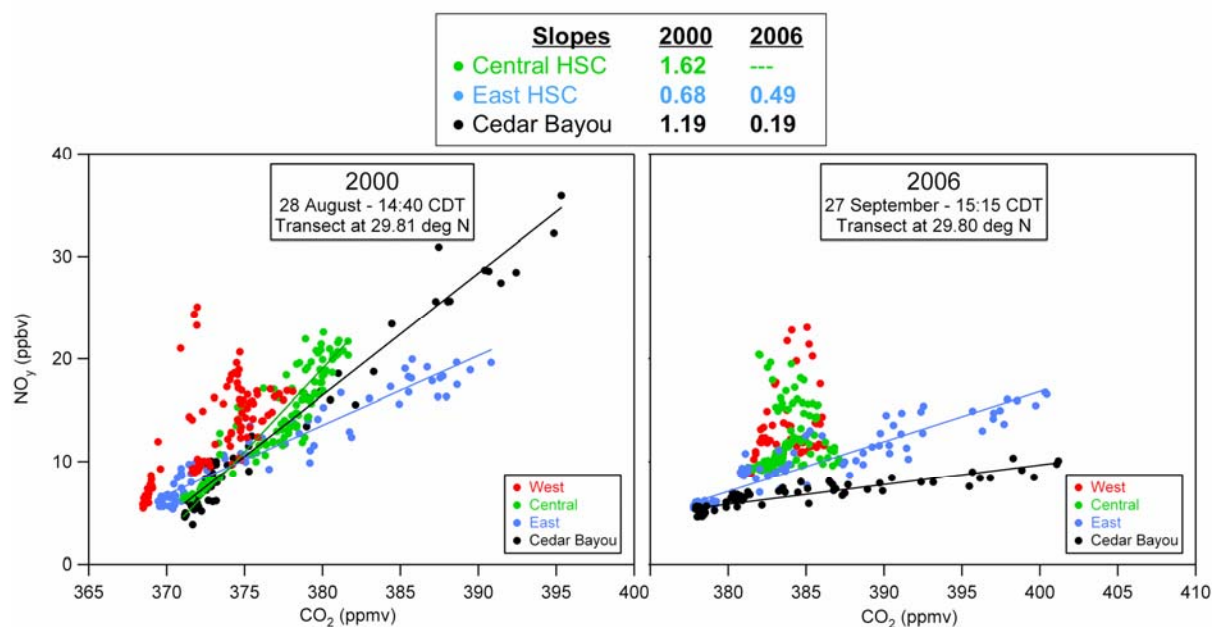

Figure C9. Relationships between NO_y and CO_2 from flights during TexAQS 2000 and 2006. Linear least squares fits are given for correlations with $r^2 > 0.80$. Slopes of the fits give the NO_x to CO_2 emission ratios.

KEY CITATIONS AND INFORMATION AND DATA SOURCES

Murphy, C.F. and D.T. Allen. 2005. Hydrocarbon emissions from industrial release events in the Houston-Galveston area and their impact on ozone formation. Atmos. Environ. 39:3785–3798.

Parrish, D.D. 2006. Critical evaluation of US on-road vehicle emission inventories. Atmos. Environ. 40:2288–2300.

Ryerson, T.B., M. Trainer, W.M. Angevine, C.A. Brock, R.W. Dissly, F.C. Fehsenfeld, G.J. Frost, P.D. Goldan, J.S. Holloway, G. Hübler, R.O. Jakoubek, W.C. Kuster, J.A. Neuman, D.K. Nicks, Jr., D.D. Parrish, J.M. Roberts, D.T. Sueper, E.L. Atlas, S.G. Donnelly, F. Flocke, A. Fried, W.T. Potter, S. Schauffler, V. Stroud, A.J. Weinheimer, B.P. Wert, C. Wiedinmyer, R.J. Alvarez, R.M. Banta, L.S. Darby, and C.J. Senff. 2003. Effect of petrochemical industrial emissions of reactive alkenes and NO_x on tropospheric ozone formation in Houston, Texas. J. Geophys. Res. 108(D8), 4249, doi:10.1029/2002JD003070.

Sather, M.E. and K. Cavender. 2007. Trends analysis of ambient 8 hour ozone and precursor monitoring data in the south central U.S. J. Environ. Monit. 9:143–150.

Response to Question D

QUESTION D
What distribution of anthropogenic and biogenic emissions of ozone and aerosol precursors can be inferred from observations?

BACKGROUND
Questions C, D, and E all deal with emissions. Question C specifically addresses highly reactive VOC and co-located NO_x emissions in the Houston area. Here, Question D addresses all other ozone and aerosol precursor emissions, biogenic as well as anthropogenic, that are included in emission inventories. Question E addresses evidence for additional, unrecognized sources of precursor emissions.

FINDINGS

Finding D1a: **Several rural electric generation units (EGU) in the Houston area and in eastern Texas have substantially decreased their NO_x emissions per unit power generated since the TexAQS 2000 study. With one exception, SO_2 emissions have not changed appreciably since 2000 for the plants sampled in 2006.**

Finding D1b: **Comparisons of emissions derived from ambient observations with those measured by continuous emission monitoring systems (CEMS) indicate that the emissions from point sources equipped with CEMS are very accurately known.**

Finding D1c: **Underreporting of CO emissions at several EGU noted in 2000 (Nicks et al., 2003) has been reconciled by large increases (by factors of 5 to 50) in the inventory values between 2000 and 2006, as a result of newly implemented CEMS monitoring of CO at these plants.**

Analysis and Data: Ryerson et al.-NOAA.

NO_x, SO_2, CO, and CO_2 are emitted directly, in varying ratios, from electric generation units (EGU). Enhancement of the first three species, relative to CO_2 enhancements when sampled in plumes immediately downwind of EGU point sources, provide a measure of pollutant emissions per unit energy generated by the plant (e.g., Ryerson et al., 2003). Comparisons of emissions ratios between the TexAQS 2000 and TexAQS 2006 studies permit an assessment of EGU emissions control strategies, intended primarily to reduce NO_x emissions, that have been implemented since 2000.

Near-field plumes from numerous rural EGU in Texas were characterized using aircraft measurements in 2000 and 2006. Data were generated as shown in Figure D1a, which depicts the NOAA WP-3D ground track for a flight designed to assess several large EGU point sources in the eastern Texas area. The data are taken from the closest transects, within 10 km downwind of the plants, and plotted in Figure D1b as enhancement ratios versus CO_2. The slopes of linear fits to these data provide a direct measure of the plant emissions ratios.

Analyses of rural EGU emissions ratios to CO_2 have been performed for Monticello, Welsh, Martin Lake, Big Brown, and W.A. Parish power plants. Table D1 compares derived emission ratios from the 2006 WP-3D data with the ratios measured from the NCAR Electra aircraft in 2000.

The TexAQS 2000 study demonstrated quantitative agreement between emissions estimates from the Electra aircraft data and the tabulated emissions from Continuous Emissions Monitoring Systems (CEMS) data, for NO_x and SO_2 at each plant. Some variability is expected on time scales of hours to years, and is reflected in the data in Table D1. Nonetheless, conclusions from the 2006 study can be drawn that are well outside of the uncertainties due to normal emissions variability over time.
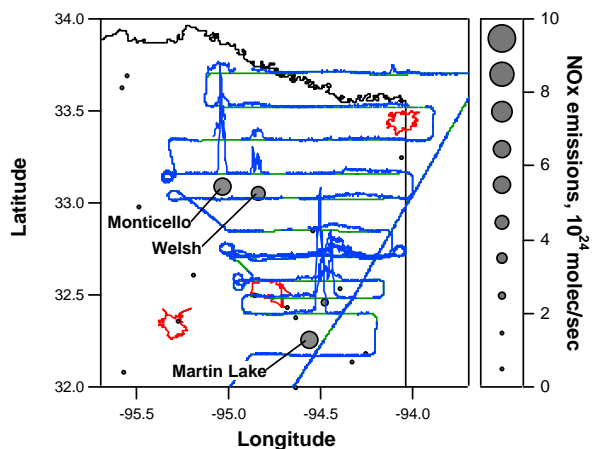

Figure D1a. Sept. 16, 2006 WP-3D ground track (green) with observed SO2 enhancements (blue) plotted along the track.
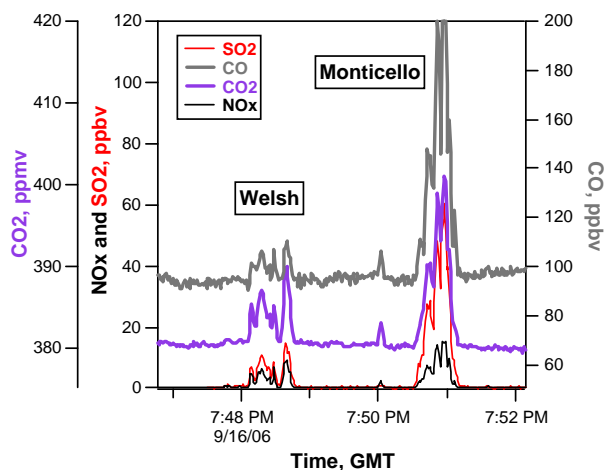
Figure D1b. Time series of CO2, SO2, NOx, and CO measured immediately downwind of Welsh and Monticello.

Table D1. Measured emissions relative to CO_2 for EGU in East Texas.

EGU name	NCAR Electra aircraft data 2000			NOAA WP-3D aircraft data 2006			NOx emissions decreased by factor of:
	SO_2	CO	NOx	SO_2	CO	NOx	
Monticello	3.5	6.4	1.0	2.8	5.4	0.80	**1.25**
Welsh	1.5	1.7	0.80	1.7	1.7	1.20	**1.5 (increase)**
Martin Lake	1.4	4.0	1.3	3.0	6.1	0.80	**1.6**
Big Brown	4.8	2.9	1.5	7.8	6.8	0.66	**2.3**
W.A. Parish	2.1	(variable)	0.88	2.1	(variable)	0.25	**3.5**

Emissions values presented as molecules per 1000 molecules of CO_2 emitted.

Analysis of all available transects of the Parish power plant plume shows that inventory values derived from CEMS data and estimates from the WP-3D are in quantitative agreement. Figure D2 shows that both the magnitude and the variability in time of emissions are captured by the data in Texas 2006 for both SO_2 and NO_x.
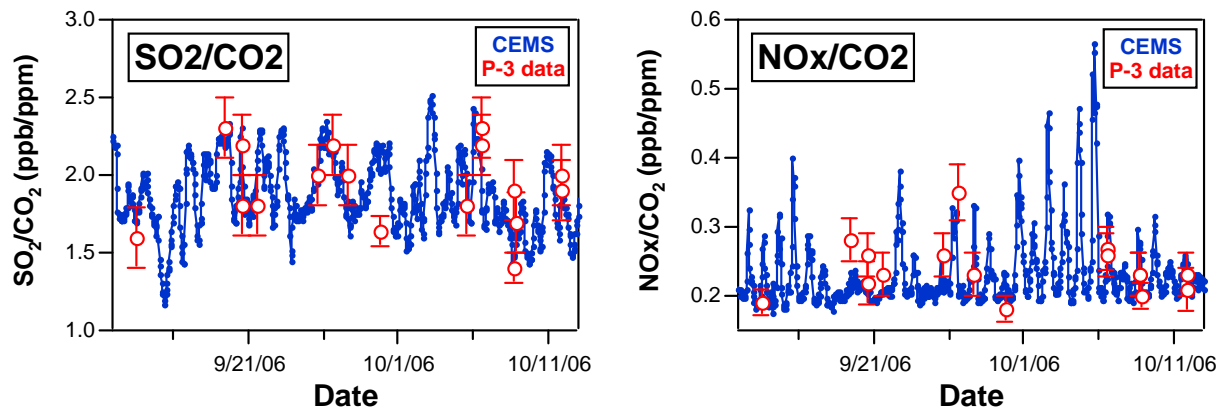
Figure D2. Ratios of SO_2 and NO_x to CO_2 emitted from the Parish power plant plume during six weeks of the TexAQS 2006 study. The ratios derived from CEMS data are compared to the determinations from multiple near-field transects of the emission plume by the WP-3D aircraft.

Conclusions from this body of evidence are:

- NO_x emissions have decreased substantially in several EGU, by factors of 2–4, qualitatively consistent with NO_x controls implemented since the 2000 study. NO_x emissions from other EGU are essentially unchanged.
- SO_2 emissions are generally unchanged between 2000 and 2006 in the plants studied to date. The small variability observed is within that expected from CEMS data due to normally changing plant loads. An exception is the Martin Lake plant, where SO_2 appears to have increased by a factor of 2 relative to CO_2 compared to the 2000 study.
- Large CO emissions discrepancies, noted in the 2000 study, have been reconciled by substantial increases in the inventory CO values for several EGU in east Texas.
- Quantitative agreement between inventory values and aircraft estimates of NO_x/CO_2 and SO_2/CO_2 emissions ratios from rural EGU suggests that emissions from point sources equipped with CEMS are very well known.

Finding D2: **On-road mobile emission inventories developed from MOBILE6 have significant shortcomings. MOBILE6 consistently overestimates CO emissions by about a factor of 2. It accurately estimated NO_x emissions in the years near 2000, but it indicates decreases in NO_x emissions since then, while ambient data suggest NO_x emissions have actually increased. Consequently in 2006, NO_x to VOC emission ratios in urban areas are likely underestimated by current inventories.**

Analysis: Parrish et al.-NOAA; Data: TCEQ, Lefer et al.-U. Houston.

Figure D3 compares CO to NO_x ratios from ambient measurements with those from emission inventories. The Dallas and Houston routine ambient data are in excellent agreement with the nationwide AIRS data. The TexAQS 2006 data from Moody tower agree reasonably well with the routine monitoring data. Significant differences are seen in El Paso and San Antonio, which have older vehicle fleets.
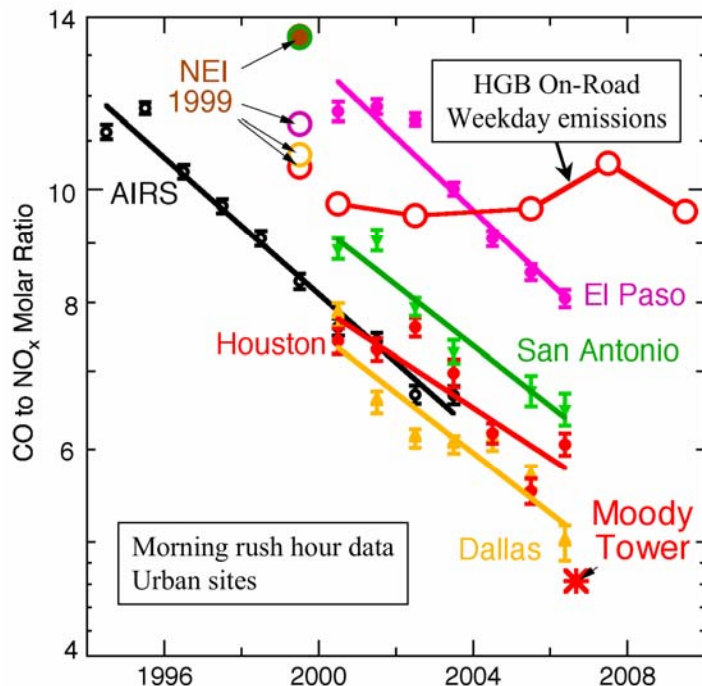
Figure D3. Determination of CO to NO_x ratio in Texas on-road mobile emissions from monitoring data (solid symbols) compared to the HGB emission inventory (open symbols), color-coded according to urban area. The black symbols are for all stations in the EPA AIRS network.

The HGB inventory overestimates the CO to NO_x emission ratio, and that overestimate becomes worse with time as the inventory does not show a significant temporal decrease. The HGB points are from the "SIP Quality" emission inventories (www.tceq.state.tx.us/assets/public/implementation/air/am/committees/pmt_set/20070424/20070 424-rthomas-0506EI_Modeling_Update.pdf; accessed 17 August 2007). It should be noted that the on-road emissions inventory value for 2000 was calculated with actual data for 2000, whereas the on-road mobile inventories for later years are projections, based upon projected population growth, economic data, and estimates of expected emission decreases. The projections, therefore, are more uncertain than the base case 2000 emissions. Parrish (2006) showed that the rapid decrease (6.6%/yr) in the ratio is partially due to a slower decrease in CO emissions (4.6%/yr), which implies a significant increase in NO_x emissions (approximately 2%/yr). The large inventory overestimates in the CO to NO_x ratio at the present time are attributed to a factor of 2 overestimate in CO emissions, and an underestimate in present NO_x emissions. This will cause NO_x to CO emission ratios in urban areas, which are often dominated by on-road mobile emissions, to be underestimated by current emission inventories.

Urban emission ratios sampled by the WP-3D aircraft in 2006 and the NCAR Electra aircraft in 2000 are consistent with measurements carried out at a Houston highway tunnel in 2000 (McGaughey et al., 2004). These measurements demonstrate the weekday increase in CO/CO_2 and CO/NO_x emission ratios from midday to the afternoon rush hour correlated with increases in the proportion of gasoline vehicles during rush hour. While aircraft and tunnel measurements were not made during the morning rush hour, their afternoon rush hour emission ratios are consistent with the routine monitoring data for the morning rush hour. Similar to the routine monitors, the aircraft and tunnel observations indicate that inventories overestimate mobile source CO by at least a factor of 2.

The VOC to NOx ratio in on-road emissions is of more critical importance to photochemical modeling in the HGB area than is the CO to NO_x ratio. Parrish (2006) showed that VOC

emissions from on-road vehicles have decreased at a similar rate to CO emissions. This correspondence is expected because catalytic converters are the principal control measure for both species. Although MOBILE6 accurately calculated the VOC to NO_x ratio in 2000, the decrease in the ratio is not accurately captured. Consequently, in 2006, NO_x to VOC emission ratios in urban areas are likely underestimated by current inventories.

***Finding D3*: Emissions from ships constitute a significant NO_x source in the HGB region. Literature results provide accurate emission factors for inventory development.**

Analysis and Data: Williams et al.-NOAA.

During TexAQS 2006, emissions in exhaust plumes from over 200 marine vessels in Galveston Bay and the Houston Ship Channel were measured on the *Ronald H. Brown*. Table D2 presents the average derived emission factors for slow speed diesel (SSD) engines, which are those with maximum power greater than ~10 MW, and medium speed diesel (MSD) engines, which are of lower power. The NO_x values are within 20% of the average values reported in the Lloyd's (1995) study for both MSD and SSD engines although the measured variability is large in both cases. These data are sufficient to provide emission factors classified by ship type (e.g., freighters, container ships, tankers, tugs, etc.). It is concluded that Lloyd's (1995) provides an accurate characterization of NO_x emissions from underway vessels in the HGB region.

Table D2. Summary of average marine vessel emission factors.

Engine type	NO_x	CO	SO_2	H_2CO	LAC
Medium speed diesel (MSD)	60	8.7	9.1	0.17	0.41
Slow speed diesel (SSD)	74	6.6	28	0.20	1.16

All units are grams of species per kilogram fuel consumed.
Emission factors for CO are median data.

The emission factors for CO are within 20% of the value reported by Lloyd's (1995). There is no trend of increasing CO at lower vessel speeds (used as a surrogate for engine load), which was seen in the Lloyd's data. Measurements of formaldehyde (H_2CO) emissions from ships show little distinction between MSD and SSD engines; emission of H_2CO is less than 5% of the emission of CO. Emission factors for SO_2 vary with fuel sulfur content. In the HGB region the mean fuel S derived from the measurements is 0.46% for MSD engines and 1.4% for SSD engines. Measurements of light absorbing carbon (LAC; also known as black carbon) were also derived.

Given detailed activity data (i.e., marine fuel consumption) for ships in the HGB region, an emissions inventory for this source could be constructed. The 2007 report from Eastern Research Group (ERG) to TCEQ (Eastern Research Group, 2007) has such data, but there appears to be a significant underestimate (factor of 2-8) of fuel consumption, when compared to an estimate from a more comprehensive model (Wang et al., 2007). The NO_2 emission factors used in the ERG report agree with our data to within 10%. Thus, for current ship emissions inventory modeling, there is less uncertainty contributed by emission factors than by activity data.

Table D3 gives emissions of NO_x, CO, and SO_2, relative to the emission of CO_2, from ships, compared to similar emission ratios from electric power generating units (EGU) from the 2004 point source emission inventory, updated to 2006 with CEMS data. This comparison shows that ships emit 10 to 100 times more NO_x (and somewhat more CO, and SO_2) per unit fuel burned (i.e. CO_2 emitted) than large stationary sources. Though the emissions from an individual vessel might be 10-100 times lower than from an EGU, the volume of ship traffic in the HGB region is sufficient that emissions from commercial shipping, in aggregate, cannot be neglected. Accurate fuel consumption or other ship activity data are needed to accurately quantify these emissions. Importantly, while emissions from stationary sources are a focus of ongoing control measures, emission controls on commercial shipping are not likely to be implemented because of technical constraints and complications arising from international law.

Table D3. Comparison of marine vessel and power plant emissions.

Emission source	NO_x/CO_2	CO/CO_2	SO_2/CO_2
Commercial vessel, SSD	22	6.1	6.1
Commercial vessel, MSD	18	8.1	2.0
Electric power generating unit			
W. A. Parish	0.23	0.51	1.9
Welsh	0.88	1.4	1.8

All units are molecules of species per 1000 molecules of CO_2.

Finding D4: **Mixing ratios of isoprene over Texas measured from the WP-3D were used for evaluation of the BEIS-3 emission inventory. On average, the isoprene emissions from the inventory and emissions derived from the measurements agree within a factor of ~2. There may be areas south of Dallas-Fort Worth and southwest of Houston, where isoprene emissions are lower than indicated by the BEIS3 inventory based upon the biogenics emission land cover data (BELD-3.0).**

Analysis and Data: de Gouw, Warneke et al.-NOAA.

Isoprene was measured from the WP-3D aircraft both in-situ by PTR-MS and off-line by laboratory analysis of whole air samples (WAS) collected in flight. Both measurements agreed within the respective measurement uncertainties. The PTR-MS has the highest time resolution, and thus spatial resolution, and the data illustrate the large variability of the isoprene concentration due to the in-homogeneity of its sources and its extremely short photochemical lifetime.

The PTR-MS data allowed the isoprene emissions to be estimated along the flight track using the measured height of the boundary layer (BL) and the concentration of OH radicals calculated from the parameterization of Ehhalt et al. (1998). The emissions were then converted to standard temperature and photo-active radiation using the formalism from Guenther et al. (1995) and compared to the BEIS3 emission inventory extracted along the flight track. The results for a flight on September 16th over NE Texas are shown in Figure D4. On this flight, the isoprene emissions from BEIS3 and those estimated from the aircraft data agree within a factor of ~2. A better agreement cannot be expected given the uncertainties in some of the relevant factors for this comparison (BL height, OH concentrations, and vertical gradients in the BL).
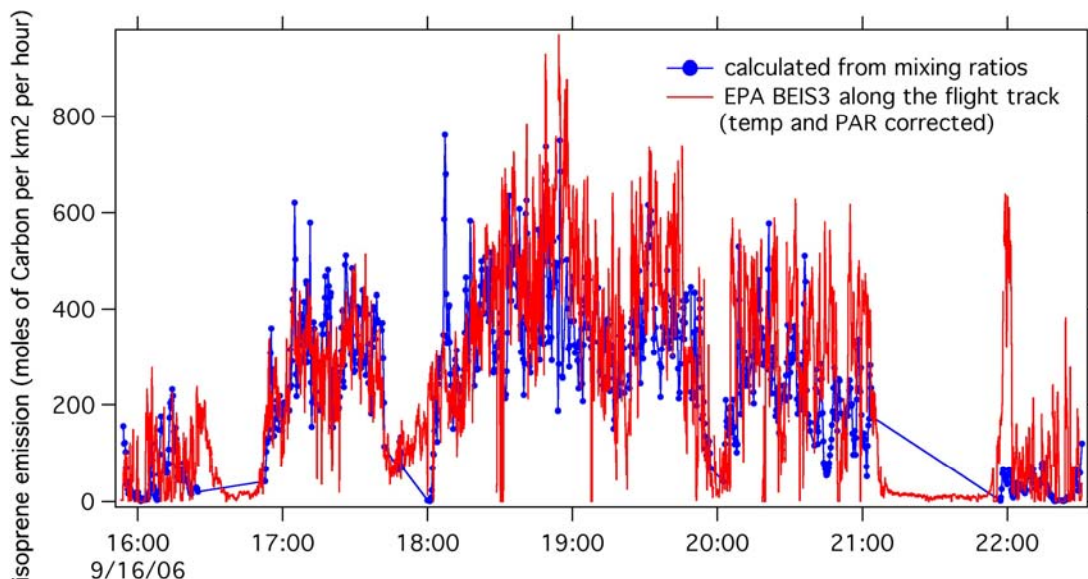
Figure D4. Isoprene emissions for a flight of the NOAA WP-3D on 16 September over NE Texas. Emissions extracted from the BEIS3 inventory based upon the biogenics emission land cover data (BELD-3.0) along the flight track are shown in red. Emissions derived from the PTR-MS data are shown in blue.

We also used the BEIS3 isoprene emission inventory as input for the Lagrangian particle dispersion transport model FLEXPART (Stohl et al., 2003). A comparison between isoprene measured by PTR-MS and modeled using FLEXPART after an average transport time of 1 hr is shown in Figure D5. As before, the model and measurements agree within a factor of ~2. Work is in progress to compare measured isoprene mixing ratios to 3-D chemistry-transport models; however, for a good comparison the models need to get boundary layer heights and OH levels correct, which is not true in all cases.
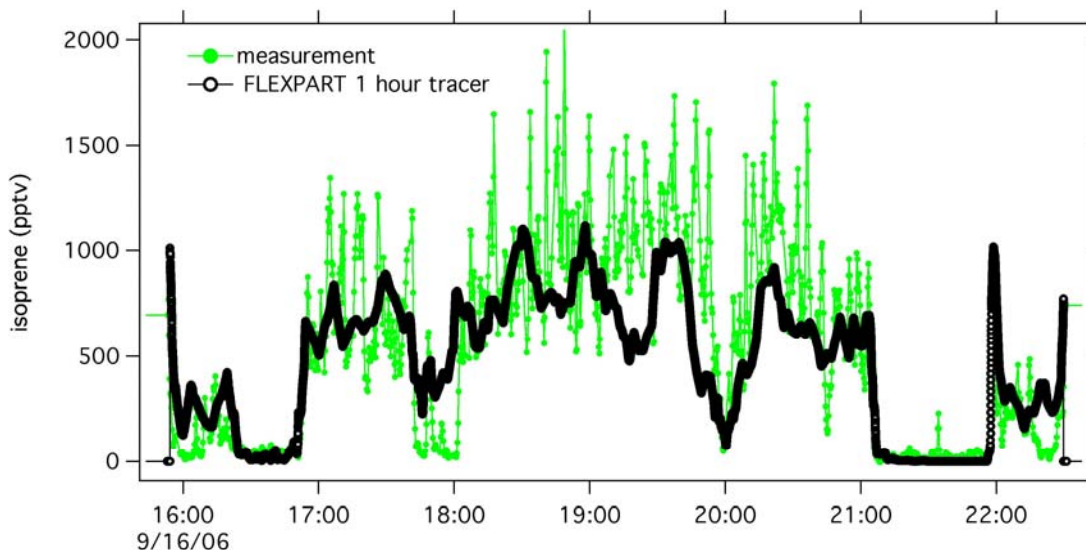

Figure D5. Comparison between isoprene mixing ratios measured by PTR-MS from the WP-3D on 16 September, and those modeled by FLEXPART.

31 August 2007

Comparisons between isoprene measurements and FLEXPART model results have been made for all flights. Figure D6 shows a map of the flight tracks in the boundary layer color-coded by the differences between measurements and model. The flight tracks in red indicate areas where measurement and model agree well. Flight tracks in yellow indicate areas where modeled isoprene was higher than the measurements; in particular to the southwest of Houston there is an area where this is the case. A possible explanation includes a difference between the actual land use and the land use assumed in the BEIS3 inventory; work is in progress to investigate this possibility. There is also an area in between Dallas-Fort Worth and Houston where the model indicates higher isoprene than the measurements. This area, however, was not as frequently sampled. Flight tracks in black indicate areas where the modeled isoprene was lower than the measurements. This is the case for NE Texas, but because isoprene was very high over this region, the difference of -400 pptv only represents a small relative difference between measurements and model.
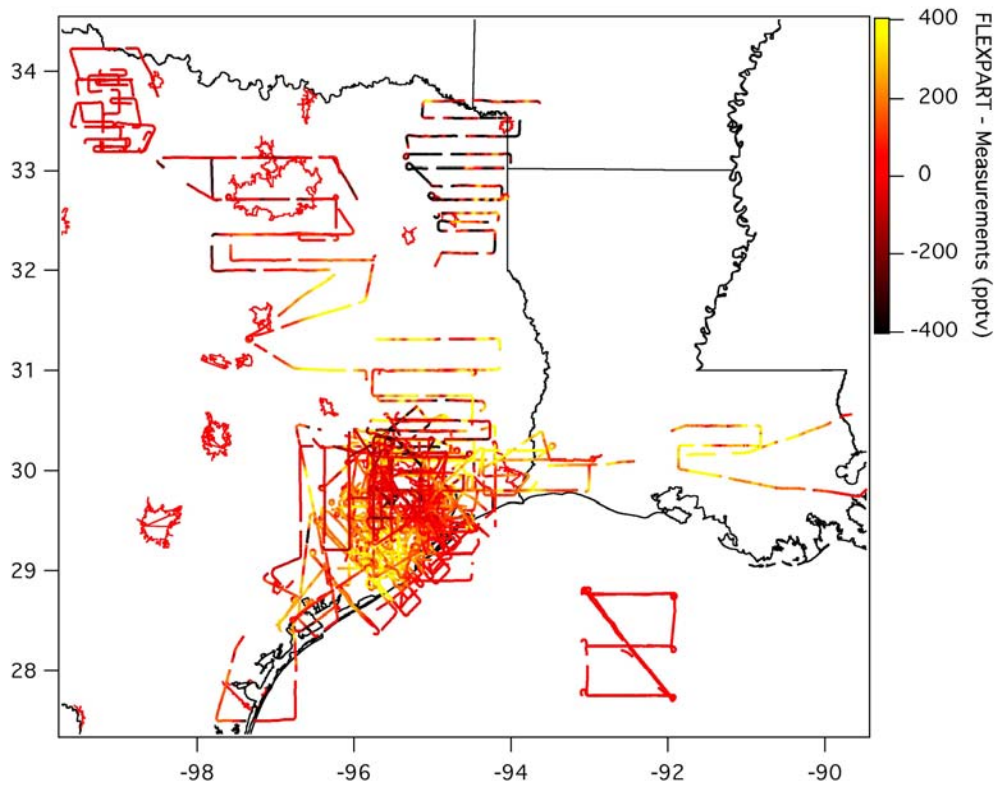

Figure D6. Flight tracks of the NOAA WP-3D aircraft in the boundary layer color-coded by the difference between modeled and measured isoprene mixing ratios.

***Finding D5*: The speciation of VOC from mobile sources in the Houston and Dallas-Forth Worth areas agrees with detailed measurements in the northeastern U.S. However, initial results suggest that the agreement with the NEI-99 emission inventory is poor.**

Analysis and Data: de Gouw, Warneke et al.-NOAA.

For specific wind directions, the emissions from urban, mostly mobile, sources in Houston are spatially separated from industrial emissions from the Ship Channel area. Specific WP-3D flights were selected based on wind direction to determine the speciation of VOC from mobile sources, using airborne data from the PTR-MS and WAS instruments. In addition, data from the flights downwind from Dallas-Fort Worth were studied. Emissions ratios of VOC versus CO were calculated from the airborne data and compared with the results of a similar study downwind from New York City in 2004 for different classes of compounds (Figure D7). There was a good quantitative agreement between urban emissions in Houston, Dallas, and New York City, which is not surprising. Warneke et al. (2007) showed previously that the VOC composition of urban emissions in New York City and Boston are not represented well in the NEI 99 emissions inventory. Initial results suggest that the same is true for Houston and Dallas-Fort Worth.
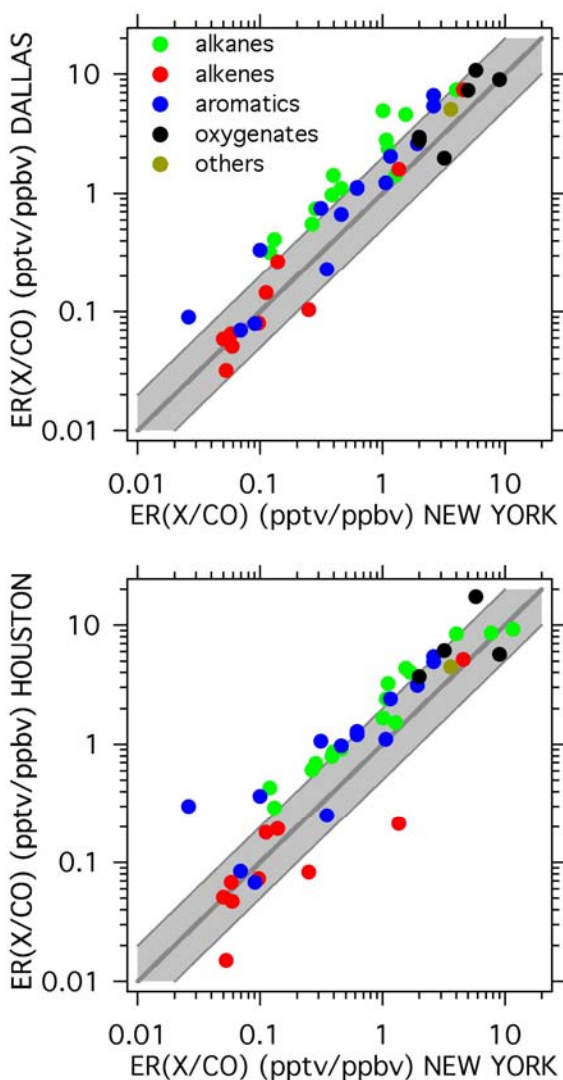

Figure D7. Emissions ratios (ER) of various VOC to CO from urban, mostly mobile, sources in Houston and Dallas-Fort Worth in 2006 versus the same ratios from New York City in 2004.

31 August 2007

KEY CITATIONS AND INFORMATION AND DATA SOURCES

Eastern Research Group. 2007. Houston/Galveston Routine Vessel Identification and Traffic Study, ERG Rep. No. 0196.00.023, TCEQ Contract No. 582-04-65564-23, January 26, 2007.

Ehhalt, D.H., F. Rohrer, A. Wahner, M.J. Prather, and D.R. Blake. 1998. On the use of hydrocarbons for the determination of tropospheric OH concentrations, J. Geophys. Res. 103:18981-18997.

Guenther, A., C. Hewitt, D. Erickson, R. Fall, C. Geron, T. Graedel, P. Harley, L. Klinger, M. Lerdau, W. McKay, T. Pierce, B. Scholes, R. Steinbrecher, R. Tallamraju, J. Taylor, and P. Zimmerman. 1995. A global model of natural volatile organic compound emissions. J. Geophys. Res. 100(D5):8873-8892.

Lloyd's Register Engineering Services. 1995. Marine Exhaust Emission Research Programme. Lloyd's Register House, London.

McGaughey, G.R., N.R. Desai, D.T. Allen, R.L. Seila, W.A. Lonneman, M.P. Fraser, R.A. Harley, J.M. Ivy, and J.H. Price. 2004. Analysis of motor vehicle emissions in a Houston tunnel during the Texas Air Quality Study 2000. Atmos. Environ. 38(20):3363-3372.

Nicks Jr., D.K., J.S. Holloway, T.B. Ryerson, R.W. Dissly, D.D. Parrish, G.J. Frost, M. Trainer, S.G. Donnelly, S. Schauffler, E.L. Atlas, G. Hübler, D.T. Sueper, and F.C. Fehsenfeld. 2003. Fossil-fueled power plants as a source of atmospheric carbon monoxide. J. Environ. Monit. 5:35-39.

Parrish, D.D. 2006. Critical evaluation of US on-road vehicle emission inventories. Atmos. Environ. 40(13):2288-2300.

Ryerson, T.B., M. Trainer, W.M. Angevine, C.A. Brock, R.W. Dissly, F.C. Fehsenfeld, G.J. Frost, P.D. Goldan, J.S. Holloway, G. Hübler, R.O. Jakoubek, W.C. Kuster, J.A. Neuman, D.K. Nicks, Jr., D.D. Parrish, J.M. Roberts, D.T. Sueper, E.L. Atlas, S.G. Donnelly, F. Flocke, A. Fried, W.T. Potter, S. Schauffler, V. Stroud, A.J. Weinheimer, B.P. Wert, C. Wiedinmyer, R.J. Alvarez, R.M. Banta, L.S. Darby, and C.J. Senff. 2003. Effect of petrochemical industrial emissions of reactive alkenes and NO_x on tropospheric ozone formation in Houston, Texas. J. Geophys. Res. 108(D8), 4249, doi:10.1029/2002JD003070.

Stohl, A., C. Forster, S. Eckhardt, N. Spichtinger, H. Huntrieser, J. Heland, H. Schlager, S. Wilhelm, F. Arnold, and O. Cooper. 2003. A backward modeling study of intercontinental pollution transport using aircraft measurements. J. Geophys. Res. 108, 4370, doi:10.1029/2002JD002862.

Wang, C., J.J. Corbett, and J. Firestone. 2007. Modeling energy use and emissions from North American shipping: Application of the ship traffic, energy, and environment model. Environ. Sci. Technol., doi:10.1021/es060752e.

Warneke, C., S.A. McKeen, J.A. de Gouw, P.D. Goldan, W.C. Kuster, J.S. Holloway, E.J. Williams, B.M. Lerner, D.D. Parrish, M. Trainer, F.C. Fehsenfeld, S. Kato, E.L. Atlas, A. Baker, and D.R. Blake. 2007. Determination of urban volatile organic compound emission ratios and comparison with an emissions database. J. Geophys. Res. 112, D10S47, doi:10.1029/2006JD007930.

Response to Question E

QUESTION E
Are there sources of ozone and aerosol precursors that are not represented in the reported emissions inventories?

BACKGROUND
Questions C, D, and E all deal with the evaluation of emission inventories. Question C specifically addresses highly reactive VOC and co-located NO_x emissions in the Houston area. Question D addresses all other ozone and aerosol precursor emissions, biogenic as well as anthropogenic, that are included in emission inventories. Here, Question E addresses evidence for ozone and aerosol precursor emissions not presently represented in inventories.

FINDINGS

Finding E1: **The observed mixing ratios and regional distribution of ambient formaldehyde are broadly consistent with daytime photochemical production from reactive VOC. An upper limit for primary formaldehyde emissions from mobile sources is obtained from nighttime measurements, and is small in comparison with the secondary, daytime formation.**

Analysis: de Gouw et al.-NOAA, Herndon et al.-Aerodyne, Rappenglück et al.-U. Houston; Data: Herndon et al.-Aerodyne, Fried et al.-NCAR, de Gouw et al.-NOAA, Atlas et al.-U. Miami, Rappenglück et al.-U. Houston.

Diurnal variations in the concentrations of ethene, propene, and formaldehyde were measured at several locations in the HSC. Figure E1 shows the data from Barbour's Cut, at the eastern end of the HSC. The mixing ratios of ethene and propene (VOC from direct emission) were highest at night, when photochemistry was absent and emissions of these species accumulated in a shallow boundary, and lowest during the day, when the boundary layer was deeper and alkenes were removed by reaction with OH. In contrast, formaldehyde is highest during the day – indicating that daytime photochemistry was the dominant source of this ozone precursor in the HSC area. Similar diurnal patterns also were observed at the Moody Tower site at the University of Houston.
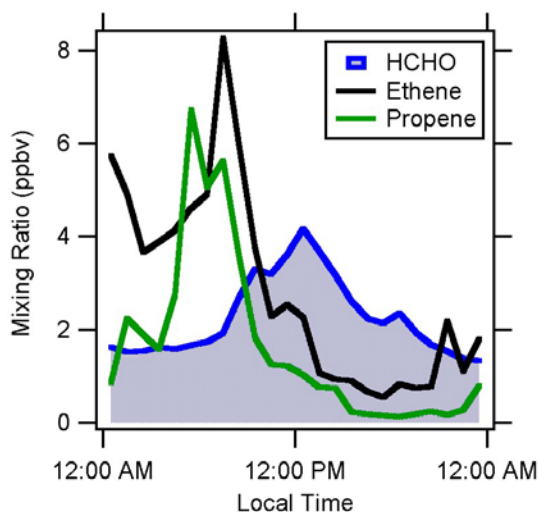

Figure E1. Average diurnal variation of mixing ratios of ethene, propene, and formaldehyde measured from the *Ronald H. Brown* over approximately ten days of measurements in Barbour's Cut.

Nighttime measurements onboard the *Ronald H. Brown* (*RHB*) and the WP-3D and at the Moody Tower site provide a useful means to estimate the direct emissions of formaldehyde from mobile sources. The left panel of Figure E2 shows the relationship of formaldehyde to CO measured in the turning basin at the western end of the HSC with winds coming from the central urban Houston area. The data are color-coded by the measured photolysis rate of formaldehyde; the nighttime points, in black, show a clear correlation between formaldehyde and CO with a slope of about 3 pptv ppbv^{-1}. After sunrise, the formaldehyde to CO ratio increased strongly due to photochemical formation of formaldehyde (daytime points in yellow). Similar observations were made onboard the WP-3D during a missed approach at Montgomery airport to the north of Houston during the night (Figure E2, right panel). In this graph the data are color-coded by altitude. Below 200 m the aircraft penetrated a shallow layer that was strongly impacted by local, primary emissions; the formaldehyde to CO ratio in this layer was 1.8 pptv ppbv^{-1}. Above the layer, the aircraft sampled the remnants of the daytime boundary layer that is isolated from primary emissions, and the formaldehyde to CO ratio was much higher. The corresponding slope from the Moody Tower measurements is somewhat higher (5 to 7 pptv ppbv^{-1}); the cause and implications of this larger slope is under investigation. From these observations we estimate the primary emissions of formaldehyde from mobile sources to be 0.18-0.3 percent of the CO emissions; this estimate is an upper limit, since it is not possible to exclude the possibility that the sampled air had been photochemically processed to at least some extent during the preceding daytime period. These findings are consistent with the conclusions of Anderson et al. (1996) who found formaldehyde to CO emission ratios of 0.10 to 0.14 percent in measurements made in Denver, Colorado.
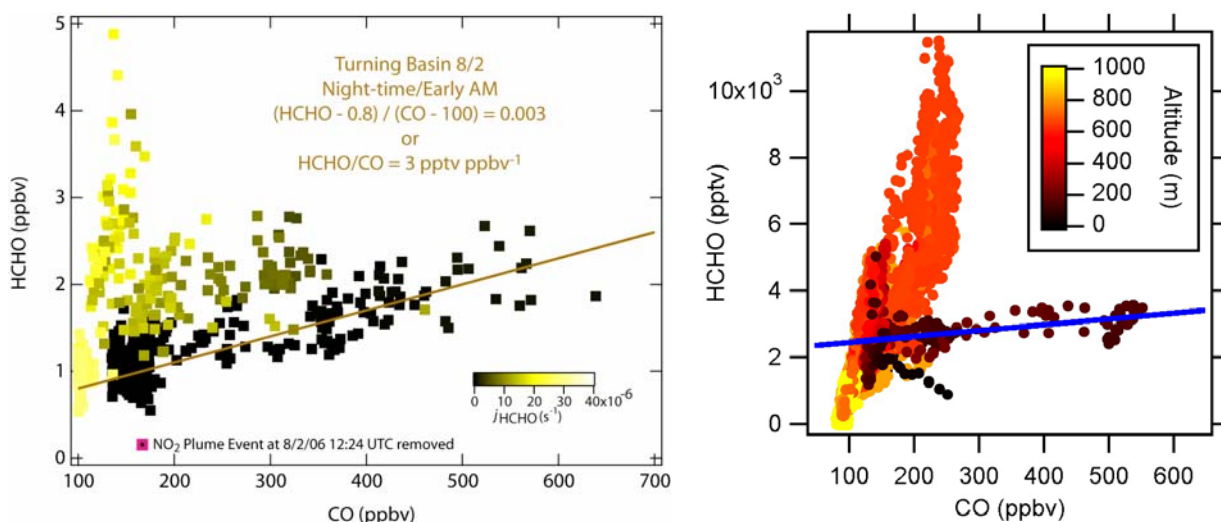
Figure E2. Relationships of HCHO to CO concentrations obtained onboard the *Ronald H. Brown* in the turning basin at the western end of the HSC (left panel), and from the WP-3D during a nighttime, missed approach at Montgomery County airport to the north of Houston.

Finding E2: **Concentrated plumes of ammonia were observed occasionally in the Houston Ship Channel area. These plumes often led to the formation of ammonium nitrate aerosol.**

Analysis and Data: Nowak et al.-NOAA.

Ammonium nitrate aerosol is formed from the reaction of gas-phase ammonia (NH_3) and nitric acid (HNO_3). Anthropogenic emissions of NH_3 and NO_x, which in sunlight is oxidized to form

HNO_3, can result in elevated concentrations of ammonium nitrate. Sources of NH_3 in the Houston area are thought to include motor vehicles, industrial facilities, outlying agricultural activity, and possibly power plants. High-time-resolution (≈1 s average) NH_3 measurements were made from the WP-3D aircraft by a Chemical Ionization Mass Spectrometry technique and from the *Ronald H. Brown* by quantum cascade laser absorption during TexAQS 2006 with the goals of characterizing sources and examining the effect of NH_3 on atmospheric aerosol formation.

Figure E3 shows the altitude profile of all 1-second average NH_3 mixing ratios measured aboard the WP-3D aircraft during the TexAQS 2006 study. Typically, NH_3 mixing ratios over the urban area ranged from 0.2 to 3 ppbv, and generally decreased with increasing altitude. Though infrequent, plumes with NH_3 mixing ratios from 5 to greater than 50 ppbv (highest values not indicated in Figure E3) were observed in the boundary layer below 1 km altitude. These plumes were encountered over the Houston metropolitan area in the vicinity of the HSC, around Beaumont, and in St. James Parish, Louisiana. NH_3 mixing ratios as high as several hundred ppbv were measured in the HSC from the *RHB*.
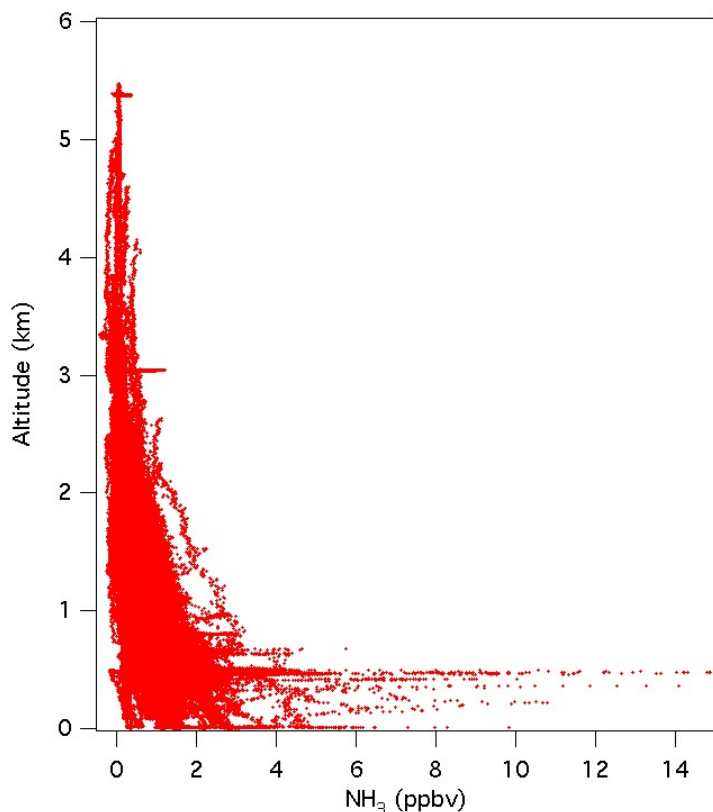
Figure E3. TexAQS 2006 NH_3 observations from the WP-3D plotted as function of altitude.

It is difficult to trace the sources of plumes with high NH_3 concentrations to particular industrial facilities. Figure E4 illustrates observations made in one of these plumes intercepted approximately 13 km downwind from the Cedar Bayou Station power plant. This plant is the location of the only significant upwind NH_3 point source listed in the National Emission Inventory of 1999 (NEI99v3). However, the lack of a strong correlation of the concentration of NH_3 with the enhancements of the CO_2 and NO_x concentrations (upper panel of Figure E4) suggests the NH_3 is not released in the Cedar Bayou stack emissions. Future analysis will focus

on using the 2006 Toxic Release Inventory along with measurements of VOC made aboard the WP-3D aircraft to unambiguously identify this NH_3 plume source.

Figure E4. Time series of concentration measurements of primary emissions (NH_3, NO_x, CO_2) and secondary products (HNO_3 nitrate aerosol) during a transect of the Cedar Bayou power plant plume.
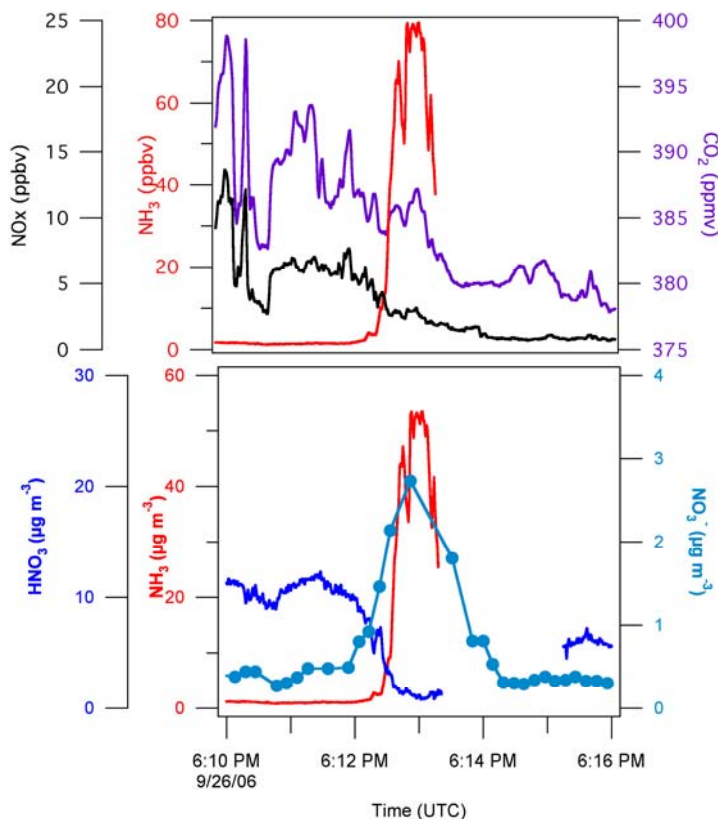
The observed NH_3 enhancements were typically found to be accompanied by corresponding increases in the particulate nitrate (NO_3^-) and decreases in HNO_3 mixing ratios as illustrated in the bottom panel of Figure E4. These correlated variations indicate the formation of ammonium nitrate. The magnitude of the observed HNO_3 lost and NO_3^- formed is consistent (within a factor of 2) with ammonium nitrate formation. The air quality implications of such ammonia plumes should be considered, particularly during cooler wintertime months when the ammonium nitrate will make a longer-lived contribution to the $PM_{2.5}$ concentrations.

Power plants that have installed Selective Catalytic Reduction (SCR) units constitute a possible NH_3 source. This process adds aqueous NH_3 to the exhaust gases as a reagent to decrease NO_x emissions. NH_3 "slippage," i.e., unwanted emissions of NH_3 into the atmosphere, occurs when exhaust gas temperatures are too low for the SCR reaction to proceed to completion, or when too much NH_3 is added. The W.A. Parish electric generating facility is equipped with these units. To characterize emissions from this plant, the WP-3D aircraft sampled the Parish plume on numerous flights during TexAQS 2006; Figure E5 shows a time series of measurements from one example transect of the plume. Clear enhancements of CO_2, NOy, and SO_2 coincide with a depletion in the ozone concentration due to its reaction with the freshly emitted NO_x, while no difference in NH_3 (black line) mixing ratios can be discerned in or out of the plume. The lack of NH_3 enhancement in the power plant plumes sampled by the WP-3D indicates that NH_3 slippage was not significant during any of the TexAQS 2006 plume transects.
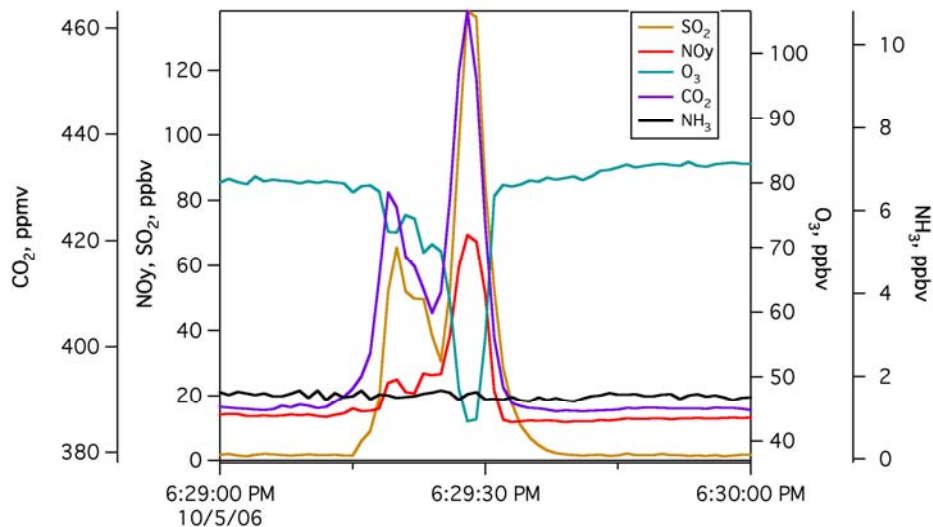
Figure E5. Time series of NH_3, NOy, SO_2, CO_2, and O_3 observations during transect of the W.A. Parish power plant plume.

Finding E3: **Concentrated plumes of gaseous elemental mercury from at least one point source were observed repeatedly in the Houston Ship Channel area and once in the Beaumont-Port Arthur area. The sources of the plumes could not be identified with current inventory sources of mercury.**

Analysis and Data: Ryerson et al.-NOAA.

High-time-resolution ($\approx$1 s) measurements of gaseous elemental mercury (Hg) were made from the *Ronald H. Brown* during TexAQS 2006. Figure E6 shows examples of the plume encounters in the HSC and Beaumont industrialized area. The magnitude of the detected plumes varied widely; the HSC plume in Figure E6 was detected during each of four transects of the HSC under southerly to easterly winds, but the magnitude of the plume varied by a factor of approximately 25. During the plume transects, the measured Hg concentration did not correlate with the measured concentrations of any other measured species. This lack of correlation rules out most known sources of Hg emissions, which can be expected to co-emit one or more of the wide range of chemical or aerosol species that were measured concurrently on the *RHB*. Further, the measured Hg concentrations are not consistent with the latest TCEQ or EPA AIRS, eGRID, and TRI inventory source locations for known Hg sources in the HSC region. A potential source not included in these inventories would be re-release of Hg from historically contaminated soils. More research into this possibility is needed to better understand the unexpectedly high concentrations of Hg observed in coastal industrial areas in eastern Texas.
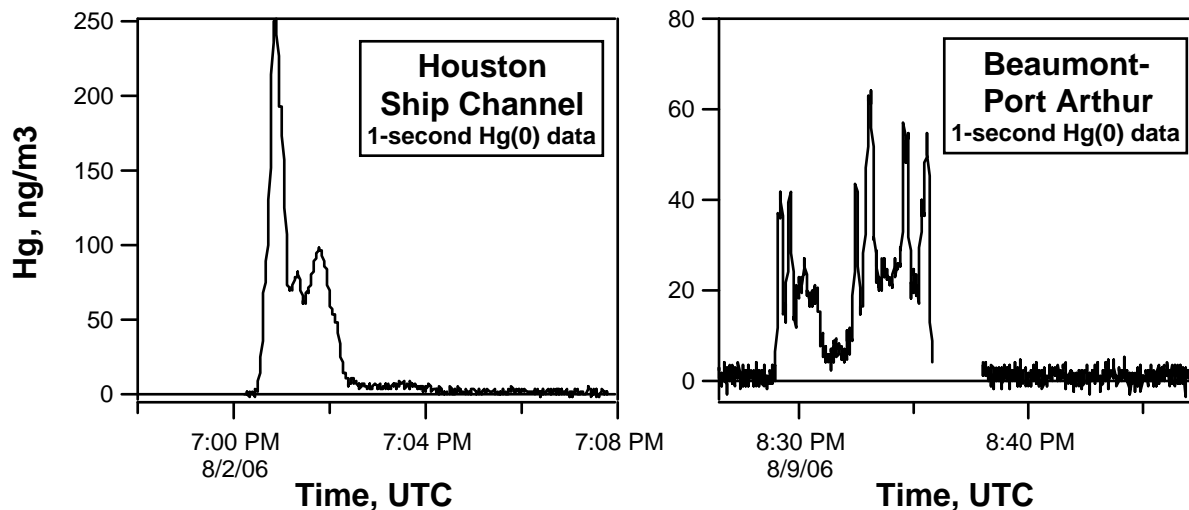
Figure E6. Measurements of gas-phase elemental mercury (Hg). Note the change in scales between the two graphs. Periods of missing data are due to automatic instrument calibration or zero procedures.

KEY CITATIONS AND INFORMATION AND DATA SOURCES

Anderson, L.G., J.A. Lanning, R. Barrell, J. Miyagishima, R.H. Jones, and P. Wolfe. 1996. Sources and sinks of formaldehyde and acetaldehyde: An analysis of Denver's ambient concentration data. Atmos. Environ. 30:2113-2123.

Ryerson, T.B., M. Trainer, W.M. Angevine, C.A. Brock, R.W. Dissly, F.C. Fehsenfeld, G.J. Frost, P.D. Goldan, J.S. Holloway, G. Hübler, R.O. Jakoubek, W.C. Kuster, J.A. Neuman, D.K. Nicks, Jr., D.D. Parrish, J.M. Roberts, D.T. Sueper, E.L. Atlas, S.G. Donnelly, F. Flocke, A. Fried, W.T. Potter, S. Schauffler, V. Stroud, A.J. Weinheimer, B.P. Wert, C. Wiedinmyer, R.J. Alvarez, R.M. Banta, L.S. Darby, and C.J. Senff. 2003. Effect of petrochemical industrial emissions of reactive alkenes and NO_x on tropospheric ozone formation in Houston, Texas. J. Geophys. Res. 108(D8), 4249, doi:10.1029/2002JD003070.

Wert, B.P., M. Trainer, A. Fried, T.B. Ryerson, B. Henry, W. Potter, W.M. Angevine, E. Atlas, S.G. Donnelly, F.C. Fehsenfeld, G.J. Frost, P.D. Goldan, A. Hansel, J.S. Holloway, G. Hübler, W.C. Kuster, D.K. Nicks Jr., J.A. Neuman, D.D. Parrish, S. Schauffler, J. Stutz, D.T. Sueper, C. Wiedinmyer, and A. Wisthaler. 2003. Signatures of terminal alkene oxidation in airborne formaldehyde measurements during TexAQS 2000. J. Geophys. Res. 108(D3), 4104, doi:10.1029/2002JD002502.

Response to Question F

QUESTION F
How do the mesoscale chemical environments (NO$_x$-sensitive ozone formation vs radical-sensitive ozone formation) vary spatially and temporally in Houston, Dallas, and eastern Texas?
Which mesoscale chemical environments are most closely associated with high ozone and aerosol?

BACKGROUND

Determination of NO$_X$ versus VOC (or Radical-Formation) Sensitive Ozone Formation
The accurate prediction of the relative response of ozone concentrations to future reductions in NO$_x$ and VOC emissions is a much sought, but very elusive goal. The prediction is central to the very important SIP-relevant question of "direction of control" – that is, should ozone control efforts in an ozone non-attainment area be focused on: a) decreasing emissions of NO$_x$ alone, b) decreasing emissions of VOC alone, or c) decreasing emissions of both NO$_x$ and VOC? The following paragraphs discuss some important considerations concerning this question.

In the period between the two TexAQS field studies, a change in the NAAQS for ozone was implemented, with at least two important implications for evaluating the "direction of control" question. The older standard, based upon a relatively high (120 ppbv) ozone concentration averaged over a short period (one hour), has been supplanted by one based on a lower (80 ppbv) concentration averaged over a longer period (eight hours). One implication is that the older, shorter-period average was much more amenable to analysis based upon in situ observations; the "snap shot" of the relationships between simultaneously measured concentrations of ozone, its precursors, and other photochemical products provided direct clues to the limiting precursor in an observed ozone exceedance. The longer-period average requires a more comprehensive analysis of the integrated accumulation of ozone over the full 8-hour exceedance period. A second implication is that the background ozone transported into an urban area will constitute a much larger fraction of the ambient ozone concentration constituting an 8-hour exceedance than was the case for a one-hour exceedance. Thus, much more attention must be paid to the effect of control strategies in upwind regions.

Some approaches to determining the "direction of control" question rely, in effect, upon comparing the response of ambient ozone to differential reductions in VOC versus NO$_x$ precursor emissions. Such approaches give useful guidance for effectively achieving incremental improvements in ozone air quality; however such approaches cannot determine if compliance with the NAAQS can be reached through such incremental emission reductions, and do not identify the most effective emission control approach for reaching compliance.

A rigorous approach to answering all aspects of the "direction of control" question would require a thoroughly tested Eulerian air quality model that treats the region of interest with sufficient accuracy. Multiple simulations would then be run with that "perfected" model to test possible NO$_x$ and VOC emission control strategies. These simulations would then provide the required ozone response information. Unfortunately however, it is not yet generally possible to develop such models because of deficiencies and uncertainties in many critical areas, including emissions, meteorological modeling, and photochemical mechanisms. The thorough testing of

the model must verify that the model adequately reproduces the observed ozone for the correct reasons. This testing would include at least two model-measurement comparisons: first, the model's ability to reproduce observed relationships between the concentrations of ozone and its precursors and, importantly, other secondary photochemical products (organic nitrates, nitric acid, formaldehyde and other oxygenated VOC, peroxides), and second, the model's ability to reproduce the observed ambient concentrations of the radicals that drive the photochemical reactions. The first comparison should pay particular attention not only to the slopes and correlation coefficients of the relationships, but also to the range of the observed and modeled concentrations of ozone and the related species. From this perspective, the air quality community is still in the early stages of the testing process; a process that is limited both by resources for model development, and by the availability of observational data with which to compare the models.

The eastern Texas region provides particular advantages, as well as particular challenges, for achieving the required model development and application. The TexAQS 2000 and TexAQS II field studies have collected data sets that provide unprecedented opportunities for model testing. However, experience has shown that development of needed emission inventories is a challenge that has not been met in all respects (see discussion in Responses to Questions C, D, and E.) A further challenge is presented by the concentrated plumes that determine the highest ozone values in the Houston area (see discussion in Response to Question A.) Such resolution may be a severe challenge for Eulerian models, especially if they attempt to include the whole eastern Texas region. At this point it is not possible to provide a rigorous answer to the "direction of control" question.

In the absence of a perfected model, it has been necessary to take a variety of heuristic approaches to provide guidance to air quality managers. Heuristic implies a model that is simplified, but that is designed and used to learn more about some specific but important aspect of the more complex air-quality system that is to be managed. In this report the closely related Questions F and K both deal with aspects of this issue. Here in Question F the application of both observation and modeling based approaches for approximately determining the sensitivity of ozone production will be discussed; the photochemical environment of the entire eastern Texas region will be considered. Question K presents an EKMA model-based approach to address the same issue, but from a different perspective; its application is restricted to the HGB area.

FINDINGS

Finding F1: **Both Eulerian and Lagrangian plume modeling approaches indicate that in 2000 high ozone concentrations in the HGB area were sensitive to both VOC and NO$_x$ emission reductions.**

Lagrangian Plume Model

Analysis: M. Trainer-NOAA; Data: Parrish et al.-NOAA, Fried et al.-NCAR, Atlas et al.-U. Miami.

Wert et al. (2003) presented a Lagrangian plume model designed to closely reproduce the emissions, ozone formation, other secondary photochemical product formation, and plume dispersion observed during the TexAQS 2000 study. Figure F1 shows that the model accurately reproduced the rapid production of ozone and formaldehyde that was measured in a concentrated plume originating from the HSC region. (Figure A3 shows the location of this plume intercept). The model required only two HRVOC – ethene and propene. To successfully reproduce the highest observed ozone concentrations, it was critical that the model reproduced two factors: a high ozone production efficiency as shown by observations (e.g. Figures A3 and A4 of this report), and a rapid rate of ozone production. High ozone production efficiency assures that high ozone can be produced from the emitted precursors, and the rapid rate of ozone production assures that high ozone is produced before the plumes of emissions dilute and disperse.
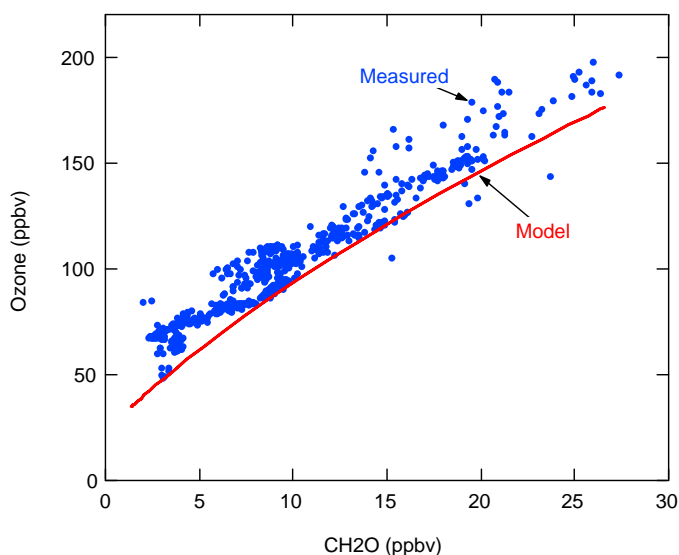
Figure F1. Relationship between ozone and formaldehyde concentrations observed from the Electra aircraft on 1 September 2000 and modeled by a Lagrangian plume model (Wert et al., 2003).

Figure F2 shows the modeled sensitivity of the ozone accumulation to both NO$_x$ and VOC emission reductions for the plume illustrated in Figure F1. The upper panel indicates that decreases in NO$_x$ emissions lead to a more rapid ozone production, but a lower peak ozone concentration, while HRVOC emission reductions lead to both slower ozone production and a lower peak ozone concentration. The lower panel indicates that HRVOC and NO$_x$ emission reductions are almost equally effective in reducing the total ozone flux in this plume. It is noteworthy that the ozone response is highly non-linear; reduction of either precursor by one-half reduces the ozone flux by only about one-quarter.

The ozone flux produced and transported in this plume from the HSC accounts for a substantial fraction of the total ozone produced in the entire Houston area. In Response to Question G of this report, the total flux from the Houston urban area is calculated from airborne ozone lidar measurements. The base case calculated plume flux in Figure F2 represents 45 to 80% of the total Houston flux determined on six days during TexAQS 2000 and 2006. These calculations led Wert et al. (2003) to conclude that targeted reductions in either or both emission categories would effectively reduce the highest observed ozone levels.

Eulerian Modeling

TCEQ (2004, 2006) has conducted Eulerian modeling of the entire HGB nonattainment area in order to determine which controls are necessary to reach attainment. This modeling indicates that both VOC and NO_x controls were effective in reducing ozone in 2000.

In particular, two tests have indicated sensitivity to both VOC and NO_x in Houston: reductions of biogenic VOC emissions by 30%, and modeling of weekend/weekday differences in mobile source emissions. However, in both cases, the effects on ozone concentrations varied by location within the HGB area and meteorological conditions, suggesting that VOC and NO_x sensitivity in HGB varies spatially and temporally.

Figure F2. Ozone sensitivity calculated by the Lagrangian plume model. The red lines give the base case calculation, and the green and red lines indicate the effect of a factor of two decrease in emissions NO_x and VOC, respectively.

TCEQ modeling for the HGB area indicates that in 2009 further NO_x emission reductions will be by far more effective than VOC emission reductions in decreasing O_3. In the 2009 future baseline scenario, the emissions of anthropogenic NO_x and VOC are projected to be reduced by 56% and 24%, respectively, relative to the 2000 emission inventory. Despite these large projected decreases in emissions, the maximum ozone design value in HGB is predicted to be 97 ppbv, well above the 84 ppbv level of the NAAQS. Thus without additional emission reductions, the HGB area is predicted to remain out of compliance with the NAAQS in 2009. Figure F3 shows the predicted effects of additional anthropogenic emission reductions beyond the 2009 future baseline. Additional reductions in VOC emissions result in only modest improvement in the ozone design value, and compliance with the NAAQS cannot be achieved with VOC decreases alone. The modeling does suggest that reductions in VOC emissions would allow compliance with the NAAQS to be reached with somewhat less drastic NO_x emission reductions (53% versus 58%) than is the case for NO_x emission reductions alone.
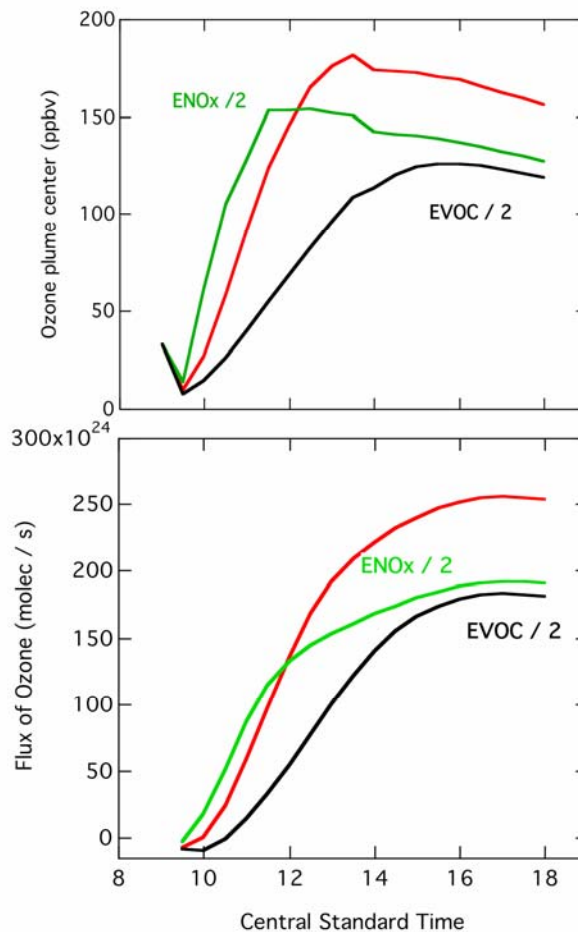
Figure F3. Predicted future ozone design values (O3 DVf; the 3-year average of the fourth-highest daily maximum 8-hour-average ozone concentration) for HGB as a function of reductions in emissions of NO_x, VOC, and both. The reference calculation (i.e. 0 percent reduction in the table in the figure) is based upon the projected emissions for 2009, and the reductions from that reference case are assumed constant across all emission categories. (Analysis by TCEQ; Figure adapted from D. Karp)

"Radical Starvation" in Selected Modeling Scenarios
A photochemical grid modeling scenario has shown that under certain conditions with high concentrations of HRVOC, ozone formation can be inhibited by "radical starvation." The radical starvation can be alleviated by adding large quantities of primary formaldehyde emissions, CO emissions, or aromatic emissions, or by changing to the SAPRC99 chemical mechanism. It is unclear at this point which, if any, of these solutions are appropriate for Houston modeling.

***Finding F2*: An observation-based approach to determine the sensitivities of high ozone in the HGB non-attainment area to the precursor VOC and NO$_x$ emissions has been investigated; it has yielded ambiguous results.**

Analysis: Parrish-NOAA; Data: Ryerson, Neuman, Parrish et al.-NOAA.

The observation-based approach selected is based upon the relationships between indicator species developed by S. Sillman (http://www-personal.engin.umich.edu/~sillman/obm.htm). This approach was selected because: 1) it addresses integrated total O$_3$ produced (not instantaneous rate of O$_3$ production), and is thus designed to answer the question of how maximum O$_3$ responds to changes in VOC versus changes in NO$_x$ emissions; 2) it is arguably the most fully developed observation-based method and is widely used; 3) it is related to the ozone production efficiency relationships exemplified in Figures A3 and A4 of this report; and 4) it utilizes measurements made with high precision and accuracy on the Electra aircraft during TexAQS 2000 and the WP-3D and *Ronald Brown* during TexAQS 2006.

Figure F4 compares the measurements made from the Electra during TexAQS 2000 with the modeled indicator species relationships of Sillman. These two relationships are those he discusses most thoroughly. The data shown include all 5-second average measurements made in the greater Houston area (94.3-96.3 deg. E Long., 28.7-30.7 deg. N. Lat.), which includes the entire urban area, all petrochemical facilities including the isolated Gulf Coast facilities, and the Parish power plant.
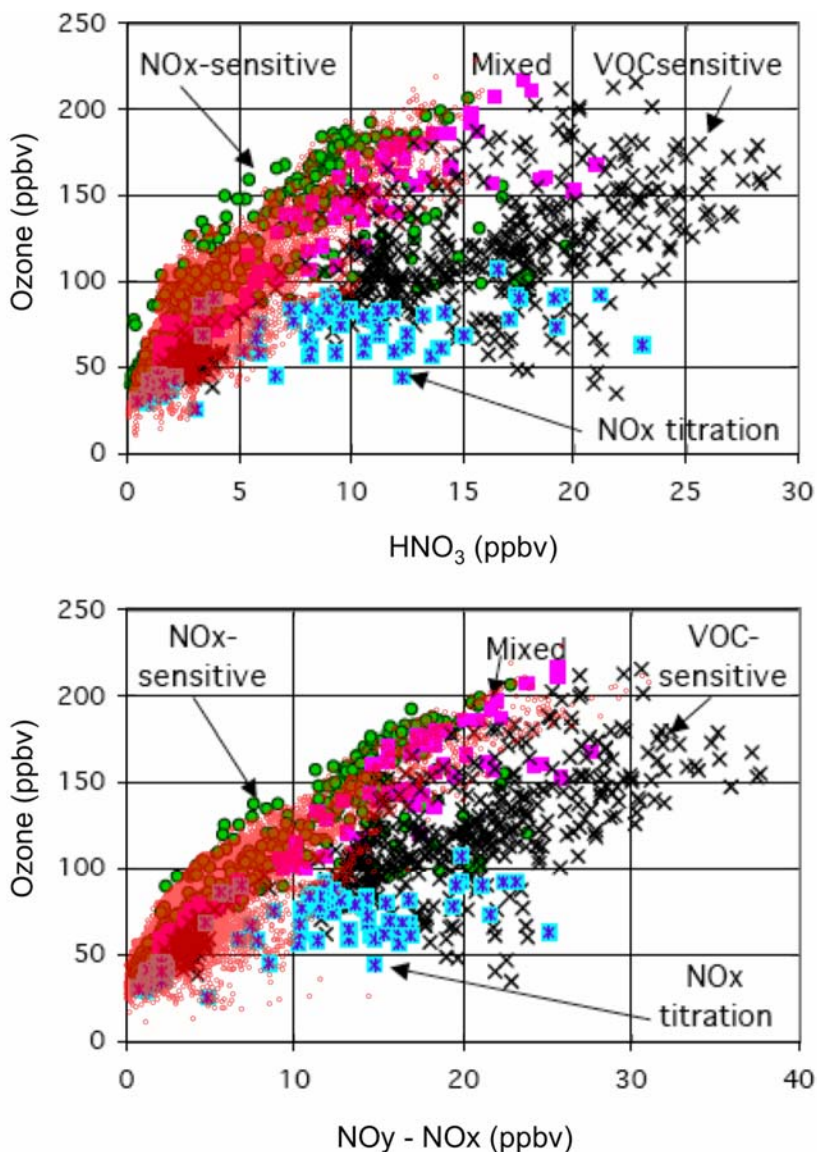

Figure F4. Indicator species relationships from models [Sillman] and from the TexAQS 2000 Electra measurements (red symbols). The relationships expected for NO$_x$-, mixed-, and VOC-sensitive ozone production are given by green, violet and black symbols, respectively. The blue highlighted symbols indicate air masses dominated by NO$_x$ titration.

The indicator species relationships in Figure F4 give ambiguous results. In both figures most of the data are localized in the predominately NO_x-sensitive region, but some points are in the mixed and predominately VOC-sensitive regions. Further, the model results themselves are interspersed between regions. Definitive conclusions cannot be drawn from these figures. This ambiguity is particularly clear in the examination of ozone data above 200 ppbv. These data were collected on three days in 2000: 25 and 30 August and 1 September (see Figure A3). The relationship of ozone with HNO_3 suggests that all three days represent NO_x-sensitive conditions, while the relationship of ozone with NO_y - NO_x suggests that the three days span the full range from NO_x-sensitive to VOC-sensitive. It is clear that no definitive conclusions can be drawn. It may be that the indicator species relationships may be most useful as a basis of comparison of models with measurements.

***Finding F3*: At the highest ozone concentrations, the observed relationship between ozone and the products of NO_x oxidation indicates less efficient ozone production in the Dallas area than in the Houston area. In the observation-based indicator species approach, this behavior corresponds to less NO_x-sensitive and more VOC- or radical-sensitive ozone formation in Dallas compared to Houston.**

Analysis: Parrish-NOAA; Data: Ryerson, Neuman, Parrish et al.-NOAA.

Figure F5 shows the relationships between ozone and the oxidation products of NO_x. These oxidation products include only nitric acid on the left plot and nitric acid plus organic nitrates on the right plot. The generally shallower slopes in the Dallas area indicate less efficient ozone production in that area. From an observation-based indicator approach, this behavior corresponds to less NO_x-sensitive and more VOC- or radical-sensitive ozone formation in Dallas compared to Houston.
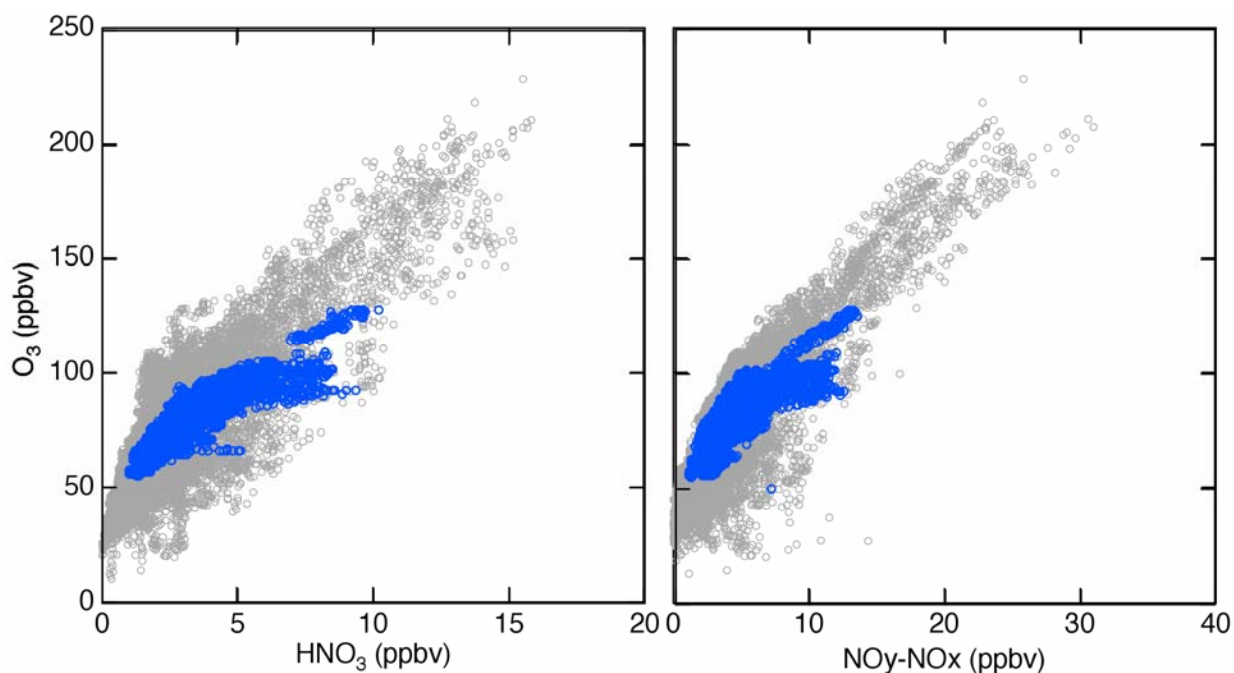

Figure F5. Indicator species relationships from the TexAQS 2000 Electra measurements. The gray and blue symbols indicate data collected in the Houston and Dallas areas, respectively.

***Finding F4*: Tests of the ability of models to reproduce observed relationships between ozone and other photochemical products have the potential to provide very fruitful approaches to improving models.**

Analysis: Parrish-NOAA; Modeling: TCEQ; Kim et al.-NOAA.

Relationships between ozone and other photochemical products, such as those illustrated in Figure F5, have been found to be remarkably robust in observations. Examination of the ability of models to reproduce these observed relationships is expected to provide powerful tests of the models' performance and to suggest possible model improvement. Figures F6 and F7 give some example model output for the relationships of O_3 with HNO_3 and with NO_y-NO_x. The figures are plotted in the same format as the observations in Figure F5 for ease of comparison.

The results of the WRF-Chem model (Figure F6), which covers most of the continental U.S. at relatively coarse (27 km x 27 km) resolution (Kim et al, 2006), shows some similarities and differences when compared to the observations (Figure F5). The model produces relatively well defined relationships, but the slopes of the relationships are significantly smaller than those observed. There is no marked difference in the modeled relationships in the different regions of eastern Texas. The very high O_3 concentrations observed in the Houston area are not reproduced by the model. Significantly higher resolution, particularly over the urban areas, is an avenue of model development that would be expected to improve the model performance. Further, the HRVOC emissions for the petrochemical facilities are undoubtedly underestimated in these calculations, since they are based upon the NEI 1999 emission inventory.

The TCEQ modeling results (Figure F7) are focused on the HGB region with much higher resolution, and generally give a better reproduction of the observed relationships. The slopes of the relationships through the majority of the data are accurately reproduced. However, there is an indication that the slopes decrease at the highest O_3 concentrations, so that the highest modeled O_3 concentrations are significantly lower than those observed. One explanation that has been suggested for this behavior is that the HRVOC emissions are underestimated in the model emissions and/or that they are not properly collocated with the NO_x emissions from the petrochemical facilities. The model also predicts relatively low concentrations of O_3 at relatively high concentrations of HNO_3 and NO_y-NO_x. Such behavior is not seen in the observations. The cause of the disagreement in these few points should be investigated.
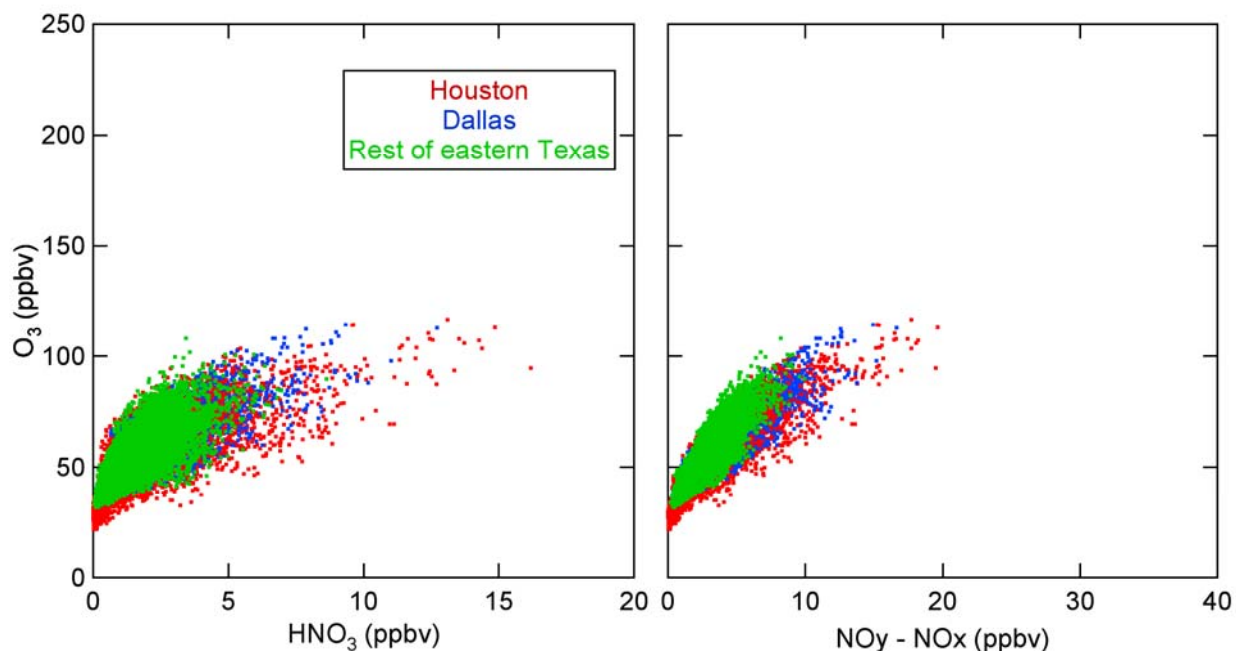
Figure F6. Indicator species relationships calculated by the WRF-Chem model for 2000 UTC each day between 1 April and 31 October 2004. The color coding indicates results for different areas of eastern Texas.
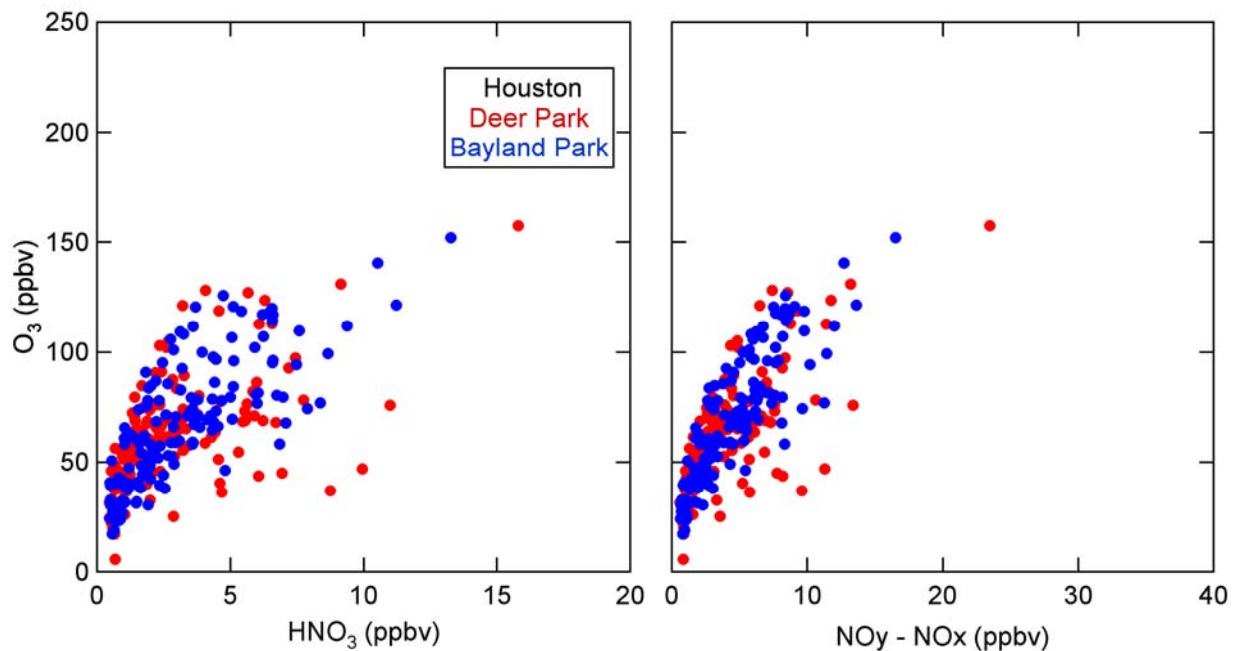
Figure F7. Indicator species relationships derived from 2006 modeling by TCEQ with the Base 1b configuration. The data points include all hours, 12:00-18:00 local time, on the days between 16 August and 6 September 2000. The color coding indicates two different monitoring sites in the HGB area.

KEY CITATIONS AND INFORMATION AND DATA SOURCES

Kim, S.-W., A. Heckel, S.A. McKeen, G.J. Frost, E.-Y. Hsie, M.K. Trainer, A. Richter, J.P. Burrows, S.E. Peckham, and G.A. Grell. 2006. Satellite-observed U.S. power plant NO_x emission reductions and their impact on air quality. Geophys. Res. Lett. 33, L22812, doi:10.1029/2006GL027749.

Sillman, S. Observation-based methods (OBMs) for analyzing urban/regional ozone production and Ozone- NO_x-VOC sensitivity (http://www-personal.engin.umich.edu/~sillman/obm.htm)

TCEQ. 2004. Houston-Galveston-Brazoria Mid-Course Review SIP Appendixes (2004-042-SIP-NR). http://www.tceq.state.tx.us/implementation/air/sip/dec2004hgb_mcr.html

TCEQ. 2006. Weekday-Weekend Effect Analysis, Part Two. Presented by Jim Smith, June 8, 2006. http://www.tceq.state.tx.us/assets/public/implementation/air/am/committees/pmt_set/20060621/20060621-smith-weekday_weekend_effects_part2.pdf

Wert, B.P., M. Trainer, A. Fried, T.B. Ryerson, B. Henry, W. Potter, W.M. Angevine, E. Atlas, S.G. Donnelly, F.C. Fehsenfeld, G.J. Frost, P.D. Goldan, A. Hansel, J.S. Holloway, G. Hübler, W.C. Kuster, D.K. Nicks Jr., J.A. Neuman, D.D. Parrish, S. Schauffler, J. Stutz, D.T. Sueper, C. Wiedinmyer, and A. Wisthaler. 2003. Signatures of terminal alkene oxidation in airborne formaldehyde measurements during TexAQS 2000. J. Geophys. Res., 108(D3), 4104, doi:10.1029/2002JD002502.

Response to Question G

QUESTION G

How do emissions from local and distant sources interact to determine the air quality in Texas?

What meteorological and chemical conditions exist when elevated background ozone and aerosol from distant regions affect Texas?

How high are background concentrations of ozone and aerosol, and how do they vary spatially and temporally?

BACKGROUND

Question G is closely related to Question H. Here Question G focuses on characterizing the background ozone and aerosol distributions, and the chemical and physical processes that affect the background concentrations of ozone and aerosol in Texas. Question H focuses on the transport processes and source-receptor relationships of those background concentrations.

FINDINGS

Finding G1: **The maximum background ozone concentrations encountered in 2006 exceeded the 8-hour NAAQS. On average, air of continental origin had higher background concentrations than marine air. The average background ozone concentrations measured in 2006 in eastern Texas complement a previously developed climatology.**

Analysis: Senff et al.-NOAA, Sullivan et al.-U. Texas; Data: Senff et al.-NOAA, TCEQ.

Daily 8-hour-average ozone maxima from upwind suburban or rural sites are taken as indicators of the local background in a particular region. In Figure G1, the red line segments indicate the average background for four areas in Texas on days in April – July 2006 when the area maximum 8-hour average reached or exceeded 80 ppbv. These segments are higher than the corresponding average curves, which were compiled for all days, not just the higher ozone days. The marine influence in the Houston area accounts for the lower background (49 ppbv) compared to the Dallas (63 ppbv), Beaumont (61 ppbv), and Northeast Texas (60 ppbv) areas.

The NOAA lidar provided a different approach for obtaining mesoscale estimates of background ozone for four regions in eastern Texas: 1) offshore over the Gulf of Mexico, 2) Gulf of Mexico coastal areas (less than 50 km from shore), 3) southeast Texas including Houston (all of southeast Texas more than 50 km from shore), and 4) northeast Texas including Dallas. Background ozone was determined by averaging lidar ozone profiles between the surface and the top of the boundary layer over all data points that were identified to be outside of pollution plumes. The blue line segments in Figure G1 indicate the background ozone values for the four regions identified above using measurements from all suitable lidar flights. The average background values for the southeast Texas and Gulf coast areas compare well with the Houston area background on high-ozone days (red line segment). The northeast Texas lidar background ozone value is close to the Dallas and northeast Texas TCEQ network-based background values for high-ozone days. This good agreement is not surprising because the lidar was typically flown on days when an ozone exceedance was forecast. The average ozone background measured over the Gulf of Mexico was the lowest of all four areas (39 ppbv) and is close to the average curves for Houston-Galveston-Brazoria (HGA) and Beaumont-Port Arthur (BPA) for the 1 August to 15 September period of the measurements. The highest observed ozone background value was 86

ppbv measured on 8 September in east central Texas near the Louisiana border, after several days of continuous easterly flow conditions.
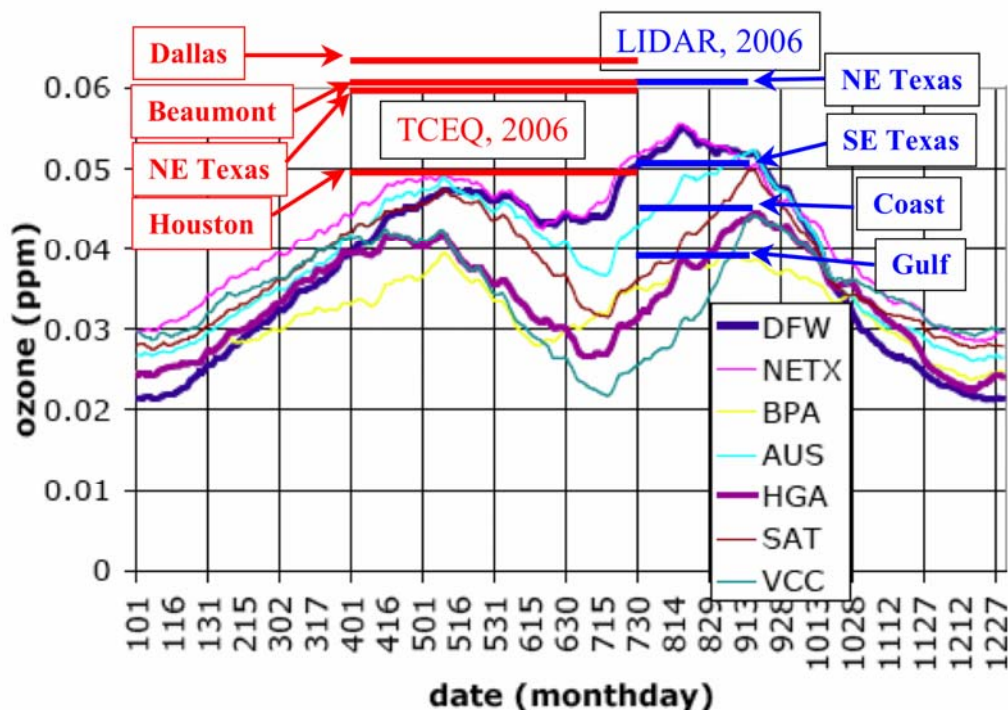

Figure G1. Continuous curves give six-year (1998-2003) average background ozone in various regions in eastern Texas, smoothed with a 31-point running mean filter (Nielsen-Gammon et al., 2005). The blue (lidar data) and red line segments (TCEQ surface network data) indicate 2006 background ozone determinations with greater emphasis on exceedance days. The widths of the line segments approximately indicate the periods considered in 2006.

A characterization of synoptic flow based on classes of regional ozone concentrations showed higher background ozone concentrations under continental air compared to maritime air. Twelve sites were selected for completeness of data coverage (>75% each year in August and September from 2001 to 2006) and regional representation (one site per county, except for two in Harris County). Each of the days included in this data set was classified as "high regional ozone," if and only if four or more stations reported maximum 8-hour-average O_3 of 75 ppbv or higher, (this included 40 days) or "low regional ozone," if and only if all stations reported maximum 8-hour-average O_3 of at least 40 but less than 50 ppbv (this included 43 days). The probability distributions for the 1-hour time step points of the HYSPLIT back trajectories (72-hour, 300 meter above ground level/mid-day starting point) for the twelve sites are given in Figure G2. On "low regional ozone" days air parcel trajectories tended to cluster to the south and southeast with relatively longer fetches from the Gulf of Mexico, while on "high regional ozone" days the trajectories cluster to the northeast with relatively short fetches, indicating transport from within eastern Texas or from areas to the northeast of Texas.
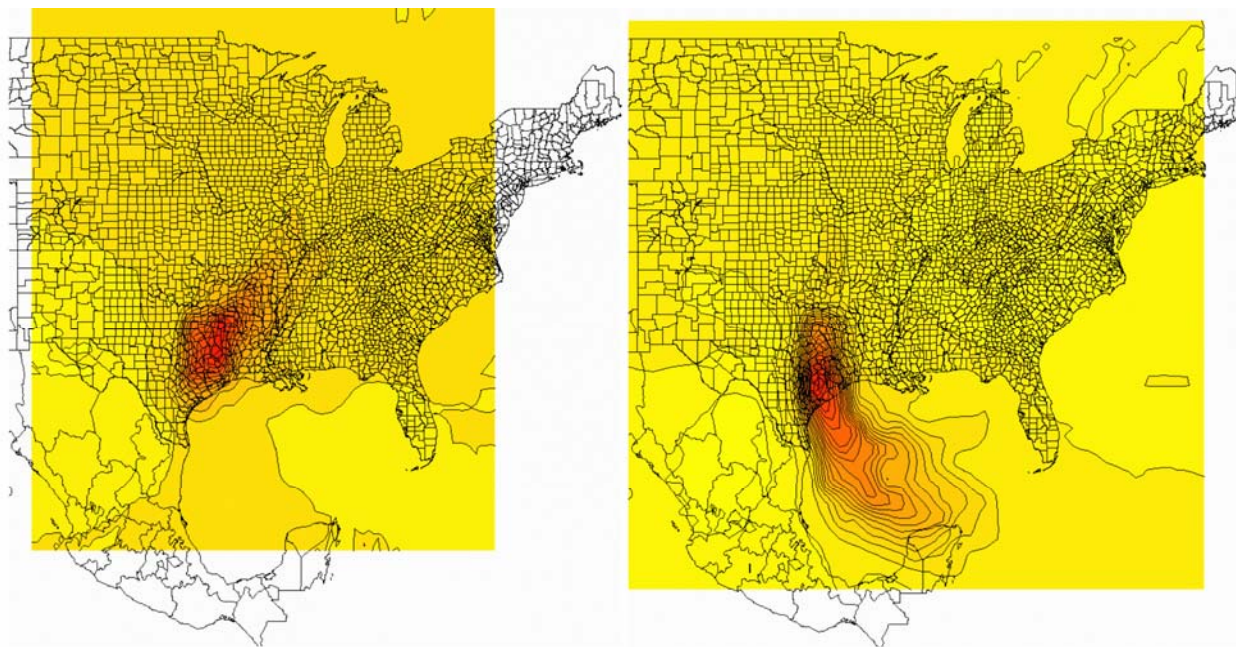
Figure G2. Contour plots showing the probability distribution of origins of 72-hour HYSPLIT back trajectories ending at 12 representative TCEQ surface ozone monitoring stations in eastern Texas. Red color denotes high probability, yellow indicates low probability. Left panel: high regional ozone days; right panel: low regional ozone days.

Finding G2: **The net ozone flux transported out of Houston averages about a factor of two to three larger than the corresponding flux from Dallas. The fluxes from these urban areas are significant contributors to the background ozone in the eastern Texas region.**

Analysis: Senff et al.-NOAA, Sullivan et al.-U. Texas; Data: Senff et al.-NOAA, TCEQ.

The horizontal flux of O_3 downwind of Houston and Dallas during TexAQS 2000 and TexAQS 2006 was calculated from airborne lidar measurements of O_3. The O_3 flux was computed by vertically integrating excess O_3 concentration in the plume (plume O_3 minus background O_3) between the surface and the top of the boundary layer and horizontally between the plume edges (see Figure G3 for example of a plume cross section). The integrated plume excess O_3 concentration was then multiplied by the horizontal wind speed (estimated from nearby wind profilers) to yield O_3 flux, which is expressed in molecules per second. Using data from the TexAQS 2000 and 2006 studies, fluxes were computed for the Houston area on five days (8/28 and 9/06/2000; 8/12, 8/14, and 8/30/2006) and the Dallas/Fort Worth area on one day (9/13/2006). The ozone flux from Houston ranged from $3.2 * 10^{26}$ to $6.0 * 10^{26}$ molec s^{-1}, and - within the uncertainties - was similar for the 2000 and 2006 cases. The average ozone flux from Houston of $4.6 * 10^{26}$ molec s^{-1}, emitted over the 8-hour photochemically active part of one day, is sufficient to produce a 10-ppbv increase in ozone over an approximately 10,000 square mile area, assuming a 2-km deep boundary layer. The flux for the one Dallas case was estimated as $1.7 * 10^{26}$ molec s^{-1}, about a factor of two to three smaller than that observed for Houston. Although this comparison is based on only one flux determination for Dallas, we expect this comparison to generally hold, since Dallas lacks the large ozone production from the petrochemical industry, which accounts for a large fraction of the ozone production in Houston.
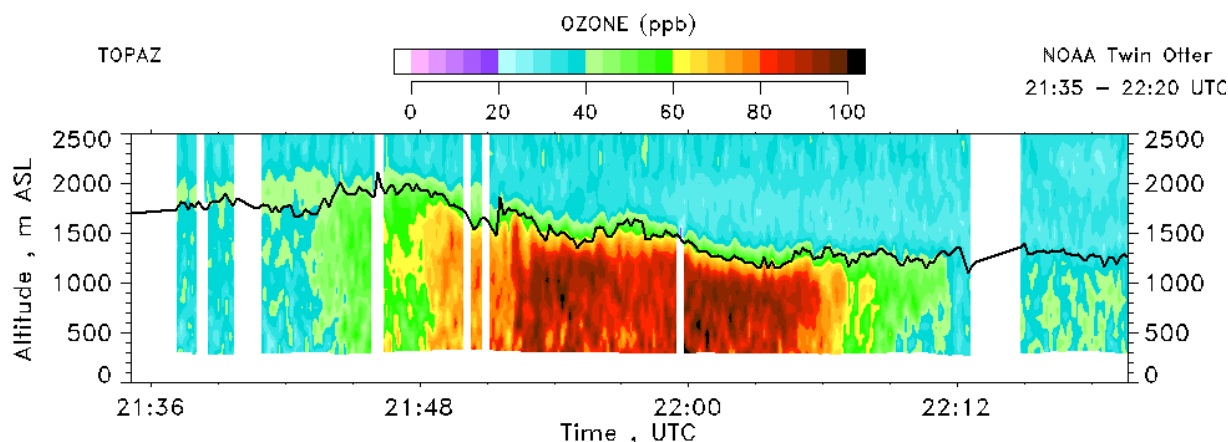
Figure G3. Time-height cross section of ozone plume about 50 km downwind of the Houston and Ship Channel area measured with NOAA's airborne ozone lidar on 8/14/2006 at about 17:00 CST. Note the strong variation of mixing height (shown as black line) across the plume.

As a complement to airborne lidar data, which are only available for rather short time periods, a similar assessment was performed using data from TCEQ's surface ozone monitoring network to estimate horizontal ozone fluxes. The horizontal plume integral was calculated from ozone measurements at downwind surface sites. The ozone was assumed constant through the mixed layer and the vertical plume extent was estimated from mixed layer height measurements from nearby wind profilers. For the days of the lidar analysis the differences between lidar- and surface-network-based flux estimates were generally on the order of 20 to 25%, except for one case where the difference was nearly 60%. This one large discrepancy may be due to uncertainties in the estimation of mixing height and horizontal plume dimensions when using surface network data. The agreement between the airborne lidar and surface monitoring results suggests that routine flux assessments using surface data may be useful.

Finding G3: **Elevated background ozone concentrations for urban areas can include contributions from the recirculation of locally produced ozone or local precursor emissions.**

Analysis: Ryerson et al.-NOAA, Sullivan et al.-U. Texas; Data: Ryerson et al.-NOAA, TCEQ.

Background ozone concentrations entering an urban area can be elevated by recirculation of the ozone produced in that same urban area on a previous day, or by ozone production from precursors emitted within that urban area and recirculated. A past example provided by TCEQ is a May 31, 2003 episode in DFW, for which O_3 concentration contours at mid-afternoon are shown in Figure G4. In this event, the one-hour-average peak O_3 was 161 ppbv, with the eight-hour-average peak at 130 ppbv. The event was influenced by a stalled frontal passage – note the contrasting direction at the wind vanes associated with monitoring sites on the north side versus the south side of DFW. The color code for ozone concentrations in the figure is: Gray 85-99 ppbv, Orange 100-124 ppbv, Red 125-149 ppbv, Purple > 149 ppbv.
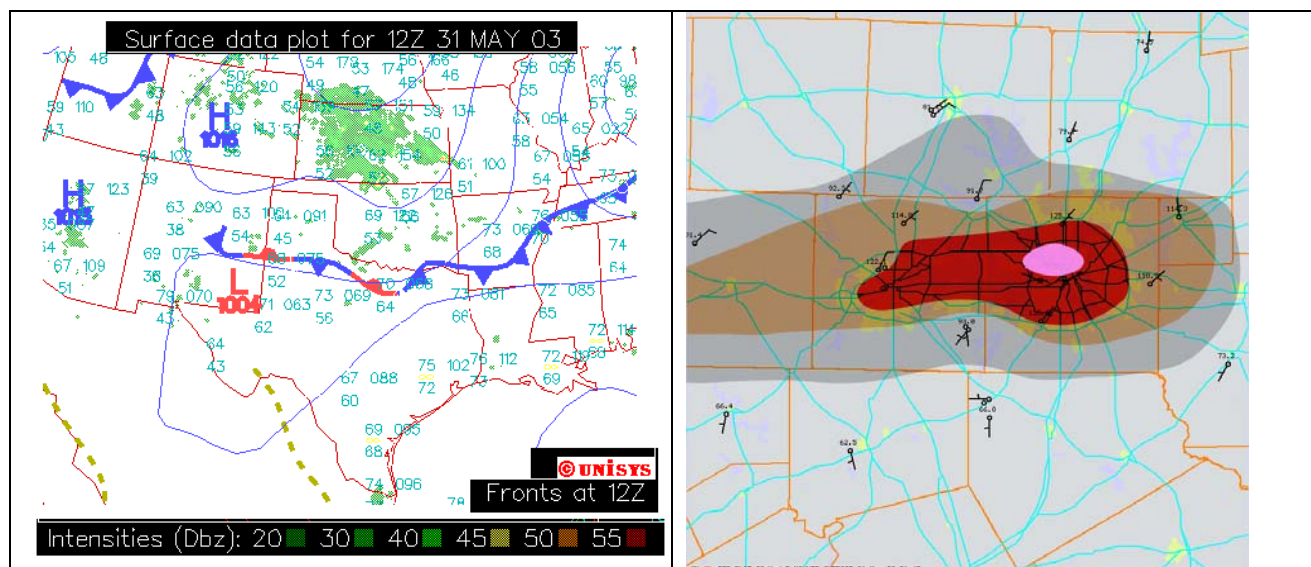
Figure G4. (Left) Surface weather map for 6 CST 31 May 2003 shows stalled front in north Texas (http://weather.unisys.com/archive/index.html). (Right) Mid-day contour of O_3 concentrations shows "pancake" of elevated O_3 between Dallas and Fort Worth. Wind barbs show northerly winds north of the city and southerly winds south of the city, trapping local pollution (TCEQ, 2003).

A recirculation example was observed in the Houston area during TexAQS 2006 (Figure G5). On 26 September the Houston plume with ozone concentrations approaching 120 ppbv was carried to the southeast by the prevailing winds. On the following day, winds from the south brought air from over the Gulf of Mexico into the Houston area. However, this background air contained ozone concentrations much higher (64 to 84 ppbv, average 74 ppbv) than the more characteristic concentrations of about 40 ppbv (see Figure G1). These elevated ozone concentrations were accompanied by elevated concentrations of other photochemical products (e.g. formaldehyde and nitric acid) and CO, a tracer of primary emissions.
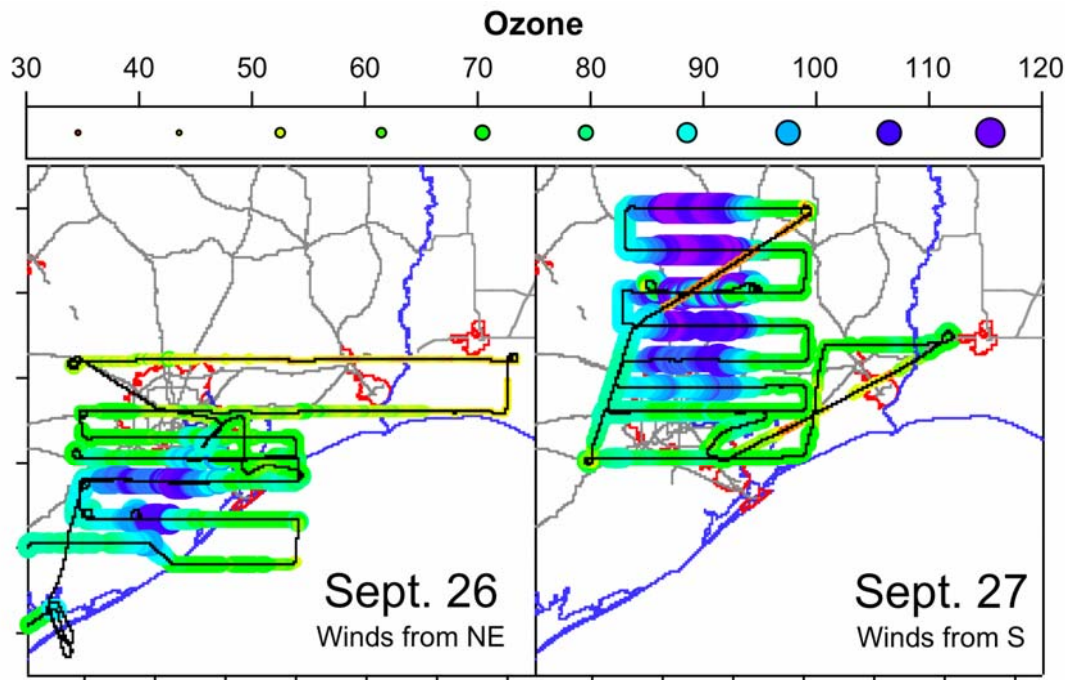
Figure G5. WP-3D flight tracks within the boundary layer in the HGB area on two successive flights color-coded and sized according to the measured O$_3$ concentration.

Results from FLEXPART particle dispersion modeling (Figure G6) and back-trajectories calculated from wind profiler data (not shown) both indicate that the elevation in background ozone concentrations on 27 September were due to recirculation of the 26 September Houston area plume back into the HGB region.
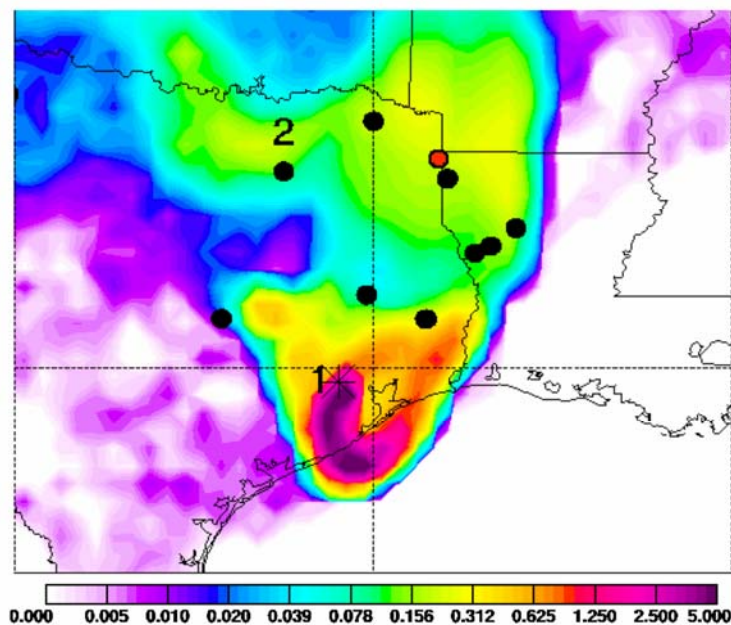
Figure G6. Footprint emission sensitivity for air sampled by WP-3D on 27 September at the position marked by the asterisk. The integral of the product of this quantity with the surface emission density gives the expected concentration that would be measured at the aircraft position. The numerals 1 and 2 indicate days of backward transport time. The near coincidence of the asterisk and the numeral 1 indicates that emissions from 26 September have been returned to near the original emission location. The shape of the red to violet colors indicates the primary transport pathways. The color scale is logarithmic in arbitrary units.

***Finding G4*: Plumes from Texas urban areas make substantial contributions to the ozone, aerosol, and precursor concentrations in the rural regions of eastern Texas.**

Analysis: Brock et al.-NOAA, Data: Middlebrook, de Gouw et al.-NOAA.

Figure G7 shows one example of model output and measurements of transported plumes of emissions and their photochemical products from the Houston area to northeastern Texas. The model results are from the FLEXPART Lagrangian particle dispersion model, and the measurements are from the WP-3D aircraft on 16 September 2006. There is excellent agreement between the model and the measurements, with both showing that the SO_2 plume, primarily from the Parish power plant, was transported parallel and to the west of the NO_x and benzene plumes, primarily from the Houston urban and Ship Channel areas. Table G1 shows that these plumes significantly increased the total aerosol concentrations in rural northeast Texas (for reference, the NAAQS for $PM_{2.5}$ aerosol are 15.0 $\mu g\ m^{-3}$ annual mean, and 35 $\mu g\ m^{-3}$ 24-hour mean).

Table G1. Measured concentrations of aerosol and gas phase species in the Parish power plant and Houston area plumes in northeast Texas.

	Background	Parish	Petrochemical Industry
Total mass ($\mu g\ m^{-3}$)	4.3	7.9	5.7
Sulfate ($\mu g\ m^{-3}$)	1.9	4.7	2.0
Organic ($\mu g\ m^{-3}$)	1.2	1.9	2.3
Black Carbon ($\mu g\ m^{-3}$)	0.08	0.12	0.17
Benzene (ppbv)	0.094	0.103	0.26
SO_2 (ppbv)	0.29	0.97	0.53
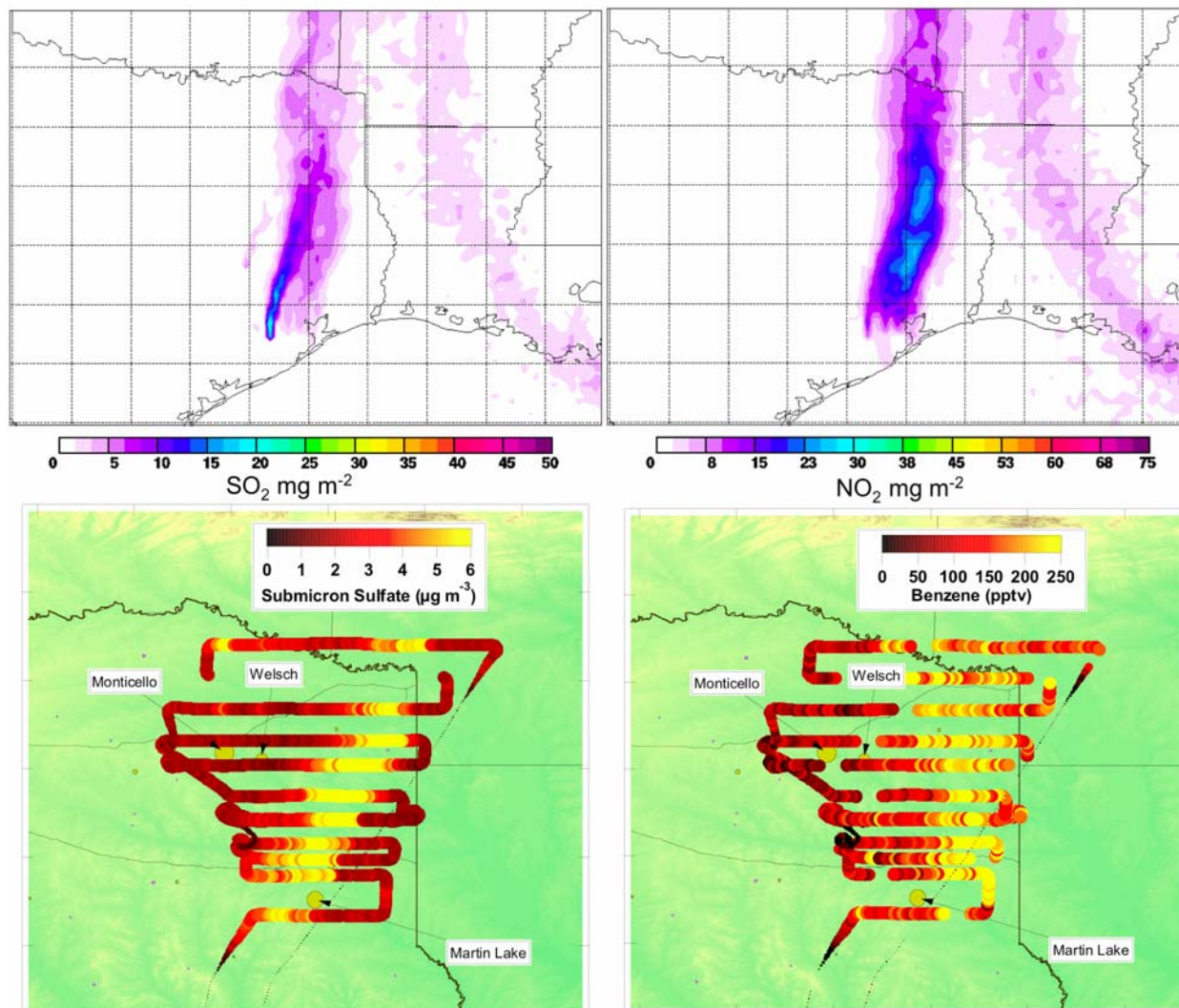
Figure G7. Modeled and measured concentrations of aerosol and gaseous species in transported plumes from the Houston area to northeast Texas. The upper panel shows the FLEXPART model calculations (Cooper et al.–NOAA) for SO_2 (primarily Parish power plant) and NO_x (primarily HSC) plumes, and the lower panel shows the measurements from the WP-3D of sulfate aerosol and benzene concentrations. A plume of sulfate aerosol associated with the Parish power plant SO_2 emission plume is evident in the measurements, as is a plume of benzene associated with HSC emissions. (Lower panel covers only a fraction of the area in the upper panel.)

Finding G5: **Dust of African origin and sulfate aerosol advected into the Houston area, under southerly flow conditions from the Gulf of Mexico, can make significant contributions to the background aerosol in the eastern Texas region.**

Analysis and Data: Bates and Quinn–NOAA.

Figure G8 summarizes 2006 aerosol chemical composition measurements made on the *Ronald H. Brown* in the Houston area. The onshore southerly flow of background aerosol (low radon concentrations indicating no contact with land for several days) was substantially impacted by Saharan dust and what appear to be ship emissions (acidic sulfate and nitrate). Mean (median) mass concentrations of the total submicrometer and supermicrometer aerosol were 6.5 (4.6) µg m^{-3} and 17.2 (8.7) µg m^{-3}, respectively. These mass loadings of "background" aerosol are much higher than typically observed in the marine atmosphere, and are large enough to substantially impact the PM loading in the Houston-Galveston area. The integrated PM$_{2.5}$ mass at ambient relative humidity (Figure G9) includes the accumulation mode (primarily acidic sulfate and dust under southerly flow conditions, seen in Figure G8) and part of the coarse mode (primarily sea salt, dust, and the acidic nitrate and sulfate absorbed by these basic components seen in Figure G8). The average PM$_{2.5}$ mass advecting into the Houston-Galveston area during TexAQS 2006 was 19 ± 11 µg m^{-3} (Figure G9). Aerosol composition and mass size distributions during northerly flow conditions are shown in Figures G8 and G9 for comparison with the "background" southerly flow. Air quality forecast models need to include ship emissions and dust transport to correctly characterize aerosol loadings in SE Texas. Compliance with PM$_{2.5}$ regulations in the Houston-Galveston area may require stricter controls on upwind aerosol sources (e.g. ship emissions).
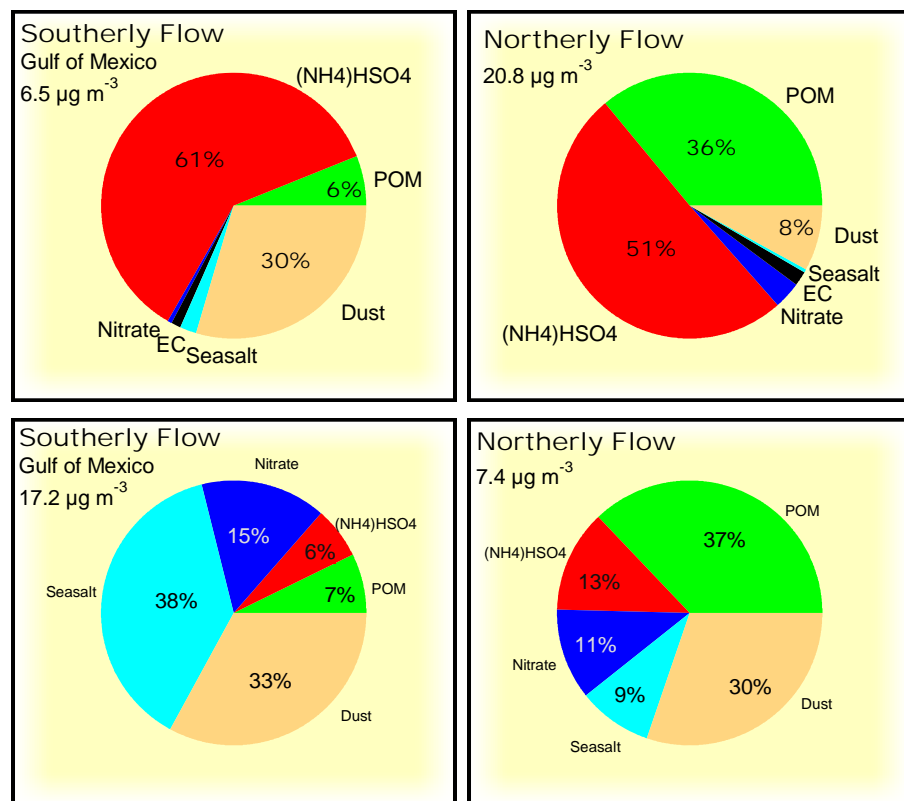

Figure G8. Average submicrometer (top) and supermicrometer (bottom) aerosol composition in the marine boundary layer, measured (at 60% RH) from the *Ronald H. Brown* in TexAQS 2006 during periods of southerly and northerly flow.
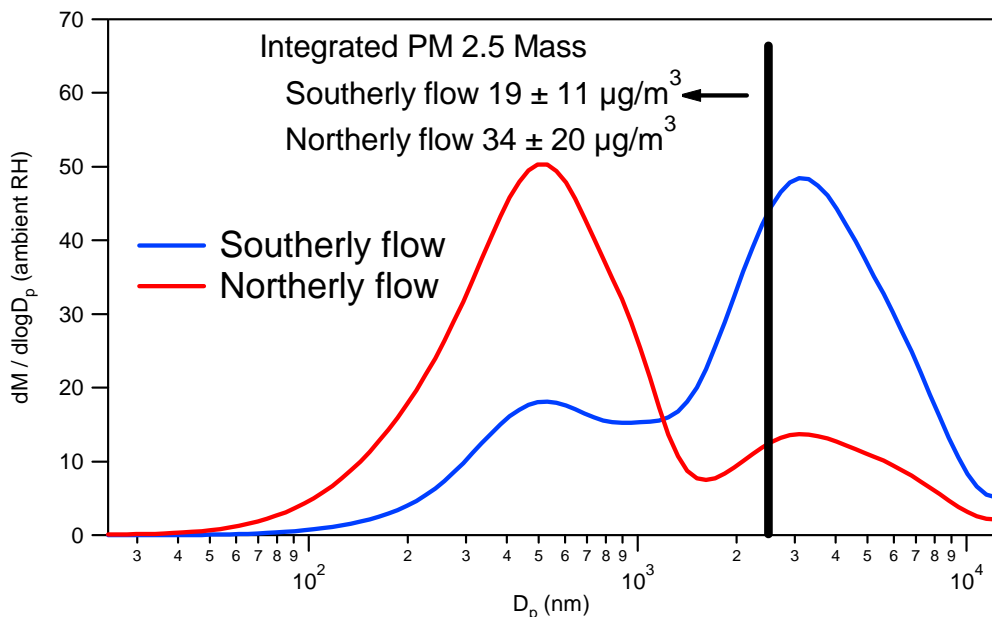
Figure G9. Average aerosol mass size distributions at ambient relative humidity measured from the *Ronald H. Brown* during TexAQS 2006.

Finding G6: Nighttime chemistry influences the availability of oxides of nitrogen (NO$_x$), highly reactive VOC (HRVOC), and O$_3$.

Analysis and Data: Brown et al.-NOAA.

Nocturnal measurements of key nitrogen oxide species, nitrate radical (NO$_3$) and N$_2$O$_5$, were made on the *Ronald H. Brown* and WP-3D. These compounds are important to regional air quality because their formation and subsequent reactions affect the nocturnal loss rates for NO$_x$, O$_3$, and HRVOC. Analysis of the measured NO$_3$ and N$_2$O$_5$ led to the following conclusions.

- Hydrolysis of N$_2$O$_5$, typically the most important reaction in the nocturnal conversion of NO$_x$ to HNO$_3$, was generally inefficient in air masses sampled aloft around Houston and elsewhere in Texas. As a result, NO$_x$ emissions occurring late in the day or at night could be transported overnight in the form of N$_2$O$_5$ to regions distant from the NO$_x$ source regions. Transport of O$_3$ was also efficient since N$_2$O$_5$ is a reservoir for odd oxygen (O$_x$) as well. This transport may affect O$_3$ concentrations well downwind of major urban and industrial areas on the following day (Figure G10).

- The reduced rate of N$_2$O$_5$ hydrolysis aloft in Houston, and the relatively warm temperatures in this area, enhanced the availability of NO$_3$ as an oxidant. This was important in plumes containing both NO$_x$ and HRVOC from industrial sources in Houston. Observed nocturnal loss rates for HRVOC due to reaction with NO$_3$ from plumes originating in the Houston Ship channel were 0.5 – 4 ppbv hr^{-1} (Figure G11).

- Surface measurements of N$_2$O$_5$ from the *RHB* and vertical profiling to low altitude from the WP-3D indicated more rapid loss rates for N$_2$O$_5$ near the surface than aloft, possibly arising from concentration of sinks for NO$_3$ and N$_2$O$_5$ from emissions within the shallow nocturnal boundary layer.
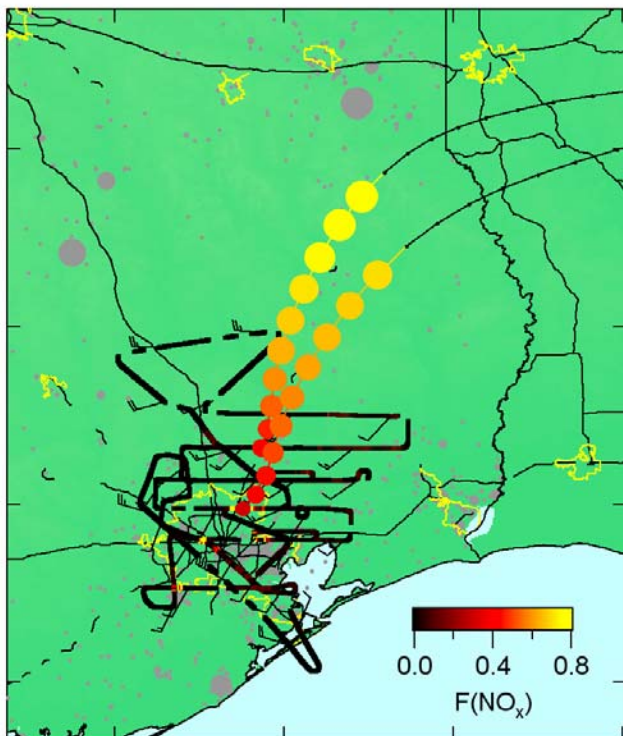
Figure G10. Fraction of NO_x $[F(NO_x) = (NO_3 + 2N_2O_5)/(NO_2 + NO_3 + 2N_2O_5)]$ present in the form of N_2O_5 and predicted to be transported overnight from the Parish power plant near Houston to northeast Texas, based on the observed N_2O_5 loss rates within the plume sampled in the Houston area and a forward overnight meteorological trajectory. The WP-3D flight track is color coded by $F(NO_x)$ and the forward trajectory is color and size coded by the predicted $F(NO_x)$ during transport. Sunrise for the trajectories occurs over east central Texas where $F(NO_x)$ quickly drops to zero, indicating re-conversion of N_2O_5 to NO_x and O_3 in a rural area.
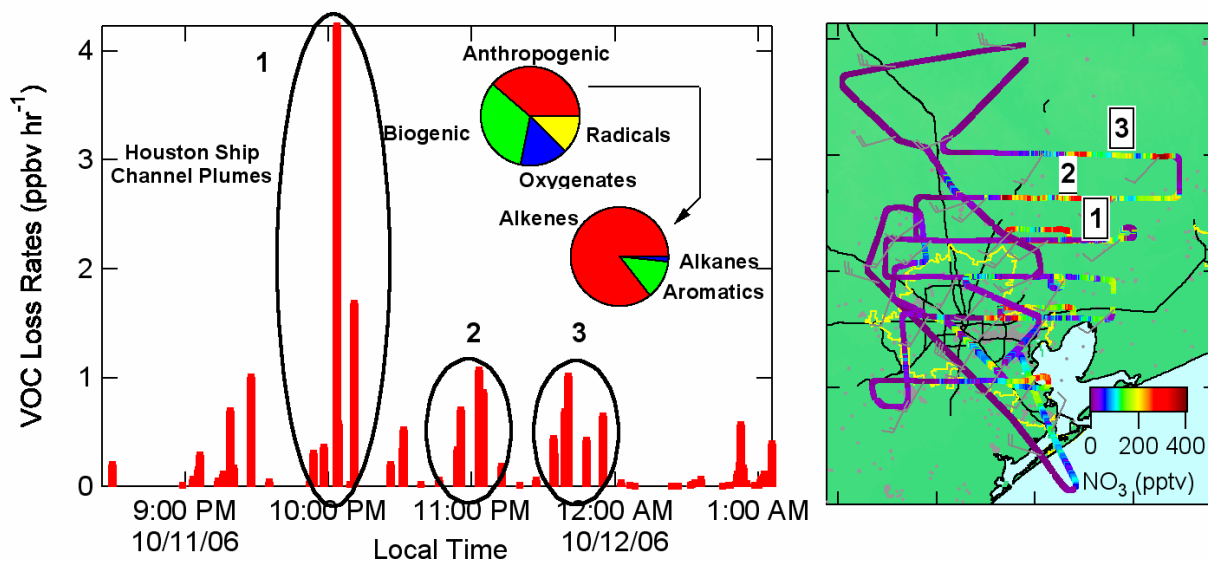
Figure G11. Total VOC loss rates due to reaction with NO_3 measured from the WP-3D on 11-12 October 2006. The flight track in the map is color-coded by NO_3 mixing ratio; these values are among the largest ever observed. The pie chart insets show the relative contributions to NO_3 loss on this flight and the relative contribution of NO_3 loss to anthropogenic VOC, which is dominated by the reaction with alkenes. Apparent "Biogenic" NO_3 losses on this chart are dominated by isoprene from anthropogenic sources.

Finding G7: **Low rural nighttime ozone concentrations have been observed at some, but not all, rural locations in northeast Texas; these low nighttime ozone concentrations are not replicated in the regulatory modeling.**

Analysis: Sullivan et al.-U. Texas; Data: TCEQ.

Photochemical models fail to reproduce the low nighttime ozone concentrations observed at some rural sites in northeast Texas (Figure G12). Possible causes of this discrepancy include the presence of: 1) shallower nighttime boundary layers than predicted by the model at the affected sites, and 2) larger local NO emissions than included in emission inventories. If the latter is the cause, then corrections to the emissions inventory are needed to accurately assess NO_x concentrations and atmospheric chemistry upwind of northeast Texas cities and the DFW area. Compressors at well-heads and on pipelines emit NO_x, and are potential sources of local NO emissions that may be underestimated in inventories. The map in Figure G12 shows that northeast Texas is a region of intense natural gas exploitation. Four other monitors in that area also consistently show lower than expected nighttime O_3 concentrations.
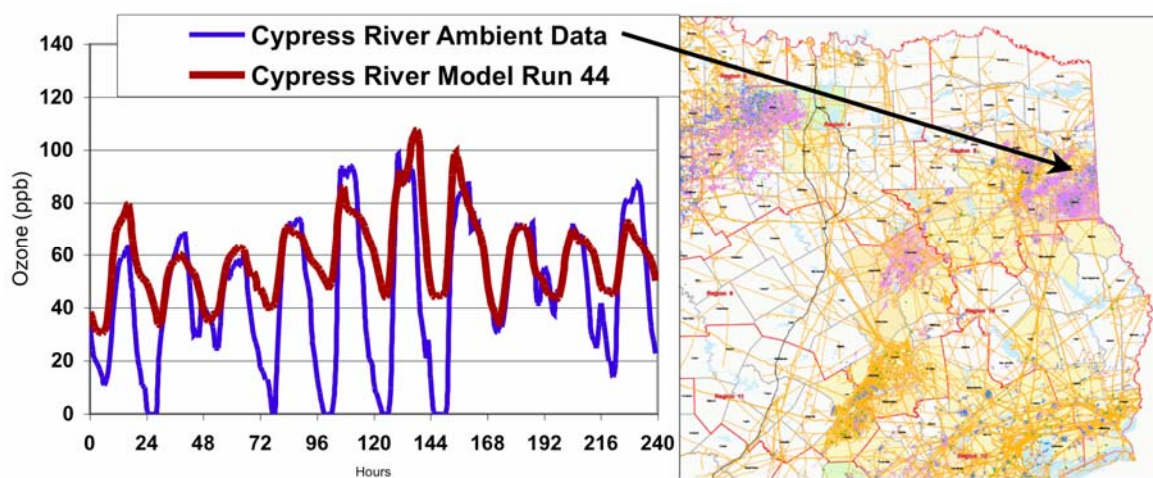
Figure G12. Time series of ozone concentrations for 19-22 August 1999, an episode included in the DFW SIP modeling (left). Ambient data at the Cypress River site in northeast Texas are compared with modeling results. The map shows natural gas well regions color-coded for production (right), and the arrow locates the Cypress River site.

KEY CITATIONS AND INFORMATION AND DATA SOURCES

Nielsen-Gammon, J.W., J. Tobin, A. McNeel, and G. Li. 2005. A Conceptual Model for Eight-Hour Ozone Exceedances in Houston, Texas - Part I: Background Ozone Levels in Eastern Texas. HARC Report No. H012.2004.8HRA, January 29, 2005. http://www.harc.edu/Projects/AirQuality/Projects/Projects/H012.2004.8HRA.

Response to Question H

QUESTION H
Which areas within Texas adversely affect the air quality of non-attainment areas in Texas?
Which areas outside of Texas adversely affect the air quality of non-attainment areas in Texas?

BACKGROUND
Question H is closely related to Question G. Here Question H focuses on the source-receptor relationships that determine the background concentrations of ozone and aerosol in Texas and the meteorologically driven transport processes. Question G focuses on characterizing the background concentrations and the chemical and physical processes that affect those background concentrations.

FINDINGS

Finding H1: **Ozone can be transported into the Dallas area from the Houston area.**

Analysis and Data: Senff et al.-NOAA.

An example of direct transport of ozone from Houston to Dallas was observed during TexAQS 2006 and is depicted in Figures H1 and H2. During 4–8 September 2006, there was a regional buildup of background ozone in eastern Texas, indicated by Dallas-Fort Worth (DFW) surface station ozone monitors (not shown) and airborne ozone lidar measurements (Figure H1). From 4–7 September, large-scale winds tended to be northerly to easterly. While the ozone was building up in Dallas, Houston also experienced a daily increase in ozone, resulting in 8-hr ozone averages up to 110 ppbv in Houston on 7 September (not shown). Between 7 and 8 September, a shift in the position of a synoptic-scale high caused the transport winds to Dallas to change from a weak northeasterly component to a stronger southerly component. This major shift in transport had a strong impact on Dallas, as 24-hour forward trajectories from Houston, beginning at 3 pm local time, indicated transport from Houston to Dallas (Figure H2). Also, elevated overnight O_3 concentrations were measured at two rural O_3 stations sited for TexAQS II (Palestine and Italy). This transport brought additional ozone to a region that was already approaching 8-hr exceedance levels, resulting in 3 stations exceeding the 80 ppbv 8-hr-average O_3 in the DFW network.
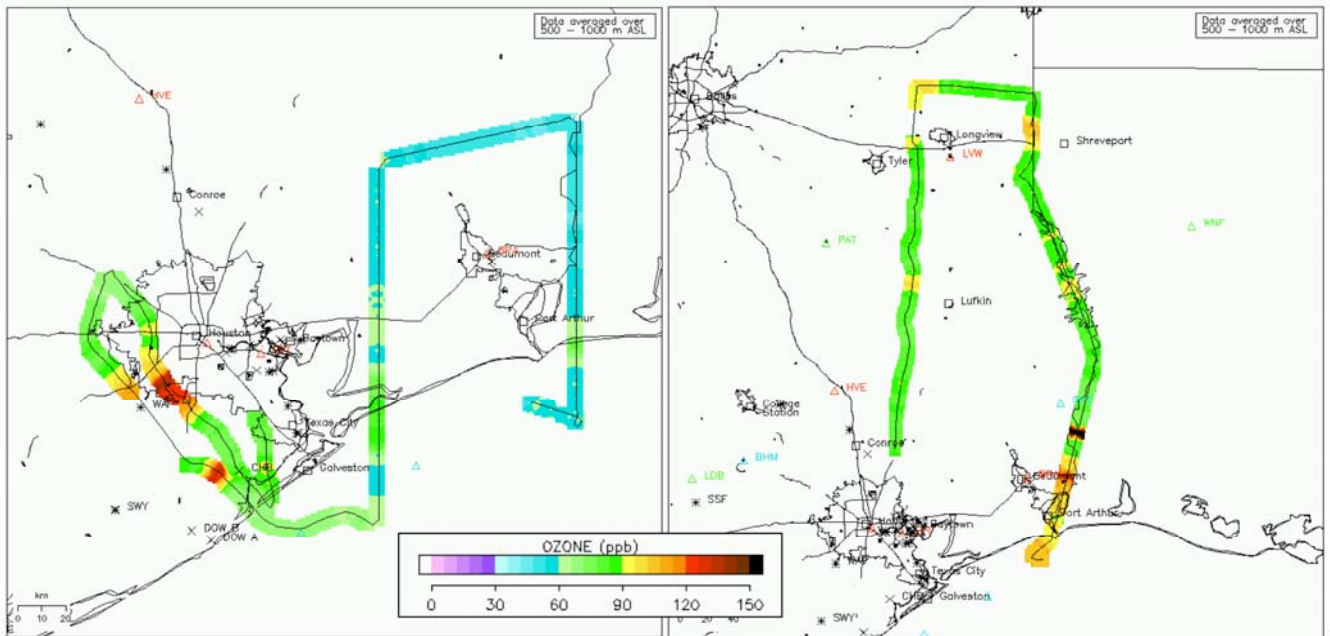
Figure H1. Airborne ozone lidar measurements on 4 and 8 September 2006, showing the large increase in background ozone in eastern Texas between the two days.
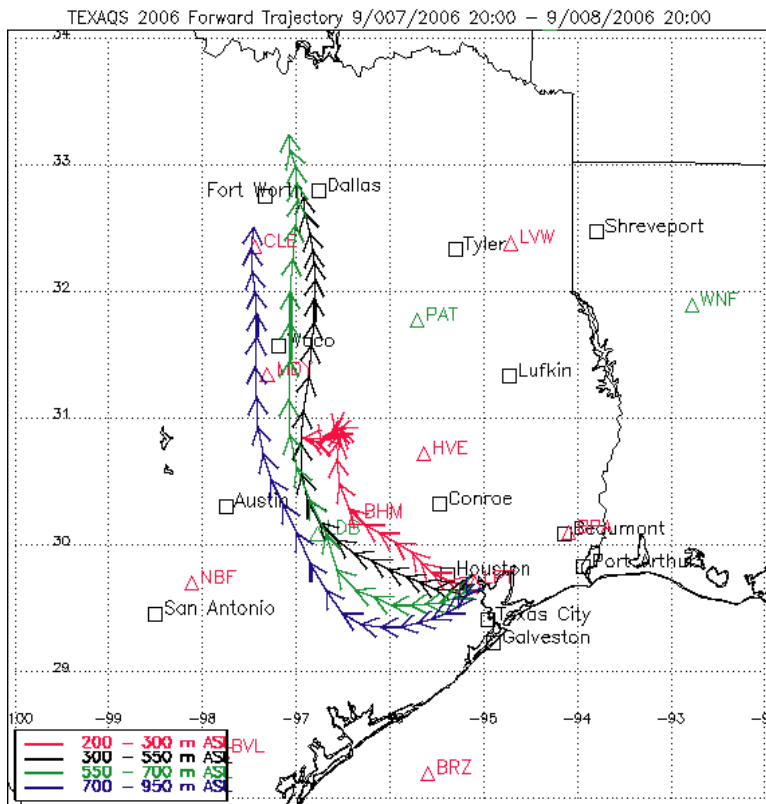
Figure H2. Forward trajectories starting at 3 pm local time in Houston, 7 September, and ending at 3 pm local time on 8 September 2006. The trajectories show direct transport from Houston to Dallas. 7 September was an exceedance day in Houston; 8 September was an exceedance day in Dallas. (The trajectory map was created using the NOAA Physical Science Division (PSD) upper air back-trajectory tool [http://www.etl.noaa.gov/programs/2006/texaqs/traj/]).

***Finding H2*: High ozone concentrations in eastern Texas result from both in-state sources and transport of continental air from the east and northeast.**

Analysis: Sullivan et al.-U. Texas.

Ensembles of historic HYSPLIT (Draxler and Rolph, 2003; Rolph, 2003) 5-day back trajectories have been run from major Texas cities on high ($\geq$ 75 ppbv 8-hr max) and low O_3 days to characterize the upwind "dirty" and "clean" typical fetches. A residence time analysis of the "dirty" fetch trajectories yields high O_3 air residence maps for northeast Texas, as exemplified in Figure H3. These maps (particularly the right one) show that transport of air from the east and northeast support many high O_3 episodes in August through October, but this analysis also shows that on high O_3 days in eastern Texas, the upwind air is resident within the state for several days, potentially building up background ozone from in-state source emissions.
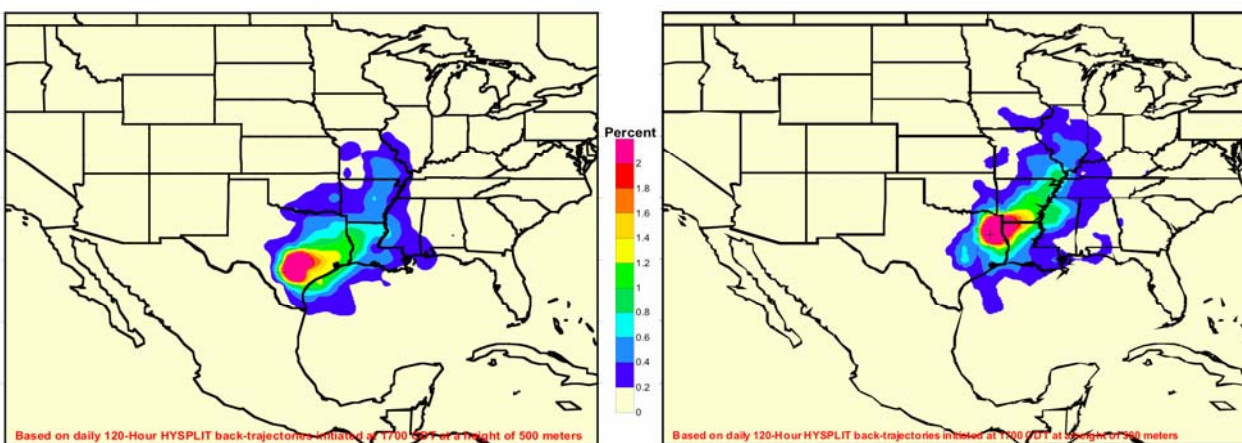
Figure H3. Contouring of HYSPLIT 500 meter 5-day back-trajectories on moderate and worse O_3 days in San Antonio (left) and Tyler/Longview/Marshall (right), color coded by density of end point frequency.

Using a new statistical analysis tool in HYSPLIT, an ensemble of back-trajectories can be categorized into clusters of similar behavior. Back-trajectories from East Texas from August and September 1997–2006 cluster into 5 categories: "short fetch" within Texas, Arkansas, and Louisiana; "E-SE" running through the southeastern US and the northern Gulf of Mexico; "S-SE" running through the Gulf to the Yucatan; "NE" running to the Midwest; and "north" running through the north-central US. An assessment of back-trajectory clusters by year compared with regional O_3 levels for August and September 1997–2006 shows that the "NE" cluster is best associated with high regional ozone, with the "short fetch" having the second highest correlation. There is some evidence that the year-to-year variation in the distribution of back-trajectory clusters helps explain the relative severity of O_3 seasons.

Finding H3: A synthesis of satellite and in situ measurements with photochemical modeling and Lagrangian trajectory analyses provides a quantification of regional influences and distant sources on Houston and Dallas air quality during TexAQS 2006.

Analysis: Pierce et al.–NASA; Data: MODIS, AIRS, CALIPSO, and TES teams–NASA, NOAA/NESDIS, UMBC.

Realtime Air Quality Modeling System (RAQMS) (http://rossby.larc.nasa.gov/RAQMS/ accessed October 2006) chemical analyses provide a means to quantify regional influences and distant sources on local air quality in Texas. Total column ozone from the Ozone Monitoring Instrument (OMI) and ozone and carbon monoxide profiles from the Tropospheric Emission Spectrometer (TES) onboard the NASA Aura satellite constrain these analyses, and fire counts from the Moderate Resolution Imaging Spectroradiometer (MODIS) instrument onboard the NASA Terra and Aqua satellites are utilized to generate biomass burning emissions. The fidelity of the RAQMS ozone analysis for the TexAQS 2006 period was assessed with independent satellite observations and aircraft data. The resulting bias-corrected RAQMS chemical analyses were used to provide estimates of background composition along ensemble back trajectories initialized daily at 18Z from surface EPA AIRNow ozone monitoring stations within the Houston and Dallas metropolitan statistical areas (MSA). Lagrangian averaged ozone production minus loss (O_3 P-L) rates along the back trajectories were used as a metric to classify back trajectories. The Lagrangian averages were computed during time periods when the back trajectories were outside the respective MSA, defined as more than 2° in longitude or latitude away from central Houston or Dallas. Three trajectory classes were considered: Class 1 (O_3 P-L > 10ppbv/day); Class 2 (0 < O_3 P-L < 10ppbv/day); and Class 3 (O_3 P-L < 0ppbv/day).

A time series depiction of the RAQMS back-trajectory analysis of regional influences on Houston and Dallas O_3 is shown in the upper panels of Figure H4. The red line shows the observed mean and variability of surface O_3 measurements in the urban area at 18 UTC extracted from EPA's AIRNow data system (http://www.airnow.gov/ accessed October 2006). The blue lines show the RAQMS chemical analysis with the solid blue for the AIRNow mean (bias-corrected), and the dashed blue for the background mean (bias-corrected) immediately prior to entering the urban area. The color bar along the upper part of each time series indicates the regional influence classification code for the modeled extent of O_3 production and loss upwind (see key). The Lagrangian analysis shows that periods of enhanced (P-L >10ppbv) regional O_3 production preceded 6 out of 9 Houston periods and 7 out of 15 Dallas periods with elevated O_3 (greater than 60 ppbv) during the 15 July – 15 October 2006 TexAQS II period. Maps of source regions for days with enhanced regional O_3 production are shown in the lower panels of Figure H4. Houston enhanced regional O_3 production events have a Midwest/Ohio River Valley source with significant O_3 P-L (40ppbv/ day) due to NO_x sources along the southern Great Lakes. Dallas enhanced regional O_3 production events have a broad Great Plains/Midwest/Ohio River Valley source with significant O_3 P-L (30ppbv/ day) due to Chicago NO_x sources along the southern Great Lakes.

Trajectory Classification

=Net O$_3$ Loss

=0< O$_3$ P-L <10 ppb/day

= O$_3$ P-L >10 ppb/day
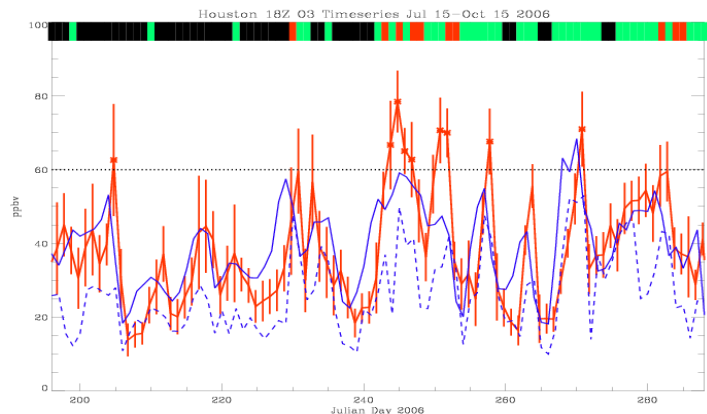
Red=AIRNow MSA mean+Std
Blue=RAQMS MSA (solid) Regional (dashed) bias corrected mean
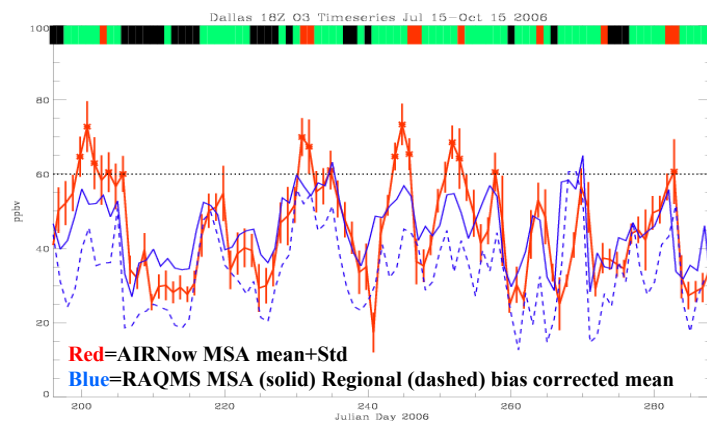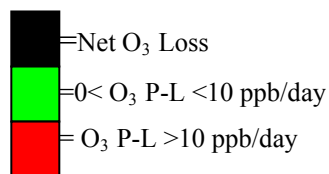
Figure H4. Lagrangian analysis of regional influences on Houston/Dallas O$_3$. Left, time series of Houston and Dallas observed, analyzed, and background ozone. Color bar along upper part of each time series indicates regional influence trajectory classification. Below, maps of Houston and Dallas Class 1 (see text) NO$_y$ source contributions (ppbv/day).
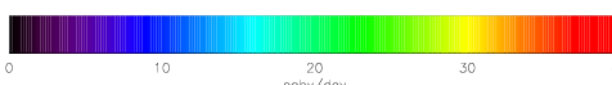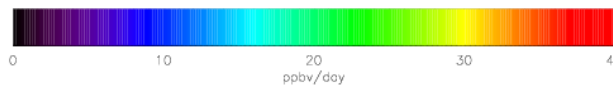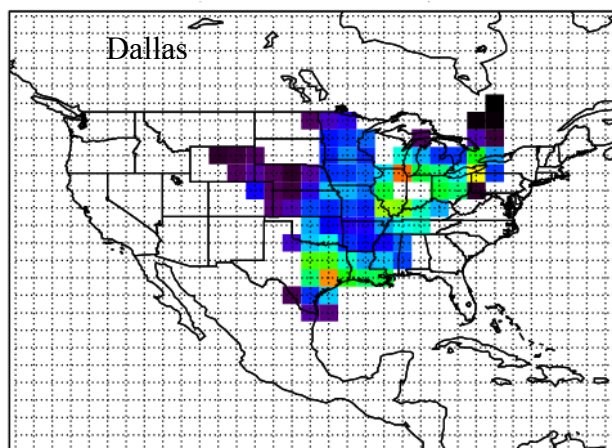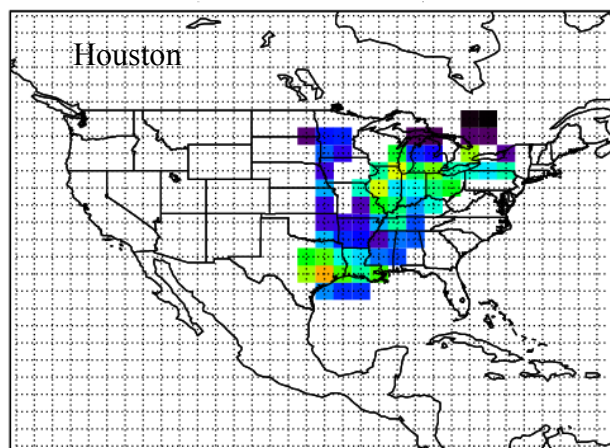
Case studies were conducted to investigate the processes responsible for enhanced regional O$_3$ production rates during the TexAQS II period. One such case is early September 2006. Twelve-day boundary layer back trajectories were initialized at locations where the High Spectral Resolution Lidar (HSRL) instrument (used to look down from the NASA King Air airplane to

assess the aerosol loading of the vertical column of air below) observed enhanced aerosol optical depths (AOD) indicating the presence of elevated particulate matter concentrations in the vicinity of Houston on 4 September 2006. Based on calculations of regional 24-hour rolling averages of TCEQ's hourly $PM_{2.5}$ concentrations, 4 September was one of only three days in the TexAQS 2006 period with widespread rolling 24-hour concentrations above 20 µg m^{-3}. In addition, a speciation monitoring site in Deer Park showed elevated sulfate and carbon material for that date. The back trajectories link the local 4 September HSRL measurements to satellite column and profile measurements from various sensors on low-earth orbit satellites (see Table H1 and Figure H5) on 23 August.

The 12-day back trajectories indicated two primary source regions: southern Canada and the eastern US. The MODIS sensor and AIRS sensor show column AOD and carbon monoxide (CO) enhancements associated with Pacific Northwest wild fire emissions within the Canadian branch, and CO enhancements associated within the eastern US branch of the back trajectories. CALIPSO attenuated aerosol backscatter cross-sections through the central US show an elevated aerosol layer associated with wild fire emissions and boundary layer aerosol enhancements over the eastern US. TES CO vertical cross-sections, which follow the same orbit as CALIPSO, show both lower and upper tropospheric CO enhancements. This case study illustrates the influence of remote emissions from the southeastern US and Pacific Northwest on Houston air quality. This analysis underscores the importance of integrating satellite, aircraft, and surface measurements of aerosol and trace gases in conjunction with advanced modeling techniques, for characterizing the impact of emissions from remote sources on local Texas air quality. Additional case studies are presented on the TCEQ website (http://www.tceq.state.tx.us), and a detailed case study is available from the 29-31 May Principal Findings Data Analysis Workshop for a 20 July 2004 O_3 and $PM_{2.5}$ episode in the Dallas area.

Table H1. Satellite sensors and resulting data products utilized for 4 September 2006 case study.

NASA Sensor	Product
MODIS - Moderate Resolution Imaging Spectro-radiometer	Aerosol optical depth
CALIPSO - Cloud-Aerosol Lidar and Infrared Pathfinder Satellite Observation	Aerosol optical depth profile
TES - Tropospheric Emission Spectrometer	Carbon monoxide profile estimate
AIRS - Atmospheric Infrared Sounder	Carbon monoxide column
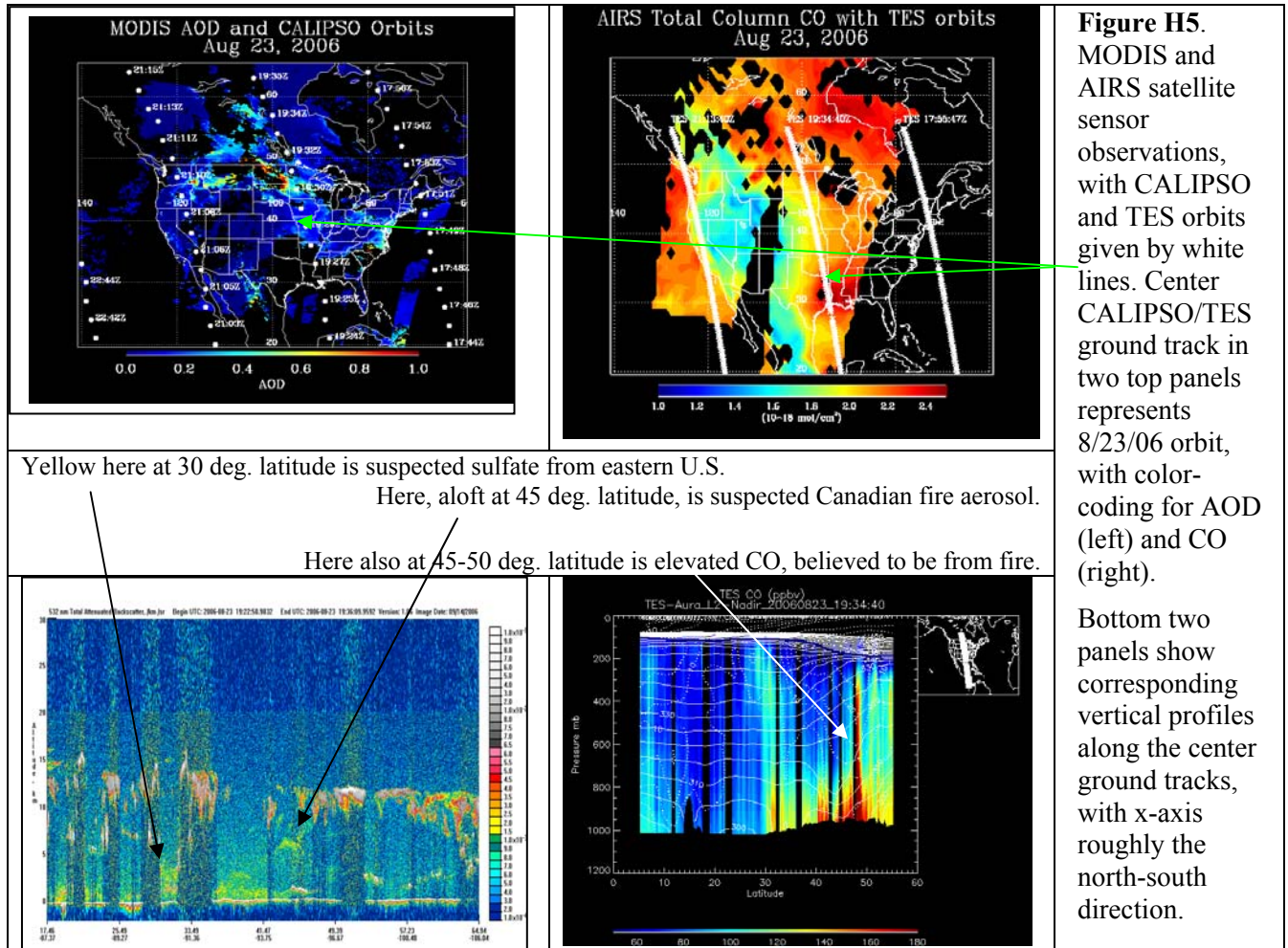
Figure H5. MODIS and AIRS satellite sensor observations, with CALIPSO and TES orbits given by white lines. Center CALIPSO/TES ground track in two top panels represents 8/23/06 orbit, with color-coding for AOD (left) and CO (right).

Bottom two panels show corresponding vertical profiles along the center ground tracks, with x-axis roughly the north-south direction.

***Finding H4*: In the Dallas area, local emissions and transport each contributed about equally to the average 8-hr ozone exceedance in 2002. Transported ozone alone can bring the Dallas area close to exceeding the 8-hour ozone standard.**

Analysis: Kemball-Cook et al. –ENVIRON; Parrish et al.-NOAA. Data: Ryerson et al.–NOAA.

Transport contributions to Dallas area O_3 were quantified for June–September 2002 using the CAMx photochemical model with emissions from EPA's 2002 National Emissions Inventory (NEI) (updated by the Central Regional Air Planning (CENRAP) consortium) and meteorology from the MM5 model (Kemball-Cook et al., 2006). The Dallas area had 35 days in 2002 with monitored 8-hour ozone levels of 85 ppbv or higher (Figure H6). Averaged over these days, Dallas area emissions contributed about 48 ppbv and other sources 54 ppbv to the total modeled ozone 8-hour maximum of 102 ppbv on the average exceedance day. The modeled average transport contribution from other parts of Texas was 6 ppbv, and there were days when northeast Texas, Houston/Beaumont, south Texas, and central Texas individually contributed 9 ppbv or more. The average modeled transport contribution from other US states was 28 ppbv, and the largest contributing states were Louisiana, Arkansas, Mississippi, Alabama, and Tennessee. These findings are consistent with back trajectory and residence time analyses. The example shown in Figure H7 compares CAMx O_3 transport contributions to back trajectories for 7 August 2002. The 5-day back trajectories cross NE Texas, Arkansas, and Tennessee, extending to the mid-Atlantic region; the CAMx modeling finds these same regions contributing to the Dallas area O_3 exceedance at the Ft. Worth NW monitor on 7 August 2002.

Estimates of the O_3 imported into the DFW area from aircraft data are in general agreement with the trend from the CAMx model, although the aircraft data suggest that the transported background ozone contributed an even larger fraction of the ozone in the DFW region than suggested by the model calculations. The Electra aircraft in TexAQS 2000 and the WP-3D aircraft in TexAQS 2006 measured O_3 upwind, across, and downwind of Dallas on two days during each field study. The green symbols in Figure H6 show the results from the 23 August and 7 September 2000 flights, and the orange symbols the results from the 13 and 25 September 2006 flights. The peak 8-hour-average O_3 for these four flights are from the monitoring data, and the DFW contribution is estimated from the difference between these peak values and the background O_3 measured upwind of DFW. 23 August 2000 is the one day investigated by the aircraft flights that had a significant exceedance of 98 ppbv. The background ozone transported into Dallas was about 72 ppbv, or 73% of the total, on that day. On some days transported ozone can bring the Dallas area close to an 8-hour exceedance without any added contribution from local emissions.
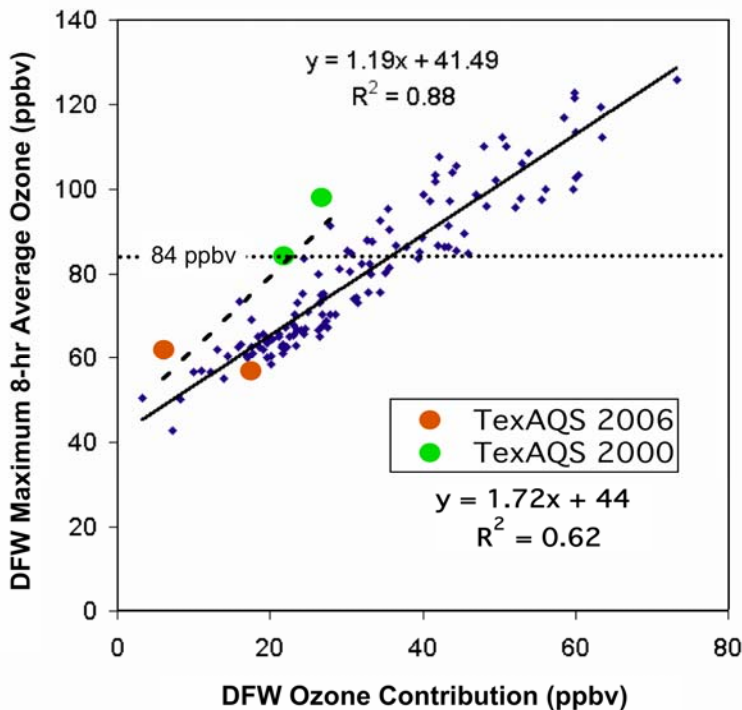
Figure H6. Measured peak 8-hour-average O_3 in the DFW area as a function of the DFW contribution to that peak. The DFW contribution is derived from the difference between the measured peak from the regional monitoring network, and the background ozone transported into the DFW region. The small symbols are from the model results from the CAMx model for each day 1 June - 30 September 2002. The larger symbols are from aircraft transects upwind and across the DFW region on four days in 2000 and 2006.

Trajectories from 3 different altitudes over Ft. Worth to characterize upwind areas for the column of air 2 pm CST on 7 August 2002.
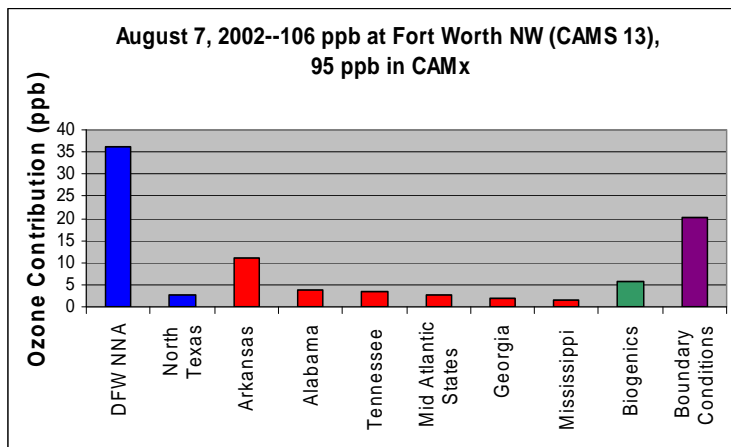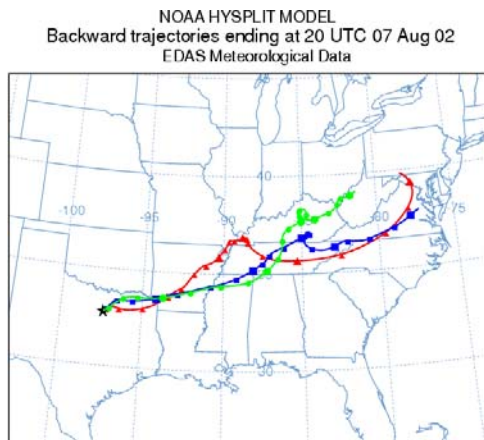
Figure H7. Modeled contributions to one monitor's ozone total concentration. Local is largest single contributor, but transport from upwind source areas significantly increase concentrations (analysis by Kemball-Cook et al., 2006).

Finding H5: **In the Houston area, local emissions and transport each contributed about equally to the average 8-hr ozone exceedances investigated by aircraft flights in 2000 and 2006. As in Dallas, transported ozone alone can bring the Houston area close to exceeding the 8-hour ozone standard.**

Analysis Parrish et al.-NOAA; Data: Ryerson et al.–NOAA.

Houston area emissions contributed about 48 ppbv and transported ozone about 59 ppbv to the average total ozone 8-hour maximum of 107 ppb on the seven exceedance days investigated by aircraft measurements during 2000 and 2006. Figure H8 shows the apportionment of the measured maximum 8-hour-average ozone for all days characterized by aircraft measurements. The linear least-square fits give slopes near unity for the separate years, and for the total data sets, which indicates that the local and transported background contributions are largely independent of each other. The background contribution was similar between the two years, but the local contribution was considerably larger in 2000 than 2006. The transported background ozone reached a maximum of 70 ppbv, which can lead to an exceedance with a relatively small additional contribution from local sources.
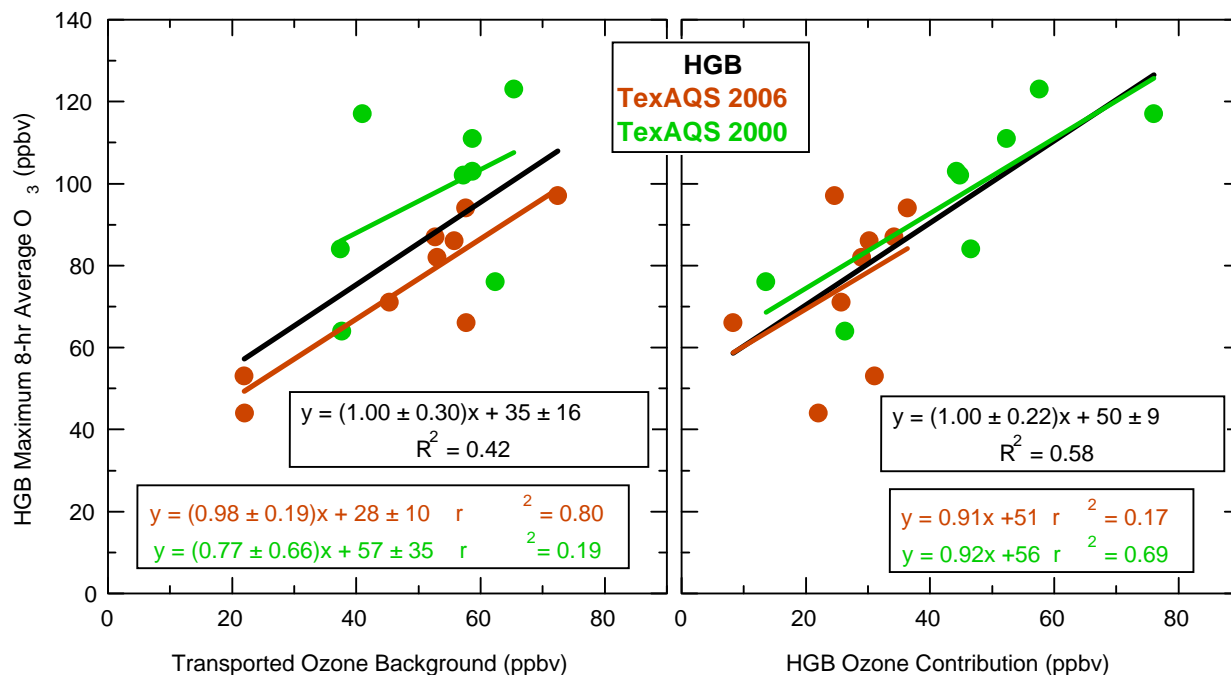
Figure H6. Measured peak 8-hour-average O_3 in the HGB area as a function of the background ozone transported into the region (left) and the local HGB contribution to that peak (right). The background ozone was determined from aircraft transects upwind and across the HGB region on seventeen days in 2000 and 2006. The HGB contribution is derived from the difference between the measured peak and the background.

KEY CITATIONS AND INFORMATION AND DATA SOURCES

Draxler, R.R. and Rolph, G.D. 2003. HYSPLIT (HYbrid Single-Particle Lagrangian Integrated Trajectory) Model access via NOAA ARL READY Website (http://www.arl.noaa.gov/ready/hysplit4.html). NOAA Air Resources Laboratory, Silver Spring, MD.

Kemball-Cook, S., M. Jimenez, and G. Yarwood. 2006. Seasonal Model of Northeast Texas Ozone for Summer 2002. http://www.netac.org/0405closeout/Task_6.1.pdf (accessed July 6, 2007).

Rolph, G.D. 2003. Real-time Environmental Applications and Display sYstem (READY) Website (http://www.arl.noaa.gov/ready/hysplit4.html). NOAA Air Resources Laboratory, Silver Spring, MD.

Response to Question I

QUESTION I
Why does the SAPRC chemical mechanism give different results than the carbon bond (CB-IV) mechanism?
Which replicates the actual chemistry better?

BACKGROUND
Gridded, regional photochemical models, used in developing State Implementation Plans (SIPs), use simplified photochemical reaction mechanisms. The two mechanisms that are most commonly used are the [California] Statewide Air Pollution Research Center (SAPRC) mechanism and the Carbon Bond (CB) mechanism. Both mechanisms are approved for use by the US EPA and are updated periodically to incorporate new experimental findings. For most urban areas, the CB mechanism, version IV (CB-IV) and the 1999 SAPRC (SAPRC99) mechanism yield similar results, but for conditions found in Houston, the SAPRC99 mechanism leads to concentrations of ozone that are up to 30-50 ppbv greater than in CB-IV and is more sensitive to reductions in NO_x emissions, especially on days with high predicted ozone concentrations (Figure I1). These differences in the sensitivity of chemical mechanisms to emission reductions could have significant consequences for determining the magnitude of decreases in emissions of ozone precursors that will be required to demonstrate attainment of the current 8-hour, 80 ppbv NAAQS for ozone.
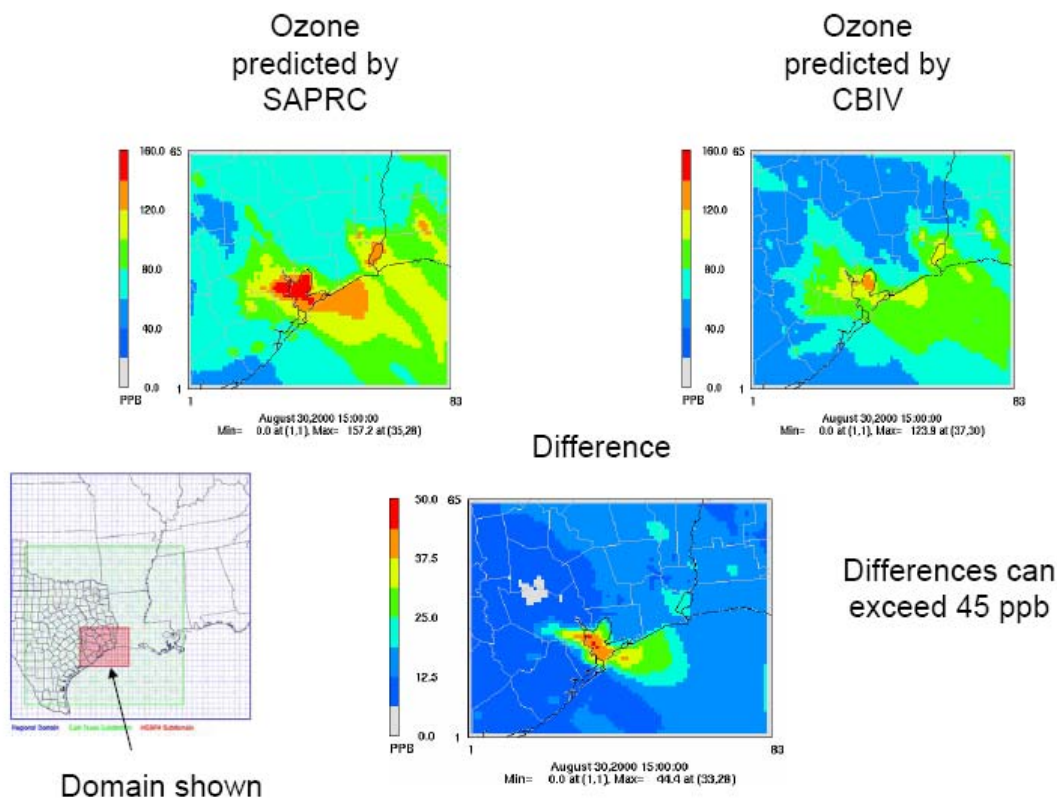
Figure I1. Predictions of domain-wide maximum O_3 concentrations in Comprehensive Air Quality Model, with extensions (CAMx) on 30 August 2000. (Faraji et al., 2007a)

FINDINGS

***Finding I1*: Air quality modeling for both 2000 and 2006 shows substantial differences in ozone concentrations predicted by the SAPRC99 and CB-IV chemical mechanisms.**

Analysis: Faraji et al. (2007a,b); Byun-U. Houston.

Simulations performed using multiple regional photochemical modeling packages (Comprehensive Air Quality Model, with extensions [CAMx] and Community Multi-scale Air Quality model [CMAQ]), and multiple emissions preprocessing systems (Sparse Matrix Operator Kernel Emissions [SMOKE] and Emissions Preprocessing System version 2 [EPS2]) for 2000 and for 2006 predicted higher ozone concentrations when the SAPRC99 mechanism was used than when the CB-IV mechanism was used. The differences in predicted ozone concentrations were greatest when predicted ozone concentrations were high.

***Finding I2*: In regions with very high VOC reactivity and high NO_x emission density, differences in ozone formation and accumulation predicted by regional photochemical models using the SAPRC99 and CB-IV mechanisms are due to differences in: (1) the chemistry of aromatics, especially mono-substituted aromatics (e.g., toluene), (2) nitric acid formation rates, and (3) the rates of free radical source terms in the SAPRC and CB-IV mechanisms.**

Analysis: Faraji et al., 2007a.

In reactions of mono-substituted aromatics, the CB-IV mechanism predicts a higher proportion of ring-retaining products, such as cresols, than SAPRC99. These ring-retaining products are less reactive than the ring opening products. The CB-IV mechanism also predicts: (1) more extensive nitric acid formation, (2) less extensive formation of peroxyacetyl nitrate (PAN), and (3) decreased formation of free radicals than the SAPRC99 mechanism. The SAPRC mechanism also has several source reactions for higher aldehydes that are not present in CB-IV. The enhanced free radical production in SAPRC99, as compared to CB-IV, leads to accumulation of higher concentrations of radicals.

***Finding I3*: The differences in the predictions of the SAPRC99 and CB-IV mechanisms can be probed using simulations of model compounds and comparisons of the simulations to environmental chamber data. For simulations involving CO and NO_x (inorganic chemistry), the predictions of the CB-IV and SAPRC99 mechanisms that are used in regional photochemical models (with no chamber wall corrections) converge if the rate constants for the $OH + NO_2$ reaction are made consistent between the two mechanisms. The predictions of the Carbon Bond mechanism, version 5 (CB05) also converge to the same predicted values if the $OH + NO_2$ rate constant is made consistent with the other mechanisms.**

Analysis: Faraji et al., 2007b.

Equating the rate constant for the $OH + NO_2$ reaction in CB-IV, CB05, and SAPRC99 mechanisms, in the form in which they are used in regional photochemical modeling, led to convergence in the concentrations of O_3, OH, HO_2, NO, and NO_2. This suggests that in photochemical modeling simulations, the major differences in the inorganic chemistry between the mechanisms are due to differences in the rate parameters of the $OH + NO_2$ reaction.

However, CO - NO$_x$ experiments may not be sensitive to all aspects of inorganic mechanisms that affect simulations under ambient conditions.

***Finding I4*: The performance of the mechanisms in simulating olefins chemistry can be improved through more explicit representation of internal olefin chemistry, which has been added in CB05. In addition, performance of the SAPRC99 mechanism in simulating chamber data was improved for some experiments when propene was modeled explicitly, as opposed to being represented by a lumped chemical species.**

***Finding I5*: For high reactivity chamber experiments involving olefins, sensitivity analyses indicated that mechanism adjustments that would lead to increased radical concentrations (increasing the radical yield in olefin-ozone reactions and changing the OH+NO$_2$ termination rate constant) had little impact on predicted ozone concentrations.**

***Finding I6*: The SAPRC99 mechanism performed better than the CB mechanisms in simulating some chamber experiments with toluene; the mechanism performances were more comparable for xylenes and other multiply substituted aromatics.**

***Finding I7*: The differences between the SAPRC and CB-IV mechanism predictions for toluene chemistry decrease substantially if the yield for the lumped species CRES, and rate constant for the OH + NO$_2$, are made consistent between the two mechanisms. The predictions of the CB05 mechanism also converge to the same predicted values if the CRES yield and the OH + NO$_2$ rate constant are made consistent with the other mechanisms.**

Analysis and Data: Faraji et al., 2007b.

The lumped group of chemical species, CRES, as used in the photochemical reaction mechanisms, is often referred to as cresol, and comparisons between chamber experiments involving aromatics and observed cresol concentrations are generally better for the SAPRC mechanism than for the CB mechanisms. However, in the CB mechanism, the CRES species is used to represent both cresol yields and other products (such as unsaturated dicarbonyls) that react rapidly with the nitrate radical. Therefore direct comparisons of CRES yields with cresol concentrations for the CB mechanisms are not appropriate. It is clear that there are substantial differences in predictions of aromatics chemistry between the CB and SAPRC mechanisms, that the toluene mechanisms all need to be revised to improve their consistency with chamber data, and that much still remains unresolved about aromatics chemistry.

***Finding I8*: For simulations of ambient surrogate mixture experiments in the UCR EPA chamber, all mechanisms underpredict O$_3$ at low ROG/NO$_x$ ratios, with the bias decreasing as the ROG/NO$_x$ ratio increases. In simulations of mixture experiments in chambers without aromatics, CB05 performs the best, and with no dependence of bias on the ROG/NO$_x$ ratio.**

Analysis and Data: Faraji et al., 2007b.

Figure I2 shows the results of comparisons of modeled simulations of environmental chamber experiments performed at University of California, Riverside (UCR). The performance of SAPRC99 in simulating the UCR EPA mixture experiments (both with and without aromatics) improved considerably if compounds are modeled explicitly, rather than in lumped groups.

Full Surrogate - Arc Lights

Full Surrogate - Blacklights

Non-Aromatic Surrogate - Blacklights

Legend:
- × Detailed SAPRC-99
- • CAMx SAPRC-99
- △ CB05
- ○ CB4

Note: Full surrogate experiments include experiments with formaldehyde removed.
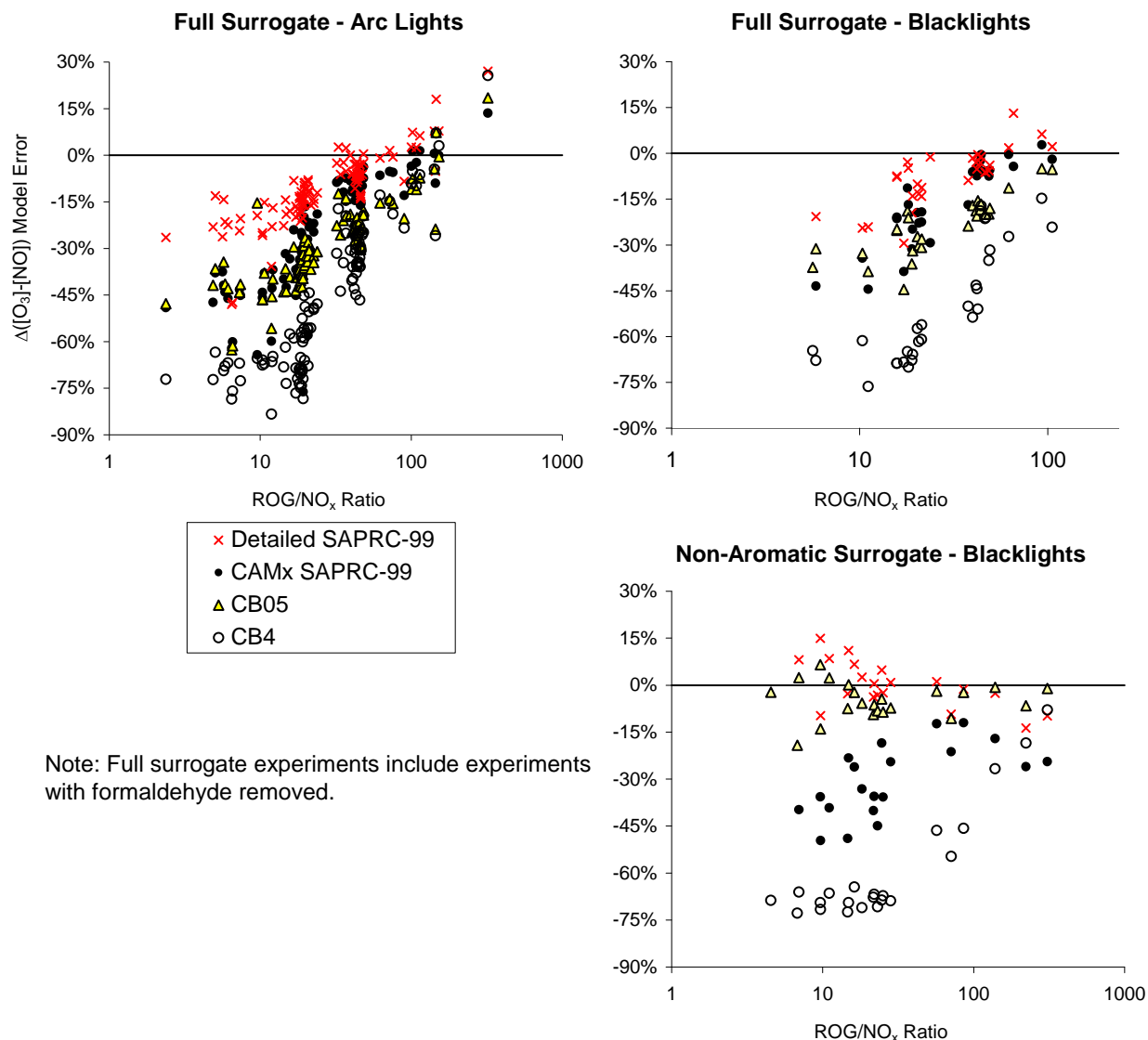
Figure I2. Comparison of CB-IV, CB05, and SAPRC99 model errors for UCR EPA surrogate runs. (Faraji et al., 2007b)

Findings I3-I8 were arrived at by analyzing model compound simulations and environmental chamber data. These six findings are consistent with Findings I1 and I2, which are based on sensitivity analyses performed using the regional photochemical models. Additional analyses were performed using ambient data from Houston collected during a stagnation event with high olefin concentrations.

***Finding I9*: SAPRC99, CB-IV, and CB05 all successfully predicted concentrations of ozone and other species during simulation of a stagnation event, if the chemical mechanisms were initialized after initial high concentrations of olefins had reacted. None of the mechanisms successfully predicted a rapid rise in radical concentrations and ozone concentration concurrent with initially high C2, C3, and CMBO concentrations during the event.**

Analysis and Data: Faraji et al., 2007b.

Analyses have been performed on ambient data collected during TexAQS 2000 at the heavily instrumented LaPorte site (Faraji et al., 2007b). Specifically, a period of stagnation at the LaPorte airport was simulated. This stagnation period had high concentrations of C2 and C3 alkanes and alkenes, as well as high concentrations of a marker of chlorine chemistry (CMBO – 1-chloro-3-methyl-3butene-2-one) that lasted for approximately one hour. The data suggest that a source of radicals, not accounted for in the current mechanisms was present, but no definitive source of the radicals was identified.

RECOMMENDATIONS

Model compound analyses and chamber data, as well as sensitivity analyses in CAMx, indicate that major causes for the differences in SAPRC and CB mechanisms under conditions encountered in eastern Texas are the chemistry of aromatics, and to a lesser extent, radical termination rates. In choosing a mechanism that will be most effective for eastern Texas, several guiding principles emerge.

1. Over the past several decades, comprehensive updates to the CB and SAPRC chemical mechanisms have been released roughly every 5-10 years. These updates incorporate changes to the mechanisms that reflect evolving knowledge about rate constants and key chemical pathways. For example, the rate parameters for the critical $OH + NO_2$ rate constant have been adjusted in CB05, as compared to CB-IV, and in SAPRC07, as compared to SAPRC99. In addition, the updates often provide explicit representations of chemical species that have recently been identified as being especially important. For example, explicit isoprene chemistry was incorporated into both SAPRC and CB mechanisms in the 1990s and the newly released CB05 incorporates internal olefins as an explicit compound class. These updates generally reflect more current knowledge, and, as a guiding principle, should be used when possible.

2. Recognizing that it may be difficult to unambiguously define the most appropriate mechanism for use in Houston, the effectiveness of proposed control strategies should be evaluated using multiple chemical mechanisms.

3. As new comprehensive updates to the CB and SAPRC mechanisms are developed, more explicit representation of both key chemical pathways (e.g., the low NO_x routes for aromatics) and key chemical species (propene, toluene, and possibly other aromatics) would likely make the mechanisms more useful in analyzing the complex industrial emission sources in the Houston area.

KEY CITATIONS AND INFORMATION AND DATA SOURCES

Carter, W.P.L. 2004. Evaluation of a Gas Phase Atmospheric Reaction Mechanism for Low NO_x Conditions. Final Report to the California Air Resources Board, Contract No. 01-305. http://pah.cert.ucr.edu/~carter/bycarter.htm.

Faraji, M., Y. Kimura, E. McDonald-Buller, and D. Allen. 2007a. Comparison of the Carbon Bond and SAPRC photochemical mechanisms under conditions relevant to southeast Texas. *Atmospheric Environment*, in press.

Faraji, M., G. Heo, Y. Kimura, E. McDonald-Buller, D. Allen, G. Yarwood, G. Whitten, and W. Carter. 2007b. Comparison of the Carbon Bond and SAPRC photochemical mechanisms. Report to the Texas Commission on Environmental Quality, August, 2007.

Yarwood, G., S. Rao, M. Yocke, and G.Z. Whitten. 2005. Updates to the Carbon Bond Mechanism: CB05. Report to the U.S. Environmental Protection Agency (December). www.camx.com/publ/pdfs/CB05_Final_Report_120805.pdf.

Response to Question J

QUESTION J
How well do air quality forecast models predict the observed ozone and aerosol formation? What are the implications for improvement of ozone forecasts?

BACKGROUND
An assessment of seven air quality forecast models (AQFMs) operating in real time during TexAQS 2006 focused on skill at predicting maximum 8-hour-average O_3 at 119 sites and 24-hr-average $PM_{2.5}$ levels at 38 sites in eastern Texas, western Louisiana, Arkansas and Oklahoma. These models included: the NCEP CMAQ-WRF model (12-km horizontal resolution), two versions of the NOAA/ESRL WRF-Chem model (12- and 36-km res.), the Canadian CMC AURAMS (28-km) and CHRONOS (21-km res.) models, one version of the Baron-AMS MAQSIP-RT model (15-km res.), and the University of Iowa STEM model (12-km res.). Details on each of these modeling systems can be found in McKeen et al. (2005), and internet web links listed below. Three standard statistical parameters, Mean Bias, Root Mean Square Error (RMSE), and correlation

Air Quality Forecast Models
AURAMS – A Unified Regional Air-Quality Modeling System
MAQSIP-RT – Multiscale Air Quality Simulation Platform-Real Time
CHRONOS – Canadian Hemispheric and Regional Ozone and NO_x System
CMAQ5x/WRF – Community Multi-scale Air Quality model/Weather Research Forecast model
University of Iowa STEM – Sulfur Transport and Emissions Model
WRF/Chem – Weather Research Forecast model/Chemistry version

coefficients were evaluated in this preliminary work. Skill for these three statistics is measured relative to a persistence forecast, or the forecast that tomorrow's AQ levels are the same as today's observed levels. In addition, bias-corrected model forecast values are calculated based on the mean O_3 or $PM_{2.5}$ bias at each site at each hour of the day, averaged over the previous 7 days. The statistical parameters are also calculated from the ensemble of the models, and the ensemble of bias-corrected models. The summary statistics for the models and their ensemble are shown in Fig. J1 for O_3 and Figure J2 for $PM_{2.5}$. Also shown are the RMSE for persistence and climatology forecasts, and correlation coefficients for persistence. Categorical statistics (measures of how well a model predicts an event) related to the predictions of daily maximum 8-hour-average O_3 levels exceeding the 85 ppbv regulatory threshold are also summarized for the seven models, their mean ensemble, and with two bias-correction options (Figures J3 and J4). The four categorical statistics evaluated in this work were: Probability of Detection, False Alarm Rate, Critical Success Index, and Bias Ratio.

The forecasts of roughly 25 chemical, aerosol, meteorological, and radiation variables from the seven models have been compared with data collected on board the WP-3D aircraft for individual transects and vertical profiles on a flight-by-flight basis for the first 12 flight legs of the aircraft deployment. These comparisons are available for viewing at the publicly available NOAA web page, http://www.esrl.noaa.gov/csd/2006/modeleval/. Concentrations and fluxes of key atmospheric constituents upwind and downwind of Houston and Dallas have also been compared, allowing assessments of model reliability in terms of emissions inventories, and efficiencies of O_3 and $PM_{2.5}$ formation from these large urban sources.

The University of Houston also made nine AQ forecasts using three model resolutions and three emission scenarios with the MM5/CMAQ model. Detailed statistical summaries for O_3 and

PM$_{2.5,}$ for each forecast, and for each of the CAMS surface monitors can be found at the University of Houston web page, http://www.imaqs.uh.edu/ftp/AQF_usa/ (password protected).
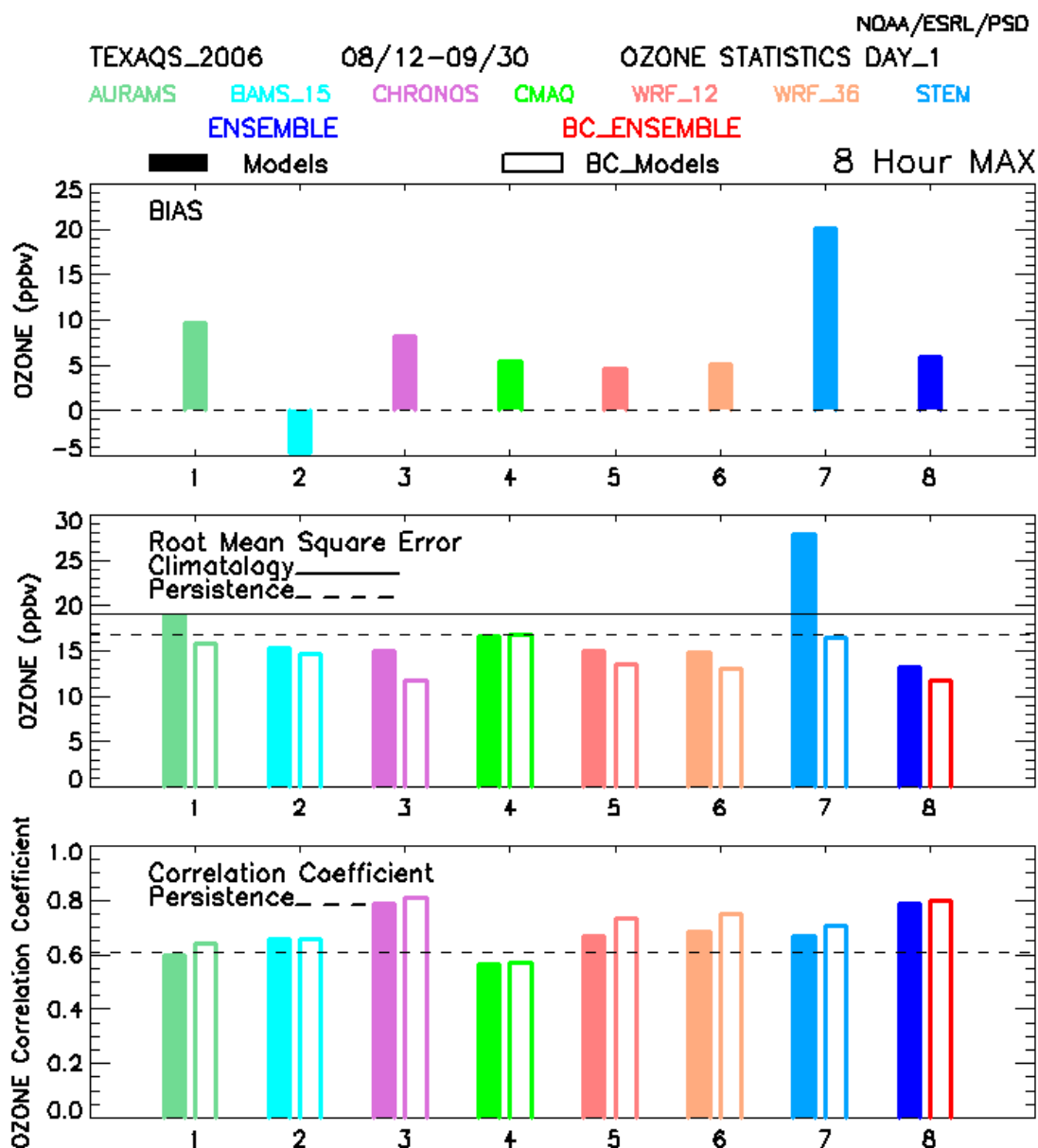
Figure J1. Summary statistics for 8-hour maximum ozone for nine air quality forecast models and their ensemble mean and bias-corrected ensemble mean.
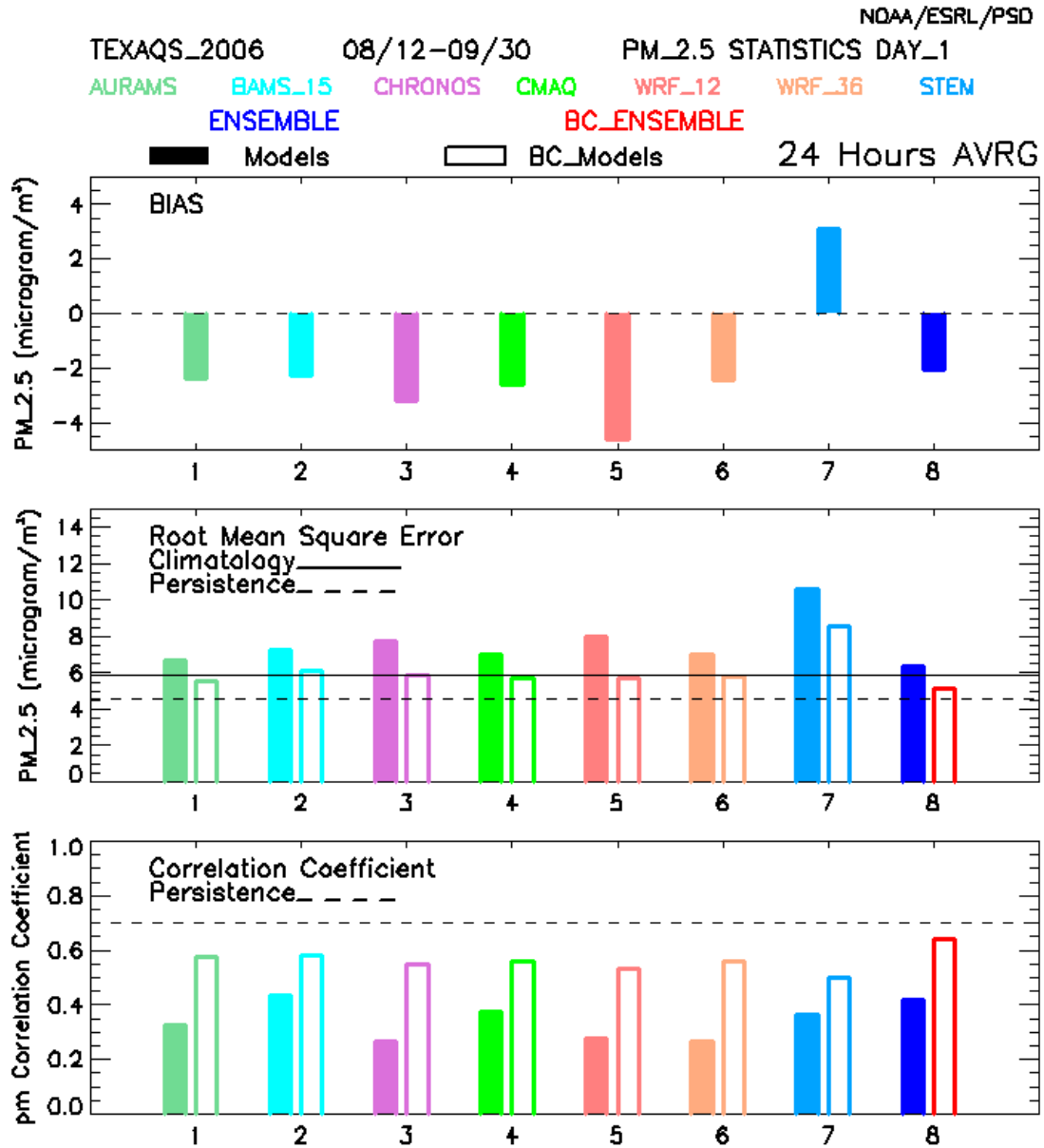
Figure J2. Summary statistics for 24-hour-average $PM_{2.5}$ for seven air quality forecast models and their ensemble mean and bias-corrected ensemble mean.

FINDINGS

Finding J1a: **Most forecast models exhibit skill in predicting maximum 8-hr-average O₃ but none of the models is better than persistence in predicting 24-hr-average PM$_{2.5}$ levels.**

Analysis: Wilczak et al.-NOAA. Model Data: McQueen et al.-NOAA/NWS, Grell et al. NOAA/GSD, Carmichael et al.-U. Iowa, McHenry et al.-Baron AMS, Gong et al.-Met. Srv. Canada, Bouchet et al.-Met. Srv. Canada.

When all O$_3$ data are considered:

- Nearly all models beat persistence RMSE and r-coefficients without bias correction.
- The ensemble performed better than all individual models, and the bias-corrected ensemble showed the best statistical performance.
- Bias correction improved RMSE scores appreciably and r-coefficients to some degree.

When all PM$_{2.5}$ data are considered:

- In contrast to O$_3$, no model or ensemble, or bias correction, beat persistence.
- All but one model was biased low, and bias correction improved r-coefficients significantly.
- Since they are not included in the models, the occurrence of Saharan dust events during August and September influenced the bulk PM$_{2.5}$ statistics. Removal of these events from the statistical evaluations is another required step in model analysis.
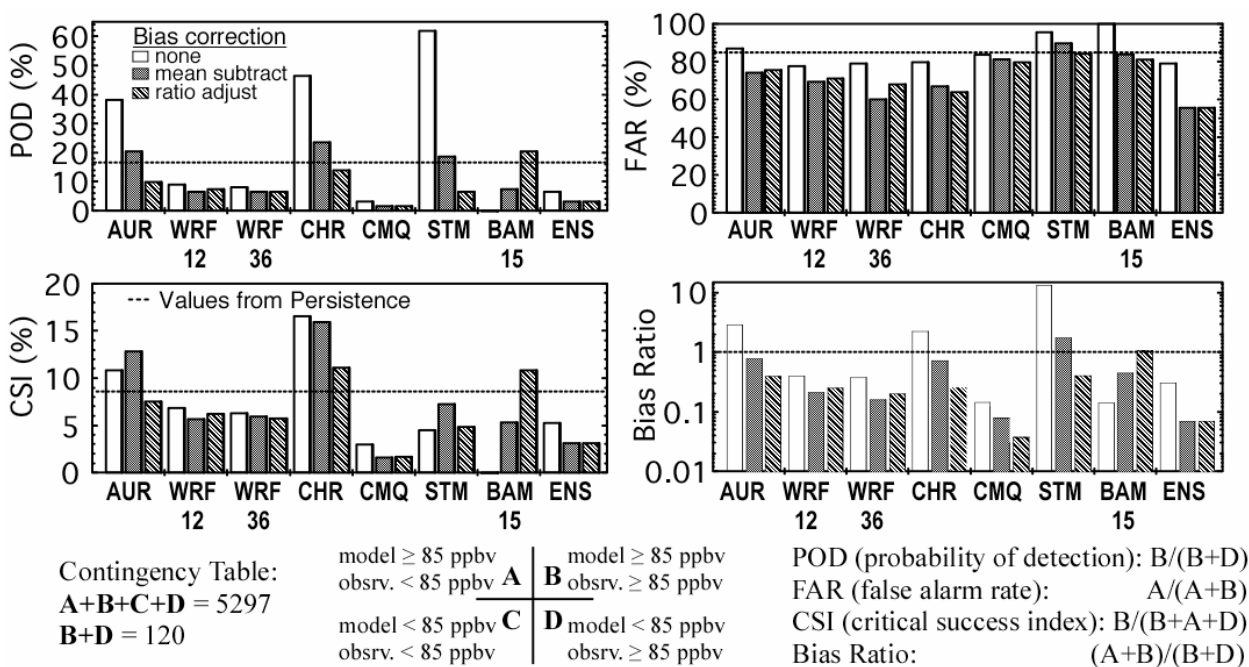
Figure J3. Categorical statistics related to the 85 ppbv exceedance for 8-hour maximum ozone for seven air quality forecast models and their ensemble.

***Finding J1b*: Seven air quality forecast models and their ensemble were generally unable to forecast 85 ppbv 8-hr-average O$_3$ exceedances with any reliability.**

Analysis: McKeen et al.-NOAA. Model Data: McQueen et al.-NOAA/NWS, Grell et al. NOAA/GSD, Carmichael et al.-U. Iowa, McHenry et al.-Baron AMS, Gong et al.-Met. Srv. Canada, Bouchet et al.-Met. Srv. Canada.

− Although the 7-model ensemble had the best overall bulk statistics, and was biased high by 5 ppbv, its ability to predict an exceedance event was significantly worse than persistence.

− The ensemble, like most of the models, predicts far fewer events, and missed most of the exceedance events in the Houston area (see Figure J4). This collective model under-prediction could be due to the lack of an important source component within all the models, such as highly reactive VOC emissions.

− Only one model beat persistence for both probability of detection and false alarm rate.

− Since most models and the ensemble are biased high, bias correction tended to reduce a model's ability to predict an exceedance event even further. This was in sharp contrast to a similar categorical analysis for New England during the summer of 2004 (McKeen et al., 2005), where bias corrections nearly always improved the critical success index.
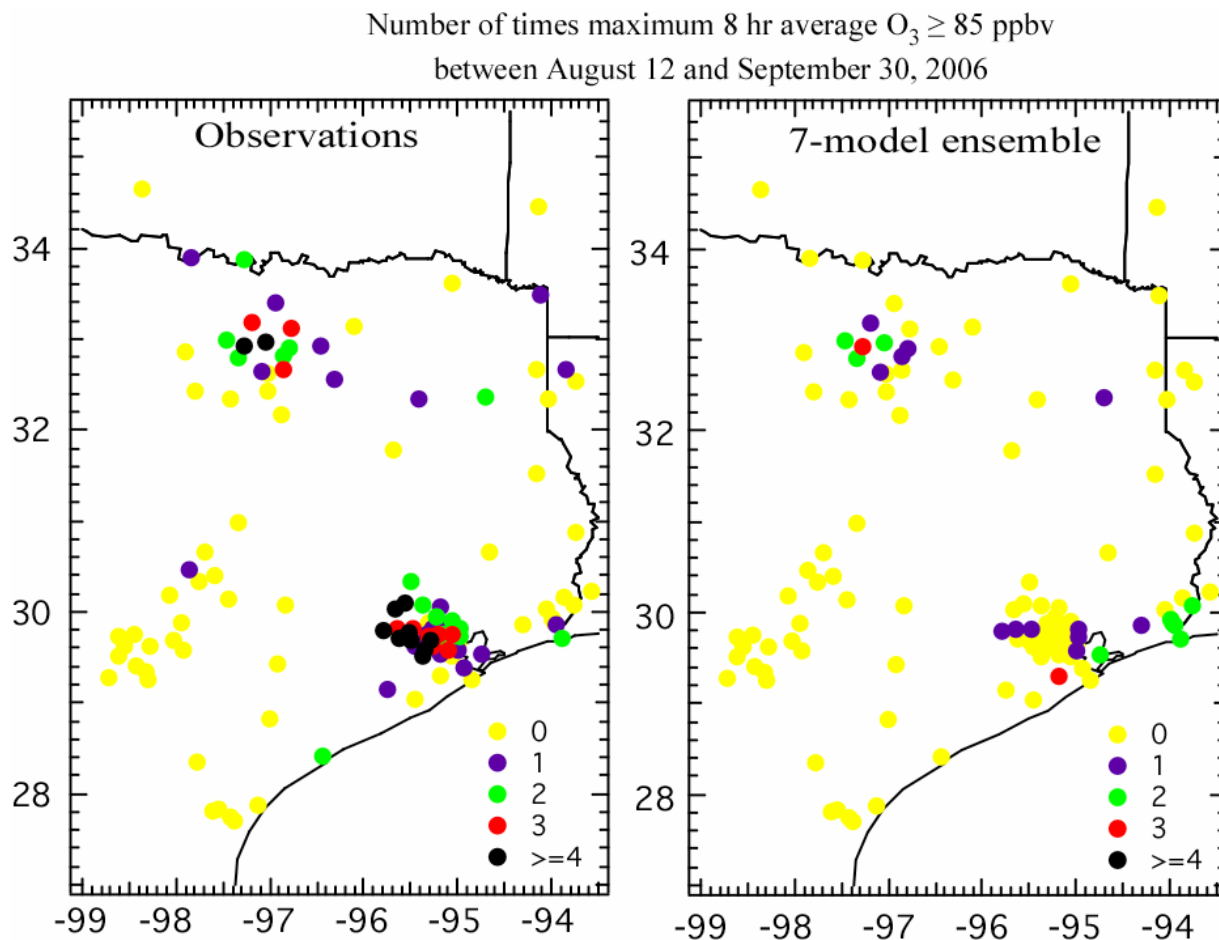
Figure J4. Number of times the 85 ppbv exceedance for 8-hour maximum ozone occurred within the reported AIRNow observations, and the 7-model ensemble forecast.

***Finding J2*: Sophisticated data assimilation of meteorological and even chemical observations is essential for improving photochemical model forecasts.**

Analysis: Nielsen-Gammon et al.-Texas A&M U., Byun et al.-U. Houston, McKeen et al.-NOAA. Model Data: Nielsen-Gammon et al.-Texas A&M U., Byun et al.-U. Houston, McQueen et al.-NOAA/NWS, Grell et al. NOAA/GSD, Carmichael et al.-U. Iowa, McHenry et al.-Baron AMS, Gong et al.-Met. Srv. Canada, Bouchet et al.-Met. Srv. Canada.

Spatial and temporal accuracy of AQ forecasts are to a large degree limited by the accuracy of the underlying meteorological forecasts within the AQ models. Most models rely on the available NCEP/NAM model product for initialization and boundary conditions, which may contribute to model biases in AQ model wind fields and pressure patterns documented throughout the field study. Retrospective forecasts and sensitivity studies are needed to assess the impact of the NAM forecasts available in the summer of 2006 to AQFMs, particularly in light of recent upgrades to the WRF-NMM model used in the NAM forecasts. Assimilation of wind profiler data (Nielsen-Gammon et al., 2006) has been shown to improve forecast meteorology in the Houston area. Similar research related to the assimilation of photochemical and aerosol data within AQFMs should be encouraged, utilizing the comprehensive data sets from the TexAQS 2006 field study.

Daytime planetary boundary layer (PBL) heights from seven of the models were compared to those derived from wind profiler measurements at several sites in east Texas. Some models showed persistent bias in daytime PBL, and no model appeared to stand out in terms of significantly better comparisons. Deficiencies in AQ forecasts from several of the models appear to be related to the formulation of PBL height and vertical transport within the PBL. This is shown in Figure J5, which shows a wide spread in the models' ability to simulate water vapor and NO_y profiles compared to WP-3D aircraft data for afternoon conditions on a particular clear day. It is quite common for models to exhibit unrealistic high biases in O_3 and $PM_{2.5}$ precursors downwind of source regions when PBL heights are under-predicted. The analogous misrepresentation of the stable PBL often affects model-predicted offshore pollutant transport and pollution precursor buildup from emissions along the coastlines. Persistent errors in the forecast of the low-level nocturnal jet are also characteristic of many models. Preliminary sensitivity studies with the MM5/CMAQ model also have demonstrated a case of over-predicted O_3 associated with a missed forecast of widespread precipitation (24, 25 August). The collection of available satellite, radar, and surface network data sets for comparing cloudiness, precipitation, and radiation with model output are needed to perform further evaluations of these parameters, and their relationships to O_3 and $PM_{2.5}$ forecasts.
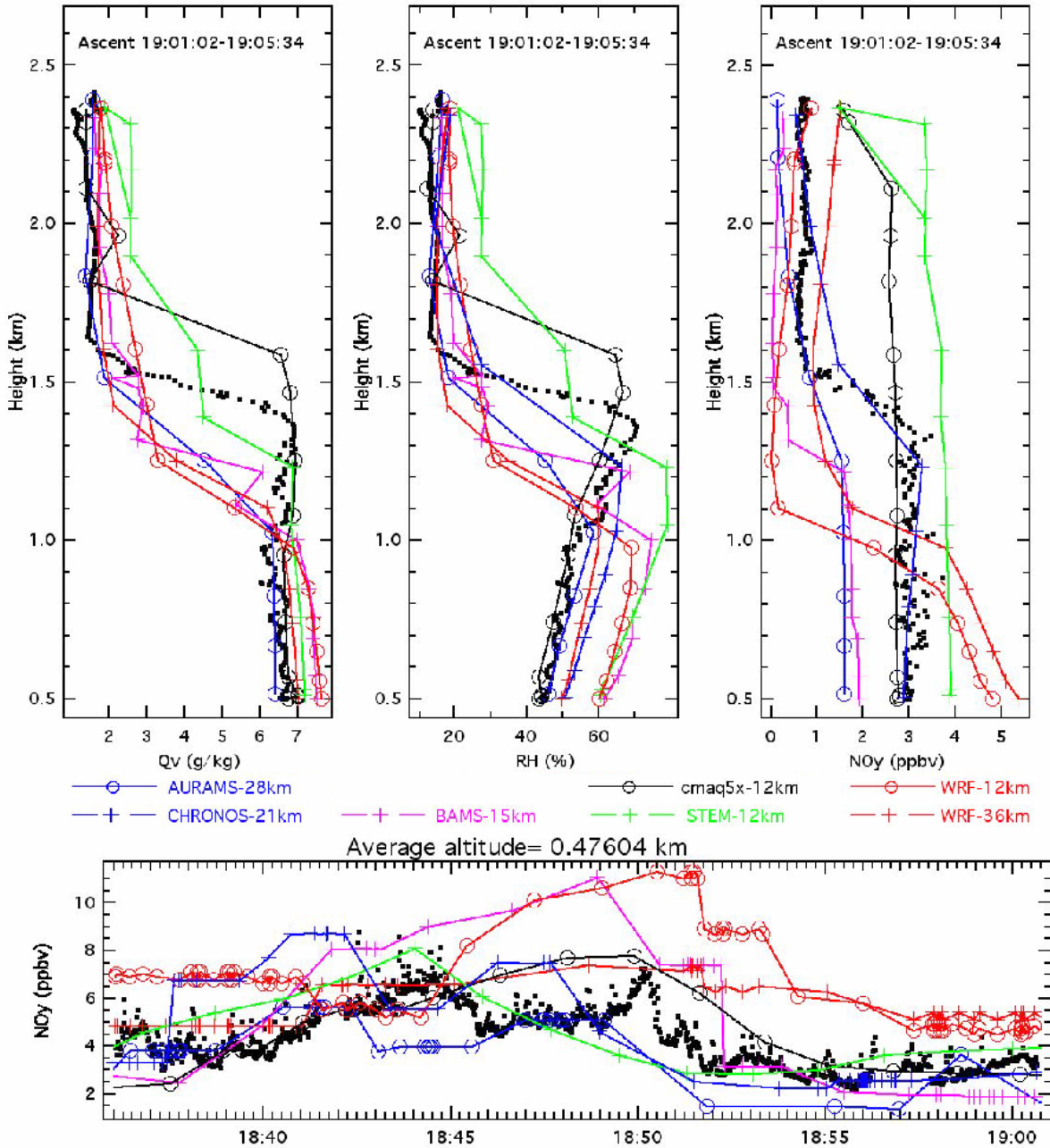
Figure J5. Profiles of water vapor, relative humidity, and NO$_y$ on 25 September 06, south and downwind of Dallas. Black dots indicate observations. The horizontal transect shows high biases of NO$_y$ for those models with the lowest PBL heights and reduced vertical transport.

Finding J3: **Model performance evaluations and intercomparisons require a comprehensive, best-guess emissions inventory for the TexAQS 2006 Field Intensive.**

Analysis: Byun et al.-U. Houston; Data: TCEQ.

Ozone and $PM_{2.5}$ forecasts are highly dependent on the emissions inventories of precursor emissions, and $PM_{2.5}$ forecasts are also dependent on primary emissions at many of the urban and suburban CAMS locations. A high priority in the model evaluation effort should be placed on using TexAQS 2006 field data to determine the accuracy of the inventories that drive AQ forecasts. Ozone forecasts are particularly sensitive to emissions estimates of HRVOC, such as ethylene and propylene, from large petrochemical facilities, especially in the Houston ship channel region. Quality-assured VOC measurements from the various platforms and comparisons with AQ model results are currently in progress in order to evaluate the model emissions inventories. Two preliminary sensitivity results from the University of Houston MM5/CMAQ model relate directly to emissions inventory validation. That model shows generally improved NO_2 and O_3 comparisons with CAMS site data using an emission inventory based on projections to 2005 as opposed to an inventory based on 2000 estimates. A narrow plume of extremely high O_3 observed downtown and west of Houston (7 September) that was significantly under-predicted by the original forecast was found to be replicated accurately in retrospective runs that included a VOC source in the ship channel region much larger than specified in the base emissions inventory.

KEY CITATIONS AND INFORMATION AND DATA SOURCES

McKeen, S., J. Wilczak, G. Grell, I. Djalalova, S. Peckham, E.-Y. Hsie, W. Gong, V. Bouchet, S. Menard, R. Moffet, J. McHenry, J. McQueen, Y. Tang, G.R. Carmichael, M. Pagowski, A. Chan, T. Dye, G. Frost, P. Lee, and R. Mathur. 2005. Assessment of an ensemble of seven real-time ozone forecasts over eastern North America during the summer of 2004. J. Geophys. Res., vol. 110, D21307, doi:10.1029/2005JD005858.

Nielsen-Gammon, J. W., R.T. McNider, W.M. Angevine, A.B. White, and K. Knupp. 2007. Mesoscale model performance with assimilation of wind profiler data: Sensitivity to assimilation parameters and network configuration. J. Geophys. Res., vol. 112, D09119, doi:10.1029/2006JD007633.

Model Acronyms and Web Links

AURAMS (A Unified Regional Air-Quality Modeling System)
http://www.msc-smc.ec.gc.ca/research/icartt/aurams_e.html

BAMS (Baron Advanced Meteorological Systems, Inc.)
http://www.baronams.com/projects/SECMEP/index.html

CHRONOS (Canadian Hemispheric and Regional Ozone and NOx System)
http://www.msc-smc.ec.gc.ca/aq_smog/chronos_e.cfm

CMAQ5x/WRF (Community Multi-scale Air Quality model/Weather Research Forecast model)
http://wwwt.emc.ncep.noaa.gov/mmb/aq/

University of Iowa STEM (Sulfur Transport and Emissions Model)
http://nas.cgrer.uiowa.edu/MIRAGE/mirage-2k6.html

WRF/Chem (Weather Research Forecast model/Chemistry version)
http://www.wrf-model.org/WG11

Response to Question K

QUESTION K
How can observation and modeling approaches be used for determining (i) the sensitivities of high ozone in the HGB non-attainment area to the precursor VOC and NO$_x$ emissions, and (ii) the spatial/temporal variation of these sensitivities?

BACKGROUND
The accurate prediction of the relative response of ozone concentrations to future reductions in NO$_x$ and VOC emissions is a much sought, but very elusive goal. This prediction is central to the very important SIP-relevant question of "direction of control" – that is, should ozone control efforts in an ozone non-attainment area be focused on: a) decreasing emissions of NO$_x$ alone, b) decreasing emissions of VOC alone, or c) decreasing emissions of both NO$_x$ and VOC? In this report the closely related Questions F and K both deal with aspects of this issue. The Background Section of the Response to Question F discusses some issues relevant to this Question and Response; the interested reader should peruse that discussion as a prelude to this Response to Question K and also review the recently revised *Guidance on the Use of Models and Other Analyses for Demonstrating Attainment of Air Quality Goals for Ozone, PM$_{2.5,}$ and Regional Haze* (USEPA, 2007). One point made in the background section of the Response to Question F is that a definitive answer to these questions requires a thoroughly tested Eulerian emissions-based air quality model that treats the region of interest with sufficient accuracy. Another point is that this model testing should involve comparisons between model results and direct observations of the relationships between ozone, its precursors, and the radicals that drive these reactions. Unfortunately however, it has not yet been possible to develop such generally applicable models because of deficiencies and uncertainties in many critical areas, including emissions, meteorological modeling, and photochemical mechanisms.

In the absence of a "perfected" Eulerian air quality model for the HGB non-attainment area, it has been necessary to take a variety of heuristic approaches to provide guidance to air quality managers. Heuristic implies a model that is simplified, but that is designed and used to learn more about some specific but important aspect of the more complex air-quality system that is to be managed. The Response to Question F discusses the application of both observation-based and emissions-based modeling approaches for approximately determining the sensitivity of ozone production and concludes that both VOC and NO$_x$ controls are presently effective in reducing the maximum observed ozone concentrations. Continued incremental reductions in emissions of either VOC or NO$_x$ emissions can be expected to yield incremental improvements in ozone design values in the HGB region.

Here the response to Question K addresses two very important questions that are related, but importantly different, in that they address how compliance with the current NAAQS for ozone can be achieved in an attainment demonstration:

- What emission controls will ultimately be necessary for the HGB area to achieve compliance with the 8-hour-average, 80 ppbv ozone standard?

- What is the most effective strategy by which to reach this compliance?

To address these questions, a very simple, emissions-based model was applied to the HGB region.

FINDINGS

Finding K1: **A simple, heuristic model based upon the Empirical Kinetic Modeling Approach (EKMA) method suggests that the HGB region may ultimately require drastic NO$_x$ emissions controls to reach compliance with the NAAQS for ozone.**

Finding K2: **The same model suggests that in a projected future scenario with very strict VOC emission controls, but without drastic NO$_x$ emission controls, biogenic VOC emissions plus background concentrations of CO and methane may be sufficient to cause ozone exceedances.**

Analysis: Dimitriades-NCSU; Luecken-USEPA.

A simplified model of an inherently complex system can sometimes provide valuable insight into the behavior of the complex system (Dimitriades, 2006; Dimitriades and Luecken, 2007). As a case in point, here we investigate a very simple, Empirical Kinetic Modeling Approach (EKMA) that includes an Ozone Isopleth Plotting Research Package (OZIPR) [see e.g. Finlayson-Pitts and Pitts, 2000]. This approach comprises a photochemical box model, and was applied to the HGB area in order to illuminate one aspect of the complex chemical-transport system that defines the near-surface atmosphere in the HGB region. The model was formulated to provide an answer to the very critical question: To reach compliance with the NAAQS ozone standard in HGB, what emission controls are necessary and most effective?

The model utilized an advanced version of the EKMA method for translating early morning (8 AM) ambient concentrations of VOC and NO$_x$ into the maximum 8-hour-average ozone concentration that accumulates by the end of the day. The model incorporates a SAPRC99 chemical mechanism and requires model and observational inputs on VOC composition, sunlight intensity, diurnally varying VOC (including biogenic VOC) and NO$_x$ emissions, diurnally varying boundary layer height, and background ozone concentration. The results presented here were obtained for:

> (i) A "typical" Harris County VOC mix, based on measurements at the LaPorte site during TexAQS 2000.

> (ii) A constant 30-ppbv concentration of background ozone.

> (iii) Time-varying post-8 AM VOC and NO$_x$ emissions based on average daily anthropogenic emissions reported for Harris county in 2002, apportioned as hourly emissions based on modeled profiles for total NO$_x$ and anthropogenic VOC emissions from EPA's 2001 National Emissions Inventory processed using the SMOKE emissions processor (http://www.smoke-model.org).

> (iv) Time-varying post-8 AM isoprene emissions estimated from the area average isoprene emissions for Harris County from the HGB 2002 emissions inventory (http://www.tceq.state.tx.us/assets/public/implementation/air/sip/hgb/hgb_sip_2007/appendices/06027SIP_Appendix_F_PEI.pdf). These emissions totaled 29 kg km^{-2}day^{-1}.

> (v) a typical time-varying mixing height based on measurements made at the Moody Tower site.

The results of the model are presented in the form of a traditional EKMA diagram in Figure K1. For illustration purposes, the method was applied to 8 AM NO$_x$ and VOC concentrations measured at five sites (Clinton, Channelview, Wallisville, Lynchburg Ferry, and HRM-3) within

Harris County during April-October of 2005 and 2006. A single ozone concentration isopleth diagram was constructed from the calculated maximum 8-hour-average ozone concentrations that accumulated in the model initiated with those 8 AM measured concentrations.
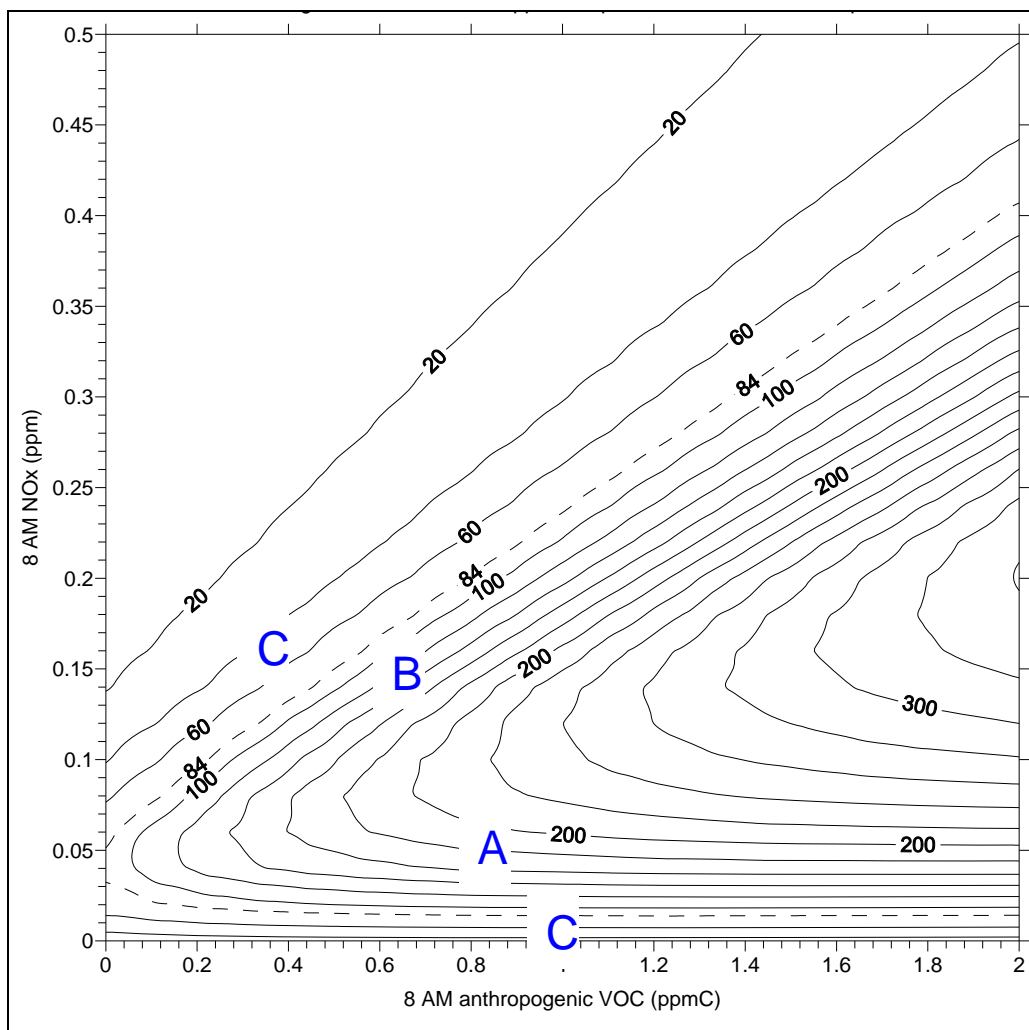
Figure K1. EKMA diagram constructed for the HGB region. The contour lines give the maximum 8-hour-average ozone concentration (in ppbv) that accumulated starting with the morning VOC and NO_x concentrations given on the respective axes. The critical, dashed line isopleth represents the maximum ozone concentration allowed in an area in compliance with the NAAQS.

Figure K1 suggests that the ozone sensitivity conditions within Harris County vary from VOC-sensitive to NO_x-sensitive from site to site and from day to day. For example, consider the points labeled A, B, and C in the figure. The two points labeled C represent non-exceedance conditions – they lie below the critical (84 ppbv) dashed line isopleth. Point A represents NO_x-limited exceedance conditions. The predicted maximum 8-hour average ozone concentration is above 84 ppbv, but by decreasing NO_x emissions sufficiently, the 8 AM NOx concentrations will decrease so that Point A will cross the critical dashed line isopleth. Similarly, Point B represents VOC-limited exceedance conditions; by decreasing VOC emissions sufficiently, the 8 AM VOC concentrations will decrease so that Point B will cross the critical dashed line isopleth.

There is a critical difference in the behavior that the EKMA model predicts for the NO_x-limited Point A and the VOC-limited Point B. Point B suggests that attainment can be most easily reached by reducing VOC emissions, but attainment can also be reached by reducing NO_x emissions if the reductions are drastic enough. Initially at point B, NO_x emission reductions alone would first increase the predicted maximum ozone concentration, but after a peak is reached, further NO_x emission reductions would lead to a decrease in the predicted maximum ozone concentration until Point B crosses the critical isopleth. In contrast, VOC reductions alone applied to Point A can never bring that point below the critical isopleth, because the maximum ozone concentration is predicted to be above 84 ppbv even when the 8 AM anthropogenic VOC concentrations are zero. This model behavior occurs because biogenic VOC emissions alone (with background CO and methane concentrations), in the presence of sufficient NO_x, can produce ozone concentrations in exceedance of the ozone standard. This behavior of Point A is similar to the predictions from the Eulerian modeling presented in Figure F3, which show that even extremely stringent VOC controls cannot decrease the HGB ozone design values enough to achieve compliance. Importantly, the EKMA model suggests that NO_x-sensitive conditions as exemplified by Point A are relatively common in HGB. Of the days investigated, 54% for Clinton, 17% for Channelview, 35% for Wallisville, 39% for Lynchburg Ferry, and 43% for HRM-3 exhibited Point A-like, NO_x-limited behavior.

Clearly the EKMA model is highly simplified, but it is notable that the NO_x-sensitive behavior exemplified by Point A may be reasonably well represented by the model. One of the most critical simplifications in the model is the assumption of a "typical" Harris County VOC mix. It is well known that the VOC composition in HGB changes markedly, from the typical urban mix of downtown Houston to the widely varying VOC emissions from the petrochemical facilities. However, the critical Point A behavior is focused at zero anthropogenic VOC concentration, so the assumed VOC composition will have no effect.

Given the EKMA model prediction that drastic NO_x emission controls will be required to eventually reach ozone compliance in HGB, the extremely difficult but central question arises:

> *How should air quality managers in the HGB area divide ozone management resources between NO_x and VOC emission controls?*

Several considerations favor control of VOC emissions, including:

- First, the Response to Question F indicates that incremental VOC emission reductions presently will result in incremental decreases in ambient ozone concentrations. Any progress in decreasing the maximum ambient ozone concentrations will have immediate health and welfare benefits.

- Second, Figure K1 does indicate that there is a modest advantage to VOC control when used in conjunction with NO_x control. For example, if the 8 AM VOC concentration is reduced from 0.4 to 0.1 ppm C, then NO_x controls need only reduce the 8 am NO_x concentration to about 25 rather than about 20 ppbv. Figure F3 also indicates a similar benefit of VOC control.

- Third, VOC emissions reductions can decrease ambient concentrations of VOC hazardous air pollutants. For example, the ambient concentrations of formaldehyde, which in the HGB area is primarily a secondary product of HRVOC oxidation, will respond to HRVOC emission controls.

Similarly, several considerations favor control of NO_x emissions, including:

- First, NO_x emissions will reduce not only locally produced ozone, but also regional background ozone. Outside of central urban areas and point source plumes, the regional ozone production environment is generally strongly NO_x-limited.

- Second, all of the modeling approaches agree that sufficiently drastic NO_x control is certain to lead to ozone attainment. Further, to the extent that the EKMA results reflect reality, such drastic control may be required to ultimately reach compliance. However, there is uncertainty whether the high degree of NO_x control required for ozone attainment is socio-economically acceptable or even technologically feasible.

- Third, NO_x controls will reduce local and regional levels of both nitrate aerosol, a significant contributor to $PM_{2.5}$ concentrations, and nitric acid, a significant component of acid deposition. Both of the nitrate contribution to $PM_{2.5}$ and the nitric acid contribution to acid deposition are particularly important issues in the western U.S.

The most efficient emission control strategies will then depend upon practical and economic considerations associated with the alternatives. Given that the Eulerian and EKMA models upon which all the preceding discussions are based are still imperfect, it is prudent to implement what VOC controls and/or NO_x controls are presently beneficial and practical, while modeling improvements are effected.

KEY CITATIONS AND INFORMATION AND DATA SOURCES

Dimitriades, D. 2006. A Proposed Study for Determining the Optimum Direction of Control in the Houston-Galveston-Brazoria Ozone Non-Attainment Area. NC State University Report to the Texas Commission on Environmental Quality. Submitted October 10, 2006. College of Natural Resources, NC State University, Raleigh, NC.

Dimitriades, B. and D. Luecken. 2007. An observational investigation of ozone sensitivity to VOC and NOx and it variation in the Houston-Galveston-Brazoria (HGB) ozone non-attainment area. Presentation at TexAQS II Principal Findings Data Analysis Workshop, 29 May-1 June 2007. Austin, TX. http://www.tceq.state.tx.us/assets/public/implementation/air/texaqs/workshop/20070529/2007.06.01/6-Spatial+Temporal_Patterns-Dimitriades.pdf

Finlayson-Pitts, B.J. and J.N. Pitts. 2000. Chemistry of the Upper and Lower Atmosphere. pp. 892-893. Academic Press, New York, NY.

US Environmental Protection Agency. 2007. Guidance on the Use of Models and Other Analyses for Demonstrating Attainment of Air Quality Goals for Ozone, $PM_{2.5}$, and Regional Haze. EPA Report 454/B-07-002. April 2007. EPA Office of Air Quality Planning and Standards, Air Quality Analysis Division, Air Quality Modeling Group, Research Triangle Park, NC. 262 pp. http://www.epa.gov/ttn/scram/guidance/guide/final-03-pm-rh-guidance.pdf

APPENDIX 1. GLOSSARY OF ACRONYMS

(The meaning of some of the acronyms more commonly used in the report are listed here.)

AIRS	Atmospheric Infrared Sounder
AIRS	Aerometric Information Retrieval System
AOD	Aerosol Optical Depth
AQ	Air Quality
AQFM	Air Quality Forecast Model
AURAMS	A Unified Regional Air-Quality System
BEIS	Biogenic Emissions Inventory System
BL	Boundary Layer
CALIPSO	Cloud Aerosol Lidar and Infrared Pathfinder Satellite Observation
CAMS	Community Air Modeling System
CAMx	Comprehensive Air Quality Model, with extensions
CB	Carbon Bond
CB05	Carbon Bond Photochemical Mechanism, version 5
CB-IV	Carbon Bond Photochemical Mechanism, version IV
CEMS	Continuous Emissions Monitoring System
CHRONOS	Canadian Hemispheric and Regional Ozone and NO_x System
CMAQ	Community Multi-scale Air Quality Model
CMBO	1-chloro-3-methyl-3butene-2-one
CRES	Lumped group of chemical species in photochemical reactions mechanisms that includes cresol
CST	Central Standard Time
DFW	Dallas-Fort Worth
DIAL	DIfferential Absorption Lidar
EGU	Electric power Generating Unit(s)
eGRID	Emissions and Generation Resource Integrated Database
EPA	US Environmental Protection Agency
EPS2	Emissions Processing System version 2
EKMA	Empirical Kinetic Modeling Approach
HGB	Houston-Galveston-Brazoria
HRVOC	Highly Reactive Volatile Organic Compound(s)
HSC	Houston Ship Channel
HSRL	High Spectral Resolution Lidar
HYSPLIT	HYbrid Single-Particle Lagrangian Integrated Trajectory model
LPAS	Laser Photo-Acoustic Spectroscopy
LST	Local Standard Time
MAE	Mean Absolute Error
MAQSIP-RT	Multiscale Air Quality SImulation Platform-Real Time
MM5	Meteorological Model version 5
MOBILE6	EPA Mobile Source Emission Factor Model version 6
MODIS	Moderate Resolution Imaging Spectroradiometer
MSA	Metropolitan Statistical Area
MSD	Medium Speed Diesel
NAAQS	National Ambient Air Quality Standards

31 August 2007

NASA	National Aeronautics and Space Administration
NCAR	National Center for Atmospheric Research
NCEP	National Centers for Environmental Prediction
NEI	National Emissions Inventory
NOAA	National Oceanic and Atmospheric Administration
NOAA/ESRL	NOAA Earth System Research Laboratory
NOAA/NESDIS	NOAA National Environmental Satellite Data and Information Service
OMI	Ozone Monitoring Instrument
OZIPR	Ozone Isopleth Plotting Research Package
PAN	PeroxyAcetyl Nitrate
PBL	Planetary Boundary Layer
$PM_{2.5}$	Particulate Matter less than 2.5 micrometers in diameter
PTR-MS	Proton Transfer Reaction-Mass Spectrometer
RAQMS	Realtime Air Quality Modeling System
ROG	Reactive Organic Gases
RHB	research vessel *Ronald H. Brown*
RMSE	Root Mean Square Error
RSST	Rapid Science Synthesis Team
SAPRC	[California] Statewide Air Pollution Research Center
SAPRC99	[California] Statewide Air Pollution Research Center (photochemical mechanism 1999 version)
SAPRC07	[California] Statewide Air Pollution Research Center (photochemical mechanism 2007 version)
SIP	State Implementation Plan
SMOKE	Sparse Matrix Operator Kernel Emissions
SOF	Solar Occultation Flux
SOS-OD	Southern Oxidants Study-Office of the Director
SSD	Slow Speed Diesel
STEM	Sulfur Transport and Emissions Model
TCEQ	Texas Commission on Environmental Quality
TES	Tropospheric Emission Spectrometer
TexAQS 2000	First Texas Air Quality Study, completed during the summer of 2000
TexAQS 2006	Intensive field measurement study conducted during 11 weeks of TexAQS II
TexAQS II	Second Texas Air Quality Study, completed during 18 months in 2005 and 2006
TRI	Toxics Release Inventory
UHI	Urban Heat Island
UTC	Coordinated Universal Time
VOC	Volatile Organic Compound(s)
WAS	Whole Air Samples
WP-3D	Instrumented aircraft operated by NOAA
WRF/Chem	Weather Research Forecast model/Chemistry version

APPENDIX 2. FINAL REPORT FROM QUESTION L WORKING GROUP.

Question L Final Report

QUESTION L
What existing observational databases are suitable for evaluating and further developing meteorological models for application in the HGB area?

QUESTION L WORKING GROUP
Leader: Lisa Darby; Participants: Robert Banta, John Nielsen-Gammon, Daewon Byun, Wayne Angevine, Mark Estes, Bryan Lambeth, Stuart McKeen.

BACKGROUND
In order to address this question, databases that are potentially useful to individuals performing air quality modeling for Texas, including both permanent measurements and enhanced measurements from TexAQS II deployments, were compiled. The databases were evaluated based on several criteria, including quality control, accessibility, regional coverage, and time resolution. Web links to the databases are given, followed by a brief description and evaluation.

FINDINGS

Surface Meteorology and Chemistry Data

COOP observations
http://www7.ncdc.noaa.gov/IPS/CDPubs?action=getstate
Consists of monthly printed pages (available as PDFs online) containing station observations. No description of QA is provided on the web site.

Because these data are not in machine-readable format, they are unlikely to be useful for any systematic study. They are redundant, in the sense that the same observations should be in the normal NWS data streams.

Crop Weather Program, Texas A&M University
http://cwp.tamu.edu/cgi-bin/htmlos.cgi/6742.2.1749378041063346623
The Crop Weather Program for South Texas (CWP) was developed to help farmers and consultants make management decisions conducive to profitable crop production. It replaces an earlier cotton monitoring system known as the Weather Station Network Program. The CWP is the gateway for access to weather data measured by a network of 21 automated weather stations spread across 10 South Texas counties and provides hourly measurements of air temperature, relative humidity, solar radiation, wind direction and speed, precipitation, and soil temperature at 1", 3", and 8" depths. The wind direction is reported based on a 16-point compass and the wind speed appears to be arithmetic (no vector average direction or speed). The wind also appears to be measured about 10 feet above ground level based on an example site photo provided (this could exacerbate exposure problems where buildings and/or trees are nearby).

Harris County Office of Homeland Security and Emergency Management
http://www.hcoem.org/
The Harris county rainfall map site allows you to enter an amount of time (in days, hours, or minutes) before the current time, and it produces a map of accumulated rainfall amounts from each site, over the time requested. The data come from 163 automatic remote sensors (part of

the flood alert system) across the metropolitan area, and they are "unofficial" (probably means not quality-controlled). The density of the network allows for detailed information regarding the horizontal distribution of the rainfall. Their locations can be found on a map link and a text link, which includes latitudes and longitudes. There is a link to an archive site where you can indicate a given amount of time before your date of interest to obtain a map of accumulated rainfall, but I could not get this part to work. If this does eventually work, this could be a useful site for modelers, although it looks like the only output would be a map (i.e., no text dump). I suggest a following up on this site to determine if there is a way to order the archived data.

Also on the main page for Harris County Office of Homeland Security and Emergency Management is a link to a real time Houston speed map. Along the outlines of the major highways the current speed of traffic is shown in color (indicating speeds <20, 20-29, 30-39, 40-49, and 50+ MPH, or no data). On this site is a link to the Houston speed map archives (http://traffic.houstontranstar.org/map_archive/map_archive.aspx). From this site you can select a date and time (down to 15-minute intervals) and you get a traffic speed map for that time. This could be useful to determine if gridlock was worse on some days compared to others.

Texas A&M data
http://dallas.tamu.edu/Weather/index.html
This web site has data from two sites near Dallas. The sites are run by the Texas A&M Dallas Agricultural Research and Extension Center (phone: 972.231.5362), and details are sketchy. The locations are not specified, although one is on a research farm (Prosper) and the other is just called "Dallas." The "Dallas" site has, by date, max/min soil temperature, max/min air temperature, max/min RH, a single column labeled "wind" (no units indicated on any of the columns), max/min soil moisture, and total rain. Some years have a column labeled ET_o (evapotranspiration?). At the end of each month is a row for monthly medians for each column and another row with the max, min, or total for each column (depending on the variable). The Prosper site has the same variables, plus "RAD" (radiation?), wind speed, wind direction and battery voltage. The Dallas site has data archived from 2000 and the Prosper site has data archived from 1997. Given how important soil moisture measurements are for modelers, it may be useful to investigate this database further to determine the location of the sites and the robustness of the soil moisture data.

Lower Colorado River Authority network
http://hydromet.lcra.org/index2.shtml
Lower Colorado River Authority network. This web page has a wealth of information regarding measurements throughout the Colorado River watershed (which extends from NW to SE of Austin, becoming quite narrow at Matagorda Bay). The network is most dense around Austin. They have: rainfall (24-hr accumulation, accumulation since midnight, and the most recent measurement); stage, flow, lake level, air temperature, relative humidity, and conductivity data, shown on maps. You can download historic data for a single site (precipitation, air temperature, relative humidity, wind speed and direction), but this is not very practical for obtaining data from many sites. It is stated that real-time data are provisional, but there is no indication about the quality of the archived data. It may be worth investigating if it is possible to obtain archived data directly from the agency.

Texas A&M agricultural weather site

http://texaset.tamu.edu/weatherstns.php

This one would be useful for Texas meteorological comparisons of precipitation (not many CAMS sites have precipitation), temp, RH, wind speed, wind direction, and solar radiation. Pretty good coverage in East Texas. Hourly data should be simple to download and compare with model results.

Soil Climate Analysis Network, US Agriculture Department

http://www.wcc.nrcs.usda.gov/scan/

This site only gives soil parameters - no standard met. There is only one site (Prairie View) in the region of Texas that may be useful to TexAQS 2006 participants. Nonetheless, it may useful for comparison of soil models and parameterizations in meteorological models, since soil data is so sparse in the east Texas region.

Louisiana agricultural weather data network

http://www.agctr.lsu.edu/subjects/weather/

This site is specific to the state of Louisiana. It gives meteorological and soil parameter data at about 20 sites evenly distributed throughout Louisiana. The data are not so convenient to download. But the soil parameters may be useful for meteorological model soil data comparisons.

Louisiana Universities Marine Consortium weather network.

http://weather.lumcon.edu/

This web site includes measurements from 5 sites in Louisiana run by LUMCOM (Louisiana Universities Marine Consortium). Four of the sites are on platforms over water. The 5th site is somewhat inland, but looks like it's in a marshy/wetlands type of area. The Lake Pontchartrain station is in the northern part of the lake. Meteorological data include: atmospheric pressure, humidity, temperature, winds, solar radiation, and precipitation. Hydrographic instrumentation include: chlorophyll probe, conductivity probe, and a sonde, 6600. Three other sites have the same instruments: Tambour Bay, Southwest Pass/Miss River and LUMCOM. The Tambour Bay and Southwest sites are off the LA coast, on platforms. LUMCOM is the slightly inland site and also has a co-located 915-mHz wind profiler with RASS. The Audubon/Miss River site is on a floating structure near the coast (from the picture is looks like it's in a harbor). It only has atmospheric pressure, humidity, and temperature for meteorological measurements. It has the same hydrographic measurements as Lake Pontchartrain, plus a wet chemical in-situ nitrate analyzer.

The web site is comprehensive, with a map and much information for each station. There are records regarding calibrations and inspections, implying that these sites are well maintained. These appear to be good sites for modelers to obtain coastal meteorological data for Louisiana. The archived files are easy to access.

CAMS (TCEQ organized surface meteorological and chemical data)
http://www.tceq.state.tx.us/nav/eq/mon_sites.html
This website includes information regarding the details of the TCEQ measurements sites. Many sites have both meteorology and chemistry measurements. Some have just one or the other. All chemistry sites appear to have ozone measurements, but some also include NO, NO2, and perhaps other important constituents. Those with meteorology tend to have temperature and winds, perhaps precipitation. This site has two links:

      1) TCEQ's Air Monitoring Sites (Regional Map) provides details about the TCEQ's air monitoring sites and air pollution, weather and other parameters measured at each site.

      2) Air Monitoring Sites (Table)

Provides a user interface to view sortable list of locations and descriptions of monitoring sites operated by the TCEQ and other entities around the state as well as link to photos of sites, lists of parameters monitored, and current measurements.

This is useful for modelers who want to know the locations of monitoring stations, and what is monitored at each station.

http://www.tceq.state.tx.us/compliance/monitoring/air/monops/historical_data.html
This page provides access to two sources of pollutant and weather data. The first source, the Texas Commission on Environmental Quality (TCEQ) and local monitoring networks, provides hourly pollutant and weather data from 1972 to 2004. The second source, the U.S. Environmental Protection Agency (EPA), provides data summaries and hourly data collected since 1982 on numerous pollutants and meteorological parameters in Texas and other states.

A useful site for modelers to download hourly surface data for model evaluation.

METARs (NWS surface data)
http://www.nndc.noaa.gov/cgi-bin/nndc/buyOL-001.cgi
The Unedited Surface Weather Observations product consists of unedited hourly observations from over 700 U.S. locations. There is a charge to access this data online, but not if your domain is .gov, .mil, or .edu. (More details on the web site.) The time range of the available data is from July 1, 1996 to two days ago. A useful site for obtaining surface observations for model evaluation.

Oklahoma air quality monitors
http://www.deq.state.ok.us/AQDnew/monitoring/index.htm
This site has the details of the air quality monitoring stations in Oklahoma. There are several monitoring sites north of the Texas-Oklahoma border that would be useful for southerly flow events (e.g., looking at transport from Dallas to Oklahoma). For a graphical display, the site links to the EPA site http://www.airnow.gov/index.cfm?action=airnow.currentconditions, where the user can click on the state of Oklahoma to see the Oklahoma observations. Text data includes real-time data (for today and yesterday). The user can sort by pollutant or by station. Archived data includes 8-hour averages of ozone and CO, organized by year. Within each year is the date and amount of the 4 highest readings for each station. One-hour ozone exceedances are also available in this format. It does not appear that data other than the 4 highest readings per year are available via the web. This site is probably somewhat useful for modelers.

Upper Air Data

ESRL (formerly ETL) Profiler Network, South Central Texas
http://www.etl.noaa.gov/et7/data/
The ESRL (formerly ETL) network page allows access to real-time and archived plots of profiler winds and other profiler data. Real-time plots are provided through a clickable map interface. Archived plots and ASCII data can be downloaded for single profilers. A trajectory tool allows the calculation of forward and backward trajectories using profiler data. The site includes all regular wind profilers from the NOAA and TCEQ network as well as all those installed for the TexAQS-II field program. The data include profiler winds and signal-to-noise ratio, RASS virtual temperature and virtual potential temperature, and surface meteorological observations from profiler sites. Data should remain available for several months after the experiment, as well as the profiler trajectory tool.

NOAA National Profiler Network graphical display
http://www.profiler.noaa.gov/npn/
The NOAA site used to include all permanent profilers, but now it appears to contain only the profilers in the NOAA demonstration network, including Ledbetter, Palestine, and Jayton in Texas. Users can request real-time plots or generate plots using archived data. There is considerable flexibility in the online data plotting interface. Archived data are available from the web site hosts.

Rapid Update Cycle (RUC) soundings
http://rucsoundings.noaa.gov/
This sounding page allows the user to generate plots or ASCII data dumps of soundings from rawinsondes, profilers, and RUC/MAPS forecasts. The output is Java-based, allowing mouse-over data information and animation/looping of soundings. The interface requires the user to know the name or site ID's of the stations to plot. Most of the data are available only in real-time or near-real-time, except that an online rawinsonde archive was begun early in 2006. Perhaps the most useful aspect of the web site is the ability to plot forecast soundings from the RUC model. These forecasts are available for any arbitrary location and extend up to 12 hours into the future, so they provide detailed guidance for mixing heights, vertical wind shear, and convection.

University of Wyoming sounding page
http://weather.uwyo.edu/upperair/sounding.html
This web site allows the user to select a station using a clickable map and generate graphical soundings or ASCII data output from real-time or archived rawinsonde observations. The output format includes all common sounding diagram types and ASCII data formats. Large amounts of data would be difficult to obtain, but this site is the best available on the web for individual archived soundings.

ACARS aircraft observations
http://amdar.noaa.gov/
ACARS observations are in situ meteorological observations made by commercial aircraft. The data include temperature, wind, and often dew point. The wind precision is not very good, but the temperature and dew point data are useful for estimating mixing heights and their diurnal variation. Most ACARS observations in Texas come from the Dallas-Fort Worth area, usually about two dozen per day. Much less frequent observations are available from Houston and other major airports. The data are not freely available in real time on the web, but they are available for research purposes upon approval by NOAA. Texas A&M presently receives ACARS data but is not funded by TCEQ to process or use the data for analysis or forecasting during 2006.

Coastal and Buoy Data

Texas Coastal Ocean Observation Network, Texas A&M Corpus Christi, Conrad Blucher Institute
http://lighthouse.tamucc.edu/TCOON/HomePage
Large network of coastal stations. Some of the reported stations are regular NOAA or other agency stations, and these are not identified as such. The additional stations seem to primarily provide water level, water temperature, and air temperature. Machine-readable historical data are available. Some QA is apparently done, but specifications are not easily found on the web site.

Possibly useful for improving resolution of model validations for simple parameters.

NDBC (National buoy data)
http://www.ndbc.noaa.gov/Maps/WestGulf.shtml
Provides listings of hourly meteorological data (air and sea-surface temperature, winds, pressure, etc.) and wave data for each meteorological buoy in the Gulf of Mexico (and elsewhere around the U.S.). Meteorological data are archived back as far as 1990 for some sites. Also a section gives data on ocean currents as a function of depth. Buoy and other instrument locations are displayed on a map, and data are obtained by clicking on the site of interest. Recent ship observations are also listed at this site, and the tri-annual *Mariners Weather Log.*

Houston/Galveston Port Meteorological Office
http://www.srh.noaa.gov/hgx/marine/pro.htm
Houston/Galveston Port Meteorological Office

Site includes a description of needs for maritime meteorological data and the role of this office in facilitation of the Voluntary Observing Ship (VOS) Program. The office also "works within the framework of the Shipboard Environmental (Data) Acquisition System (SEAS), by which meteorological data are collected and transmitted to NCEP, for inclusion in the major data bases. Under *Past Weather*, this site has climatological data and daily information for several Texas land stations around the Gulf of Mexico, including daily high and low temperatures, wind, precipitation, and some other meteorological data. The monthly Texas Climatic Bulletins and other climatological products and information are available at this site. We were unable to locate any actual shipboard data from this site (however, some current data could be found on the NDBC site).

Satellite Data

Space Science and Engineering Center, University of Wisconsin, Madison
http://www.ssec.wisc.edu/
Comprehensive archive of data, products, and downloadable processing software for geosynchronous and polar-orbiting satellites, including GOES-11 and -12 and MODIS data from Terra and Aqua. A host of real-time satellite images and products are also available, some stored for 7 days. Routine meteorological data are also available for McIdas users.

NASA Aura TES step and stare observations
http://tes.jpl.nasa.gov
TES is an infrared, high resolution, Fourier Transform spectrometer covering the spectral range 650 - 3050 cm-1 (3.3 - 15.4 µm) at a spectral resolution of 0.1 cm-1 (nadir viewing) or 0.025 cm-1 (limb viewing). Launched into a polar sun-synchronous orbit (13:38 hrs local mean solar time ascending node) on July 15, 2004, the TES orbit repeats its ground track every 16 days (233 orbits), allowing global mapping of the vertical distribution of tropospheric ozone and carbon monoxide along with atmospheric temperature, water vapor, surface properties (nadir), and effective cloud properties (nadir). TES has a fixed array of 16 detectors, which in the nadir mode, have an individual footprint of approximately 5.3 x .5 km. In order to increase the signal-to-noise ratio, these detectors are averaged together to produce a combined footprint of 5.3x8.4 km. TES has two basic observational modes: the global survey mode, where observations are taken 1.3 degrees apart in latitude, and the "step-and-stare" mode, where the separation between observations is approximately 35 km along the orbit. This step-and-stare mode was used extensively throughout the TexAQS 2006 campaign.

Maps of these profiles can be found at
http://tes.jpl.nasa.gov/TexAQS_2006/main_SS_TEXAQS_2006.html

Contact information: kevin.bowman@jpl.nasa.gov

NASA CALIPSO observations
http://www-calipso.larc.nasa.gov/
The Cloud-aerosol lidar and Infrared Pathfinder satellite Observations (CALIPSO) satellite mission was launched on April 28, 2006 for a planned 3-year mission. CALIPSO is flying in formation with Aqua, Aura, CloudSat, and Parasol satellites as part of the Afternoon Constellation or A-train. The CALIPSO payload consists of three instruments: the Cloud-Aerosol LIdar with Orthogonal Polarizaton (CALIOP); the Infrared Imaging Radiometer (IIR) and the Wide Field Camera (WFC). CALIPO is a nadir-pointing instrument which provides profile measurements of aerosol backscatter at 532 and 1064 nm and depolarization at 532 nm. The IIR provides calibrated radiances at 8.65 µm, 10.6 µm, and 12.05 µm over a 64 km swath centered on the lidar footprint and a pixel resolution of 1 km. The WFC consists of a single channel covering the 620 nm to 670 nm spectral region providing images of a 61 km swath with a spatial resolution of 125 m in a band 5 km about the nadir track and 1000 m elsewhere. For TexAQS 2006 campaign, CALIPSO *quick turn-around* browse images were produced to identify aerosol and cloud layers for flight planning activities. Observations were also synthesized into aerosol modeling systems to better understand the origin of surface and elevated aerosol features from regions outside the experiment domain.

Examples of aerosol browse images used during TexAQS can be found at
http://www-calipso.larc.nasa.gov/products/lidar/

Contact information: Charles.R.Trepte@nasa.gov

NOAA and DoD satellite images
http://www.class.noaa.gov/nsaa/products/welcome;jsessionid=1C0E54F015C2813E5A9ACFC22C675F90
The National Oceanic and Atmospheric Administration (NOAA) Comprehensive Large Array-data Stewardship System (CLASS) is NOAA's premier on-line facility for the distribution of NOAA and US Department of Defense (DoD) Polar-orbiting Operational Environmental Satellite (POES) data and derived data products. CLASS is operated by the Information Processing Division (IPD) of the Office of Satellite Data Processing and Distribution (OSDPD), a branch of the National Environmental Satellite, Data and Information Service (NESDIS).

CLASS maintains an active partnership with NOAA's National Climatic Data Center (NCDC). NCDC, the permanent US Archive for POES data and derived data products, supports CLASS through a user-interactive Help Desk facility and through the provision of POES supporting documentation, including the NOAA Polar Orbiter Data (POD) User's Guide and the NOAA KLM User's Guide. Additionally, NCDC and CLASS share data distribution responsibilities for Defense Meteorological Satellite Program (DMSP) data under a Memorandum of Understanding with the National Aeronautics and Space Administration (NASA) for the Earth Observing System (EOS) Program.

CLASS provides data free of charge. Anyone can search the CLASS catalog and view search results through CLASS's World Wide Web (WWW) site. Users who wish to order data are required to register with their names and email addresses. CLASS distributes data to those users via FTP services.

CLASS (originally called Satellite Active Archive), was established as a demonstration prototype for electronic distribution of POES data in 1994, and became operational in July 1995. During that first month, 379 Advanced Very High Resolution Radiometer (AVHRR) Level 1b data sets were distributed to 27 customers via the emerging Internet. During the first five years of operation, the average monthly volume of data distribution increased to 65,000 data sets with a total size of 1.2 TB, and the SAA customer base grew to more than 10,000 registered customers. The active archive was expanded during that period to include TIROS Operational Vertical Sounder (TOVS) data, Defense Meteorological Satellite Program (DMSP) data, Radarsat Synthetic Aperture Radar (SAR) imagery, operational (near-term) satellite-derived products, and climatic (time-series) satellite-derived products.

NASA Earth Observatory natural hazards
http://earthobservatory.nasa.gov/NaturalHazards/
This is a NASA site that has awesome satellite images due to the following natural phenomena: crops & drought; dust & smoke, fires, floods, severe storms, and volcanoes. The images are organized by event, and are free to all. They just ask for proper acknowledgment. This site is probably of limited value to modelers, but for certain events, such as the Saharan dust events that occurred during TexAQS II, the images may add some visual interest for a case study presentation.

NASA MODIS Rapid Response System images
http://rapidfire.sci.gsfc.nasa.gov/realtime/2006297/
This site has images from MODIS (Terra and Aqua). Images are archived by day, and can be downloaded. This site may be somewhat useful for modelers.

NASA Aqua AIRS retrieved CO profiles
http://asl.umbc.edu/pub/mcmillan/www/index.html#calendar
AIRS output for the TexAQS II field campaign. There is a clickable calendar for a view of the data. Please work with Dr. Wallace McMillan if interested in using the data (contact information is on the web site).

Solar Radiation Data

Texas Solar Radiation data, from a solar energy research group at UT
http://www.me.utexas.edu/~solarlab/tsrdb/
This site has solar radiation data for 15 sites throughout Texas. The data intervals and times of coverage vary by station, ranging from 15 minute data to monthly averages. Data stops in 2003 or earlier for many of the stations. Data reported: Global horizontal, direct normal, and diffuse horizontal (W m^{-2}). Monthly averages include temperature (degrees C). Data are easy to access. This site may be moderately useful for modelers.

National Renewable Energy Lab (solar radiation data)
http://rredc.nrel.gov/solar/new_data/confrrm/
Cooperative Networks for Renewable Resource Measurements (CONFRRM). This network was designed to capture long-term solar radiation and wind measurements. There are 5 sites in Texas, however the last month showing data for all sites is March 2000. Therefore, data on this site are not useful for modelers working on summers 2000 – 2006.

Large, Multi-field Data Sets

MADIS
http://madis.noaa.gov/
The Meteorological Assimilation Data Ingest System (MADIS) is dedicated toward making value-added data available from the National Oceanic and Atmospheric Administration's (NOAA) Earth System Research Laboratory (ESRL) Global Systems Division (GSD) (formerly the Forecast Systems Laboratory (FSL)) for the purpose of improving weather forecasting, by providing support for data assimilation, numerical weather prediction, and other hydro-meteorological applications.

MADIS subscribers have access to an integrated, reliable and easy-to-use database containing the real-time and archived observational datasets described below. Also available are real-time gridded surface analyses that assimilate all of the MADIS surface datasets (including the very dense integrated mesonet data). The grids are produced by the Rapid Update Cycle (RUC) Surface Assimilation System (RSAS) that runs at ESRL/GSD, which incorporates a 15-km grid stretching from Alaska in the north to Central America in the south, and also covers significant oceanic areas. RSAS grids are valid at the top of each hour, and are updated every 15 minutes.
- Observations
    - Meteorological Surface
        - METAR
        - SAO
        - Maritime
        - Modernized NWS Cooperative Observer
        - Integrated Mesonet
            - Observations from local, state, and federal agencies and private mesonets (including GPSMET water vapor)
    - Radiosonde
    - NOAA Profiler Network
    - Hydrological Surface
    - Automated Aircraft
        - Automated Aircraft Reports
        - Profiles at Airports
    - Multi-Agency Profiler
    - Radiometer
    - Satellite Wind
        - GOES Operational 3-Hour
        - GOES Experimental 1-Hour
    - Satellite Sounding
        - NOAA POES
    - Satellite Radiance
        - NOAA POES
    - Snow
- Grids
    - RSAS Surface Analyses

TCEQ Air Pollution Events
http://www.tceq.state.tx.us/compliance/monitoring/air/monops/sigevents06.html
The TCEQ Air Pollution Events web pages provide preliminary analyses of large-scale high ozone and/or particulate events in Texas. The analyses include satellite imagery, webcam imagery, ozone contour animations, ozone plume animations, backward air trajectories, upper air

data graphs, and pollution data time series graphs. The discussions describe the intensity and geographic coverage of each event. The discussions also report any transport related aspects to the pollution, if appropriate, and provide an estimate of background levels and local add-on for ozone cases.

EDAS (NCEP grid reanalysis)

http://www.cdc.noaa.gov/cdc/reanalysis/reanalysis.shtml

It is a website for the NCEP/NCAR Reanalysis Project at the NOAA/ESRL Physical Sciences Division

This page points you to information on the NCEP/NCAR Reanalysis project and the implementation of a netCDF-based, internet-accessible, data service at NOAA/ESRL PSD for this set of data products.

   * The 6-hourly and daily data currently available on-line.
   * The monthly and other derived data currently available on-line.

This site also has links to other reanalysis project sites (e.g., ECMWF).

NCEP/NCAR Reanalysis

http://dss.ucar.edu/pub/reanalysis/

This site includes the following NCEP/NCAR REANALYSIS databases.

   * DSS Reanalysis archives.

Project Overview

   * Project Description -

      The project motivation and objectives, cooperative arrangement between NCEP and NCAR, and other published documentation are outlined

   * Model Description
   * Project Status
   * Other Related Sites

Data Product Description

More than 20 different data products are output from the Reanalysis data assimilation, model run, and model forecast. These products are defined in terms of the NCAR archive names, physical variables, resolutions (temporal and spatial), and media storage size. CDROMS are also used to distribute selected reanalysis products.

This web site includes much detail on all of the data bases used, etc.

   * 2006AUG10 --All 1948-2006JUL pgb.f00 and grb2d files are now available on line for registered users.
   * 2006AUG10 --JUL 2006 data files are released. All 1948-2006JUL reanalysis files are available.
   * 2006APR20 --Public (non-restricted) version of 200309-200602 prepqm files are released.
   * 2006APR11 --2005 annual cdrom is released. All 1950-2005 reanalysis annual cdroms are available.
   * 2006MAR28 --2005OCT-2006FEB reanalysis forecasts are released.

* 2005Apr20 --2004OCT-2004DEC reruns to fix sea-ice problems are released.

* 2005Apr19 --2004AUG and 2004SEP reruns to fix sea-ice problems are released.

* 2005Apr08 --There will be a rerun from 2004080100 to 2005032212 due to sea-ice data problem. The 200501 and 200502 results are in.

* 2003Aug04 --NCEP-NCAR Reanalysis Temperature Change Plots, 1948-2002

* DSS Reanalysis archives.

Project Overview

* Project Description -

The project motivation and objectives, cooperative arrangement between NCEP and NCAR, and other published documentation are outlined

* Model Description

* Project Status

* Other Related Sites

Data Product Description

More than 20 different data products are output from the Reanalysis data assimilation, model run, and model forecast. These products are defined in terms of the NCAR archive names, physical variables, resolutions (temporal and spatial), and media storage size. CDROMS are also used to distribute selected reanalysis products.

This web site includes much detail on all of the data bases used, etc.

APPENDIX 3. INSTITUTIONAL AFFILIATIONS AND E-MAIL ADDRESSES FOR MEMBERS OF THE RAPID SCIENCE SYNTHESIS WORKING GROUPS AND OTHER COOPERATORS

Dave Allen, University of Texas at Austin — allen@che.utexas.edu
Wayne Angevine, NOAA Earth System Research Laboratory — wayne.m.angevine@noaa.gov
Elliot Atlas, University of Miami — e.atlas@miami.edu
Bob Banta, NOAA Earth System Research Laboratory — robert.banta@noaa.gov
Tim Bates, NOAA Pacific Marine Environmental Laboratory — tim.bates@noaa.gov
Carl Berkowitz, DOE Pacific Northwest Laboratory — carl.berkowitz@pnl.gov
Veronique Bouchet, Meteorological Service of Canada — veronique.bouchet@aec.gc.ca
Kevin Bowman, NASA Jet Propulsion Laboratory, Caltech — kevin.bowman@jpl.nasa.gov
Pete Breitenbach, Texas Commission on Environmental Quality — pbreiten@tceq.state.tx.us
Chuck Brock, NOAA Earth System Research Laboratory — charles.a.brock@noaa.gov
Steve Brown, NOAA Earth System Research Laboratory — steven.s.brown@noaa.gov
Daewon Byun, University of Houston — daewon.byun@mail.uh.edu
Greg Carmichael, University of Iowa — gregory-carmichael@uiowa.edu
Bill Carter, University of California, Riverside — carter@mail.cert.ucr.edu
Ellis Cowling, North Carolina State University — ellis_cowling@ncsu.edu
Lisa Darby, NOAA Earth System Research Laboratory — lisa.darby@noaa.gov
Joost de Gouw, NOAA Earth System Research Laboratory — joost.degouw@noaa.gov
Basil Dimitriades, North Carolina State University — basildi@hotmail.com
Bright Dornblaser, Texas Commission on Environmental Quality — bdornbla@tceq.state.tx.us
Mark Estes, Texas Commission on Environmental Quality — mestes@tceq.state.tx.us
Alan Fried, National Center for Atmospheric Research — fried@ucar.edu
Maedeh Faraji, University of Texas at Austin — mfaraji@mail.utexas.edu
Cari Furiness, North Carolina State University — cari_furiness@ncsu.edu
Noor Gillani, University of Alabama in Huntsville — gillani@nsstc.uah.edu
Wanmin Gong, Meteorological Service of Canada — wanmin.gong@ec.gc.ca
Georg Grell, NOAA Forecast Systems Laboratory — georg.a.grell@noaa.gov
Mike Hardesty, NOAA Earth System Research Laboratory — mike.hardesty@noaa.gov
Scott Herndon, Aerodyne Inc. — herndon@aerodyne.com
John Holloway, NOAA Earth System Research Laboratory — john.s.holloway@noaa.gov
Harvey Jeffries, University of NC at Chapel Hill — harvey@unc.edu
John Jolly, Texas Commission on Environmental Quality — jjolly@tceq.state.tx.us
Dick Karp, Texas Commission on Environmental Quality — dkarp@tceq.state.tx.us
Siwan Kim, NOAA Earth System Research Laboratory — siwan.kim@noaa.gov
Susan Kemball-Cook, Environ Corp — skemballcook@environcorp.com
Bryan Lambeth, Texas Commission on Environmental Quality — blambeth@tceq.state.tx.us
Barry Lefer, University of Houston — blefer@uh.edu
Deborah Luecken, US Environmental Protection Agency — luecken.debora@eps.gov
John McHenry, Baron Advanced Meteorological Systems — john.mchenry@baronams.com
Stuart McKeen, NOAA Earth System Research Laboratory — stuart.a.mckeen@noaa.gov
Wallace McMillan, University of Maryland, Baltimore County — mcmillan@umbc.edu
Jeffery McQueen, NOAA National Weather Service — jeff.mcqueen@noaa.gov
Johan Mellqvist, University of Göteborg, Sweden — johan.mellqvist@rss.chalmers.se

Ann Middlebrook, NOAA Earth System Research Laboratory ann.m.middlebrook@noaa.gov
Gary Morris, Valparaiso University gary.morris@valpo.edu
John Nielsen-Gammon, Texas A&M University n-g@tamu.edu
Jonathan Andy Neuman, NOAA Earth System Research Laboratory andy.neuman@noaa.gov
John Nowack, NOAA Earth System Research Laboratory john.nowak@noaa.gov
Hans Osthoff, NOAA Earth System Research Laboratory hans.osthoff@noaa.gov
David Parrish, NOAA Earth System Research Laboratory david.d.parrish@noaa.gov
Ryan Perna, University of Houston ryan.perna@mail.uh.edu
Brad Pierce, NOAA Satellite and Information Service robert.b.pierce@nasa.gov
Particia Quinn, NOAA Pacific Marine Environmental Laboratory particia.k.quinn@noaa.gov
Bernhard Rappenglück, University of Houston brappenglueck@uh.edu
James Roberts, NOAA Earth System Research Laboratory james.m.roberts@noaa.gov
Ted Russell, Georgia Institute of Technology trussell@ce.gatech.edu
Tom Ryerson, NOAA Earth System Research Laboratory thomas.b.ryerson@noaa.gov
Ken Schere, US Environment Protection Agency schere.kenneth@epa.gov
Christoph Senff, NOAA Earth System Research Laboratory christoph.senff@noaa.gov
David Sullivan, University of Texas at Austin sullivan231@mail.utexas.edu
Michael Trainer, NOAA Earth System Research Laboratory michael.k.trainer@noaa.gov
Youhua Tang, University of Iowa youhua.tang@noaa .gov
Sara Tucker, NOAA Earth System Research Laboratory sara.tucker@noaa.gov
William Vizuete, University of North Carolina at Chapel Hill vizuete@email.unc.edu
Carsten Warneke, NOAA Earth System Laboratory carsten.warneke@noaa.gov
Allen White, NOAA Earth System Research Laboratory allen.b.white@noaa.gov
Jim Wilczak, NOAA Earth System Research Laboratory james.m.wilczak@noaa.gov
Eric Williams, NOAA Earth System Research Laboratory eric.j.williams@noaa.gov
David Winker, NASA Langley Research Center d.m.winker@larc.nasa.gov
Yulong Xie, DOE Pacific Northwest Laboratory yulong.xie@pnl.gov
Greg Yarwood, Environ Corp gyarwood@environcorp.com

APPENDIX 4. GUIDELINES FOR FORMULATION OF SCIENTIFIC FINDINGS TO BE USED FOR POLICY PURPOSES

The following guidelines in the form of checklist questions were developed by the NAPAP Oversight Review Board to assist scientists in formulating presentations of research results to be used in policy decision processes.

1) **IS THE STATEMENT SOUND?** Have the central issues been clearly identified? <u>Does each statement contain the distilled essence of present scientific and technical understanding of the phenomenon or process to which it applies</u>? Is the statement consistent with all relevant evidence – evidence developed either through NAPAP [or TexAQS] research or through analysis of research conducted outside of NAPAP [or TexAQS II]? Is the statement contradicted by any important evidence developed through research inside or outside of NAPAP [or TexAQS II] Have apparent contradictions or interpretations of available evidence been considered in formulating the statement of principal findings?

2) **IS THE STATEMENT DIRECTIONAL AND, WHERE APPROPRIATE, QUANTITATIVE?** Does the statement correctly quantify both the direction and magnitude of trends and relationships in the phenomenon or process to which the statement is relevant? When possible, <u>is a range of uncertainty given for each quantitative result</u>? Have various sources of uncertainty been identified and quantified, for example, does the statement include or acknowledge errors in actual measurements, standard errors of estimate, possible biases in the availability of data, extrapolation of results beyond the mathematical, geographical, or temporal relevancy of available information, etc. In short, <u>are there numbers in the statement? Are the numbers correct? Are the numbers relevant to the general meaning of the statement</u>?

3) **IS THE DEGREE OF CERTAINTY OR UNCERTAINTY OF THE STATEMENT INDICATED CLEARLY?** <u>Have appropriate statistical tests been applied to the data used in drawing the conclusion</u> set forth in the statement? If the statement is based on a mathematical or novel conceptual model, has the model or concept been validated? Does the statement describe the model or concept on which it is based and the degree of validity of that model or concept?

4) **IS THE STATEMENT CORRECT WITHOUT QUALIFICATION?** <u>Are there limitations of time, space, or other special circumstances in which the statement is true</u>? If the statement is true only in some circumstances, are these limitations described adequately and briefly?

5) **IS THE STATEMENT CLEAR AND UNAMBIGUOUS?** <u>Are the words and phrases used in the statement understandable by the decision makers of our society</u>? Is the statement free of specialized jargon? Will too many people misunderstand its meaning?

6) **IS THE STATEMENT AS CONCISE AS IT CAN BE MADE WITHOUT RISK OF MISUNDERSTANDING?** Are there any excess words, phrases, or ideas in the statement which are not necessary to communicate the meaning of the statement? Are there so many caveats in the statement that the statement itself is trivial, confusing, or ambiguous?

7) **IS THE STATEMENT FREE OF SCIENTIFIC OR OTHER BIASES OR IMPLICATIONS OF SOCIETAL VALUE JUDGMENTS?** Is the statement free of influence by specific schools of scientific thought? Is the statement also free of words, phrases, or concepts that have political, economic, ideological, religious, moral, or other personal-, agency-, or organization-specific values, overtones, or implications? <u>Does the choice of how the statement is expressed rather than its specific words suggest underlying biases or value judgments</u>? Is the tone impartial and free of special pleading? If societal value judgments have been discussed, have these judgments been identified as such and described both clearly and objectively?

8) **HAVE SOCIETAL IMPLICATIONS BEEN DESCRIBED OBJECTIVELY?**
Consideration of alternative courses of action and their consequences inherently involves judgments of their feasibility and the importance of effects. For this reason, it is important to ask if a reasonable range of alternative policies or courses of action have been evaluated? Have societal implications of alternative courses of action been stated in the following general form?:

"If this [particular option] were adopted then that [particular outcome] would be expected."

9) **HAVE THE PROFESSIONAL BIASES OF AUTHORS AND REVIEWERS BEEN DESCRIBED OPENLY?** Acknowledgment of potential sources of bias is important so that readers can judge for themselves the credibility of reports and assessments.